THE SUPERCRITICAL PROCESSING OF MAMMALIAN CELLS FOR APPLICATIONS IN TISSUE ENGINEERING

Patrick J. Ginty, BSc., MSc.

Thesis submitted to the University of Nottingham for the degree of Doctor of Philosophy, April 2006

"They say Rome wasn't built in a day, but I wasn't on that particular job".

Brian Clough

Abstract

Conventional methods of combining mammalian cells and synthetic polymers for tissue engineering applications are frequently problematic. This is due to the incompatibility between the sensitive cell component and the harsh polymer processing environments required to form the desired porous scaffold e.g. high temperatures and organic solvents. This results in the necessity for an often inefficient and time consuming two-step scaffold seeding process, whereby mammalian cells are added to a pre-fabricated polymer scaffold. High pressure or supercritical CO_2 ($scCO_2$) processing is a method of fabricating porous polymer scaffolds at ambient temperatures and without using organic solvents. When pressurised, CO_2 becomes highly soluble in a variety of amorphous polymers such as poly(DL-lactic acid) ($P_{DL}LA$) to produce a high viscosity liquid. Subsequent decompression causes the formation of gas bubbles that become permanent as the polymer vitrifies. Based upon technology at the University of Nottingham, we hypothesised that mammalian cells could be incorporated into poly(DL-lactic acid) ($P_{DL}LA$) scaffolds using a single step $scCO_2$ process. This would not only make the process more rapid, but it would remove the inefficient scaffold seeding step required in most cell based tissue engineering strategies.

Mammalian cells were subject to a range of high pressure CO_2 and N_2 processing conditions and assessed for cell survival. It was discovered that primary hepatocytes, meniscal fibrochondrocytes, myoblastic C2C12s and 3T3 fibroblasts could survive after exposure to both high pressure gases on a time and pressure dependent basis. Cells exposed to $scCO_2$ for one minute were then assessed for both gene and enzyme function. Using a microarray, it was found that only eight genes (out of 9000) in murine C2C12 cells were significantly down-regulated when compared to untreated cells. Continued cell function was confirmed by measuring BMP-2 induced alkaline phosphatase activity as a measure of osteogenic differentiation in myoblastic C2C12 cells. Alkaline phosphatase activity was indistinguishable between untreated cells and cells exposed to $scCO_2$ for one minute. Additional enzyme and receptor function was confirmed by measuring cytochrome P450 activity in primary hepatocytes after one minute of $scCO_2$ processing.

In the second half of the study, these short processing times were found to be sufficient to plasticise and foam porous $P_{DL}LA$ scaffolds. Therefore, cells were incorporated into the biodegradable $P_{DL}LA$ foams by pre-mixing the cell suspension with the polymer powder and exposing to $scCO_2$. Subsequent decompression caused the polymer to foam with the cells trapped within the porous structure. Despite the presence of the plasticised $P_{DL}LA$, cell survival was confirmed by both an Alamar Blue™ assay and LIVE/DEAD™ staining. Osteogenic differentiation on the scaffolds was confirmed by a stain and assay for BMP-2 induced alkaline phosphatase activity.

Finally, a second generation processing piece of processing apparatus was designed that permitted mammalian cells to be passed into a pressurised vessel containing pre-plasticised $P_{DL}LA$ using a novel high-pressure CO_2 injection system. This was made possible by constant optimisation of the high pressure apparatus and the introduction of a cell delivery valve. When injected at high pressures cell survival was found to be reduced when compared with previous experiments although this was likely to be due to the additional mechanical trauma caused by the injection process. Despite this, the live cell population was shown to retain its osteogenic differentiation capacity when induced with BMP-2. With further optimisation of the delivery method, cells may survive this process in sufficient numbers to suggest that it could be used as a method of seeding tissue engineering scaffolds in the future. This development could remove the limitations place on polymer processing time by the finite survival period of the cells, permitting tuning of the scaffold structure to suit the application

In summary, this study has demonstrated that mammalian cells can be incorporated into biodegradable $P_{DL}LA$ scaffolds using a rapid, one-step $scCO_2$ process without the use of toxic solvents or elevated temperatures. Furthermore, the development of the high pressure injection system could allow cells to be incorporated during the fabrication step, removing the restrictions on polymer processing. This technique could be used for the rapid production of tissue cell loaded engineering scaffolds and other associated biotechnological applications where cells and synthetic polymers are combined, such as cell therapy and recombinant protein production.

Contents

Abstract	II
Acknowledgments	XI
Publications	XII
Conference Abstracts	XIII
List of Figures	XIV
List of Tables	XX
List of Abbreviations	XXII
Chapter 1: Introduction	1
1.1 Tissue Engineering: A Potential Alternative to Organ Replacement	2
1.2 Tissue Engineering Strategies: Cells, Growth Factors and Scaffolds	2
1.2.1 Cells and Tissues	3
1.2.2 The Role of the Scaffold	5
1.2.3 Growth Factors used in Tissue Engineering Applications	8
1.2.3.1 The Bone Morphogenetic Proteins	9
1.3 Materials used as Tissue Engineering Scaffolds	12
1.3.1 Synthetic Polymers	12
1.3.2 Biopolymers	16
1.3.3 Non-Polymeric Materials used in Tissue Engineering	20
1.4 A Summary of Scaffold Fabrication Techniques	21
1.5 The Introduction of Cells into Tissue Engineering Scaffolds	23
1.6 Supercritical Fluid Technology	24
1.6.1 Supercritical Fluid Extraction and Impregnation	24
1.6.2 The Role of Supercritical Carbon Dioxide in Polymer Synthesis and Processing	27
1.6.3 The Role of Supercritical Carbon Dioxide in the Pharmaceutical Industry	28
1.6.4 Supercritical Carbon Dioxide and Tissue Engineering	31
1.6.5 Processing Mammalian Cells in Supercritical Carbon Dioxide	35
1.7 Aims	36

Chapter 2: Assessment of Mammalian Cell Survival After Processing in Supercritical Carbon Dioxide 37

2.1 Introduction – High Pressure CO_2 and Cell Survival 38
2.1.1 Aims 40

2.2 Methods 41
2.2.1 Culture of Secondary Cell Lines 41
2.2.2 Isolation and Culture of Primary Cells 41
2.2.3 Exposure of Mammalian Cells to High Pressure CO_2 and Associated Conditions 41
2.2.3.1 The Effect of Gas Bubble Formation on Cell Survival 42
2.2.3.2 The Effect of Decompression Rate on Cell Survival 42
2.2.3.3 The Effect of Processing Temperature on Cell Survival 42
2.2.3.4 The Effect of Cell Suspension Volume on Cell Survival 43
2.2.3.5 The Effect of an Acidic Environment on Cell Survival 43
2.2.3.6 The Effects of Supercritical CO_2 on Different Cell Types 43
2.2.4 Cell Survival Assessment 44

2.3 Results and Discussion 45
2.3.1 The Effects of Processing Time and Pressure on Mammalian Cell Survival 45
2.3.2 The Effects of Gas Bubble Formation and Decompression Rate on Mammalian Cell Survival 49
2.3.3 The Effects of Temperature and pH on Mammalian Cell Survival 54
2.3.4 The Effect of Cell Suspension Volume on Mammalian Cell Survival 58
2.3.5 The Effect of Changing Cell Type on Resultant Cell Survival 58

2.4 Conclusions 61

Chapter 3: Elucidating The Cause and Extent of Damage to Mammalian Cells After Exposure to Supercritical Carbon Dioxide 62

3.1 Introduction 63

3.1.1 Investigating Potential Causes of Cell Death after Processing in Supercritical CO_2 63
3.1.2 Measuring the Effects of Supercritical CO_2 on Gene Expression and Cell Function 63
3.1.3 Aims 64

3.2 Methods 65
3.2.1 Culture of the Murine C2C12 Cell Line 65
3.2.2 Exposure of Mammalian Cells to Supercritical CO_2 and High Pressure N_2 65
3.2.3 Measuring the Survival of Murine C2C12 Cells after Processing in High Pressure N_2 65
3.2.4 Assessment of Cell Membrane Rupture after Processing in Supercritical CO_2 66
3.2.5 Assessment of Cellular Apoptosis after Processing in Supercritical CO_2 66
3.2.6 Assessment of Gene Expression in Murine C2C12 Cells after Processing in Supercritical CO_2 67
3.2.7 Cell Functionality Assessment by BMP-2 Induced Osteogenic Differentiation of the C2C12 Cell Line after Exposure to Supercritical CO_2 67
3.2.8 Cell Functionality Assessment by Measurement of Cytochrome P450 Activity in Rat Hepatocytes after Exposure to Supercritical CO_2 68

3.3 Results and Discussion 69
3.3.1 Investigating the Possible Causes of Cell Death 69
3.3.2 The Effects of Supercritical CO_2 on Gene Expression in C2C12 Cells 72
3.3.3 The Effects of Supercritical CO_2 on Important Aspects of Mammalian Cell Function 75

3.4 Conclusions 78

Chapter 4: Co-Processing Mammalian Cells and Poly(DL-Lactic Acid) in Supercritical Carbon Dioxide 79

4.1 Introduction 80
4.1.1 Characterising Tissue Engineering Scaffolds 80
4.1.1.1 Light and Fluorescence Microscopy 81
4.1.1.2 Scanning Electron Microscopy 81
4.1.1.3 Micro-Computed Tomography 82
4.1.2 Aims 85

4.2 Methods 86
4.2.1 Fabrication of $P_{DL}LA$ Scaffolds 86
4.2.2 Characterisation of $P_{DL}LA$ Scaffolds 86
4.2.2.1 Light and Fluorescence Microscopy 86
4.2.2.2 Scanning Electron Microscopy 86

4.2.2.3 Micro-Computed Tomography 87
4.2.3 Investigation of the Cell/Polymer Mixing Technique 87
4.2.3.1 Investigating the Effects of Pre-Mixing a Liquid Dye and $P_{DL}LA$ Powder on the Final Distribution of the Dye in the Scaffold 87
4.2.3.2 Investigating the Effects of Pre-Mixing Cells Fixed with Osmium Tetroxide and $P_{DL}LA$ Powder on the Final Distribution of the Cells in the Scaffold 88
4.2.3.3 Co-processing Dead and Fixed Cells with $P_{DL}LA$ in Supercritical CO_2 88
4.2.3.4 Light Microscopy Analysis 88
4.2.3.5 Micro-Computed Tomographic Analysis of Cell Loaded Scaffolds 88
4.2.4 Co-Processing Live Cells with $P_{DL}LA$ 89
4.2.4.1 Cell Isolation and Culture 89
4.2.4.2 Fabrication of Cell-Loaded $P_{DL}LA$ Scaffolds using Supercritical CO_2 89
4.2.4.3 Assessment of Cell Survival in $P_{DL}LA$ scaffolds 89
4.2.4.4 Histological Assessment of Cell Survival and Distribution 90
4.2.4.5 Scanning Electron Microscopy of Cell Loaded $P_{DL}LA$ Scaffolds 90
4.2.5 Assessment of Cell Function using BMP-2 Induced Alkaline Phosphatase Activity 91
4.2.5.1 Addition of BMP-2 after Scaffold Fabrication 91
4.2.5.2 Addition of BMP-2 before Scaffold Fabrication 91
4.2.5.3 Assay and Stain for Alkaline Phosphatase Activity 92

4.3 Results and Discussion 93
4.3.1 Characterisation of $P_{DL}LA$ Scaffolds Fabricated in Supercritical CO_2 93
4.3.2 Investigation of the Cell/Polymer Mixing Technique 99
4.3.3 Confirmation of Cell Attachment and Survival in $P_{DL}LA$ Scaffolds 103
4.3.4 Confirmation of Alkaline Phosphatase Activity in Cell Loaded Scaffolds 108

4.4 Conclusions 112

Chapter 5: Passing Mammalian Cells into Plasticised Poly(DL-Lactic Acid) using a High Pressure Carbon Dioxide Injection System 113

5.1 Introduction 114
5.1.1 Designing the Cell Injection System 114

5.1.2 Aims 115

5.2 Methods 117
5.2.1 Testing the Injection Mechanism with Dead Cells 117
5.2.1.1 Preparation of Dead C2C12 Cells for Injection Experiments 117
5.2.1.2 Delivering Cell Suspensions into the 60 ml Vessel using High Pressure CO_2 117
5.2.1.3 Delivering Cell Suspensions into a High Pressure CO_2 Environment 118
5.2.1.4 Delivering Cell Suspensions into a Collection Mould using High Pressure CO_2 120
5.2.2 The Injection of Live Cells into High Pressure CO_2 123
5.2.2.1 Cell Culture 123
5.2.2.2 Investigating the Effect of Injection Pressure on Cell Survival 123
5.2.2.3 Investigating the Effect of the Injection Mechanism and Medium on Cell Survival and Function 123
5.2.2.4 Assessment of Cell Survival after Injection with High Pressure CO_2 and N_2 124
5.2.2.5 Assessment of Cell Membrane Rupture after Injection with High Pressure CO_2 124
5.2.2.6 Assessment of Cell Functionality after Injection with High Pressure CO_2 125
5.2.3 The Injection of Live Cells into Plasticised $P_{DL}LA$ 125
5.2.3.1 Cell Culture 125
5.2.3.2 The Injection of Fixed and Live Mammalian Cells into Plasticised $P_{DL}LA$ 126
5.2.3.3 Microscopic Analysis of Foamed $P_{DL}LA$ Scaffolds 126
5.2.3.4 Micro-Computed Tomographic Analysis of Cell Loaded $P_{DL}LA$ Scaffolds 126
5.2.3.5 Assessment of Cell Survival after Injection into Plasticised $P_{DL}LA$ 127
5.2.3.6 Assessment of Cell Functionality after Injection into Plasticised $P_{DL}LA$ 127
5.3 Results and Discussion 128
5.3.1 Testing the Injection Mechanism 128
5.3.2 The Injection of Live Cells into High Pressure CO_2 132
5.3.3 The Injection of Live Cells into Plasticised $P_{DL}LA$ 140
5.3.4 Cell Functionality Studies 145

5.4 Conclusions 147

Chapter 6: General Discussion and Conclusions 148

6.1 Discussion 149

6.2 Conclusions 155

Chapter 7: Materials and Methods 156

7.1 Cell Culture 157
7.1.1 Culture of Primary and Secondary Cells 157
7.1.2 Isolation of Primary Cells 157
7.1.3 Viable Cell Counts using Trypan Blue Exclusion 160

7.2 High Pressure Carbon Dioxide Processing 162
7.2.1 Processing of Mammalian Cells in High Pressure CO_2 and N_2 162
7.2.2 Supercritical Processing of $P_{DL}LA$ Scaffolds 165
7.2.3 Supercritical Processing of Live Mammalian Cells with $P_{DL}LA$ 165
7.2.4 Injecting Cells into High Pressure Environments and $P_{DL}LA$ 165

7.3 Biochemical Assays 168
7.3.1 Alamar Blue™ Cell Metabolic Activity Assay 168
7.3.2 DNA Assay 169
7.3.3 Assay for LDH Release from Mammalian Cells as an Indicator of Cell Rupture 169
7.3.4 Enzyme–Linked Immunosorbent Assay for Histone Complexes as an Indicator of Apoptosis 170
7.3.5 Testosterone Assay for Cytochrome P450 Activity using High Performance Liquid Chromatography 170

7.4 Alkaline Phosphatase Studies using the Murine C2C12 Cell Line 172
7.4.1 BMP-2 Induced Osteogenic Differentiation of the C2C12 Cell Line 172
7.4.2 p-NPP Assay for Alkaline Phosphatase Activity 172
7.4.3 Alkaline Phosphatase Staining of the C1C12 Cell Line 173

7.5 Genomic Analysis 174
7.5.1 RNA Isolation, Purification and Hybridisation 174
7.5.2 Microarray Analysis 175

7.6 Biological Stains and Histology 176
7.6.1 Ethidium Homodimer-1: Calcein AM (LIVE/DEAD™) Stain 176
7.6.2 Histology of Cell Loaded Scaffolds with LIVE/DEAD™ and Propidium Iodide Staining 176

7.7 Techniques used in the Characterisation of Polymer Scaffolds 177

7.7.1 Light and Fluorescence Microscopy 177
7.7.2 Scanning Electron Microscopy 177
7.7.2.1 Preparation of Samples 177
7.7.2.2 Gold (Sputter) Coating 178
7.7.2.3 Imaging and Scaffold Characterisation 178
7.7.3 Micro-Computed Tomography 179

References 180

Acknowledgements

First and foremost I would like to acknowledge all of my PhD supervisors, Professors Kevin Shakesheff, Steve Howdle and Dr Felicity Rose for their help, expertise and guidance throughout the last three and a half years.

Many thanks go to Dan Howard for carrying out the histology work on the polymer scaffolds samples and answering my constant questions about the alkaline phosphatase assay! Many thanks must also go to John Barry for my training on the micro-CT unit and Marta Silva for my training on the supercritical CO_2 equipment.

I must also acknowledge Paddy Tighe and Stacey Mutch for the genomic analysis and Robert Thomas for the hepatocyte isolation, as this work was carried out on my behalf and when I was not present.

The following people have all also helped me at some stage during the 3 years, but are mentioned in no particular order; Jennifer Unsworth, Chris Duxbury, Ben Wong, Martin Whitaker, Katrina Teare and Mieke Heyde. I am hugely grateful to Pete and Rich in Chemistry workshops for manufacture of the high pressure kit and Teresa and Christi in Pharmacy for helping with my strange requests. I would also like to thank all of the researchers in both tissue engineering (Pharmacy) and clean technology (Chemistry).

I must acknowledge the people who have not contributed to this work directly, but without their contribution, I would have found it more difficult to complete this PhD. This includes all of my family members, particularly my mum and my brother Simon, as well as all of my friends. Specific thanks go to my former housemates Omar and Adam who have made those three years in Nottingham more tolerable and very eventful to say the least.

Finally, very special thanks go to Carly, from whom I have received greater support than anyone else in the last three to four years. I promise that all of my hard work will be worth it in the end and I would not have got this far without you.

Publications

The following publications have contributed to this PhD thesis:

Ginty, PJ, Whitaker, MJ, Shakesheff, KM, Howdle, SM. (2005) Drug Delivery goes Supercritical. *Materials Today*, **8** (8) S1, p42-48.

Ginty, PJ, Rose, FRAJ, Howdle, SM, Shakesheff, KM. (2006) *The role of polymers for drug delivery in tissue engineering applications*. In 'Polymers in Drug Delivery' Eds. Uchegbu, I & Schatzlein, A. G., p63-80. Taylor & Francis.

Ginty, PJ, Howard, D, Rose, FRAJ. *et al.* (2006) Mammalian cell survival and processing in supercritical CO_2. *Proceedings of the National Academy of Sciences of the United States of America*, **103**, 7426-7431.

Ginty, PJ, Howard, D, Barry, JA, Rose, FRAJ, Shakesheff, KM, Howdle, SM. A high-pressure CO_2 injection system for the rapid production of polymer:cell composites. *Submitted*.

Conference Abstracts

The following abstract was submitted for an oral presentation at the Tissue and Cell Engineering Society meeting at Keele University, Staffordshire, UK in June 2004:

Ginty, PJ, Rose, FRAJ, Howdle, SM and Shakesheff, KM. *Cell loaded scaffolds using a one-step supercritical mixing technique*. TCES conference, Keele University, June (2004).

The following abstract has been accepted for the British Pharmaceutical Conference in Manchester (September 2006):

Ginty, PJ, Howard, D, Rose, FRAJ, Howdle, SM and Shakesheff, KM. *A Rapid Supercritical Route to Cell Loaded Scaffolds for Tissue Engineering.*

List of Figures

Chapter One

Figure 1-1 Phase diagram showing the point at which a substance ceases to be either a liquid or a gas and becomes a supercritical fluid.

Figure 1-2 The plasticisation and foaming of $P_{DL}LA$ using $scCO_2$ processing as viewed through the sapphire window of a high pressure viewing vessel.

Chapter Two

Figure 2-1 Survival of the murine 3T3 fibroblast cell line after exposure to $scCO_2$ for increasing time periods as measured by the Alamar Blue assay.

Figure 2-2 Survival of mammalian cells exposed to high pressure and supercritical CO_2 for increasing exposure times as measured by the Alamar Blue assay.

Figure 2-3 Effects of a one-step and a two-step decompression on gas bubble formation in cell culture medium (200 µl) as seen through the sapphire window of a high pressure viewing vessel.

Figure 2-4 Survival of mammalian cells after exposure to $scCO_2$ using a one step or two step pressure quench as illustrated in figure 2-3.

Figure 2-5 Survival of mammalian cells after exposure to $scCO_2$ for one minute and increasing decompression times as measured by an Alamar Blue assay.

Figure 2-6 Survival of mammalian cells exposed to $scCO_2$ for one minute at different processing temperatures as measured by an Alamar Blue assay.

Figure 2-7 Survival of mammalian cells exposed to acidic conditions (pH3) for increasing exposure times, with and without the addition of Hepes buffer (pH7) as measured by an Alamar Blue assay.

Figure 2-8 Survival of mammalian cells exposed to $scCO_2$ when suspended in different volumes of cell culture medium as measured by an Alamar Blue assay.

Figure 2-9 Master chart for the survival of four different mammalian cell types when subjected to $scCO_2$ for increasing exposure times as measured by an Alamar Blue assay.

Chapter Three

Figure 3-1 Survival of C2C12 cells when subjected to 74 bar pressure of $scCO_2$ or N_2 for increasing exposure times as measured by an Alamar Blue assay.

Figure 3-2 Measurement of cell rupture using an LDH assay and apoptosis using an ELISA for DNA-histone complexes, after exposure of C2C12 cells to $scCO_2$ for increasing time periods.

Figure 3-3 Log-log plots of normalised intensity (arbitrary units on both axes) for genes after microarray analysis of the murine C2C12 cell line after exposure to $scCO_2$.

Figure 3-4 Specific alkaline phosphatase activity of C2C12 cells after $scCO_2$ processing for one minute as measured by the p-NPP substrate system.

Figure 3-5 Assay data measuring the metabolism of testosterone by cytochrome P450 activity in rat hepatocytes after $scCO_2$ processing for increasing exposure times.

Chapter Four

Figure 4-1 A typical SEM image showing the internal pore structure of a $P_{DL}LA$ scaffold fabricated by $scCO_2$ processing at the University of Nottingham.

Figure 4-2 Micro-computed tomography mages of $P_{DL}LA$ scaffolds fabricated by $scCO_2$ processing at the University of Nottingham.

Figure 4-3 Images of $P_{DL}LA$ scaffolds taken using a light microscope after $scCO_2$ processing for 10, 30 and 60 seconds (A, B and C respectively) at 74 bar, 35°C.

Figure 4-4 Scanning electron micrographs of $P_{DL}LA$ scaffolds after $scCO_2$ processing for 10, 30 and 60 seconds (A, B and C respectively) at 74 bar, 35°C.

Figure 4-5 Pore size distributions calculated from SEM for $P_{DL}LA$ scaffolds after $scCO_2$ processing for up to 60 seconds at 74 bar, 35°C.

Figure 4-6 Pore size distributions calculated from micro-CT for $P_{DL}LA$ scaffolds after $scCO_2$ processing for up to 60 seconds at 74 bar, 35°C.

Figure 4-7 Gross morphology of $P_{DL}LA$ scaffolds showing the effects of pre-mixing the polymer powder with a food dye solution on the final distribution of the liquid in the foamed scaffold.

Figure 4-8 Cross sections of pre-mixed and unmixed $P_{DL}LA$/food dye scaffolds as viewed on the light microscope.

Figure 4-9 Distribution of pre-mixed, osmium stained cells (right) in a $P_{DL}LA$ scaffold (left).

Figure 4-10 SEM images of 3T3 fibroblasts spreading on $P_{DL}LA$ scaffolds.

Figure 4-11 Survival data for four cell types after processing into $P_{DL}LA$ scaffolds using $scCO_2$ for 30 seconds as measured by an Alamar Blue assay.

Figure 4-12 Images of cell loaded $P_{DL}LA$ scaffolds processed in $scCO_2$ for 30 seconds and stained with LIVE/DEAD™.

Figure 4-13 Thin cut sections of $P_{DL}LA$ scaffolds loaded with C2C12 cells using a one-step $scCO_2$ process.

Figure 4-14 Confirmation of alkaline phosphatase activity in $P_{DL}LA$ scaffolds loaded with C2C12 cells using a one-step $scCO_2$ process after induction into the osteogenic lineage with 500 ng/ml rhBMP-2.

Figure 4-15 Visual confirmation of alkaline phosphatase activity in $P_{DL}LA$ scaffolds loaded with C2C12 cells using $scCO_2$ after subsequent osteogenic culture in 500 ng/ml rhBMP-2

Figure 4-16 Confirmation of alkaline phosphatase activity in $P_{DL}LA$ scaffolds loaded with C2C12 cells and 500 ng of rhBMP-2 using $scCO_2$ processing

Chapter Five

Figure 5-1 Original set-up for the high pressure CO_2 injection system. The gas reservoir is pressurised along with the 60 ml collection vessel.

Figure 5-2 Modifications made to the high pressure CO_2 injection system in order to incorporate a collection mould.

Figure 5-3 A PTFE mould used to collect samples from the high pressure CO_2 injection system.

Figure 5-4 Percentage recovery of a dead cell suspension after high pressure CO_2 injection into a 60 ml vessel retained at atmospheric pressure.

Figure 5-5 Percentage recovery of a dead cell suspension after high pressure CO_2 injection into a vessel already pressurised with CO_2.

Figure 5-6 Percentage recovery of a dead cell suspension after high pressure CO_2 injection into a PTFE mould within a vessel pressurised with CO_2.

Figure 5-7 Cell survival data and visual confirmation after injection into high pressure CO_2 using the A-B valve opening sequence.

Figure 5-8 Cell survival and visual confirmation after a slow injection into high pressure CO_2 using the A-B valve opening sequence.

Figure 5-9 Cell survival data after injection into high pressure CO_2 using the B-A valve opening-sequence.

Figure 5-10 Cell survival data after injection into high pressure CO_2 using the B-A valve-opening sequence and N_2 as the injection medium.

Figure 5-11 Measurement of cell rupture using an LDH assay after exposure of C2C12 cells to increasing pressures of CO_2.

Figure 5-12 Specific alkaline phosphatase activity of C2C12 cells after injection into a high pressure environment with $scCO_2$.

Figure 5-13 Gross morphology of a $P_{DL}LA$ scaffold produced using the $scCO_2$ injection system.

Figure 5-14 Micro-computed tomographic images of (A) whole $P_{DL}LA$ scaffolds and (B) scaffold cross sections, showing the distribution of mammalian cells pre-fixed with electron dense osmium tetroxide and subsequently injected into the polymer using $scCO_2$.

Figure 5-15 Scanning electron micrographs of $P_{DL}LA$ scaffolds after the injection of mammalian cells using $scCO_2$

Figure 5-16 LIVE/DEAD™ images of $P_{DL}LA$ scaffolds loaded with mammalian cells using the high pressure CO_2 injection system.

Figure 5-17 $P_{DL}LA$ scaffolds loaded with C2C12 cells using the high pressure CO_2 injection system and stained for BMP-2 induced alkaline phosphatase activity

Chapter Seven

Figure 7-1 Isolation of the cartilage menisci from the ovine knee joint.

Figure 7-2 Layout of the five chambers on the haemocytometer (1-5) used to calculate cell number.

Figure 7-3 Schematic of the equipment used to process mammalian cells and synthetic polymers in sub-critical and supercritical CO_2.

Figure 7-4 Apparatus used to process of both mammalian cells and $P_{DL}LA$ scaffolds in high pressure and supercritical CO_2.

Figure 7-5 A PTFE mould used to collect samples from the high pressure injection system.

List of Tables

Chapter One

Table 1-1 Desirable characteristics for tissue engineering scaffolds.

Table 1-2 Growth factors commonly used in tissue engineering applications.

Table 1-3 Molecular structures of synthetic polymers commonly used in tissue engineering applications.

Table 1-4 Molecular structures of biopolymers commonly used in tissue engineering or drug delivery applications

Table 1-5 Techniques commonly used in the fabrication of tissue engineering scaffolds from synthetic polymers.

Chapter Two

Table 2-1 Temperature changes inside the pressure vessel during the supercritical processing of mammalian cells.

Table 2-2 Changes in temperature recorded during increasing decompression times.

Table 2-3 Changes in temperature recorded when mammalian cells are processed at 74 bar for one minute at different starting temperatures.

Chapter Three

Table 3-1 Genes shown to have significant down regulation when analysed with the SAM algorithm, as implemented within MEV.

Chapter Four

Table 4-1 A summary of pore size and porosity data for $P_{DL}LA$ scaffolds after $scCO_2$ processing at 74 bar and 35°C. All data is given with standard deviation.

Chapter Five

Table 5-1 Processing matrix for the injection of cells into reduced pressures with CO_2.

List of Abbreviations

ASES	aerosol solvent extraction system
BMP-2	bone morphogenetic protein-2
BMP-3	bone morphogenetic protein-3
BMP-7	bone morphogenetic protein-7
CYP450	cytochrome p450
DNA	deoxyribonucleic acid
DMEM	Dulbecco's modified eagle's medium
EBSS	Earl's buffered salt solution
ECM	extra-cellular matrix
ELISA	enzyme-linked immunosorbent assay
ES	embryonic stem (cells)
FCS	foetal calf serum
FDA	food and drug administration
FGF	fibroblast growth factor
GAS	gas anti solvent
HA	hydroxyapatite
HBSS	Hanks' buffered salt solution
HPLC	high-performance liquid chromatography
HUVECs	human umbilical vein endothelial cells
IL-1	interleukin-1
KGF	keratinocyte growth factor
LDH	lactate dehydrogenase
μ-CT	micro-computed tomography
MEV	multi-experiment viewer
MSC	mesenchymal stem cell
NGF	nerve growth factor
OP-1	osteogenic protein-1
OSF-1	osteoblast stimulating factor-1
PBS	phosphate buffered saline

PCA	precipitation with a compressed anti-solvent
PCL	poly(caprolactone)
PDGF	platelet derived growth factor
$P_{DL}LA$	poly(DL-lactic acid)
PEG	poly(ethylene glycol)
PEMA	poly(ethyl methacrylate)
PGA	poly(glycolic acid)
PGSS	particles from gas saturated solutions
PLA	poly(lactic acid)
PLGA	poly(lactic-co-glycolic acid)
P_LLA	poly(L-lactic acid)
p-NP	p-nitrophenol
p-NPP	p-nitrophenyl phosphate
PS	polystyrene
PTFE	poly(tetrafluoroethylene)
RESS	rapid expansion of supercritical solutions
RGD	arginine-glycine-aspartic acid
rhBMP-2	human recombinant bone morphogenetic protein-2
RNA	ribonucleic acid
SAM	statistical analysis of microarrays
SAS	supercritical anti solvent
$scCO_2$	supercritical carbon dioxide
SCF	supercritical fluid technology
SEDS	solution enhanced dispersion of supercritical fluids
SEM	scanning electron microscopy
SFE	supercritical fluid extraction
SFI	supercritical fluid impregnation
T_c	critical temperature
Tg	glass transition temperature
TGF- β	transforming growth factor
T_p	critical pressure

VEGF	vascular endothelial growth factor
2D	two dimensional
3D	three dimensional

Chapter 1

GENERAL INTRODUCTION

1.1 Tissue Engineering: A Potential Alternative to Organ Replacement

Tissue engineering is driven by the need for new tissues to replace those lost or damaged due to illness or injury (Langer & Vacanti, 1993, Levenberg & Langer, 2004). Traditionally, there has been little alternative to the millions of intrusive and painful surgical procedures carried out every year and the financial costs incurred as a result. To put this into figures, in 1999 there were 34 million procedures costing a total of $400 million carried out in the USA alone (Langer & Vacanti, 1999). However, tissue engineering provides a real alternative to these painful and costly surgical procedures, guiding the repair and regeneration of biological tissue through the application and control of cells, materials and protein growth factors (Langer & Vacanti, 1993, Bonassar & Vacanti, 1998). Porous scaffolds made from a variety of materials, are used as the substrate for cell attachment and proliferation (Langer & Vacanti, 1993), whilst protein growth factors can control the very cellular processes that instigate and control tissue growth (Mckay and Leigh, 1993). This mixture of synthetic and biological materials makes tissue engineering a complex field that lies at the interface of several disciplines including polymer chemistry, biochemistry and drug delivery, whilst retaining its traditional roots in medicine and biology.

1.2 Tissue Engineering Strategies: Cells, Growth Factors and Scaffolds

Many strategies have been developed in order to regenerate functional tissue, most of which involve the use of polymer scaffolds specifically designed to direct tissue growth, as discussed later (Freed *et al*, 1993a). For example, a technique commonly used in cartilage engineering applications is the cell transplantation method (Brittberg *et al*, 2001). Here, tissue is taken from the donor patient and the desired cells are isolated from this tissue using enzymatic digestion to remove the extra-cellular matrix (ECM). The cells can then be cultured (*ex-vivo*) to achieve a large cell population and can either be 'seeded' onto a biodegradable pre-fabricated polymer scaffold or implanted back into the patient directly.

If a scaffold is used as a carrier, the seeded construct (as it is then known) can be transplanted into the wound or defect. This method uses the inherent regenerative capabilities of the body to produce new tissue. An alternative approach that is commonly taken in cartilage engineering is where functional tissue is regenerated *in-vitro* with the use of a bioreactor or alternative 3D culture system (Freed *et al*, 1998). A bioreactor mimics the physiological environment inside the body, providing the necessary nutrition and optimal conditions for tissue formation. It is of particular use in cartilage engineering, as it can also provide the mechanical forces often required to produce phenotypically correct cartilage. This use of bioreactors for the synthesis of cartilage tissue has already been comprehensively reviewed (LeBaron & Athanasiou, 2000, Darling & Athanasiou, 2003).

Other techniques have been used which do not involve the transplantation of cells or tissues. Conduction for example, is a passive method of engineering new tissue that involves the placement of a material, normally a synthetic polymer that simply occupies the tissue space left behind. This allows the cells in the surrounding tissues to move into that space and regenerate the tissue (Alsberg *et al*, 2001). There is also a more active method known as induction that involves the delivery of peptides and proteins to the defective site. This has been used successfully in the formation of bone through the delivery of osteoblast stimulating factor-1 (OSF-1) (Yang *et al* 2002, Yang *et al*, 2003a) and bone morphogenetic protein-2 (BMP-2) (Yang *et al*, 2003b). Such bioactive molecules are normally delivered by a polymeric device to a specific area where the molecules bind to cells and induce their migration to this area, encouraging tissue growth.

1.2.1 Cells and Tissues

The ability to take a small population of mammalian cells and provide them with an environment that will facilitate the growth of new tissue is the fundamental goal of tissue engineering (Langer & Vacanti, 1993). Combine this fact with the clinical demand for a variety of tissues and organs and the result is a growing number of cell and tissue types under investigation for possible tissue engineering applications.

Tissues and organs as diverse as retinas (Dutt *et al*, 2000), kidney (Humes *et al*, 1999) and blood vessels (Peters *et al*, 2002) have all been investigated for potential cell-based tissue engineering applications in recent years. The requirement for blood vessel formation (angiogenesis) is of particular importance because of the need for a blood supply to provide essential nutrients to many tissues and organs in the body (L'Heureux *et al*, 1998, Levenberg *et al*, 2005). In fact, large, multi-cellular and highly vascular organs such as the liver provide a great challenge to tissue engineers due to the requirement for a constant flow of nutrients provided by oxygenated blood (Dixit, 1994). This is further complicated by the fact that some cell types can only survive for a relatively short period of time when in culture (Bhandari *et al*, 2001). These facts make the possibility of engineering a whole organ very much a long term aim, although a more realistic short term aim may be to produce realistic cellular models for the testing of new drugs *in-vitro* or as pre-cursors to replacement organs (Griffith *et al*, 1997, Kulig & Vacanti, 2004). Some of the 'less complex' tissues such as skin (Orgill & Skrabut, 1985, Parenteau *et al*, 1992), cartilage (Freed *et al*, 1993a, Fuchs *et al*, 2005) and bone (Laurencin *et al*, 1996, Yang *et al*, 2004, Service, 2005, Stevens *et al*, 2005) have been successfully engineered.

Cartilage, has a largely load bearing or supportive function, with only one cell type (chondrocytes) and does not require a blood supply. Along with skin, it was among the first tissues to be investigated for tissue engineering applications and as a result there have been significant developments from both a clinical and commercial viewpoint. In addition to the first cartilage-based product (Genzyme's Carticel™) several skin-based tissue engineering products are also on the market, such as Epicel™ (also Genzyme) and Alloderm™ (LifeCell).

Development of stem cell technologies alongside tissue engineering has provided an augmentation of the traditional strategies previously mentioned, largely as a result of the advantages associated with being pluri-potent. In simple terms, when a stem cell divides, each new cell has the ability to either remain a stem cell (self-renewal) or differentiate into cell with a more specialised function (Kotobuki *et al*, 2004).

Embryonic stem (ES) cells are of great interest in medicine and biology because of their ability to develop into virtually any other type of cell present in the human body. However, their use in research as well as therapy is encumbered by ethical considerations. In contrast to stem cells from embryonic origin, adult stem cells such as mesenchymal stem cells (MSCs) are also multipotent cells that can be isolated from adult bone marrow and can be induced *in vitro* and *in vivo* to differentiate into a variety of mesenchymal tissues of interest to tissue engineers, including bone, cartilage and tendon (Oghushi & Caplan, 1999). Recent studies have also demonstrated the possibility that MSCs can differentiate into other types of tissue-specific cells, such as cardiac myoblasts (Makino *et al*, 1999), endothelial cells (Reyes *et al*, 2002), hepatocytes (Schwartz *et al*, 2002) and neural cells (Deng *et al*, 2001). In particular, mesenchymal stem cells have been recognised for their potential use in cartilage and bone engineering applications. Some researchers have already utilised MSCs in the repair of bone tissue (Quarto *et al*, 2001, Partridge *et al*, 2002).

1.2.2 The Role of the Scaffold

Within the body cells are surrounded by a physically strong supporting structure known as the extracellular matrix (ECM). For example, in cartilage the cells (chondrocytes) are surrounded by an ECM made up of collagen, the major structural protein of the tissue, and a number of other proteins such as glycosaminoglycan (GAG) proteins. These proteins provide the necessary physical and biological support to the cellular constituents to produce a mechanically strong but flexible tissue that is fit for purpose. Therefore, the role of the polymer scaffold is to provide a 3-D micro-environment for cell attachment and growth, thus mimicking the ECM. Such is the pivotal role of the ECM, any scaffold made for implantation into the body must fulfil a number of stringent criteria in order for it to receive medical approval and be fit for purpose. These criteria include; biodegradability, high levels of porosity and low toxicity (Table 1-1). In most tissue engineering applications, it is important that the scaffold material is biodegradable.

However, the material must degrade at such a rate, so as to allow the growth of new tissue in the space left behind. High levels of porosity are also required to facilitate the spread and growth of cells and to provide a network for the free passage of nutrients throughout the construct. In addition to its role as a support for cell attachment and growth, many tissue engineering strategies require the scaffold to be capable of the delivery of bioactive molecules such as protein growth factors, molecules that can promote or inhibit a number of important cellular processes (discussed in section 1.2.3). Therefore, the porosity and rate of biodegradation are also crucial in determining the release kinetics of the entrapped growth factor(s).

A number of materials have been trialled as tissue engineering scaffolds including synthetic polymers, natural polymers and ceramics. However, once a material has been deemed suitable for tissue engineering, there are still issues with immunogenicity and toxicity that must pass the stringent guidelines set by the food and drug administration (FDA). However, several materials have been approved by the FDA for use in medical applications, including synthetic polymers such as the poly(α-hydroxy acids) and natural or biopolymers such as collagen.

Table 1-1 Desirable characteristics for tissue engineering scaffolds.

Desired property or criteria	**Justification**
Non-toxic	To prevent the release of toxic metabolites into the bloodstream
Large surface area	To allow adequate seeding densities
Highly porous	For growth factor release, gas and nutrient exchange
Biocompatibility	To allow the cells to adhere to the scaffold without adverse reactions to the material
Biodegradability	To complement proliferation of cells, release of growth factors and tissue formation
Good mechanical strength	To provide physical support to the growth of the new tissue
Economical	To retain feasibility on a large scale
Ease of processing	To provide a rapid, reproducible method of scaffold fabrication without the need for toxic organic solvents

1.2.3 Growth Factors used in Tissue Engineering Applications

Growth factors are polypeptides that produce and transmit signals to control cellular activities. They can either stimulate or inhibit a number of cellular processes including proliferation and differentiation as well as altering gene expression and triggering angiogenesis (the formation of blood vessels). As a result, they have a key role in the regeneration of both vascular tissue (e.g. skin) and non-vascular tissue (e.g. cartilage) (Mckay & Leigh, 1993). Growth factors can initiate their action by binding to specific receptors on the surface of target cells. They can act locally (paracrine) or systemically (endocrine) and even upon the same cell from which they are released (autocrine) (Mckay & Leigh, 1993). Each growth factor can have a specific or non-specific role within the body to instigate cellular processes. For example, transforming growth factor-β (TGF-β) is a protein that stimulates ECM production in cartilage and bone regeneration (Nicoll *et al*, 1995, Lind *et al*, 2001, Mann *et al*, 2001), whilst vascular endothelial growth factor (VEGF) stimulates endothelial cell proliferation in blood vessel formation (angiogenesis) (Weatherford *et al*, 1996, Sheridan *et al*, 2000). However, the situation is much more complex than this as the local environment and the concentration of the growth factor are influential factors. A summary of the growth factors commonly used in tissue engineering can be seen in Table 1-2.

There are a number of challenges that must be overcome in order to achieve tissue regeneration with the use of growth factors. One such challenge is to mimic the release profile of growth factors *in-vivo*, as the release of these molecules is intermittent, in response to the needs of the body. They may also have very short biological half-lives, sometimes of only a few minutes, leading to a rapid turnover. In addition, it may be that a number of growth factors are needed at different stages throughout the regeneration process, requiring the independent control of two or more growth factor types (Richardson *et al*, 2001). For example, for the regeneration of skin both fibroblastic growth factor (FGF) and keratinocyte growth factor (KGF) are required for cell proliferation, whilst interleukin-1 (IL-1) and VEGF are required for macrophage activation and angiogenesis respectively (Eming *et al*, 2002).

In addition, the same growth factor can have different effects on different cells and even on the same cell at different concentrations. This complicates growth factor delivery and it is for this reason that much work has been done to provide effective and efficient drug delivery systems in order to target cells and promote tissue growth. Ultimately, the main aims, when producing a protein growth factor delivery device are: to mimic the release profile, kinetics, dosage, duration and cellular targeting found *in-vivo* (Maquet & Jerome, 1997). In addition to these factors, there is the issue of maximising the protein loading capacity of the polymer. By incorporating these protein growth factors, into polymeric devices, it is hoped that controlled and sustained release profiles can be achieved. Furthermore, by implanting the device into the area where regeneration is required, the delivery of the protein can be made more efficient. Such devices have been made from a number of synthetic polymers and biopolymers, in a variety of morphologies, dependent upon the processing method. Indeed, once the target cell is identified, the selection of the polymer/fabrication method is crucial to the successful controlled release of the protein. For example, adverse processing conditions, such as the use of a toxic solvent, can denature the conformation of a sensitive protein or cause aggregation and this needs to be avoided (Van de Weert *et al*, 2000). Similarly, a poor release mechanism as a result of an unsuitable choice of polymer may result in poor release kinetics or loss of efficacy. This is because in most cases, the release mechanism for the protein is by diffusion through the porous matrix or by degradation of the polymer and subsequent release of the entrapped molecules.

1.2.3.1 The Bone Morphogenetic Proteins

The first protein growth factors to become commercially available as tissue engineering products were the bone morphogenetic proteins (BMPs). BMPs are endogenous growth factors that can be extracted from pulverised bone. With the exception of bone morphogenetic protein-3 (BMP-3), they are all osteoinductive proteins that can be used to repair bone via local administration. Products such as Stryker Biotech's OP-1 putty™ and the InFuse implant™ (Wyeth-Ayerst), have both become commercially available after FDA approval.

Both of these devices use the induction technique previously described whereby the protein growth factor is combined with collagen to provide a controlled release device. In the case of the OP-1™ product, bone morphogenetic protein-7 (BMP-7) is mixed with type I collagen to form a powder that when hydrated with a saline solution forms putty. This putty is then used to fill wound defects and deliver BMP-7 to the affected area, actively recruiting stem cells from the surrounding tissue and initiating the bone formation cascade starting with osteoblast activity. The InFuse™ implant (licensed to Medatronic Sofamor Danek) contains bone morphogenetic protein-2 (BMP-2) absorbed onto a highly porous collagen sponge. The sponge acts as a controlled release system for the protein that is used to induce spinal fusion when rolled inside a titanium cage.

In addition to the collagen-based systems, BMPs have also been used in tissue engineering applications that utilise synthetic polymers as controlled release matrices. For example, BMP-2 has been incorporated into porous poly(DL-lactic acid) scaffolds to repair both bone and cartilage (Yang *et al*, 2003b, Yang *et al* 2004). It is also useful for the assessment of functionality in cell based tissue engineering applications as it can induce an osteogenic response in myogenic cells (Tare *et al*, 2002). This osteogenic response is measured by using markers of mineralization such as alkaline phosphatase and osteocalcin (Okubo *et al*, 1999, Han *et al*, 2003).

Table 1-2 Growth factors commonly used in tissue engineering applications.

Factor	**Action/activity**	**Use in tissue engineering**	**References**
Platelet derived growth factor (PDGF)	Promotes proliferation of endothelial cells	Angiogenesis, bone and wound healing	Lohmann *et al*, 2000, Park *et al*, 2000a & b, Richardson *et al*, 2001
Fibroblast growth factor (FGF)	Cell proliferation	Nerve growth, endothelial cell proliferation, angiogenesis	Hile *et al*, 2000, Sakiyama-Elbert & Hubbell, 2000b, Tabata *et al*, 2000.
Epidermal growth factor (EGF) and basic fibroblast growth factor (bFGF)	Cell proliferation	Wound healing, differentiation of neural stem cells	Mooney *et al*, 1996b, Chen *et al*, 1997, Von Recum *et al*, 1999, Hile *et al*, 2000, Kanematsu *et al*, 2004.
Nerve growth factor (NGF)	Axonal growth and cholinergic cell survival	Promotes neurite extension and neural cell survival	Krewson & Saltzman, 1996, Cao & Shoichet, 1999, Sakiyama-Elbert and Hubbell, 2000b.
Transforming growth factor (TGF-β)	ECM protein production	Angiogenesis, bone and cartilage repair	Nicoll *et al*, 1995, Mann *et al*, 2001.
Vascular endothelial growth factor (VEGF)	Endothelial cell proliferation	Angiogenesis	Ishihara *et al*, 2003, Weatherford *et al*, 1996, Sheridan *et al*, 2000, Sun *et al*, 2004.
Bone morphogenetic protein-2 (BMP-2)	Cell proliferation	Bone repair	Partridge *et al*, 2002, Yang *et al*, 2003b, Yang *et al*, 2004.

1.3 Materials used as Tissue Engineering Scaffolds

A large variety of materials have been used successfully in medical applications such as metallic prostheses for hip replacements and synthetic polymers for surgical sutures. However, so specific are the desirable criteria for a successful tissue engineering scaffold, many materials are not deemed suitable. In this section, the materials that have figured most frequently in tissue engineering applications are described.

1.3.1 Synthetic Polymers

Synthetic polymers have featured in tissue engineering applications more often than natural or biopolymers. This is because man-made polymers offer several advantages over natural polymers, such as relatively low toxicity and tuneable degradability (Lu & Mikos, 1996). However, a key disadvantage of using synthetic polymers is their lack of biocompatibility. The surface chemistry of many synthetic polymers is not biomimetic, in other words, there is a lack of the functional groups required for the long-term adhesion and function of mammalian cells. Therefore a number of methods have been used to both alter surface chemistry (Dsouza *et al*, 1991, Yang *et al*, 2001) and screen for compatible polymers (Anderson *et al*, 2004).

Table 1.3 shows the structures of the most commonly used synthetic polymers in tissue engineering applications. One family of synthetic polymers has featured most frequently in tissue engineering applications, namely the poly(α-hydroxyacid)s and associated esters such as poly(lactic acid) (PLA), poly(glycolic acid) (PGA), the co-polymer poly(lactic-co-glycolic acid) (PLGA) and poly(ε-caprolactone) (PCL). Several members of this group of synthetic polymers have been given approval by the FDA for applications such as orthopaedic implants, surgical sutures and drug delivery devices. These polymers fulfil most of the criteria required by a tissue engineering device, as they are non-toxic, biodegradable and economical.

However, it is the variability in both stereochemistry and co-polymer ratios that, has made these polyesters a popular choice in tissue engineering strategies, as this can allow the degradation rate to be tailored to match the application. For example, poly(DL-lactic acid) ($P_{DL}LA$) is an amorphous polymer that undergoes hydrolysis more slowly than the rigid but hydrophilic PGA (a largely crystalline polymer). This is because the large number of methyl groups in the polymer structure and its highly hydrophobic nature combine to slow hydrolysis of the ester bonds and increase the degradation time when compared to PGA. In contrast poly(L-lactic acid) (P_LLA) is a semi-crystalline polymer that has the combination of both methyl groups and a crystalline structure. Therefore, this can result in longer degradation times, limiting its use in tissue engineering applications. However, it is still more popular than the D-form, with respect to tissue engineering as it yields the naturally occurring L+-lactic acid during hydrolysis (Göpferich, 1996). In addition to changing the molecular weight and stereochemistry, degradation times for PLA can also be reduced or increased by varying the pore wall thickness and the pore surface to volume ratio of the polymer matrix (Lu *et al*, 2000a).

Frequently, it has been shown that by changing the surface properties of PLA, a more biomimetic environment for mammalian cells can result. This has been achieved by methods such as the addition of RGD peptides (Dsouza *et al*, 1991, Yang *et al*, 2001) and plasma deposition (Barry *et al*, 2005). However, despite its naturally hydrophobic surface properties, PLA has been used as a supporting matrix for the culture and growth of many cell types without surface modification. Examples include: bone progenitors (Howard *et al*, 2002), chondrocytes (Park *et al*, 2004) and hepatocytes (Riccalton-Banks *et al*, 2003). Poly(DL-lactic acid) also finds many uses in drug delivery applications where it is important to have a homogenous dispersion of the bioactive species within a one-phase matrix. As a result, $P_{DL}LA$ has been used successfully in the controlled release of model enzymes such as lysozyme (Young *et al*, 1999) and ribonuclease A (Howdle *et al*, 2001, Watson *et al*, 2002).

The more hydrophilic PGA is often used in tissue engineering applications but almost exclusively for the reconstruction of hard tissues, such as cartilage and bone, due to its rigidity and improved mechanical strength (Dunkelman *et al*, 1995, Cao *et al*, 1998, Kellner *et al*, 2002). It has also been shown that PGA encourages chondrocytes to produce more proteoglycans than cells cultured on PLA (Freed & Vunjak-Novakovic, 1998). When both lactic and glycolic acid, are co-polymerised to form PLGA, the degradation kinetics can be further tailored by altering the ratio of lactic acid to glycolic acid (Lu *et al*, 2000b). In addition, the increased mechanical strength and hydrophilicity provided by the PGA molecules provide additional properties suitable for cell culture/tissue growth. As a consequence, PLGA scaffolds have been used for the culture of smooth muscle cells (Harris *et al*, 1998), osteoblasts (Ishaug-Riley *et al*, 1998) and mesenchymal stem cells (Uematsu *et al*, 2005). In addition to their role as cell support devices, PLGA scaffolds have been successfully employed as controlled release matrices in a number of tissue engineering applications such as protein release (Howdle *et al*, 2001, Watson *et al*, 2002) and DNA delivery (Shea *et al*, 1999, Jang & Shea, 2003).

Other synthetic polymers used in tissue engineering applications include poly(ε-caprolactone) (PCL) and poly(ethylene glycol) (PEG). Poly(ε-caprolactone) is a polyester that has found use in tissue engineering despite the fact that it has a very long degradation profile (up to one year). This semi-crystalline polymer can be blended more easily and is generally more compatible with other polymers (Göpferich, 1996). For example, mechanically strong PCL scaffolds have been coated with collagen to provide a more biomimetic environment for dermal fibroblast culture (Zhang *et al*, 2005) and smooth muscle cells (Venugopal *et al*, 2005). Despite being crystalline, PEG is a very different type of polymer from PCL as it is highly soluble in water and has physical properties that are dependent upon the molecular weight. By combining PEG molecules with other polymers, the surface properties of tissue engineering scaffolds can be changed by reducing non-specific protein interactions (Cannizzaro *et al*, 1998) and increasing the hydrophilicity (Han & Hubbell, 1997).

Table 1-3 Molecular structures of synthetic polymers commonly used in tissue engineering applications. Note the methyl group present in the structure of poly(lactic acid) but absent in the otherwise identical poly(glycolic acid).

Polymer	Structure
Poly(lactic acid)	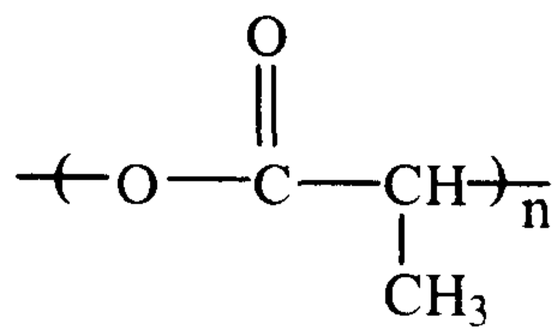
Poly(glycolic acid)	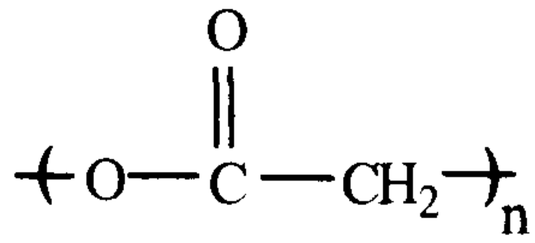
Poly(lactic-co-glycolic acid)	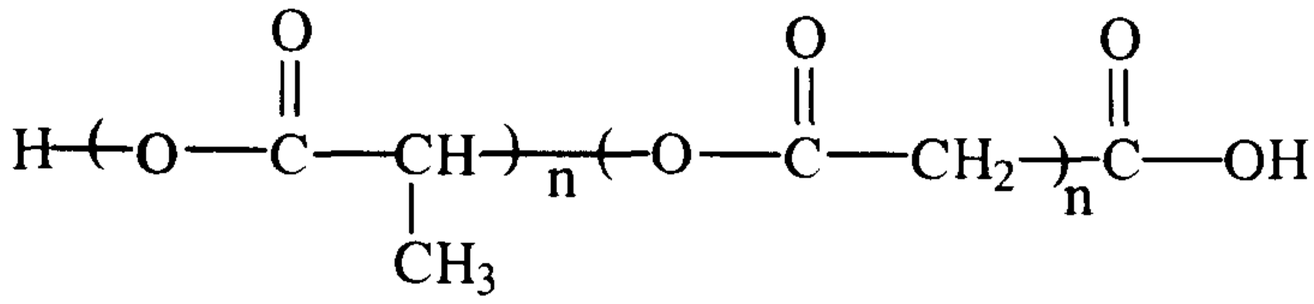
Poly(ε-caprolactone)	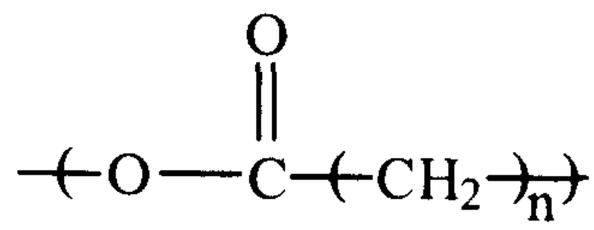
Poly(ethylene glycol)	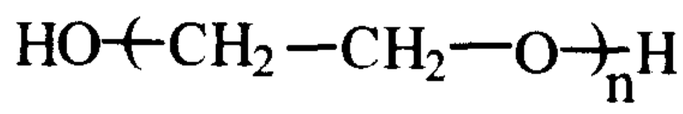

1.3.2 Biopolymers

Table 1.4 shows the molecular structures of the biopolymers most commonly used in tissue engineering applications. These natural polymers such as collagen, gelatin, alginate and chitosan have featured frequently as they carry a number of advantages over the synthetic polymers already mentioned. One example is the reduced need for harsh processing conditions e.g. high temperatures and organic solvents. These natural macromolecules can be easily converted into physical or chemical gels that can entrap cells and growth factors.

Collagen is an abundant ECM protein found in many tissues and structures in the body. Because its natural function is that of physical support, it is a logical choice as a tissue-engineering device (Auger *et al*, 1995). As a result of variations in this structure, collagen comes in many forms (19 types in humans) dependent upon the tissue in question. Type I collagen constitutes the main protein component of natural ECMs of skin and bone and has an important role in the conduit of tissue repair. In addition, type I collagen matrices can be produced as highly porous interconnecting networks and as a result have been used as scaffolds to grow skin, bone and blood vessels (Auger *et al*, 1995). Collagen matrices typically exhibit very poor loading capacities for growth factors, although this has been modified by varying the cross-linking density with glutaraldehyde, thereby reducing the degradation rate and prolonging the delivery of VEGF (Tabata *et al*, 2000). More significantly, FDA approval has also lead to the use of bovine type I collagen being used in several tissue engineering devices, such as the OP-1 and InFuse™ bone induction products already described. However, despite the clinical success of these two devices there are a number of disadvantages associated with the use of collagen carriers. Immunogenicity arising from the use of collagen, including collagen type I, has been recorded in a number of instances (Wangerin & Wottge, 1994, Van de Vord *et al*, 2005) and there is also a risk of pathogen transmission if using allograft collagen (Tomford, 1995).

Perhaps most crucially, control over collagen degradation time is limited by the properties of the material resulting in poor release kinetics (Wallace & Rosenblatt, 2003). Collagen can also come in a denatured form known as gelatin, a substance used for some time in both the pharmaceutical and food industries (Wood, 1965, Reichelt & Joyner, 1965). Denaturation occurs through a harsh acidification process that changes the structure and form of the protein. However, despite this treatment, gelatin does retain all of collagen's biological qualities such as adhesiveness and proteolytic degradability. This form of collagen has been utilised successfully for the culture of chondrocytes with the aid of FGF-9 (Côté *et al*, 2004), and for the delivery of FGF-2 (Au *et al*, 2004). Gelatin has also found use as a carrier for BMP-2 to induce bone regeneration in animal models (Talwar *et al*, 2001).

Alginate is an anionic polysaccharide derived from brown algae. It comes in the form of a block co-polymer composed of two sub units: β-D-mannuronic acid (M) and α–L-guluronic acid (G), the ratio of which is dependent on the source of the alginate (Martinsen *et al*, 1989). When complexed with divalent cations (Ca^{2+}), alginate forms a gel almost independent of temperature, unlike many other biopolymers that require ~37°C. The gelation of alginates is based on their affinity towards specific ions, with the G-blocks responsible for specific ionic binding. This high level of binding gives the G blocks more rigidity and mechanical strength. Therefore, the ratio of G to M blocks can be altered to change the properties of the gel, a useful tool when designing drug delivery devices for tissue engineering applications (Draget *et al*, 1997). Alginate gels have been frequently used as cell supporting scaffolds for tissue engineering applications and in the majority of cases, for the culture of chondrocytes (Guo *et al*, 1989, Paige *et al*, 1995). It has also been used in a recent bone regeneration study where mesenchymal stem cells were layered in an artificial space between the tibia and the periosteum to form an in vivo bioreactor (Stevens *et al*, 2005). Despite the fact that alginate has been shown to induce an inflammatory response (Smidsrod & Skjak-Braek, 1990, Otterlei *et al*, 1991) it is generally well tolerated and as a gel offers many advantages.

These advantages include: controllable levels of porosity in the final gel, simple protein entrapment and no requirement for cross-linking agents or solvents in the gelation process (Hou *et al*, 2004).

Another naturally derived protein used in tissue engineering applications is chitosan. Chitosan is a linear glycosaminoglycan made up of D-glucosamine units derived from chitin, a natural product found in the shells of crustaceans (Berscht *et al*, 1994). Chitosan is a material that has received much attention in tissue engineering applications because of its low cost and ready availability (Suh & Howard, 2000). However, because of its weak mechanical properties and limited ability to support cells, it is rarely used in tissue engineering applications without the addition of another material (Sarasam & Madihally, 2005). Chitosan is often is blended with gelatin due to the presence of the Arg-Gly-Asp (RGD) peptide in the latter providing a more cell adhesive surface. For example, this combination has been used successfully for the culture of human umbilical vein endothelial cells (HUVECs) (Huang *et al*, 2005) and hepatocytes (Moon *et al*, 2005).

Table 1-4 Molecular structures of biopolymers commonly used in tissue engineering or drug delivery applications. The primary sequence of type I collagen is made up of polypeptides containing the repeating amino acid sequence Gly-X-Y with X and Y representing different amino acids with unique functional groups (R_1 and R_2). The structure for alginate is composed of two sub-units: α-(1-4)-L-guluronic acid (a) and β-(1-4)-mannuronic acid (b). Chitosan is made up of repeating D-glucosamine units.

Polymer name	Structure
Collagen type I (primary structure)	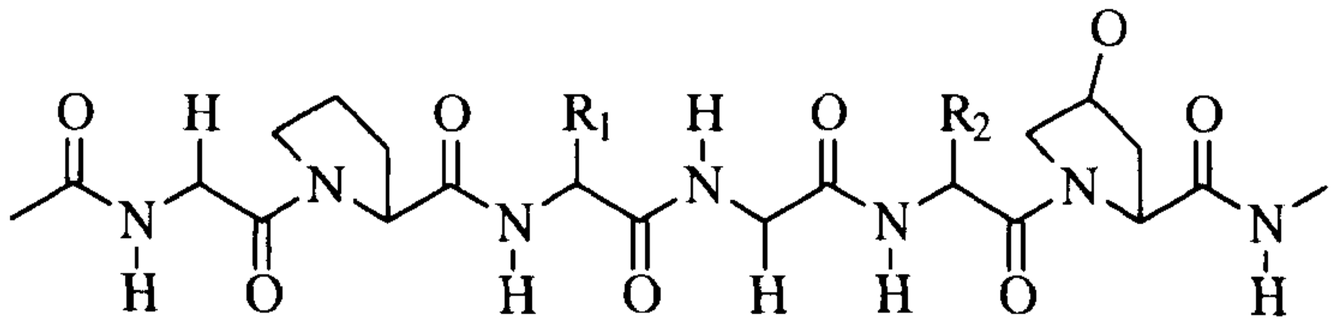
Alginate	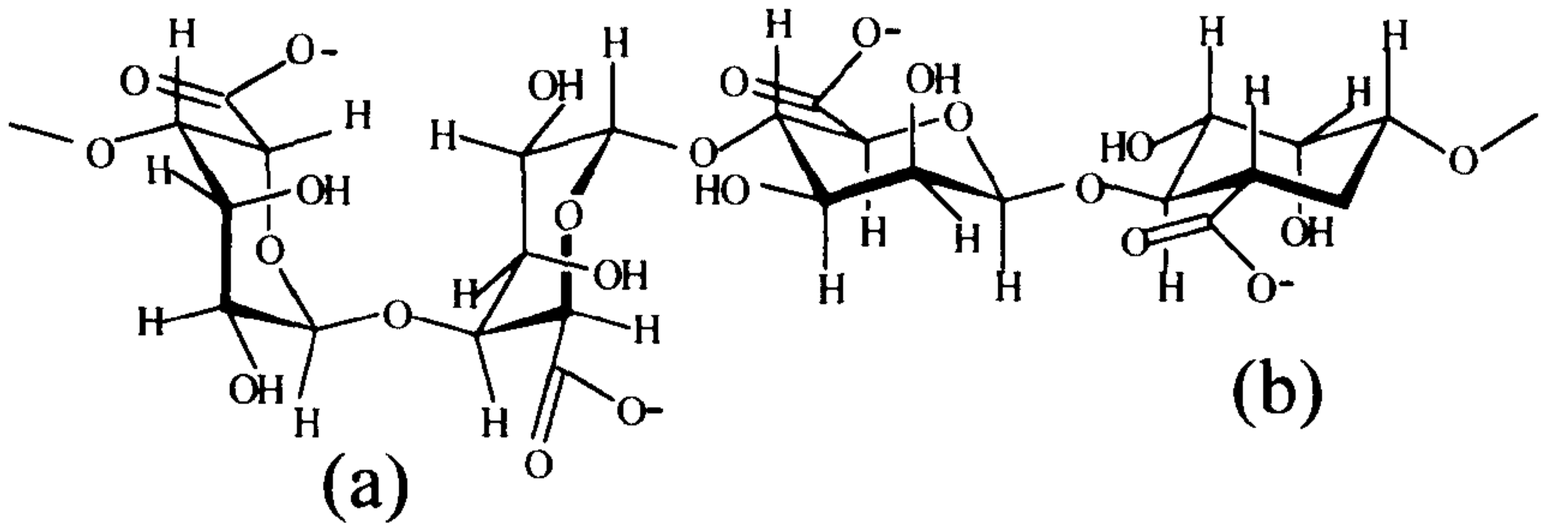 (a) (b)
Chitosan	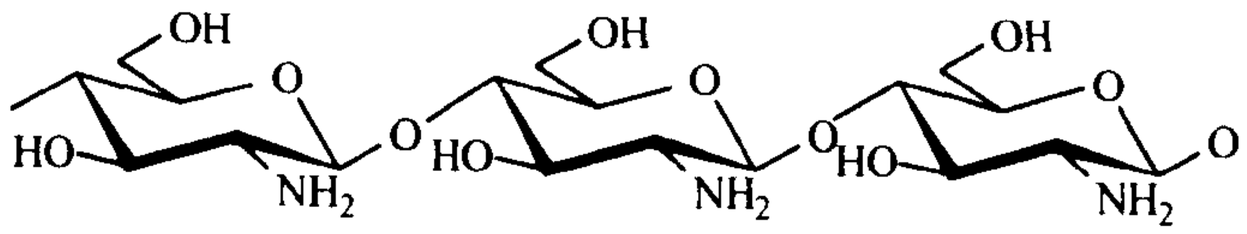

1.3.3 Non-Polymeric Materials in Tissue Engineering

In addition to natural and synthetic polymers, there are a number of other materials that have been utilised in tissue engineering strategies. After polymers, metallic prostheses and ceramics have been used most extensively in medical applications, although the latter are most associated with tissue engineering. Ceramics are known for their hard, but sometimes, brittle properties making them useful in medicine and dentistry (Denry, 1996). Calcium phosphate is a ceramic material that is particularly useful in bone tissue engineering applications as it is analogous to the inorganic phase of bone. For example, hydroxyapatite (HA) is a calcium phosphate that is frequently used in orthopaedic tissue engineering as it can interact with new bone and is therefore known as osteoconductive (Ducheyne & Qui, 1999). In addition, HA is approved for human clinical use by the FDA and has been used as a macroporous scaffold capable of supporting cell growth (Rose *et al*, 2004).

Another ceramic, Bioglass® was also developed as a replacement for osseous defects. Bioglass® is a product made from calcium salts, phosphorous, sodium salts and silicon, which bonds with living bone tissue, repairing and promoting bone regeneration. Bioglass® has been used as both a scaffold material for the culture of osteoblasts (Xynos *et al*, 2000) and as a coating to improve the osteoconductive properties of synthetic polymers (Roether *et al*, 2002).

1.4 A Summary of Scaffold Fabrication Techniques

The choice of scaffold fabrication technique depends largely on the material. Water soluble biopolymers such as alginate can form porous cross-linked hydrogels that can act as tissue engineering matrices, using simple ion-exchange techniques (Draget *et al*, 1997, Suh & Howard, 2000). Collagen can also form networked matrices but only when the polymer is induced by cross linking agents such as glutaraldehydes (Tabata *et al*, 2000). However, synthetic polymers frequently require the use of toxic organic solvents or high temperatures and/or pressures in order to produce tissue engineering scaffolds (table 1-5). Natural hydrogels do offer several advantages over synthetic systems as they often provide a more biomimetic and porous environment (Zisch *et al*, 2003). However, synthetic polymers are used more frequently in tissue engineering applications as they are non-immunogenic, versatile and more economical than natural polymers. The use of toxic organic solvents (solvent casting) and high temperatures (compression moulding) have frequently been used to fabricate tissue engineering scaffolds (Mooney *et al*, 1996a, Khang *et al*, 2002). However, high temperatures impose many processing restrictions such as the exclusion of thermally labile materials whilst many organic solvents are toxic and often leave residues in the resultant scaffolds that exceed the safe limits imposed by the authorities (Hile *et al*, 2000). As a result, new methods of processing synthetic polymers into porous tissue engineering scaffolds without the use of organic solvents or high temperatures are becoming more attractive. Techniques such as gas foaming (Harris *et al*, 1998) and supercritical fluid technology (Howdle *et al*, 2001) utilise high pressure carbon dioxide as a porogen and are known as a form of 'clean technology'. Particulate leaching is another commonly used method of producing tissue engineering scaffolds, although it can only be used as a method of altering or increasing porosity and so must combined with another technique such as solvent casting (Khang *et al*, 2002) or supercritical fluid technology (Jang & Shea, 2003). An addition, the use of toxic particulates, such as sodium chloride, can also result in high residual levels in the final scaffold (Harris *et al*, 1998).

Table 1-5 Techniques commonly used in the fabrication of tissue engineering scaffolds from synthetic polymers.

Fabrication Technology	**Pore size (μm)**	**% Porosity**	**Advantages**	**Disadvantages**	**Reference**
Solvent Casting/Salt Leaching	50-500	30-60	Pores were uniform, good inter-connectivity,	Uses toxic solvents, NaCl residues, time consuming	Khang *et al*, 2002
Gas Foaming/Salt Leaching	193-439	97%	No toxic solvents, High porosity, pore size is controllable,	NaCl residues in scaffolds	Harris *et al*, 1998
Supercritical Fluid Technology	20-30, & 300-600	70%	No toxic solvents or high temperatures, controllable pore size	Limited to polymers with amorphous regions	Watson *et al*, 2002
Supercritical Fluid Technology/ Particulate Leaching	Not given	94	Good interconnectivity, controllable pore size, controlled release of DNA	NaCl residues in scaffold	Jang and Shea, 2003
Compression Moulding/Salt Leaching	~500	77	Very large pores, good interconnectivity	Very high temperatures and pressures, NaCl residues in scaffold	Sohier *et al*, 2003
Polymer Extrusion	3-33	~90	Suitable for tissue requiring tubular scaffolds	Very high temperatures	Widmer *et al*, 1998
Electrospinning of Polymeric Fibres	25-100	97	High porosity, tensile strength	Requires toxic solvents	Li *et al*, 2002
Emulsion Templating	50-100	Not given	Good inter-connectivity	Requires toxic solvents	Hayman *et al*, 2005

1.5 The Introduction of Cells into Tissue Engineering Scaffolds

The introduction of cells into a supporting matrix is of critical importance in many tissue engineering strategies as the distribution of cells throughout the porous material is one critical component determining the success or failure of the device. This can influence both the successful integration of the device with the host tissue as well as the development of a vascularised network throughout the entire scaffold. Therefore, a variety of culture methods have been developed for the 'seeding' of cells into porous supporting scaffolds. These include: static, dynamic (e.g. stir flask, agitation) and perfusion bioreactor cultures (Burg *et al*, 2000). Scaffold seeding was originally performed by adding cells drop-wise (Langer & Vacanti, 1993), before other methods were developed, including: culturing in an incubator able to circulate cells for attachment (Freed *et al*, 1993a), incorporation into a material such as alginate encapsulation (Atala *et al*, 1993), self forming peptides (Zhang *et al*, 1995) or addition using a bubble jet type system (Mironov *et al*, 2003). The latter methods are of particular interest as the authors have been able to incorporate living cells into the fabrication process. Incorporation of living cells into a scaffold at production could allow the distribution of cells throughout the scaffold and negate the requirement for the time consuming and often, inefficient second seeding stage (Burg *et al*, 2000). The removal of the additional seeding step could also result in a lower risk of infection. However, these novel fabrication methods have been restricted to using biopolymers such as alginate that can form porous hydrogels without the need for harsh processing environments (Hou *et al*, 2004). This prevents damage to the sensitive cell component without compromising the structural properties of the scaffold. This is important, as when combining mammalian cells and polymer scaffolds it is important to minimise disruption to the cell component from fluctuations in solvent composition, temperature, pressure and shear forces (Atala *et al*, 1993, Anson *et al*, 1995). However, when fabricating porous scaffolds using synthetic polymers, organic solvents, elevated temperatures and/or pressures are frequently required to, produce the required three-dimensional form. This has thus, prevented the inclusion of cells within the scaffold fabrication process.

1.6 Supercritical Fluid Technology

The excitement about supercritical fluid (SCF) technology first materialised because of the apparent environmental benefits associated with their replacement of toxic organic solvents. Supercritical fluids have since been shown to have a number of interesting properties that enhance many types of chemical process operations and have consequently found numerous applications throughout industry and scientific research. By definition, supercritical fluids are substances that have been pressurised and heated to above their critical values and have a density close to or above their critical density (Darr & Poliakoff, 1999). Once above this critical point, a substance can exhibit unique properties that are exclusive to neither a gas or liquid. For example, when carbon dioxide is raised above its critical point of 73.8 bar and 31.1°C, it forms a single phase with liquid-like densities and hence, solvating characteristics that are similar to those of liquids, yet with mass transfer properties similar to gases (Cooper, 2000) (see figure 1-1). The solvating power of supercritical CO_2 ($scCO_2$) can be tuned very precisely by small alterations to the processing temperature and because CO_2 is relatively inert, there are few issues with toxicity. The use of CO_2 also has a number of other advantages such as its low cost, ready availability, stability and environmental acceptability over organic solvents. These factors, along with its relatively low critical point, make CO_2 the most widely used supercritical solvent.

1.6.1 Supercritical Fluid Extraction and Impregnation

The high level of diffusivity of CO_2 in a number of substances has made it a very useful tool for extractions (Maddocks & Gibson, 1977). Carbon dioxide can diffuse into a substance and then be used as a vehicle to remove unwanted material during decompression into a collection vessel or chromatographic instrument. The most common use of supercritical fluid extraction (SFE) is in the removal of caffeine from coffee (Peker *et al*, 1992). This is in preference to using chlorinated solvents which could impair the flavour of the coffee. The applications for SFE are now becoming numerous, with the extraction of wide variety of materials.

A number of anti-oxidants have been extracted from fruit and vegetables using $scCO_2$, such as lycopene and beta-carotene (Cadoni *et al*, 1999). Also, in forensic science, a number of extractions have been carried out using $scCO_2$ to remove drugs such as cocaine and morphine from hair (Brewer *et al*, 2001, Goodpaster *et al*, 2003).

Synthetic polymers have been the subject of both extractions and impregnations using $scCO_2$. For example, attempts have been made to remove impurities from polymers intended for medical applications in order to improve biocompatibility, although ultimately an improvement in biocompatibility was not achieved (Popov *et al*, 2004). Similarly, the reverse process of supercritical impregnation (SFI) is used to incorporate a number of substances into materials. This can be achieved by the dissolution of $scCO_2$ laden with a solute into a synthetic polymer. This is made possible by the plasticisation of the polymer by $scCO_2$ without the use of high temperatures (see section 1.6.2). Upon decompression, the gas escapes from the polymer whilst the solute remains trapped within the polymer. This technique has been used to successfully incorporate thermally labile proteins into polymers to produce films with bioactive surfaces (Sproule *et al*, 2004). Guney and Akgerman (2002) used a continuous flow method to impregnate PLGA with two drugs: 5-fluorouracil (for chemotherapy) and β-estradiol (for oestrogen hormone therapy). Both of these drugs were previously shown to be soluble in $scCO_2$ (Guney & Akgerman, 2000) and as a result were incorporated into PLGA matrices.

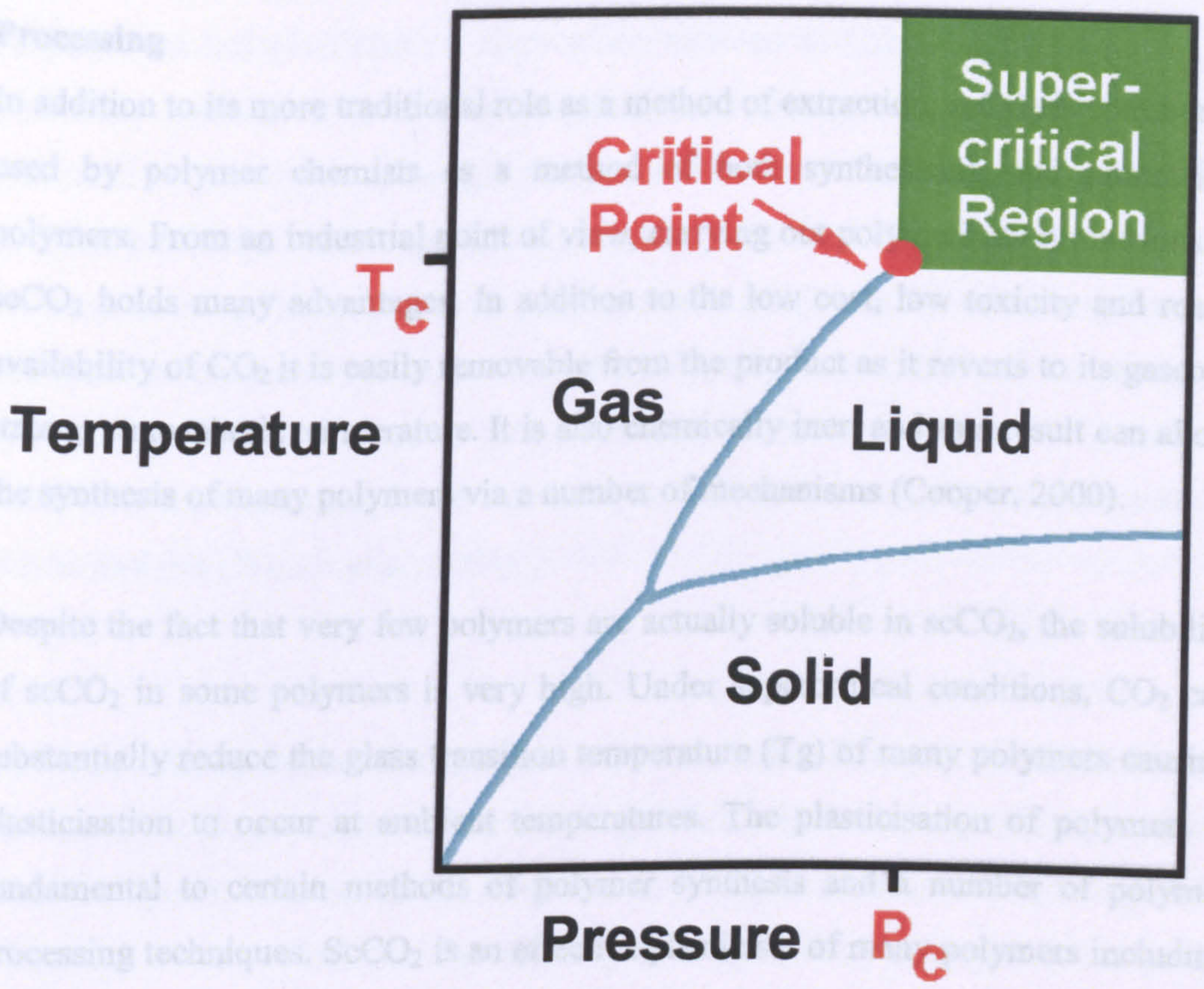

Figure 1-1 Phase diagram showing the point at which a substance ceases to be either a liquid or a gas and becomes a supercritical fluid. This occurs when a substance is raised above its critical temperature (T_c) and pressure (P_c).

1.6.2 The Role of Supercritical Carbon Dioxide in Polymer Synthesis and Processing

In addition to its more traditional role as a method of extraction, $scCO_2$ is commonly used by polymer chemists as a method of both synthesising and processing polymers. From an industrial point of view, carrying out polymerisation reactions in $scCO_2$ holds many advantages. In addition to the low cost, low toxicity and ready availability of CO_2 it is easily removable from the product as it reverts to its gaseous state at atmospheric temperature. It is also chemically inert and as a result can allow the synthesis of many polymers via a number of mechanisms (Cooper, 2000).

Despite the fact that very few polymers are actually soluble in $scCO_2$, the solubility of $scCO_2$ in some polymers is very high. Under supercritical conditions, CO_2 can substantially reduce the glass transition temperature (Tg) of many polymers causing plasticisation to occur at ambient temperatures. The plasticisation of polymers is fundamental to certain methods of polymer synthesis and a number of polymer processing techniques. $ScCO_2$ is an effective plasticiser of many polymers including polystyrenes (Arora *et al*, 1998), polyethylene (Busby *et al*, 2003), polymethacrylates (Goel & Beckman, 1993a) and polyurethanes (Briscoe & Kelly, 1995). As a result, $scCO_2$ has been used in the production of porous foams or matrices (Goel & Beckman, 1994a, Goel & Beckman, 1994b, Parks *et al*, 1996). It is this ability to produce porous materials that has made $scCO_2$ processing an attractive method of producing tissue engineering scaffolds and controlled release matrices. At high pressure CO_2 dissolves into the amorphous regions of polymers such as PMMA, PLGA and $P_{DL}LA$ causing a depression of the Tg and allowing them to be plasticised at ambient temperatures. A drop in pressure then leads to a thermodynamic instability causing the gas molecules to cluster or nucleate, in order to minimise the free energy (Goel and Beckman, 1994a). The nucleated gas bubbles form pores that become permanent as the Tg rises and the polymer vitrifies (Goel & Beckman, 1994b). The resultant three dimensional porous scaffold can then act as a support for cell attachment and proliferation or as a controlled release device for the delivery of growth factors (Howdle *et al*, 2001, Yang *et al*, 2004).

The weak solvating power of CO_2 is the only major limitation, as a number of polymers do not plasticise or foam when exposed to CO_2 at high pressure. As previously mentioned, it is only polymers with amorphous regions that can be processed in this way. It is thought that the electron donating carbonyl groups on the polymer backbone exhibit specific interactions with the CO_2 of a Lewis acid-base nature (Kazarian, 1996). Therefore polymers with a high number of carbonyl groups and some amorphous regions, such as the poly(α-hydroxy acids) can be processed into porous foams. For those polymers that cannot be processed by $scCO_2$, surfactants have been employed that have an affinity for both the polymer and the pressurised gas (Woods *et al*, 2004).

1.6.3 The Role of Supercritical Carbon Dioxide in the Pharmaceutical Industry

The use of $scCO_2$ processes to produce drug delivery devices has gathered pace over the last 10 years, with one of the most successful applications of $scCO_2$ being in the production of microparticles. The majority of drug delivery strategies focus on the production of drug particles, with approximately two thirds of the products used in the pharmaceutical industry coming in the form of particulate solids (Roberts & Debenedetti, 2002). Control over drug particle size is essential for good targeting and efficacy as a smaller particle size leads to higher rates of dissolution. This increases the bioavailability of the drug leading to smaller dosages and enhancing controlled release (Tom & Debenedetti, 1991). The use of $scCO_2$ has provided a more controlled route to producing a variety of drug delivery systems, whilst circumventing many of the problems associated with traditional techniques (Foster *et al*, 2003). Despite being successful, traditional drug micronisation techniques such as milling, grinding and spray-drying do not provide this level of control and often use toxic solvents, high temperatures or mechanical stresses that cause degradation of the drug. Furthermore, residual levels of toxic solvents can remain in the product after processing, making them unsuitable for pharmaceutical applications (Falk & Randolph, 1998).

Methods traditionally used for the encapsulation of drugs within polymer particles such as phase separation, spray drying and double emulsion techniques are beset with the same problems (Hile *et al*, 2000). Because the use of $scCO_2$ does not require high temperatures, toxic solvents or mechanical stresses, it has obvious advantages when processing sensitive pharmaceuticals.

A number of SCF techniques have been used for the micronisation of drug particles. Many pharmaceuticals can be dissolved or liquefied in $scCO_2$ before being sprayed through a nozzle upon decompression to produce fine drug particles. This can be achieved with non-solvent techniques such as the rapid expansion of supercritical solutions (RESS) and particles from gas saturated solutions (PGSS). The rapid expansion of supercritical solutions (RESS) is the most simplistic SCF technique used to produce fine drug particles. Here, the solute (the drug) is dissolved within the supercritical gas without the need for additional organic solvents (Debenedetti *et al*, 1993). The mixture is then depressurised through a nozzle resulting in the rapid precipitation of the drug particles into a collection chamber (Matson *et al*, 1986, Matson *et al*, 1987). This method has been used for the precipitation of drug particles such as ibuprofen, resulting in greater dissolution rates (Charoenchaitrakool *et al*, 2000, Kayrak *et al*, 2003). The PGSS process works on the basis that pressurised gas can diffuse into a solute, by means of lowering both its melting point and viscosity. By continuing to increase the pressure of the gas, the molten solute forms a highly saturated solution (Sencar-Bozic *et al*, 1997). Particles can then be formed by depressurising the solution through a nozzle, as the gas is released from the condensed phase. Particle size distribution can be controlled by changing the processing parameters such as temperature and pressure, although the nozzle diameter is the single most important factor. This technique used for the micronisation of pharmaceuticals such as nifedipine, an anti-hypertensive drug (Kerc *et al*, 1999).

It has been shown that the incorporation or encapsulation of a drug within a biodegradable polymer can greatly enhance the controlled release of the particles (Sencar-Bozic *et al*, 1997). The PGSS technique has been used to process nifedipine with PEG 4000. The levels of drug dissolution were greater than five times quicker than a non-treated mixture of the same material (Sencar-Bozic *et al*, 1997). An anti-angina drug, felodipine, has also been co-precipitated with PEG using $scCO_2$, with dissolution rates that better those of the Sencar-Bozic study (Kerc *et al*, 1999). In fact, PEG has been shown to compare favourably to $P_{DL}LA$ when micronised using the PGSS technique, in terms of the uniform spherical particle morphology and ease of processing (Hao *et al*, 2004, Hao *et al*, 2005). Despite this, a number of proteins have been incorporated into $P_{DL}LA$ particles using the PGSS process (Whitaker *et al*, 2005). The RESS technique has also been used for this application, the earliest example of which involved loading lovastatin, an anti-cholesterol drug, into the polymer (Tom *et al*, 1991). However, the PGSS technique has several benefits when compared with RESS including its versatility in terms of the polymers and drugs that can be processed in this way. Also, because the PGSS technique does not require the polymer/drug to be soluble in the $scCO_2$, it uses lower pressures than RESS resulting in lower gas consumption.

Alternatively, $scCO_2$ can be employed as an anti-solvent for the precipitation of drugs already dissolved in organic solvents (Foster *et al*, 2003). Gas anti-solvent techniques differ from either the RESS or the PGSS process, because the gas is used as an anti-solvent to reduce the solvating power of the organic solvent in which the solute is contained. Because of the ability of pressurised gases such as CO_2 to dissolve and expand organic solvents, they can be used for the precipitation of solids from organic solutions (Foster *et al*, 2003). The expanded solvent can then be purged from the system, with the particular solid washed by the anti-solvent (CO_2). The particles can then be removed from the collection chamber upon decompression (Yeo *et al*, 1993). A number of gas anti-solvent techniques exist, each with a small change required in the processing technique to suit a particular application.

Some of these techniques include the original gas anti-solvent (GAS) technique (Yeo *et al*, 1993), precipitation from a compressed anti-solvent (PCA) (Falk *et al*, 1997) and the aerosol solvent extraction system (ASES) (Bleich *et al*, 1993). Alternative anti-solvent techniques include such as supercritical assisted atomization (SAS) (Reverchon, 2002) and solution enhanced dispersion by supercritical fluids (SEDS) (Hannah & York, 1995).

1.6.4 Supercritical Carbon Dioxide and Tissue Engineering

Both supercritical and high pressure CO_2 processing techniques are commonly used to fabricate porous materials for tissue engineering applications (Mooney *et al*, 1996a, Howdle *et al*, 2001). Compared to other methods of scaffold fabrication, scCO_2 has a number of processing advantages. There is no requirement for toxic organic solvents or elevated temperatures in order to plasticise the polymer, so there are no toxic residues in the final product and less processing restrictions. In addition, CO_2 is also relatively inert, environmentally friendly and inexpensive. Supercritical CO_2 was first used to form micro-porous polymeric structures by Goel & Beckman (Goel & Beckman, 1993b). However, the first use of pressurised CO_2 to produce tissue engineering scaffolds was by Mooney *et al*, where sub-critical CO_2 was used to produce porous PLGA foams (Mooney *et al*, 1996a). Here, PLGA discs formed by compression moulding were exposed to sub critical CO_2 before rapid decompression resulted in the formation of a macroporous structure (100 μm pores, 93% porosity). In this technique, the CO_2 was used as a blowing agent to form pores in the already softened polymer. This technique has also been combined with other methods such as salt leaching, with the size of the leached particles governing the pore size (Harris *et al*, 1998). It has since been demonstrated that scCO_2 can be used as a single step process to produce porous scaffolds for tissue engineering applications with a variety of polymers such as poly(ethyl methacrylate) (PEMA) (Barry *et al*, 2004), $P_{DL}LA$ (Yang *et al*, 2001) and PLGA (Howdle *et al*, 2001, Singh *et al*, 2004). By changing the polymer processing conditions, including the operating temperature and/or pressure, CO_2 exposure time (soak time) and decompression speed, the final properties of the scaffold can be tuned to a specific purpose.

For example, the operating pressure and the polymer soak time are both directly linked to the level of porosity (Goel & Beckman, 1994a, Goel & Beckman, 1994b) and interconnectivity in the scaffold (Park *et al*, 1995, Baldwin *et al*, 1995). By increasing the pressure and/or processing time, the level of soluble gas molecules in the polymer can also be increased, preventing the depletion of dissolved gas in the regions around the nucleating pores and allowing the pores to become interconnected (Park *et al*, 1995, Baldwin *et al*, 1995). Pore interconnectivity is a desirable property in tissue engineering scaffolds as it allows cells to interact with one another, removing the barrier between host cells and tissues and transplanted cells and tissues (Langer and Vacanti, 1993). An open, interconnected structure also facilitates the free passage of nutrients to surrounding cells and tissues.

Pore sizes in scaffolds made by sub and supercritical processing methods in this way are largely controlled by both the level of CO_2 molecules dissolved in the polymer and the rate of the decompression (Parks *et al*, 1996, Goel & Beckman, 1994b). Howdle and co-workers demonstrated the effect of decompression rate on pore size and pore size distribution in $P_{DL}LA$ scaffolds, by comparing a slow (two hours) and a fast (two minutes) decompression rate. With an equal amount of CO_2 dissolved in the polymer, the 'slow' material possessed a small population of large pores (diameter 100–500 μm) whereas the 'fast' material had higher porosity and the pore size distribution was more heterogeneous. However, producing tissue engineering scaffolds with pre-determined pore structures is complicated by factors such as interfacial tension, viscosity, molecular weight and polymer stereochemistry (Baldwin *et al*, 1996a, Baldwin *et al*, 1996b). Despite this seemingly complex scaffold formation process, simple systematic changes in the processing conditions have provided the information for the successful production of scaffolds with pre-determined porosities. This ability to control porosity facilitates the use of different cell types, as the optimum pore size is dictated by the type and morphology of the cells. For example, hepatocytes, the main functional cellular constituent of the liver, require a smaller pore size (~100 μm) than osteoblasts, the main cellular constituent of bone (250-400 μm) (Klawitte & Hulbert, 1973, Klawitte *et al*, 1976).

In addition to providing a suitable environment for cell growth and the passage of nutrients, these porous scaffolds can also be used as way of controlling protein release from tissue engineering scaffolds. In an interesting development, thermally labile proteins and growth factors have been incorporated into the scaffold fabrication process. A one-step $scCO_2$ mixing technique developed at the University of Nottingham has been used to successfully incorporate several proteins into $P_{DL}LA$ scaffolds (Howdle *et al*, 2001, Watson *et al*, 2002). The protein becomes incorporated into the polymer during the plasticisation process and is permanently entrapped within the porous matrix as the polymer solidifies during the pressure quench (figure 1-2). Because this process does not use elevated temperatures or organic solvents, the activity of the protein is retained, despite the fact that pressures of 200 bar are used. This work was taken a step further by the incorporation of BMP-2 into the polymer matrix during processing, with subsequent controlled release of the molecule inducing the formation of new bone tissue *in-vivo* (Yang *et al*, 2003b, Yang *et al*, 2004).

The sub-critical CO_2 technique first used to produce tissue engineering scaffolds (Mooney *et al*, 1996) has also been used to form porous gene delivery matrices for tissue engineering applications, by fusing together microspheres containing plasmid DNA (Shea *et al*, 1999). Poor transfection data, likely to be due to the minimal exposure of the DNA plasmids to the cells in question, has cast doubt over the use of this method (Ledley, 1996, Jang & Shea, 2003). However, this gas foaming technique has been used to deliver plasmid DNA encoding for platelet-derived growth factor (PDGF) into PLGA matrices with controlled release achieved (Shea *et al*, 1999).

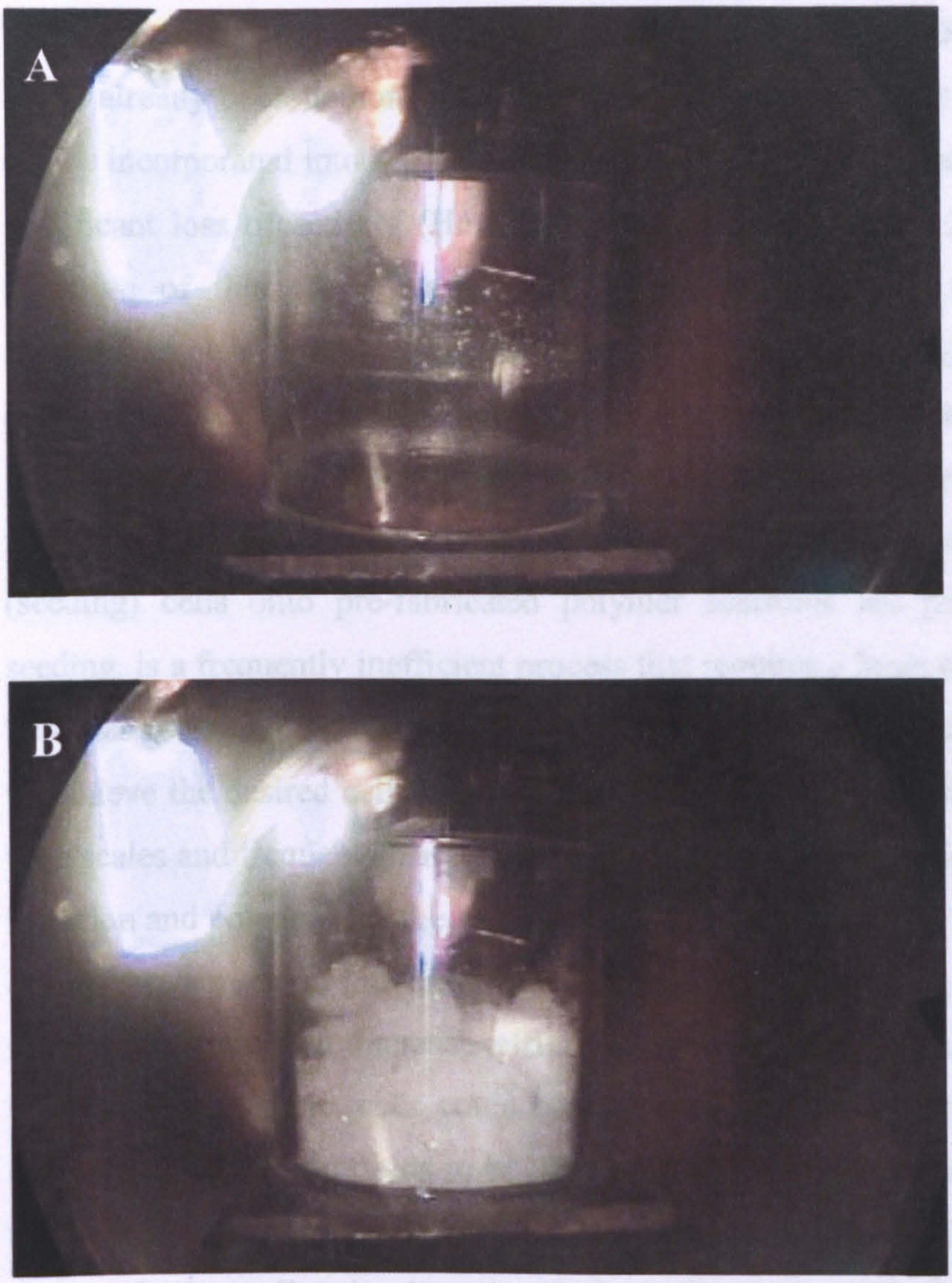

Figure 1-2 The plasticisation and foaming of $P_{DL}LA$ using $scCO_2$ processing as viewed through the sapphire window of a high pressure viewing vessel. Supercritical CO_2 (200 bar, 35°C) has been used to plasticise the $P_{DL}LA$ (A) before subsequent decompression causes nucleation of the CO_2 bubbles inside the polymer to produce a porous foam as the polymer solidifies (B).

1.6.5 Processing Mammalian Cells in Supercritical Carbon Dioxide

It has already been demonstrated that thermally labile proteins and growth factors can be incorporated into $P_{DL}LA$ scaffolds using a $scCO_2$ fabrication process without significant loss of activity (Howdle *et al*, 2001, Yang *et al*, 2004). The ultimate objective of this thesis was to use a similar processing technique to allow mammalian cells to be incorporated into $scCO_2$-plasticised $P_{DL}LA$ to produce cell-loaded scaffolds for tissue engineering. The incorporation of cells into the scaffold fabrication step, could potentially lead to a number of benefits over traditional method of incorporating cells into scaffolds. Conventional methods of loading (seeding) cells onto pre-fabricated polymer scaffolds are problematic. Scaffold seeding, is a frequently inefficient process that requires a large population of cells to be added to a solid, porous structure followed by weeks or months of careful culture to achieve the desired cell density (Freed *et al*, 1998, Burg *et al*, 2000). With these time scales and frequent changes in the cellular environment comes increased risk of infection and potential for the patient's condition to worsen. If cells were introduced during the fabrication process in sufficient densities, it could not only significantly reduce this time and increase efficiency, but also have several other potential benefits. For example, cells could be suspended in a cryo-preserving medium that enables cell-loaded scaffolds to be frozen after processing and remain 'on the shelf' until required. Alternatively, cell loaded scaffolds could be fabricated in surgical theatres for immediate implantation back into the patient. This would not only make the process more rapid, but it would also be less stressful for the patient as there would be only one surgical procedure necessary with a potentially reduced risk of infection.

However, processing mammalian cells in $scCO_2$ has previously never been reported with logic suggesting that the combination of high pressure and high concentrations of CO_2 would result in rapid cell death. In fact, $scCO_2$ has been used as a technique for the inactivation of bacterial cells for sterilisation purposes (Fraser, 1951, Dillow *et al*, 1999).

1.7 Aims

We hypothesised that the high solubility of CO_2 in amorphous polymers such as $P_{DL}LA$ would facilitate the incorporation of mammalian cells into the scaffold fabrication process, provided that they could survive for sufficient time to allow the CO_2 to plasticise and foam the polymer. Therefore there were five main aims to this project:

1. To investigate the effect of $scCO_2$ and associated processing conditions on mammalian cell survival
2. To investigate the possible causes of cell death and effects of $scCO_2$ upon gene and cell function.
3. To investigate the possibility that mammalian cells can be co-processed with $P_{DL}LA$ under supercritical CO_2 conditions and remain both metabolically active and functional.
4. To design and build a second generation injection system capable of introducing liquid suspensions into plasticised $P_{DL}LA$ at high pressure.
5. To investigate the possibility that mammalian cells can be injected into $P_{DL}LA$ at high pressure with cell survival and function retained.

Chapter 2

ASSESSMENT OF MAMMALIAN CELL SURVIVAL AFTER PROCESSING IN SUPERCRITICAL CARBON DIOXIDE

2.1 Introduction – High Pressure CO_2 and Cell Survival

The survival of mammalian cells after exposure to high pressure CO_2 is fundamental to the success of fabricating cell loaded tissue engineering scaffolds using a one-step process. However, there is no literature describing the effects of high-pressure CO_2 upon mammalian cell survival. In fact, the closest comparison that can be made is with that of bacterial systems. There have been a number of studies into the effects of high-pressure CO_2 on micro-organisms, as this technique has been employed to induce bacterial cell death (Fraser, 1951, Foster *et al*, 1962). Both sub-critical and supercritical CO_2 have been used to kill bacterial cells when injected into poly(lactic acid) for medical sterilisation (Dillow *et al*, 1999) and for the sterilisation of food stuffs (Haas *et al*, 1989). Even over short exposure times (less than three minutes) it has been demonstrated that CO_2 at just above its critical point (74 bar, 38°C) is sufficient to inactivate both gram-negative and gram-positive bacteria (Spilimbergo *et al*, 2002). A number of conflicting mechanisms have been produced to explain this method of inactivation. Cell wall rupture caused by the increase in internal pressure (Nakamura *et al*, 1994) or the extraction of lipids from the cell membrane (Enomoto *et al*, 1997) have been proposed as potential causes of cell death. However, changes in the cellular environment that are indirectly linked to the use of high pressure such as an increase in acidity or physical trauma are also likely to affect cell survival. Increased acidity is caused by the reaction between CO_2 and water to form carbonic acid (H_2CO_3). This increase in acidity has been suggested as a mechanism for cell death in sterilisation techniques, with $scCO_2$ thought to diffuse through the bacterial cell wall and reduce the intracellular pH (Dillow *et al*, 1999). The pH of water/CO_2 mixtures under supercritical conditions has been measured at 3.0 (Holmes *et al*, 1999) and calculated as 3.12 (Spilimbergo *et al*, 2002). These values are well below the neutral conditions required for normal cellular metabolism, although the intracellular pH under $scCO_2$ conditions is not known.

Along with the changes in the chemical environment inside the vessel during supercritical processing, there are physical forces that need to be considered.

A temperature range of 30-37°C is often found to be optimal for the culture of mammalian cells and therefore, the effect of temperature increases and decreases on cell survival during supercritical processing provide an area for investigation. Heat treatment is known to be very effective at killing both mammalian (Gregoriades *et al*, 2003) and bacterial cells (Keswani & Frank, 1998). However, low temperatures such as between 0°C and 10°C have been known to reduce the numbers of mammalian cells such as hepatocytes, although this has only been seen over the course of hours or days, not seconds or minutes (Rauen & de Groot, 1998). Combinations of high/low temperatures with high pressures have also been used to successfully inactivate bacteria (Spilimbergo *et al*, 2002). However, the effects of rapid changes in temperature on mammalian cells (induced by the rapid increase and decrease of pressure) are not known. The act of increasing or decreasing the pressure of the gas inside the vessel can cause the temperature to rise or fall very quickly. This temperature change is the result of the rapid expansion of a gas through a small orifice, a phenomenon known as Joule-Thompson cooling/heating.

In addition to the changes in temperature, rapid compression and decompression can cause the formation of gas bubbles not only in plasticised polymers, but also in water-based solutions or suspensions. Bubbles can be problematic in the culture of cells for biotechnological applications, such as recombinant protein production and can result in reduced cell survival (Kunas & Papoutsakis, 1990, Wu, 1995). However, bubble formation in a cell suspension cannot be investigated as easily as the chemical changes previously mentioned as it needs to be assessed during and not after supercritical processing. The effects of decompression rate have been thoroughly investigated in bacterial systems, demonstrating that a more rapid or 'explosive' pressure drop can have a more lethal effect (Fraser, 1951, Foster *et al*, 1962 & Nakamura *et al*, 1994). Furthermore, the rate of decompression has been shown to be crucial in determining the pore structure of tissue engineering scaffolds (Howdle *et al*, 2001). Therefore, the effect of decompression rate on bubble formation and cell survival could have implications when determining conditions and processing times for scaffold fabrication.

2.1.1 Aims

The main aim of this first chapter was to investigate the effects of high pressure and supercritical CO_2 on mammalian cell survival. In addition to the effects of processing time and pressure, a number of other conditions that are intrinsically linked to the use of high pressure and supercritical CO_2 were investigated. Ultimately, this provides a set of optimum processing conditions to be taken into the rest of the study, ensuring maximum cell survival before the introduction of the polymer component.

2.2 Methods

2.2.1 Culture of Secondary Cell Lines

Both murine 3T3 fibroblasts and C2C12 cells were cultured in complete Dulbecco's Modified Eagle's Medium (DMEM) for all cell survival and functionality studies. Details of cell culture for 3T3s and C2C12s are given in the materials and methods chapter (section 7.1.1). A viable cell count was carried out for both cell lines using trypan blue exclusion, full details of which can be seen in the materials and methods chapter (section 7.1.3).

2.2.2 Isolation and Culture of Primary Cells

Primary rat hepatocytes and ovine fibrochondrocytes were first isolated and then cultured in Williams Medium E and complete DMEM respectively. Details of both cell isolation and culture techniques can be found in the materials and methods chapter (section 7.1.1 and 7.1.2). A viable cell count was carried out for both cell types using trypan blue exclusion as described in materials and methods chapter (section 7.1.3).

2.2.3 Exposure of Mammalian Cells to High Pressure CO_2 and Associated Conditions

In order to process mammalian cells in supercritical CO_2 ($scCO_2$) a generic method was used prior to the method optimisation carried out during the course of the study. Full details of this can be found in the materials and methods chapter (section 7.2.1). Briefly, 3T3 fibroblasts (250,000) were suspended in 200 µl of complete DMEM and then placed into custom-made 8-well poly(tetrafluorethylene) (PTFE) moulds. Eight samples were processed in triplicate using in CO_2 (food grade, Cryoservice) at 37 or 74 bar (supercritical) with a starting temperature of 35°C. Cells were processed at maximum pressure for between 10 seconds and three minutes with an additional 40 seconds required to depressurise the vessel. After processing, the cells in each well were re-suspended in 1 ml of complete DMEM and incubated for 24 hours in 48-well tissue culture plates (Falcon) before assay.

2.2.3.1 The Effect of Gas Bubble Formation on Cell Survival

Gas bubble formation was determined in 200 µl of complete DMEM during the decompression stage using a 60 ml clamp sealed autoclave complete with a sapphire window for observation. In addition to a standard 40 second pressure drop, a second experiment was carried out used whereby a second stage was introduced in order to slow the release of the last 25% of the pressure. Therefore, the first 56 bar (~75%) of pressure was released within the first twenty seconds and the last 18 bar (~25%) was released during the second stage, making it a two-step decompression. Live images of this decompression were captured using a video camera (JVC) and edited using the Windows movie maker software to form a series of images that show the formation of bubbles and foaming during the entire process. The experiment was then repeated with a 200 µl cell suspension containing 3T3 fibroblasts, in a standard 60 ml pressure vessel. All of the other conditions were kept the same as in 2.2.3. After processing, the cells in each well were re-suspended in 1 ml of complete DMEM and incubated for 24 hours in 48-well tissue culture plates (Falcon) before assay.

2.2.3.2 The Effect of Decompression Rate on Cell Survival

To test resilience to prolonged decompression, 3T3 fibroblasts were also subject to increasing decompression times (one to seven minutes) after being held at maximum pressure for one minute (74 bar & 35°C). After processing, the cells in each well were re-suspended in 1 ml of complete DMEM and incubated for 24 hours in 48-well tissue culture plates (Falcon) before assay.

2.2.3.3 The Effect of Processing Temperature on Cell Survival

To test the effects of the processing temperature on the survival of 3T3 fibroblasts, the starting temperatures of each experiment were varied between 4, 22, 35, 50 and 65°C. Otherwise the method is identical to that used in section 2.2.3 (74 bar, 35°C). After processing, the cells in each well were re-suspended in 1 ml of complete DMEM and incubated for 24 hours in 48-well tissue culture plates (Falcon) before assay.

2.2.3.4 The Effect of Cell Suspension Volume on Cell Survival

To show the effect of the suspension volume on 3T3 fibroblast survival, the volume of DMEM making up the cell suspension was varied between 25 and 400 µl with all of the other conditions kept the same as in section 2.2.3 (74 bar, 35°C). After processing, the cells in each well were re-suspended in 1 ml of complete DMEM and incubated for 24 hours in 48-well tissue culture plates (Falcon) before assay.

2.2.3.5 The Effect of an Acidic Environment on Cell Survival

In this study, the cells were not exposed to high pressure, but rather the DMEM was adjusted to pH3.0 using 1M HCL in order to mimic the acidic conditions inside the pressure vessel under supercritical conditions. The exposure times used mirror those used in previous experiments (10 seconds to three minutes) and the cells were kept in ambient conditions throughout (25-37°C). In order to show the effects of such an acidic pH on cell viability, subsequent experiments were carried out with Hepes buffer (pH of 7.0) added to the DMEM at two different concentrations (0.25M and 0.5M) in order to neutralise the effects of the acid conditions. After exposure to the acidic conditions, the cells were re-suspended in 1 ml of complete DMEM and incubated for 24 hours in 48-well tissue culture plates (Falcon) before assay.

2.2.3.6 The Effects of Supercritical CO_2 on Different Cell Types

A number of cell types were subjected to supercritical conditions to show if the effect of the high pressure CO_2 is cell type dependent. Rat hepatocytes, ovine chondrocytes 3T3 fibroblasts and C2C12's were processed in scCO_2 (74 bar, 35°C) to show any differences in survival between primary cells and secondary cell lines. Hepatocytes and C2C12 cells were of particular interest as they were to be used for subsequent functionality assays. The conditions used were identical to those used in 2.2.3 with the cells suspended in appropriate culture media. After exposure to the supercritical conditions, the cells were re-suspended in 1 ml of complete DMEM and incubated for 24 hours in 48-well tissue culture plates (Falcon) before assay.

2.2.4 Cell Survival Assessment

Cells were assayed for metabolic activity by the Alamar Blue™ (Serotech) cell metabolic activity assay as described in the materials and methods chapter (section 7.3.1). Briefly, cells were removed from culture and the complete media covering the cells replaced with an Alamar Blue™ solution (10% in Hank's Balanced Salt Solution (HBSS), Sigma UK). After a 90 minute incubation at 37°C (5% CO_2) 200 µl of solution from each well was transferred to a 96-well plate (Falcon). Fluorescence readings were then obtained at an emission wavelength of λ590 nm using λ560 nm excitation.

2.3 Results and Discussion

2.3.1 The Effects of Processing Time and Pressure on Mammalian Cell Survival

Alamar Blue™ data for 3T3 fibroblast survival can be seen in figure 2-1. The optimum exposure time for cell survival is between 10 seconds and 30 seconds (~82% for both times). After 30 seconds exposure, there is a steep drop in cell survival from 70±5% to 32±7% between one minute and one minute 30 seconds. This indicates that there is an exposure time dependent relationship, with little or no cell survival after two minutes and 30 seconds. There is also a possible link between survival and temperature, as at shorter times there less of a net temperature drop resulting in a more stable temperature for the cells (table 2-1). This is caused by a combination of the increase in temperature during compression and the short time for temperature equilibration before decompression (as previously discussed). These data show that there is a very finite time for which cells can be exposed to this pressure, although there is no indication that the supercritical pressure is significant. Therefore, cells were exposed to a sub-critical pressure of 37 bar to show the effects of a reduced pressure on cell survival. The comparison between cells exposed to 37 and 74 bar can be seen in figure 2-2. These data indicate that the effect of dropping the pressure by half is only statistically significant at 10 seconds, with a survival rate of 98±4% at 37 bar compared to 82±6% at 74 bar. Any subsequent increase in cell survival does not appear to be significant although there is a general increase at all of the time points. This would indicate that it is largely the exposure time at maximum pressure that is causing this reduction in cell survival and not the pressure.

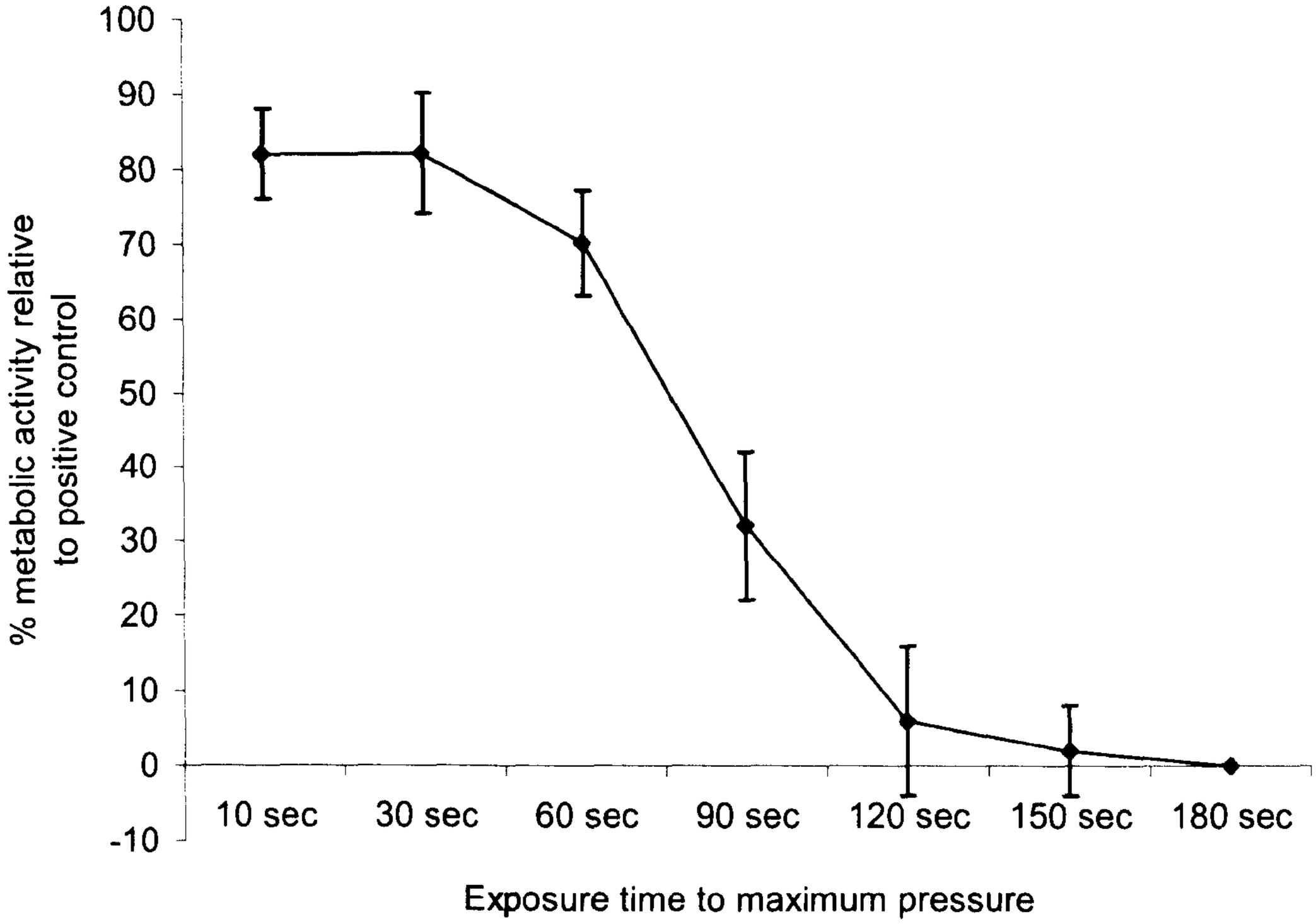

Figure 2-1 Survival of the murine 3T3 fibroblast cell line after exposure to $scCO_2$ for increasing time periods as measured by the Alamar Blue assay. Mean (n=3) ± SD.

Table 2-1 Temperature changes inside the pressure vessel during the supercritical processing of mammalian cells.

Exposure time to maximum pressure at 35°C	Temperature at 74 bar (°C)	Temperature at start of decompression (°C)	Temperature at end of decompression (°C)	**Net temperature drop from 74 to 0 bar (°C)**
10 sec	46	46	21	**25**
30 sec	46	42	18	**28**
60 min	46	39	17	**29**
90 sec	46	38	15	**31**
120 min	46	36	12	**34**
150 sec	46	35	11	**35**
180 sec	46	35	11	**35**

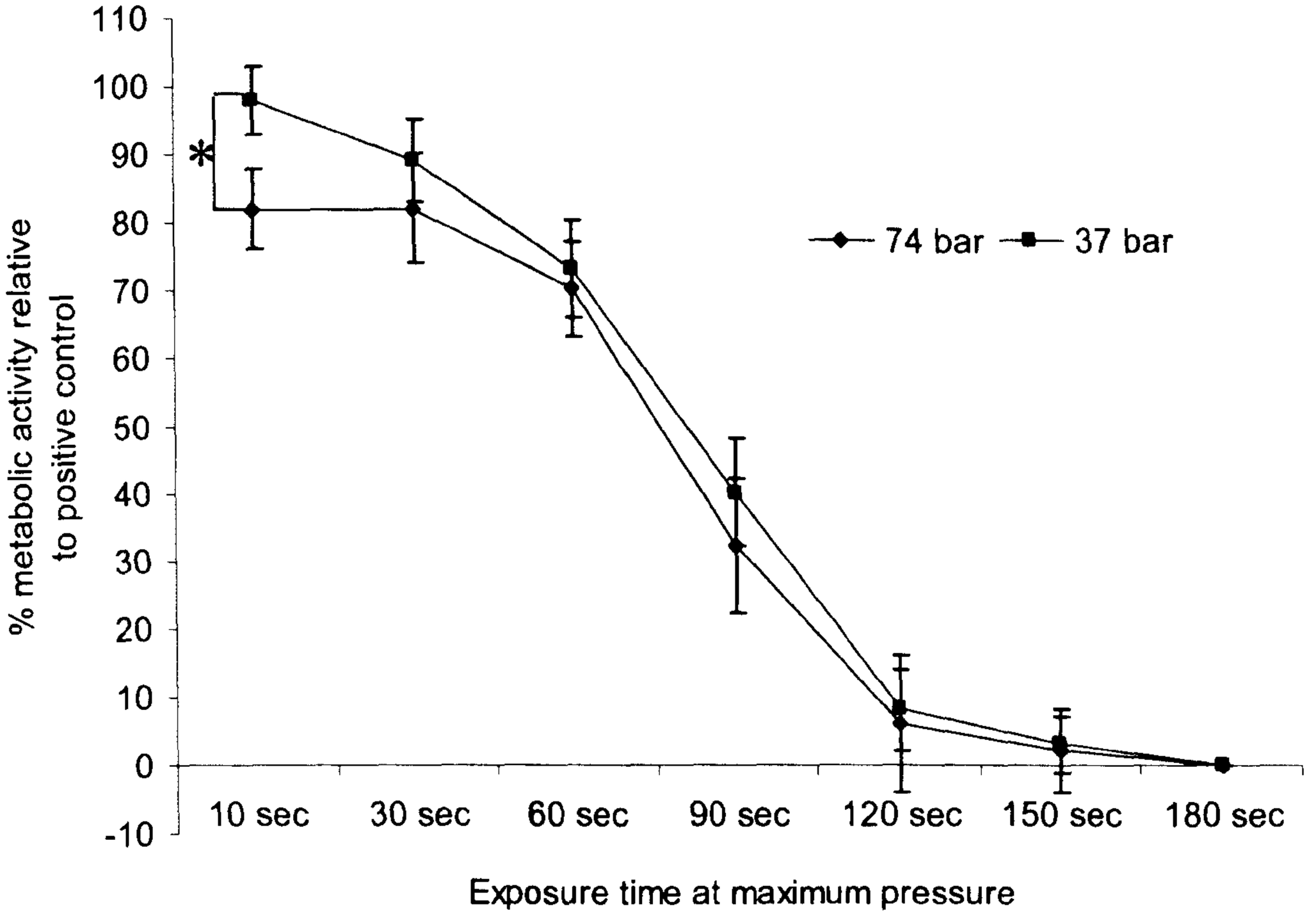

Figure 2-2 Survival of mammalian cells exposed to high pressure and supercritical CO_2 for increasing exposure times as measured by the Alamar Blue assay. Mean (n=3) ± SD. * indicates $p<0.05$ using T-test.

2.3.2 The Effects of Gas Bubble Formation and Decompression Rate on Mammalian Cell Survival

Gas bubble formation during the compression and subsequent decompression of 200 µl DMEM can be observed in figure 2-3A-H. Figures 2-3E and 2-3F show the foaming effect induced by the formation of gas bubbles during the rapid one-step decompression from 74 to 0 bar. However, in the case of the two-step decompression, there is clearly less foaming visible to the naked eye after the decompression (see figures 2-3G and 2-3H). This indicates that a slower release of the gas during the second part of the decompression, reduces the number of gas bubbles and hence the formation of foam is minimised. Despite this, the cell survival data presented in figure 2-4 indicates that the bubble formation and foaming of the DMEM does not have an obvious effect on the survival of the cells.

The effects of the decompression speed from 74 bar to atmospheric pressure can be seen in figure 2.5. These data show that there is still 71±7% cell survival after four minutes and 47±8% after six minutes of decompression, added to the one minute of initial exposure at 74 bar. This suggests that the gradual decrease in pressure results in a less physically stressful environment for the cells, such as a reduced net temperature change (see table 2-2). This evidence would certainly concur with the literature on bacterial systems where a more rapid decompression time was found to increase cell inactivation (Nakamura *et al*, 1994, Enomoto *et al*, 1997). However, there was also some 'pressure dumping' during the initial stages of this investigation, resulting in a decompression speed that was not constant. Therefore, during the latter stages of decompression the pressure would not be as high as would be expected with a constant decompression rate.

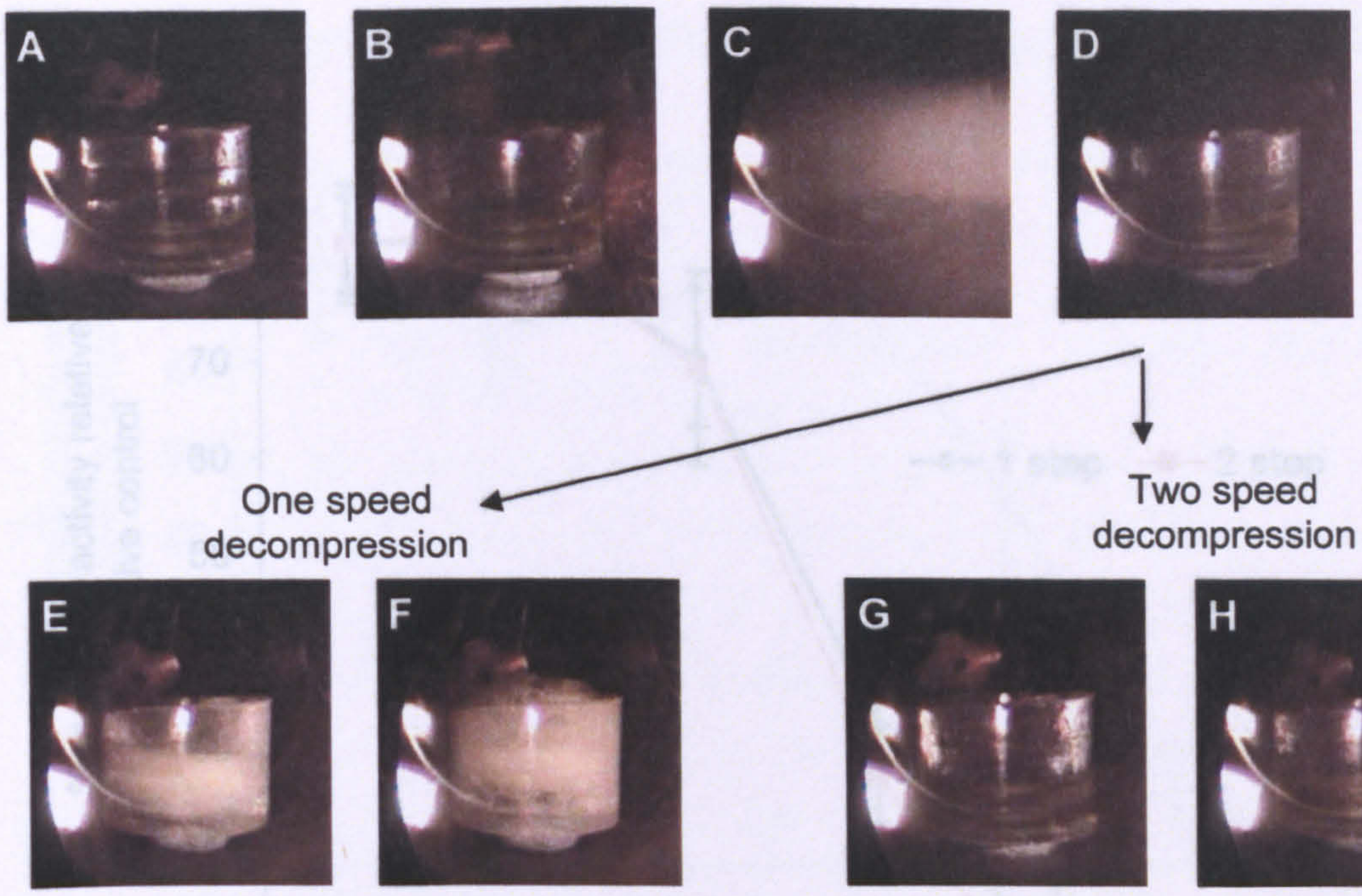

Figure 2-3 Effects of a one-step and a two-step decompression on gas bubble formation in cell culture medium (200 µl) as seen through the sapphire window of a high pressure viewing vessel. Compression from 0-74 bar in 40 seconds (A-B) is followed by decompression from 74-37 bar in 20 seconds (C-D) and then from 37-0 bar in 20 seconds (E-F) (one step decompression). In the two-step decompression, only 18 bar of pressure is released during the last 20 seconds (G-H).

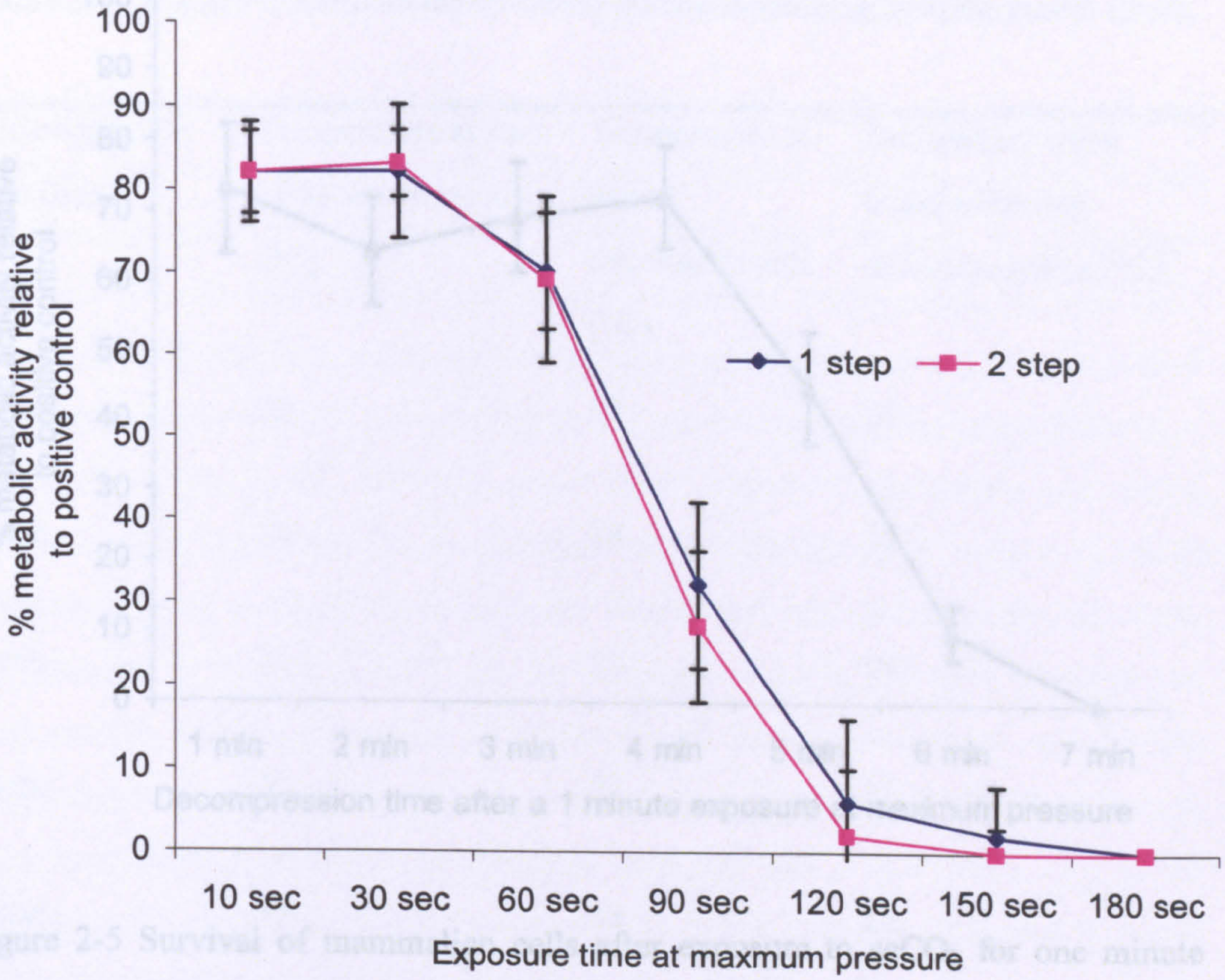

Figure 2-4 Survival of mammalian cells after exposure to $scCO_2$ using a one step or two step pressure quench as illustrated in figure 2-3. Compression from 0-74 bar in 40 seconds (A-B) is followed by decompression from 74-37 bar in 20 seconds (C-D) and then from 37-0 bar in 20 seconds (E-F) (one step decompression). In the two-step decompression, only 18 bar of pressure is released during the last 20 seconds (G-H). Mean (n=3) ± SD.

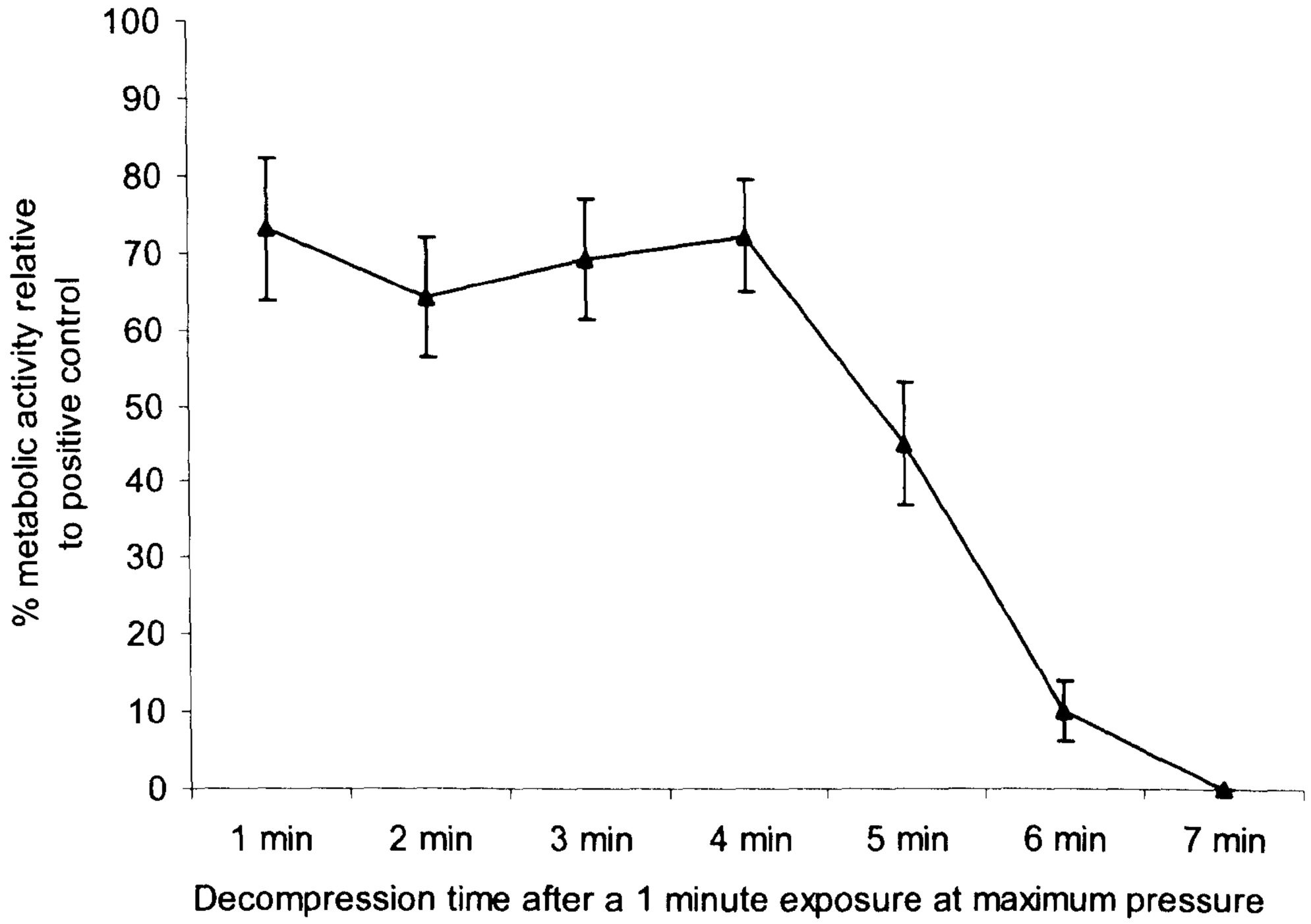

Figure 2-5 Survival of mammalian cells after exposure to $scCO_2$ for one minute followed by increasing decompression times as measured by an Alamar Blue assay. Mean (n=3) ± SD.

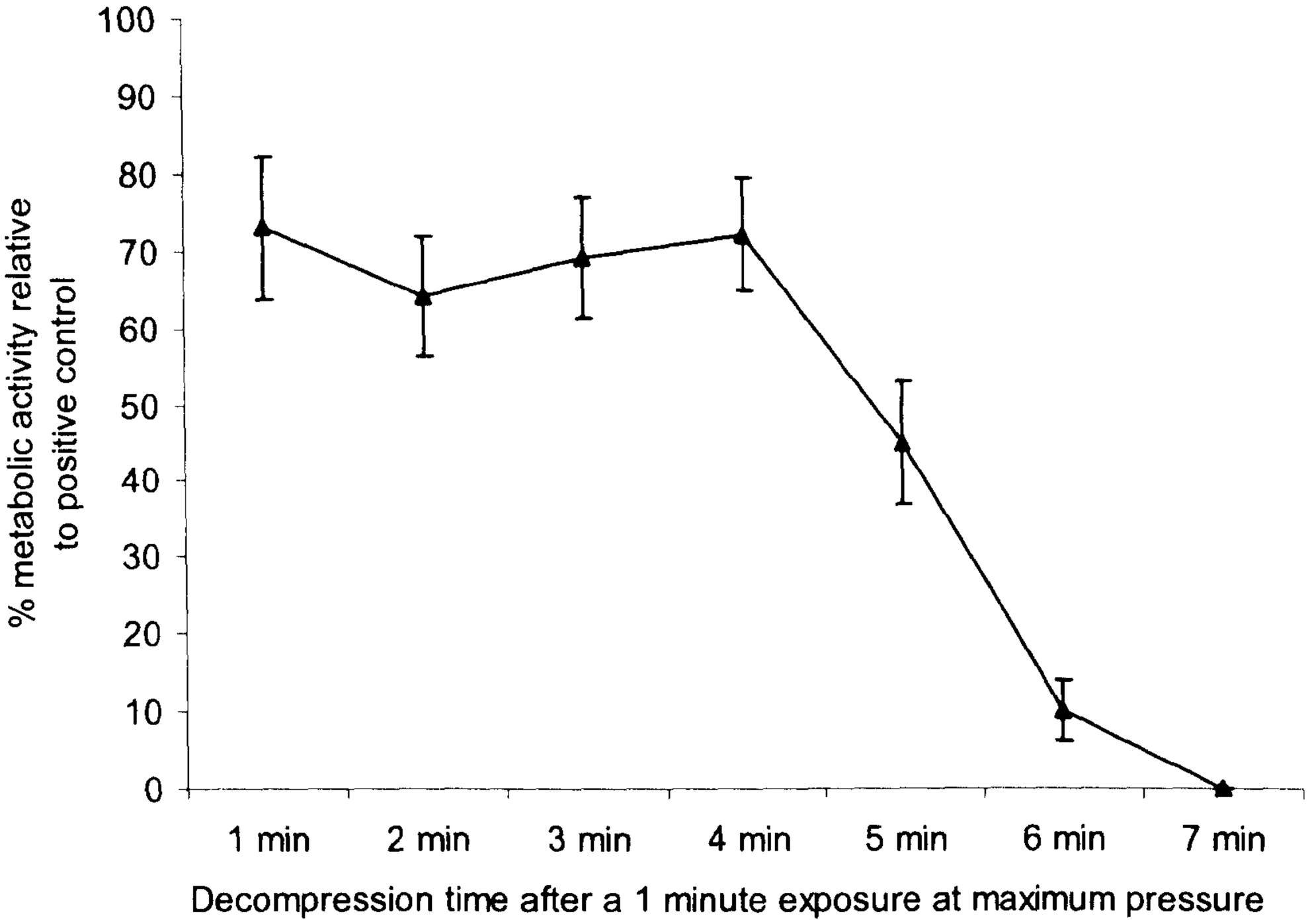

Figure 2-5 Survival of mammalian cells after exposure to $scCO_2$ for one minute followed by increasing decompression times as measured by an Alamar Blue assay. Mean (n=3) ± SD.

Table 2-2 Changes in temperature recorded during increasing decompression times.

Decompression time (min)	Temperature at start of decompression (°C)	Temperature at end of decompression (°C)	**Net temperature change during decompression (°C)**
40 sec	39	17	**22**
1 min	39	18	**21**
2 min	39	20	**19**
3 min	39	23	**16**
4 min	39	28	**11**
5 min	39	34	**5**
6 min	39	35	**4**
7 min	39	35	**4**

2.3.3 The Effects of Temperature and pH on Mammalian Cell Survival

The effects of the processing temperature followed by $scCO_2$ processing on cell survival are shown in figure 2-6. These data indicate that cell survival is only significantly reduced at temperatures below 22°C when exposed to supercritical pressures (23±8% at 4°C). The cells appear to tolerate temperatures of up to 60°C, concurring with previous evidence where only very high temperatures such as 80°C have significantly reduced cell survival in such short time periods (Gregoriades *et al*, 2003). However, at 4°C the cells never reach optimal temperatures and during decompression, are exposed to a rapid temperature drop from 24°C, to just above the freezing point of water (2°C). It has been shown that with some mammalian cells, temperatures of between 0-10°C can be sufficient to cause a drop in survival over long periods of time (Rauen & de Groot, 1998) but the effects of such a rapid temperature drop under these conditions is unknown. However, the fact that the cells were suspended in water-based substance suggests that temperatures near to the freezing point of water would have a detrimental effect. One possible solution to this maybe to suspend the cells in a cryo-preserving reagent such as dimethylsulfoxide (DMSO) to prevent cold damage.

Despite not being able to recreate the supercritical pH by using high pressure CO_2, the pH value of 3.0 has been used to examine the effects of increased acidity on mammalian cell survival, as shown figure 2-7. These data indicate that even without the addition of buffer, exposure times of 10 and 30 seconds do not have any significant effect on cell survival. However, at a one minute exposure there is a noticeable drop in survival for those cells processed in standard DMEM to 90±5% and those buffered with Hepes. This also coincides with the point at which there is a large drop in cell survival in figure 2.1 indicating that the drop in pH could exacerbate the effects of high pressure CO_2. However, this drop in cell survival is only of 7% and was easily corrected by the addition of 0.25M Hepes. In addition, because the optimum processing time to be taken forward to the latter stages of the thesis from figure 2.1 was 10-30 seconds, the effects of the low pH on cell survival are not likely to be of concern.

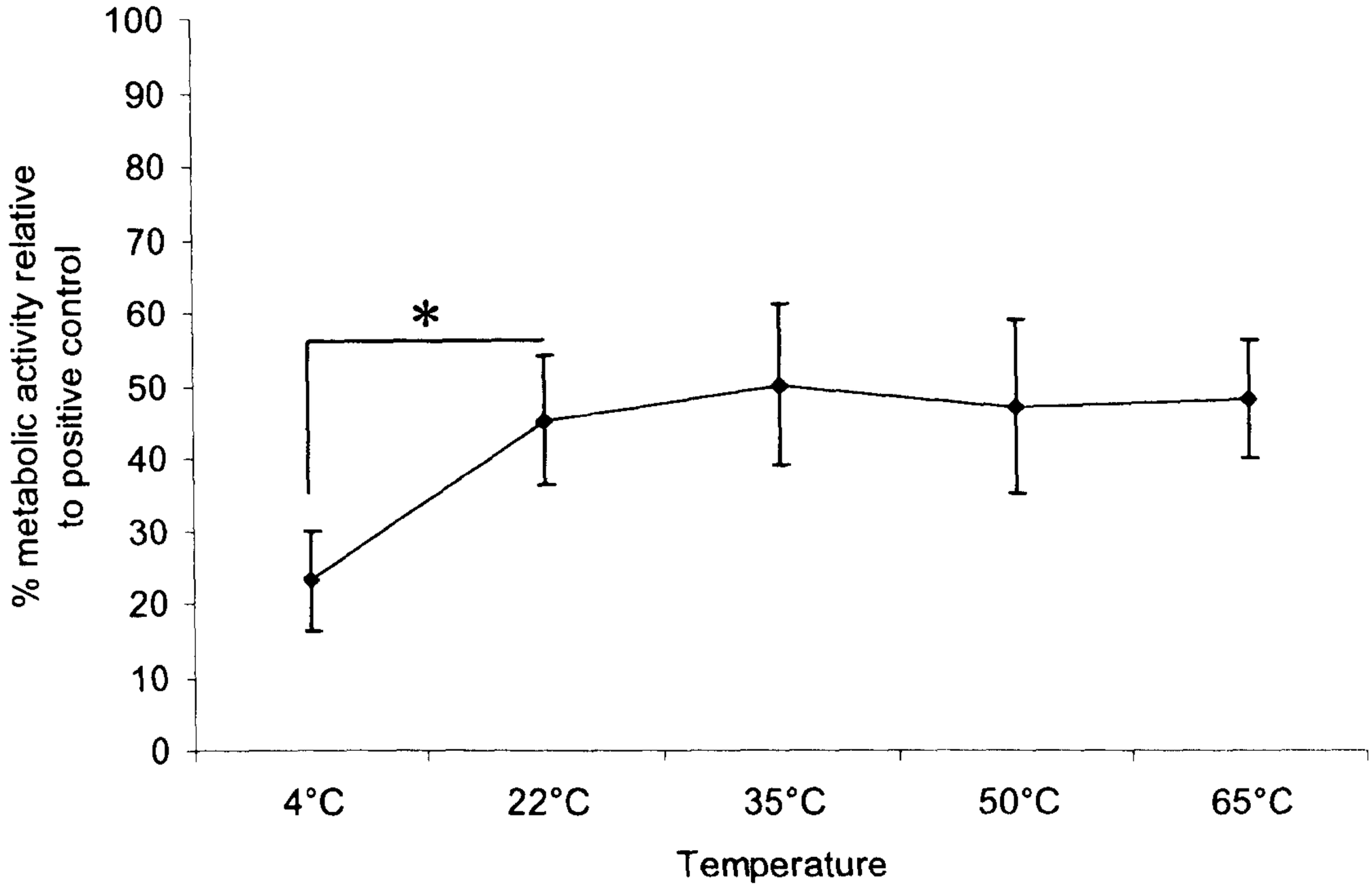

Figure 2-6 Survival of mammalian cells exposed to $scCO_2$ for one minute at different processing temperatures as measured by an Alamar Blue assay. Mean (n=3) ± SD. * indicates $p<0.05$ using T-test.

Table 2-3 Changes in temperature recorded when mammalian cells are processed at 74 bar for one minute at different starting temperatures.

Starting temperature (°C)	Temperature at 74 bar (°C)	Temperature at start of decompression (°C)	Temperature at end of decompression (°C)	**Net temperature change: 74 to 0 bar (°C)**
4	18	24	2	**16**
22	36	35	12	**24**
35	46	39	17	**29**
50	60	58	32	**28**
60	66	67	40	**26**

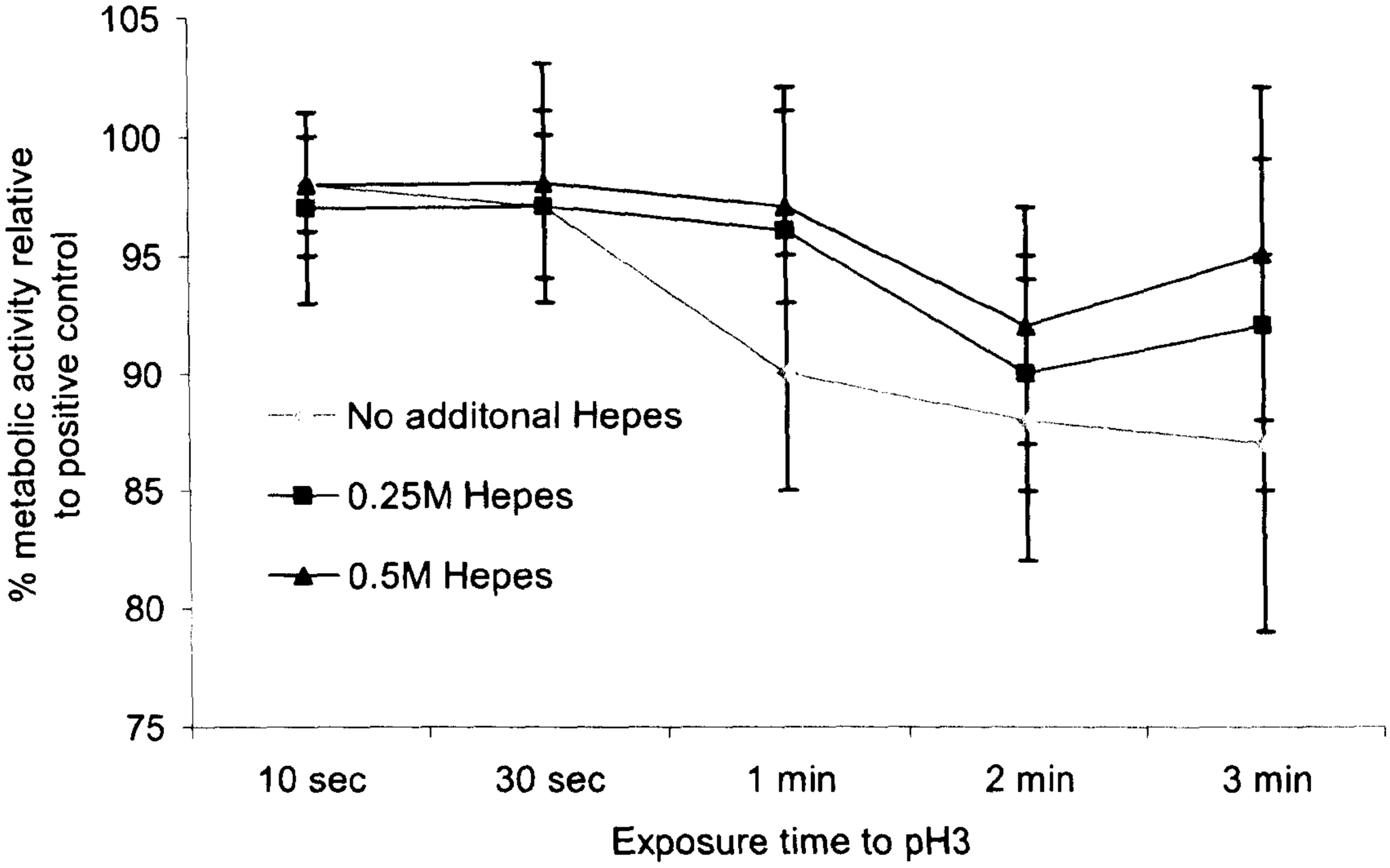

Figure 2-7 Survival of mammalian cells exposed to acidic conditions (pH3) for increasing exposure times, with and without the addition of Hepes buffer (pH7) as measured by an Alamar Blue assay. Mean (n=3) ± SD.

2.3.4 The Effect of Cell Suspension Volume on Mammalian Cell Survival

The effects of processing mammalian cells in different volumes of cell culture medium (DMEM) under supercritical conditions are presented in figure 2-8. These data show that the volume of the cell suspension is crucial in the determining the rate of cell survival, with only 30±8% survival recorded with 50 µl of DMEM compared with 75±5% survival when using 400 µl. This evidence would suggest that higher volumes provide some kind of protection for the cells and act as a physical barrier. A greater supply of nutrients and oxygen from the increasing volume of media throughout the processing step may be one reason for this increase in survival. Despite the highest rate of survival being at 400 µl, this value does not appear significantly different to that at 200 µl (70±7%). Furthermore, it is possible that the increased volume of the cell suspension may interfere with the polymer processing step (due to the presence of water) in future applications. Therefore, 200 µl was selected as the optimal volume for the processing of mammalian cells in $scCO_2$.

2.3.5 The Effect of Changing Cell Type on Resultant Cell Survival

The effect of supercritical processing on the survival of four different cell types are shown in figure 2-9. Cell survival at 10 seconds, in comparison to an untreated control, was over 80% for all cell types (over 90% for the C2C12 cell line). Cell survival remained at or above 50% for all cell types at one minute. Between one and two minutes exposure, there was a steep decline in cell survival, with little or no metabolic activity recorded after three minutes. The secondary murine cell lines (3T3 and C2C12) appear to show more resistance to $scCO_2$ than the primary cells suggesting a cell type dependent survival rate. However, this could be explained by the faster growth rates of 3T3 fibroblasts and C2C12 cells during the post processing 24 hour culture stage.

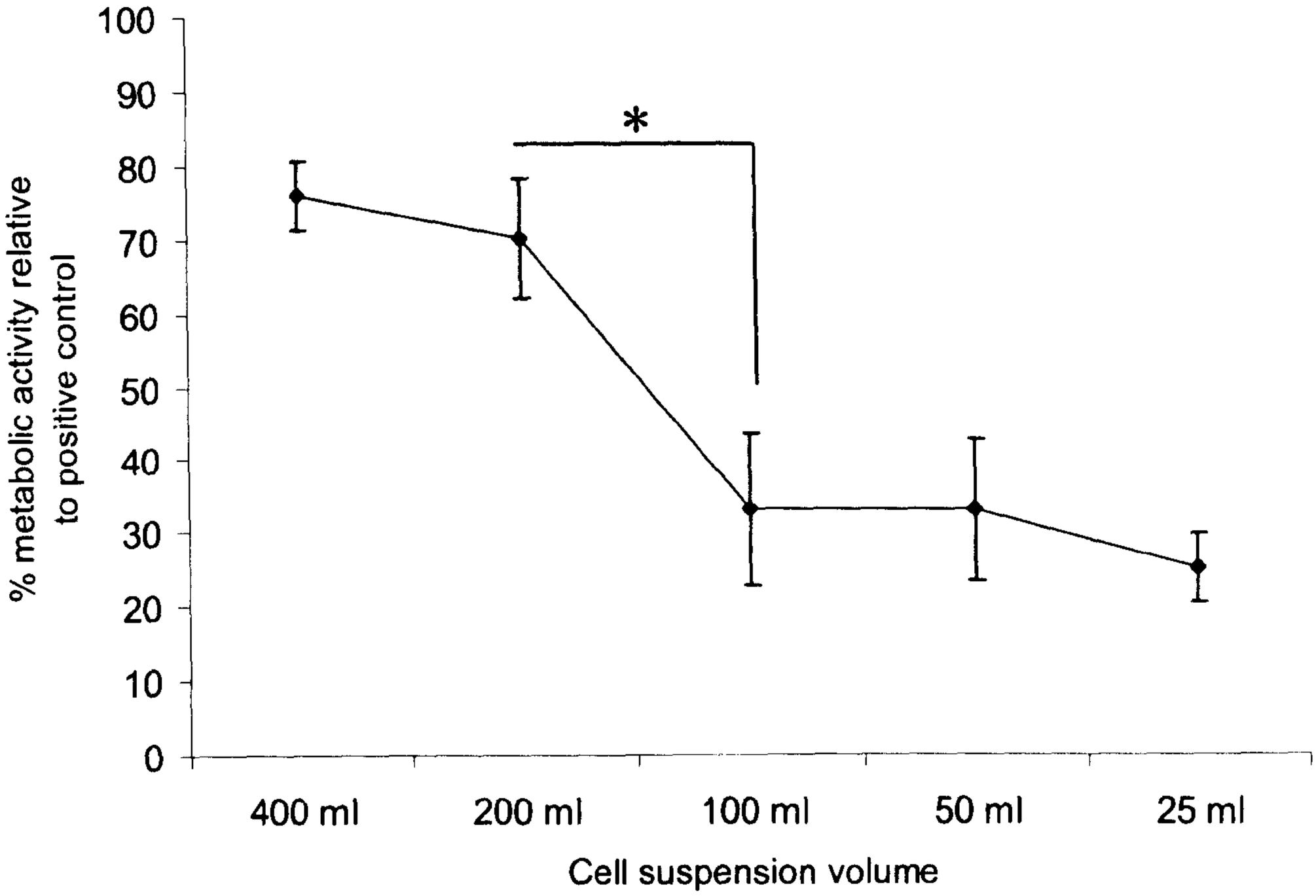

Figure 2-8 Survival of mammalian cells exposed to $scCO_2$ when suspended in different volumes of cell culture medium as measured by an Alamar Blue assay. All data is given with standard deviation. * indicates $p<0.05$ using T-test.

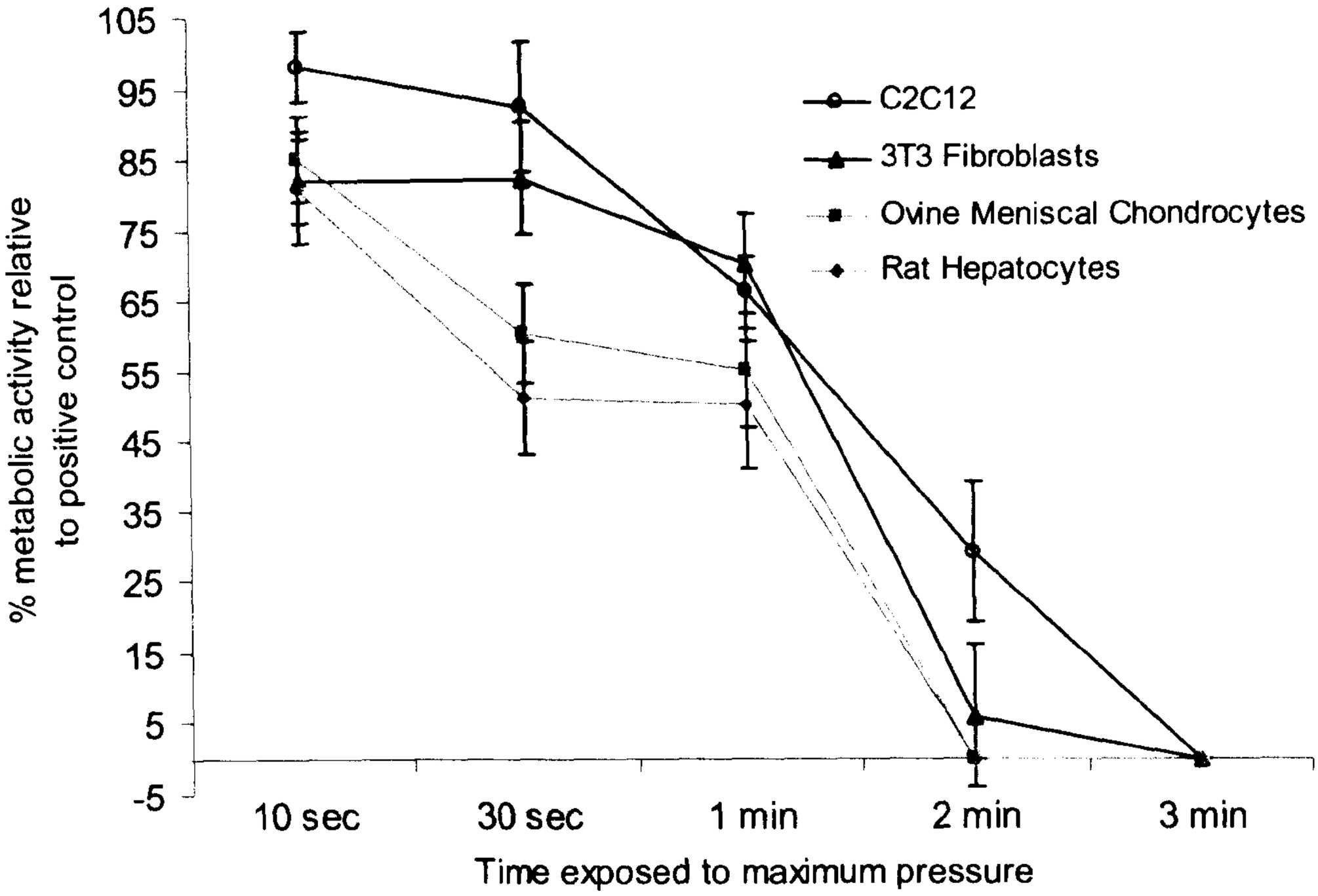

Figure 2-9 Master chart for the survival of four different mammalian cell types when subjected to $scCO_2$ for increasing exposure times as measured by an Alamar Blue assay. Mean (n=3) ± SD.

2.4 Conclusions

In order to satisfy the aims set out at the beginning of the study, mammalian cells have been subjected to all manner of $scCO_2$ processing conditions in order to produce optimal conditions for the latter stages of this investigation (measuring cell function and co-processing with $P_{DL}LA$. Of all of the conditions used here, the effects of processing time, decompression time and pressure appear to have the most obvious effects on cell survival. Processing time is crucial, with anything more than 60 seconds at maximum pressure resulting in less than 35% survival for all cell types and less than 10% for the primary cells (see figure 2-9). Therefore a processing time of 10 or 30 seconds would provide the highest live cell population. However, with the addition of the polymer phase, a processing time of 30 seconds would allow more CO_2 to become dissolved in the polymer and provide and longer window for any subsequent mixing that may be necessary. The pressure used for co-processing was always likely to be 74 bar irrespective of the data at sub critical pressures as this would offer polymer processing advantages, particularly over short periods of time. The use of a lower pressure did not significantly increase cell survival and may not be sufficient to produce a porous structure. Although when increased beyond 40 seconds the decompression time acted to prolong the survival of the cells under pressure, this did not actually increase cell survival. Therefore the decompression time subsequently used was retained at 40 seconds for future experiments. The effects of bubble formation and foaming during the decompression were not found to be detrimental to cell survival. Any changes in temperature and pH were insignificant over these short time periods and as a result no change from the starting temperature of 35°C was required, nor was the use of buffers to neutralise the pH.

Chapter 3

ELUCIDATING THE CAUSE AND EXTENT OF DAMAGE TO MAMMALIAN CELLS AFTER EXPOSURE TO SUPERCRITICAL CARBON DIOXIDE

3.1 Introduction

3.1.1 Investigating Potential Causes of Cell Death after Processing in Supercritical CO_2

The discovery that mammalian cells can survive in high pressure and supercritical CO_2 using a variety of processing conditions provided the basis for further investigation. However, there was no investigation as to the mechanism or cause of cell death from these experiments, except for the observation of a time-dependent survival. It was quite possible that cell death was caused by elevated and/or rapid changes in pressure as reported with bacterial systems (Fraser, 1951, Foster *et al*, 1962. It has also been proposed that weak solvent effects of CO_2 are a cause of cell death at high pressure either by causing a drop in the intracellular pH (Dillow *et al*, 1999) or by lipid extraction through the perforation of the cell membrane (Nakamura *et al*, 1994, Enomoto *et al*, 1997). Therefore it was considered that a study of CO_2 and a second processing medium would enable a comparison of the effects of both high pressure and more specifically high pressure CO_2 upon cell survival. Nitrogen (N_2) was chosen as an alternative processing medium as it is relatively inert. Despite the fact that the critical point of N_2 is reached at a pressure of 34 bar and a temperature of -147°C, the conditions had to remain the same from the initial experiments so that a direct comparison could be made.

3.1.2 Measuring the Effects of Supercritical CO_2 on Gene Expression and Cellular Function

In addition to investigating the cause of cell death, it was vital that the effects of $scCO_2$ processing on more complex aspects of cell machinery were assessed. Determining the effect of high pressure CO_2 on levels of gene expression is crucial to the future success of such a technique. Therefore a gene chip was used to compare gene regulation in murine C2C12 cells with and without being processed in $scCO_2$. To demonstrate cell function, the murine C2C12 cell line and primary rat hepatocytes were selected.

Myoblastic C2C12 cells were chosen for their ability to differentiate into the osteogenic lineage when prompted by BMP-2 (Katagiri *et al*, 1994). This change is shown by the production of protein markers indicative of bone formation, two of which are alkaline phosphatase (Okubo *et al*, 1999) and osteocalcin (Han *et al*, 2003). Therefore, induced protein activity, is seen as evidence of differentiation and thus, cellular function. Also chosen were primary hepatocytes, which are the main cellular constituent of the liver. Hepatocytes were selected as they have a number of important metabolic and catabolic activities. One such important activity is the metabolism of testosterone by the cytochrome P450 (CYP450) super-family of protein enzymes. Therefore, the activity of cytochrome P450 is used as a suitable marker of liver function in the pharmaceutical industry due to its role in the metabolism of many drugs. Function of CYP450 enzymes in culture systems is assayed via the hydroxylation of testosterone. The 6β-hydroxylation of testosterone is predominantly mediated by CYP 3A, the major isoform being 3A1 in rats (Sonderfan *et al*, 1987). Oxidation of testosterone to 4-androstene-3, 17-dione in rats is predominantly catalysed by CYP 2B1 (greater than 80%) with minor contribution by CYP 2C11 and CYP 2B2. 2α-hydroxylation is predominantly CYP 2C11 mediated in rats. Presence of these metabolites is detected via the use of high performance liquid chromatography (HPLC).

3.1.3 Aims

The central aim of this chapter was to investigate some of the possible causes of cell damage/death after processing in high pressure and supercritical CO_2 with a comparison made between the effects of CO_2 and N_2. In addition, it was also important to ascertain to what extent damage was affecting those cells that survived. Thus, the effects upon important aspects of gene function were estimated using a gene chip specific for murine. Finally, important aspects of cell machinery were investigated using the differentiation capacity of C2C12 cells and hormone metabolism in primary hepatocytes as markers of retained cell function after $scCO_2$ processing.

3.2 Methods

3.2.1 Culture of the Murine C2C12 Cell Line

Murine C2C12 cells were cultured in complete DMEM for all cell survival and functionality studies. Details of cell culture for 3T3's and C2C12's are given in the materials and methods chapter (section 7.1.1). A viable cell count was carried out for both cell lines using trypan blue exclusion, full details of which can be seen in the materials and methods chapter (section 7.1.3).

3.2.2 Exposure of Mammalian Cells to Supercritical CO_2 and High Pressure N_2

Briefly, C2C12 cells (250,000) were suspended in 200 µl of complete DMEM (without phenol red and FCS for the lactate dehydrogenase (LDH) assay) and then placed into custom-made 8-well PTFE moulds. Eight samples were processed in triplicate using either CO_2 (food grade, Cryoservice) or N_2 (BOC gases, UK) at 74 bar with a starting temperature of 35°C. Cells were processed at maximum pressure for between 10 seconds and 3 minutes with an additional 40 seconds required to depressurise the vessel. After processing, the cells in each well were re-suspended in 1 ml of complete DMEM and incubated for 24 hours (3 hours for apoptosis assay) in 48-well tissue culture plates (Falcon) before assay. For the LDH assay, the cell suspensions were immediately centrifuged to remove the cells and the assay carried out on the 200 µl aliquots of supernatant. For gene expression and functionality studies the cells were exposed to $scCO_2$ (74 bar, 35°C) for one minute with the additional 40 seconds required for both compression and decompression.

3.2.3 Measuring the Survival of Murine C2C12 Cells after Processing in High Pressure N_2

Cells were assayed for metabolic activity by the Alamar Blue™ cell metabolic activity assay as described in the materials and methods chapter (section 7.3.1). Briefly, the complete medium covering the cells in culture was replaced with 1 ml per well of an Alamar Blue™ solution (10% in HBSS, Sigma UK).

After a 90 minute incubation at 37°C (5% CO_2) 200 µl of solution from each well was transferred to a 96-well plate (Falcon). Fluorescence readings were then obtained at an emission wavelength of λ590 nm using λ560 nm excitation.

3.2.4 Assessment of Cell Membrane Rupture after Processing in Supercritical CO_2

As cells release cytosolic LDH when the membrane is ruptured, an assay for levels of LDH after exposure to $scCO_2$ was carried out as described in chapter 7.3.3. Briefly, C2C12 cells (250,000 per well) were suspended in DMEM (without phenol red and FCS) and processed in $scCO_2$ (74 bar, 35°C) for increasing times (10 seconds – three minutes) as in previous experiments. The cells were then removed by centrifugation and the remaining DMEM assayed for release of LDH using a LDH colour substrate system as per manufacturer's instructions (Roche, Penzberg, Germany). The results were then compared to a set of controls consisting of both live cells (intact) and dead cells (lysed).

3.2.5 Assessment of Cellular Apoptosis after Processing in Supercritical CO_2

To further elucidate the cause of cell death, C2C12 cells were assessed for $scCO_2$ induced apoptosis by way of an enzyme-liked immuno sorbent assay (ELISA) used to detect the histone-DNA complexes indicative of apoptotic cells. The full methodology can be found in chapter 7.3.4. In brief, C2C12 cells (250,000 per well) were suspended in DMEM (without phenol red) and processed in $scCO_2$ (74 bar, 35°C) for increasing times (10 seconds – three minutes) as in previous experiments. The cells were then cultured for a further 3 hours in fresh DMEM (so as to observe apoptosis rather than cell mechanical damage) and then assayed for histone associated DNA fragment indicative of cell death. Induced cell death was detected via the cell death detection ELISA+ kit (Roche, Penzberg, Germany) used as per manufacturers instructions.

3.2.6 Assessment of Gene Expression in Murine C2C12 Cells after Processing in Supercritical CO_2

A microarray of over 9000 genes was used to indicate any changes in gene expression after processing in $scCO_2$. In brief, murine C2C12 cells were processed for one minute at 74 bar and 35°C as described in the materials and methods chapter (section 7.2.1) and cultured for a further three hours in DMEM before being homogenised in an RLT (unknown abbreviation) buffer containing β-mercaptoethanol (10 µl per ml). Total RNA content of the cell homogenate was assessed using the RNeasy kit (Qiagen, Germany) according to the manufacturer's instructions. Slides were OciChip™ 30k set-A arrays (Ocimum Biosolutions) and indirectly labelled probes were generated from 5 µg of total sample RNA with ambion messageamp II amplification (as per manufacturers instructions). The probes were labelled with alexa 555 or 647 NHS ester dyes (InVitrogen) and 0.5 µg (approximately 40 pM of dye-label) of each was used for each channel of 2 colour hybridisations. Hybridisations were performed for 16 hours on a TEcan HTS 4800 hybridisation station with moderate agitation, using the Ocimum recommended solutions and temperatures. Arrays were scanned with a GenePix 4000b laser scanner and primary data obtained using GenePix Pro 6.0 software (Axon). Filtering of array data and normalisation using the LOWESS algorithm were performed within the University of Nottingham microarray database (a version of BASE v1.2.16, Lund University, Sweden). Further analysis was performed on this data set using Multi Experiment Viewer (MEV) software and the statistical analysis of microarrays (SAM) algorithm.

3.2.7 Cell Functionality Assessment by BMP-2 Induced Osteogenic Differentiation of the C2C12 Cell Line after Exposure to Supercritical CO_2

For osteogenic culture, C2C12 cells that had been processed in $scCO_2$ for one minute at 74 bar (35°C) were cultured overnight in complete DMEM before the addition of 500 ng/ml recombinant human bone morphogenetic protein-2 (rhBMP-2) in 2% FCS supplemented DMEM.

After seven days in osteogenic culture, C2C12 cells were assayed for the soluble end product of alkaline phosphatase activity using the assay described in the materials and methods chapter (section 7.4.2). In brief, cell cultures were fixed in 75% ethanol for 10 minutes and homogenised in 600 µl of distilled water containing 0.001% Tween detergent after 3 cycles of freeze-thawing. The substrate (p-nitrophenyl phosphate) (p-NPP) was added to equal volumes of the cell samples, incubated at 37°C for 1 hour and the rate of conversion into p-nitrophenol (p-NP) measured by a change in fluorescence at 405 nm. Values were compared against known p-NP standards and the data was corrected to DNA content as a measure of cell number and presented as nM of p-NP per hour per ng DNA. The DNA content of the cells was assayed using a method also found in the materials and methods chapter (section 7.3.2). To observe the osteogenic status of C2C12 cells, a red colour substrate was precipitated on the cells by the action of cellular alkaline phosphatase activity. The substrate system comprised of Napthol AS-MX buffer solution containing 1 mg/ml Fast Violet B salt, as previously described (Oreffo *et al*, 1998) and can be found in more detail in the materials and methods chapter (section 7.4.3).

3.2.8 Cell Functionality Assessment by Measurement of Cytochrome P450 Activity in Rat Hepatocytes after Exposure to Supercritical CO_2

After exposure to $scCO_2$ and 24 hours in culture, rat hepatocytes were assayed for function by measuring the metabolic activity of three key cytochrome P450 enzymes as described in the materials and methods chapter (section 7.3.3). In brief, rat cell cultures were incubated for 1 hour at 37°C in 1.5 ml or 320 µl respectively of Earl's buffered saline solution (EBSS) supplemented with 1 mM Ca^{2+}, 1 mM Mg^{2+} and containing 100 µM testosterone. The supernatant was analysed using a Beckman HPLC 1090, with UV absorbance detected at 245 nm using an integral diode array detector. The sample injection volume was 40 µl with each run controlled by intermittent injection of a 6β-hydroxytestosterone standard, as well as a mix of all metabolite standards. The peak height of each sample was recorded and compared to a series of known metabolite standards to calculate the percentage of each metabolite present (DNA corrected).

3.3 Results and Discussion

3.3.1 Investigating the Possible Causes of Cell Death

Mammalian cells were exposed to N_2 using identical conditions to those used for the CO_2 studies and assayed for metabolic activity 24 hours later. The results of these studies were compared with values already ascertained for $scCO_2$ and can be seen in figure 3-1. C2C12 survival was a 99±8% after exposure to high pressure N_2 (74 bar, 35˚C) compared with a survival rate of 66±3% after exposure to CO_2 at the same pressure and temperature, a difference which has been confirmed as significant by a standard T-test. Furthermore, the levels of cell survival are maintained above 70% after three minutes exposure to nitrogen compared with total cell death after exposure to similar periods of $scCO_2$. Thus, these data indicate that mammalian cells are more susceptible to the effects of CO_2 than N_2 and that elevated pressures are not the only mechanism of cell death. The increased cell death after exposure to $scCO_2$ indicates that it may be a CO_2 specific interaction with the cell suspension that is adding to the effects of pressure. This would concur with previous literature where a CO_2-instigated drop in pH has been suggested as a mechanism of cell death (Dillow *et al*, 1999). Figure 3-2 shows the data from two separate experiments conducted to provide further information as to the cause of cell death.

The measured release of LDH from the cells exposed to $scCO_2$ under the same conditions shows the presence of ruptured cells but not in a consistent manner. This indicates that there is some perforation of, or damage to, the cell membrane during the rapid compression/decompression of CO_2 as reported by Nakamura *et al* (1994) & Enomoto *et al* (1997). This rupture could be both a direct cause of cell death whilst also possibly facilitating a reduction in the intracellular pH. The measurement of histone complexes by ELISA showed no observable induced apoptosis (in surviving cells) over that of control cells, as can be seen in figure 3.2. Therefore it would appear that apoptosis is not a primary cause of the cell death.

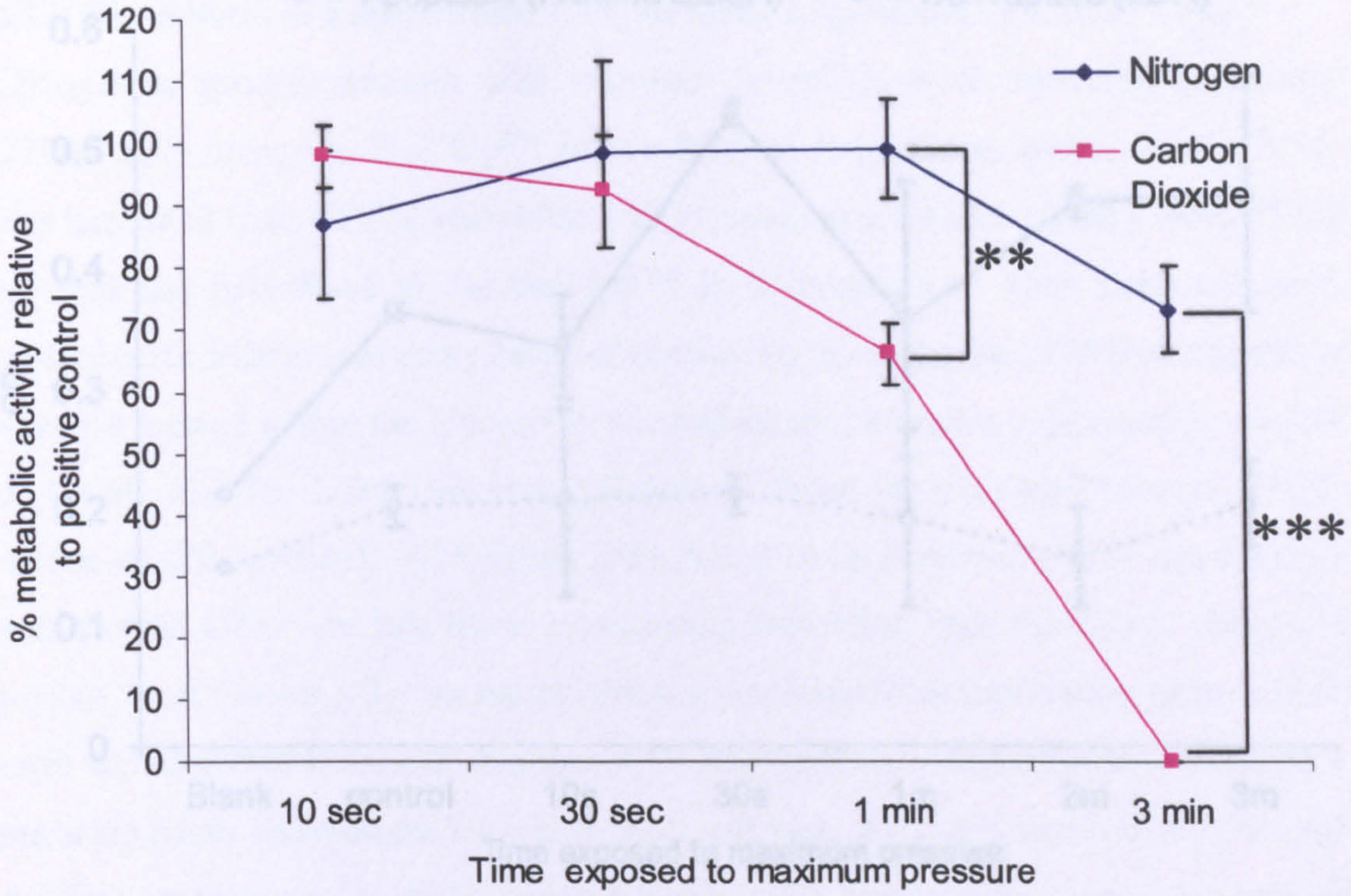

Figure 3-1 Survival of C2C12 cells when subjected to 74 bar pressure of $scCO_2$ or N_2 for increasing exposure times as measured by an Alamar Blue assay. Mean (n=3) ± SD. ** indicates $p<0.01$ and *** $p<0.001$ using T-test. An additional T-test was carried between the data sets at three minutes exposure in order to further demonstrate the significance of the result.

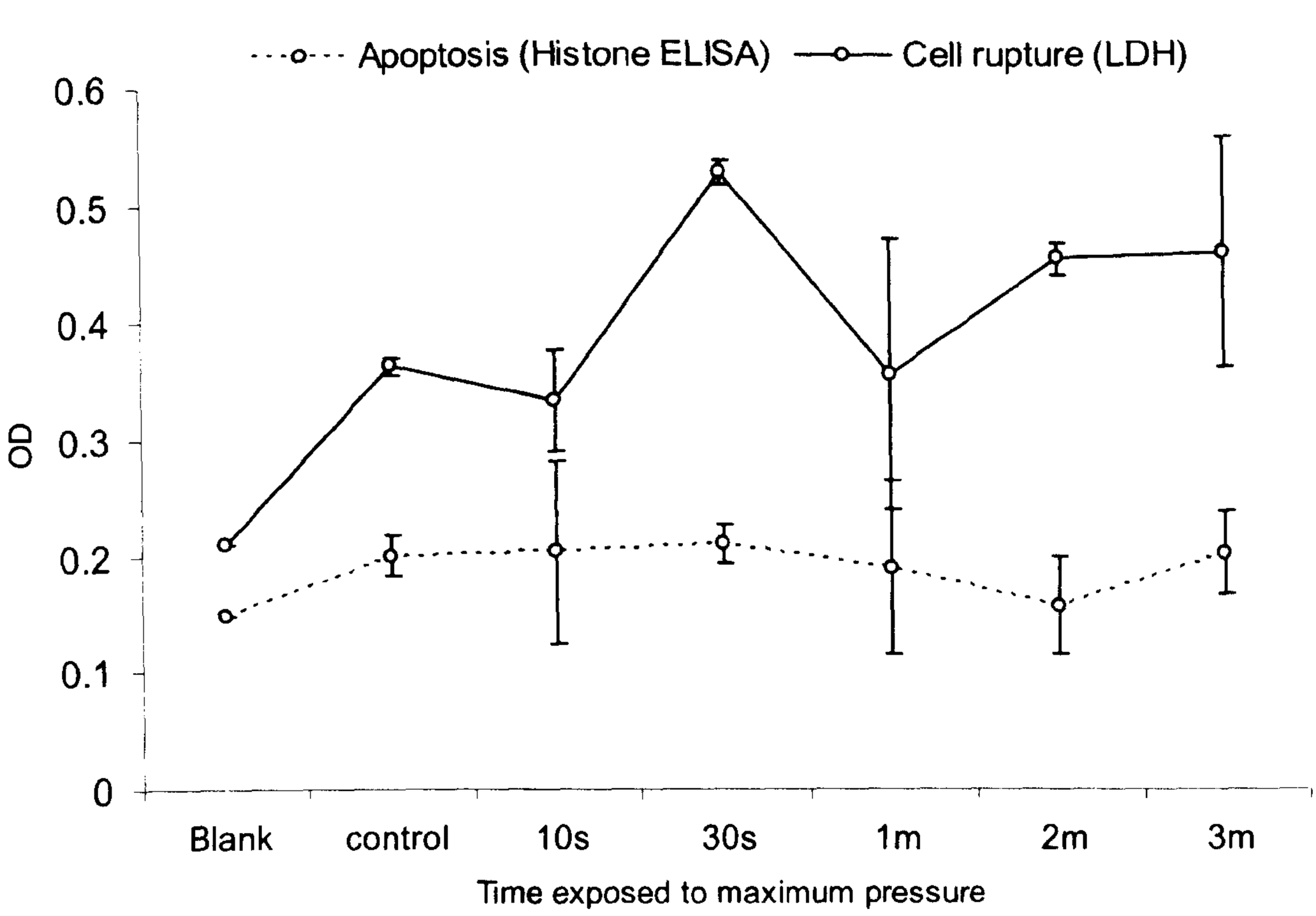

Figure 3-2 Measurement of cell rupture using an LDH assay and apoptosis using an ELISA for DNA-histone complexes, after exposure of C2C12 cells to $scCO_2$ for increasing time periods. Mean (n=3) ± SD.

3.3.2 The Effects of Supercritical CO_2 on Gene Expression in C2C12 Cells

Changes in gene expression after exposure to $scCO_2$ were measured in murine C2C12 cells using the OciChip™ mouse 30k set A (Ocimum Biosolutions). RNA was harvested from C2C12 cells after $scCO_2$ processing for one minute (74bar/35˚C) labelled and hybridised to the OciChip™ in comparison to RNA from untreated control cells. Filtering of array data and normalization using the LOWESS algorithm were performed within the University of Nottingham microarray database (a version of BASE v1.2.16, Lund University, Sweden). From the OciChip™ arrays, (9853 mouse specific probes), 4418 genes were found to be detected in 3 or more arrays and showed a reproducible linear relationship indicating little significant change at mRNA level (figure 3-3). Stringent filtering was used to examine only genes which were well detected across all samples. A Further analysis was performed on this data set using Multi Experiment Viewer (MEV) software. An initial single class T-test of the data set (against threshold P values = 0.01 with standard Bonferroni correction) did not reveal any significant changes from the control samples.

The statistical analysis of microarrays (SAM) algorithm as implemented with MEV found eight significantly down-regulated genes based on a δ value of 1.0125 and false discovery of 0 (table 3-1). Of the eight genes that were significantly down-regulated, survivin121, clast4 protein and glutathione-s-transferase could play a role in a biochemical response from the cell to the extreme changes in environment. Survivin121 is a component of the chromosomal passenger complex that acts as an inhibitor of apoptosis (Wheatley & McNeish, 2005). Down-regulation of survivin121 is the only marker of an apoptotic response recorded here further indicating that apoptosis is not a major cause of cell death.

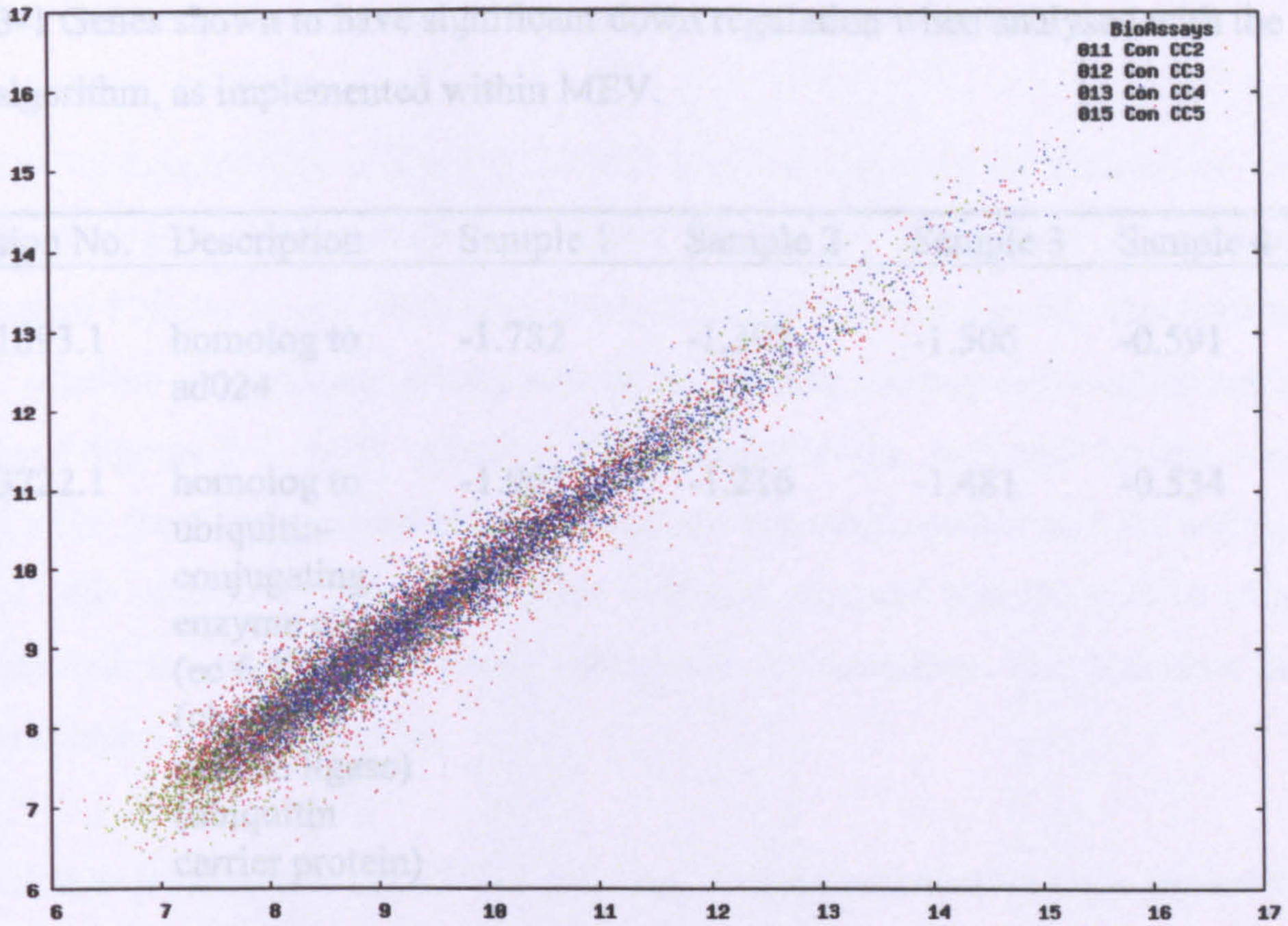

Figure 3-3 Log-log plots of normalised intensity (arbitrary units on both axes) for genes after microarray analysis of the murine C2C12 cell line after exposure to $scCO_2$. Sample genes (channel 1, x-axis) are plotted against control genes (channel 2, y-axis) with colours used to identify the four biological replicates.

Table 3-1 Genes shown to have significant down regulation when analysed with the SAM algorithm, as implemented within MEV.

Accession No.	Description	Sample 1	Sample 2	Sample 3	Sample 4
AK011893.1	homolog to ad024	-1.782	-1.398	-1.506	-0.591
AK003722.1	homolog to ubiquitin-conjugating enzyme e2 h10 (ec 6.3.2.19) (ubiquitin-protein ligase) (ubiquitin carrier protein)	-1.963	-1.216	-1.481	-0.534
AF115517.1	survivin121	-1.272	-1.227	-1.003	-0.391
NM_011526.1	transgelin; tagln	-0.660	-0.575	-0.496	-0.579
AK010877.1	homolog to ran binding protein 11	NaN*	-0.821	-1.166	-0.898
NM_023743.1	clast4 protein; 2610509l04rik	-0.677	NaN*	-0.806	-0.795
NM_010358.1	glutathione-s-transferase; mu 1; gstm1	-0.789	-0.516	-0.877	-0.523
NM_025377.1	riken cdna 1110001a07; 1110001a07rik	-0.922	NaN*	-0.881	-0.728

*NaN = Not a Number

3.3.3 The Effects of Supercritical CO_2 on Important Aspects of Mammalian Cell Function

Retention of functionality in the C2C12 cell line was assessed by their ability to undergo osteogenic differentiation as observed by the expression of alkaline phosphatase (Okubo *et al*, 1999, Han *et al*, 2003) after a one minute exposure to $scCO_2$. Alkaline phosphatase activity was detected using staining and a colorimetric assay (see figures 3-4 A/B). Alkaline phosphatase levels, indicated by the red-stained cells, were indistinguishable between the untreated control and the $scCO_2$-exposed cells after DNA correction. This evidence suggests that the C2C12 cells have retained the ability to undergo osteogenic differentiation and therefore an important aspect of their function.

In addition to studies with the C2C12 cell line, primary hepatocytes were treated to three $scCO_2$ exposure times (10, 30, 60 seconds) and assayed for important aspects of cytochrome P450 activity. The levels of each metabolite are presented as a percentage of an untreated control as detected by HPLC analysis and are seen in figure 3-5. These data indicate that several important metabolic functions of cytochrome P450 in rats are unaffected by exposure to $scCO_2$ for up to 60 seconds. The presence of 6-β-OH testosterone despite $scCO_2$ processing, provides evidence for the continued functioning of CYT 3A1. Furthermore, there is no significant difference between the increasing exposure times, indicating that this function is unaffected after up to 60 seconds exposure to $scCO_2$. 2α-hydroxylation in rats also appears to be unaffected by this treatment, with no indication of a loss in enzyme activity (CYP 2C11) irrespective of the exposure time. Oxidation of testosterone to 4-androstene-3, 17-dione in rats is predominantly catalysed by CYP 2B1 (greater than 80%) with minor contributions by CYP 2C11 and CYP 2B2 (Sonderfan *et al*, 1989). Therefore the continued production of this metabolite after $scCO_2$ processing also indicates continued function of these three enzymes, although this does appear to be reduced after 60 seconds of exposure to $scCO_2$.

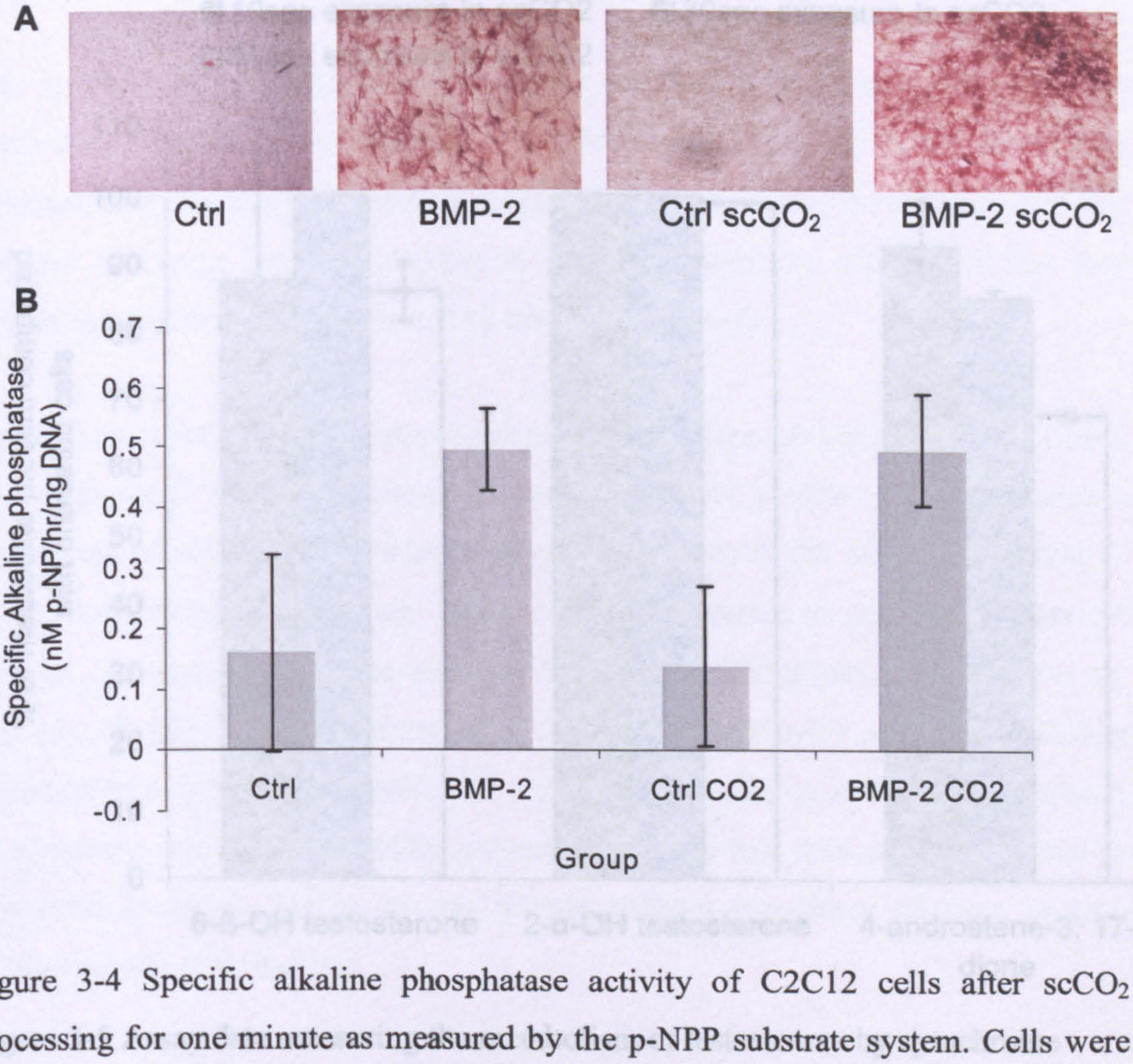

Figure 3-4 Specific alkaline phosphatase activity of C2C12 cells after $scCO_2$ processing for one minute as measured by the p-NPP substrate system. Cells were both stained (A) and assayed (B) for alkaline phosphatase activity after supercritical CO_2 processing and subsequent osteogenic culture in cell culture medium containing 500 ng/ml BMP-2. Mean (n=3) ± SD.

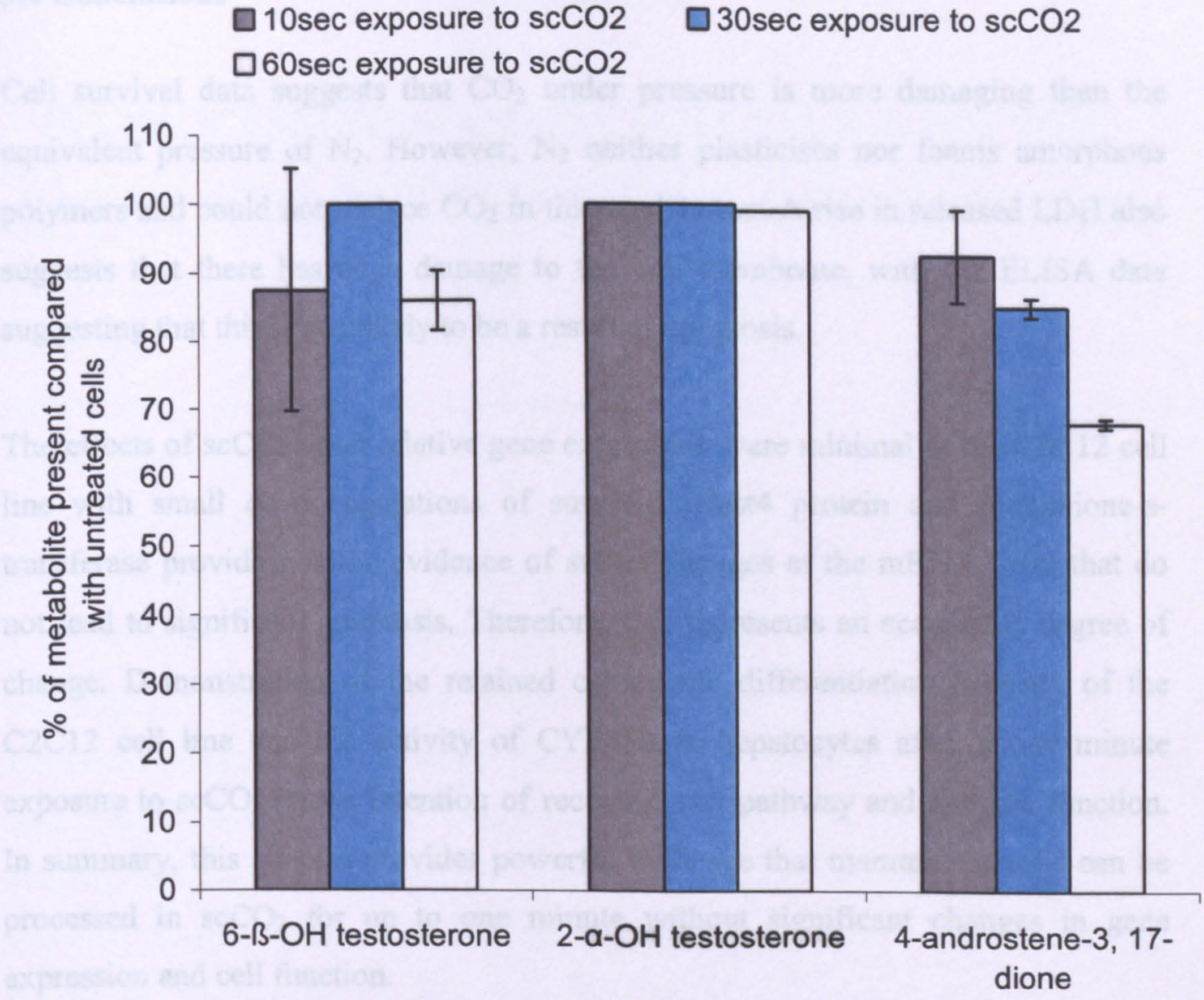

Figure 3-5 Assay data measuring the metabolism of testosterone by cytochrome P450 activity in rat hepatocytes after $scCO_2$ processing for increasing exposure times. The presence of each metabolite is detected by high performance liquid chromatography and all data is corrected to recovered DNA. Mean (n=2) ± SD.

3.4 Conclusions

Cell survival data suggests that CO_2 under pressure is more damaging than the equivalent pressure of N_2. However, N_2 neither plasticises nor foams amorphous polymers and could not replace CO_2 in this application. A rise in released LDH also suggests that there has been damage to the cell membrane, with the ELISA data suggesting that this is not likely to be a result of apoptosis.

The effects of $scCO_2$ upon relative gene expression were minimal in the C2C12 cell line with small down-regulations of survivin, clast4 protein and glutathione-s-transferase providing some evidence of subtle changes at the mRNA level that do not lead to significant apoptosis. Therefore, this represents an acceptable degree of change. Demonstration of the retained osteogenic differentiation capacity of the C2C12 cell line and the activity of CYP450 in hepatocytes after a one minute exposure to $scCO_2$ shows retention of receptor, cell pathway and enzyme function. In summary, this chapter provides powerful evidence that mammalian cells can be processed in $scCO_2$ for up to one minute without significant changes in gene expression and cell function.

Chapter 4

CO-PROCESSING MAMMALIAN CELLS & POLY(DL-LACTIC ACID) IN SUPERCRITICAL CARBON DIOXIDE

4.1 Introduction

With the exception of the work done with micro-organisms (Dillow *et al*, 1999) there has been no documented evidence describing the co-processing of mammalian cells with synthetic polymers under high pressure or otherwise. However, as previously discussed, synthetic polymers have been mixed with sensitive biological species such as nucleic acids, proteins and growth factors under high pressure or supercritical CO_2 conditions and co-processed into porous controlled release devices (Shea *et al*, 1999, Howdle *et al*, 2001, Watson *et al*, 2002, Yang *et al*, 2003b, Yang *et al*, 2004). In all of these studies, the amorphous $P_{DL}LA$ has been used either individually or as part of the PLGA co-polymer, as a cell support and or controlled release device for tissue engineering and drug delivery applications. Poly(DL-lactic acid) fulfils most of the desirable criteria as a support for cellular attachment as it is non-toxic, economical and biodegradable. Most importantly however, $scCO_2$ is highly soluble in $P_{DL}LA$ at ambient temperatures facilitating the plasticisation and foaming of the polymer without toxic solvents or chemical foaming agents. Therefore $P_{DL}LA$ was selected as the most suitable choice of polymer for this application.

4.1.1 Characterising Tissue Engineering Scaffolds

A number of techniques have been used to characterise tissue engineering scaffolds and ensure that they are fit for purpose. The type of technique/test used is largely dependent upon the material and the application. Properties such as low toxicity, biodegradability and biocompatibility are generally considered to be pre-requisites for most tissue engineering applications. However, the desired levels of porosity, pore size and mechanical strength are largely dependent upon the cell or tissue type and final use of the scaffold. Most scaffold characterisation techniques focus on measuring these parameters as they often govern the success or failure of any tissue engineering device.

This $scCO_2$ techniques discussed in this study (Howdle *et al*, 2001, Yang *et al*, 2004) have never previously been used to fabricate $P_{DL}LA$ scaffolds using the short processing times imposed by mammalian cell survival in $scCO_2$. Thus, it was necessary to confirm that solid 3D porous structures could be formed using such truncated processing times and that these structures could support cell attachment and growth over days and weeks. To further assess the properties of these scaffolds, basic information on the gross morphology, porosity and pore size distribution of the scaffolds was required. A number of methods can be used to assess the porosity and pore architecture of tissue engineering scaffolds. In this study, three techniques were chosen that are commonly used in tissue engineering applications: light microscopy, scanning electron microscopy and micro computed tomography.

4.1.1.1 Light and Fluorescent Microscopy

Light microscopy is a simple technique that can provide a two dimensional image of an object. In terms of scaffold characterisation this technique is very limited, but it is useful as a quick and simple method of observing the gross morphology of scaffolds and has the added advantage of providing colour images. When fluorescent light is added to a sample of interest that has been impregnated or tagged with a fluorescent marker, the microscope can be used to select this fluorescent marker against the background. As a result, fluorescence microscopy has been used in tissue engineering applications (Patz *et al*, 2005).

4.1.1.2 Scanning Electron Microscopy

Scanning electron microscopy (SEM) is a commonly used characterisation technique for tissue engineering and drug delivery applications (Mooney *et al*, 1996a, Howdle *et al*, 2001). SEM works by passing a concentrated beam of electrons through an electrically charged (gold coated) sample, whilst under vacuum. This beam is focussed by a series of lenses to displace secondary electrons in the sample, which when counted and detected, build up into a topographical image of the specimen.

Because the SEM has a relatively high resolution (2 nm) when compared to the light microscope (approximately 0.2 μm) it can provide a more detailed 2D image of scaffold pore structure at high magnification, as shown in figure 4-1. As a result, the pore size and morphology of tissue engineering scaffolds or micro/nano particles can be determined (Howdle *et al*, 2001, Whitaker *et al*, 2005). In addition to this, SEM is also an effective way to show the distribution of mammalian cells that have been seeded onto polymer scaffolds for tissue engineering applications (Murphy *et al*, 2000, Unsworth 2003). However, SEM is limited as it can only provide a 2D, grey scale image of the scaffold topography.

4.1.1.3 Micro-Computed Tomography

Micro-computed tomography (μ-CT) is a non-destructive, non-invasive technique that uses a sealed x-ray source to produce both 2D and 3D images of porous structures (see figure 4-2). The x-rays are passed through the scaffold and isotropic slice data are obtained and reconstructed into 2D images, which are compiled and analysed to generate 3D images and obtain quantitative morphological detail. This gives it several advantages over SEM as a technique for the characterisation of tissue engineering scaffolds. Micro-CT has frequently been used to examine porous ceramic and polymeric structures and found particular application in orthopaedic tissue engineering strategies as it can be used to measure and quantify bone repair (Cartmell *et al*, 2004, Lin *et al*, 2003). In addition, organic matter within porous scaffolds can be visualised by staining with x-ray absorptive agents that provide contrast in the resulting tomograms (Thurner *et al*, 2003, Thurner *et al*, 2004). Therefore, the distribution of cells within porous scaffolds can be assessed by pre-staining samples with electron dense chemicals.

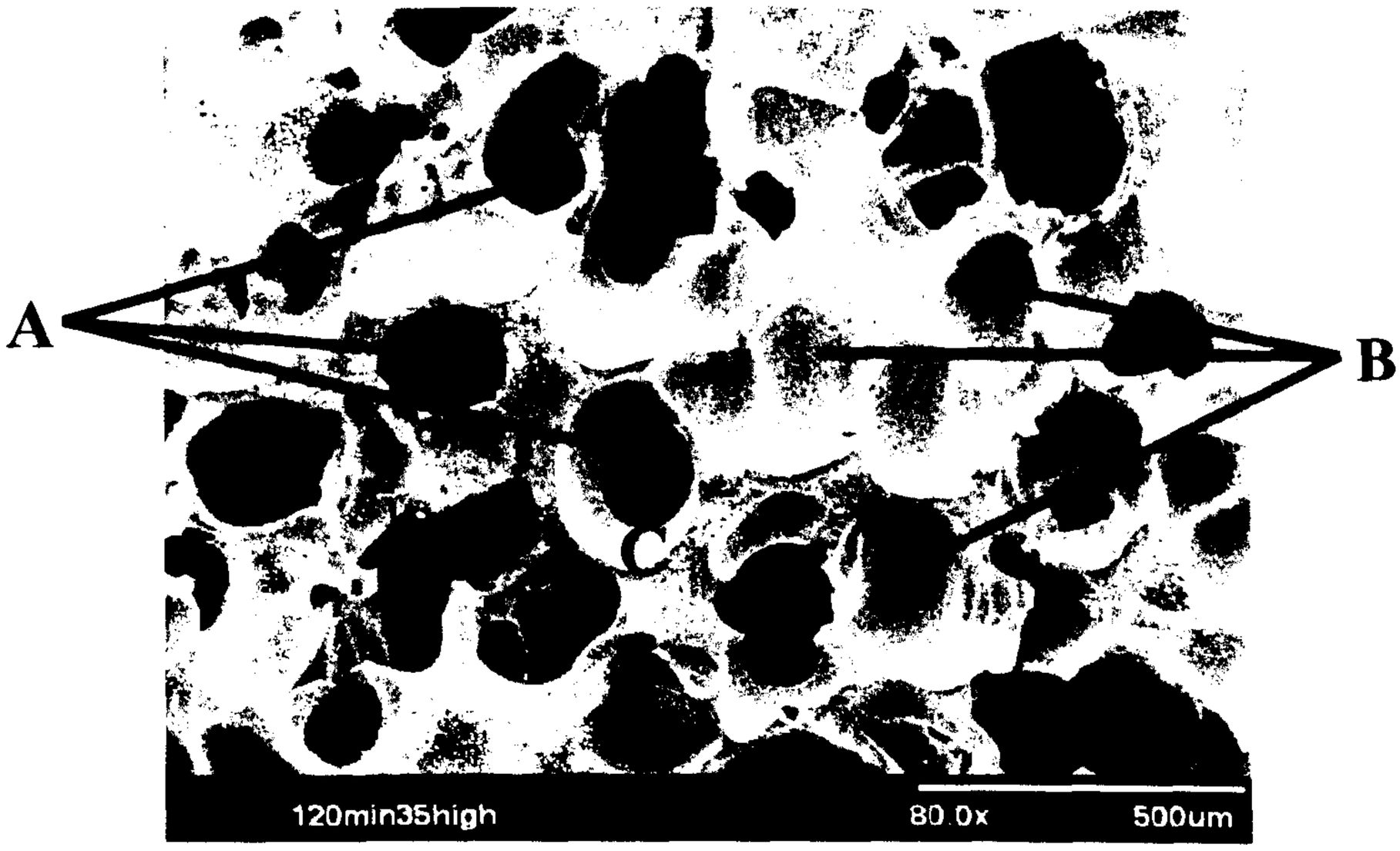

Figure 4-1 A typical SEM image showing the internal pore structure of a $P_{DL}LA$ scaffold fabricated using $scCO_2$ processing at the University of Nottingham. Note the presence of both open (A) and closed (B) pores. Open pores are so-called as they are connected to others permitting the passage of nutrients and gaseous exchange unlike closed pores which are isolated from the rest of the porous structure. The pore window size (C) is defined as the diameter across the opening of the pores and does not take into account the size of the channel itself due to the limitations of the 2D image.

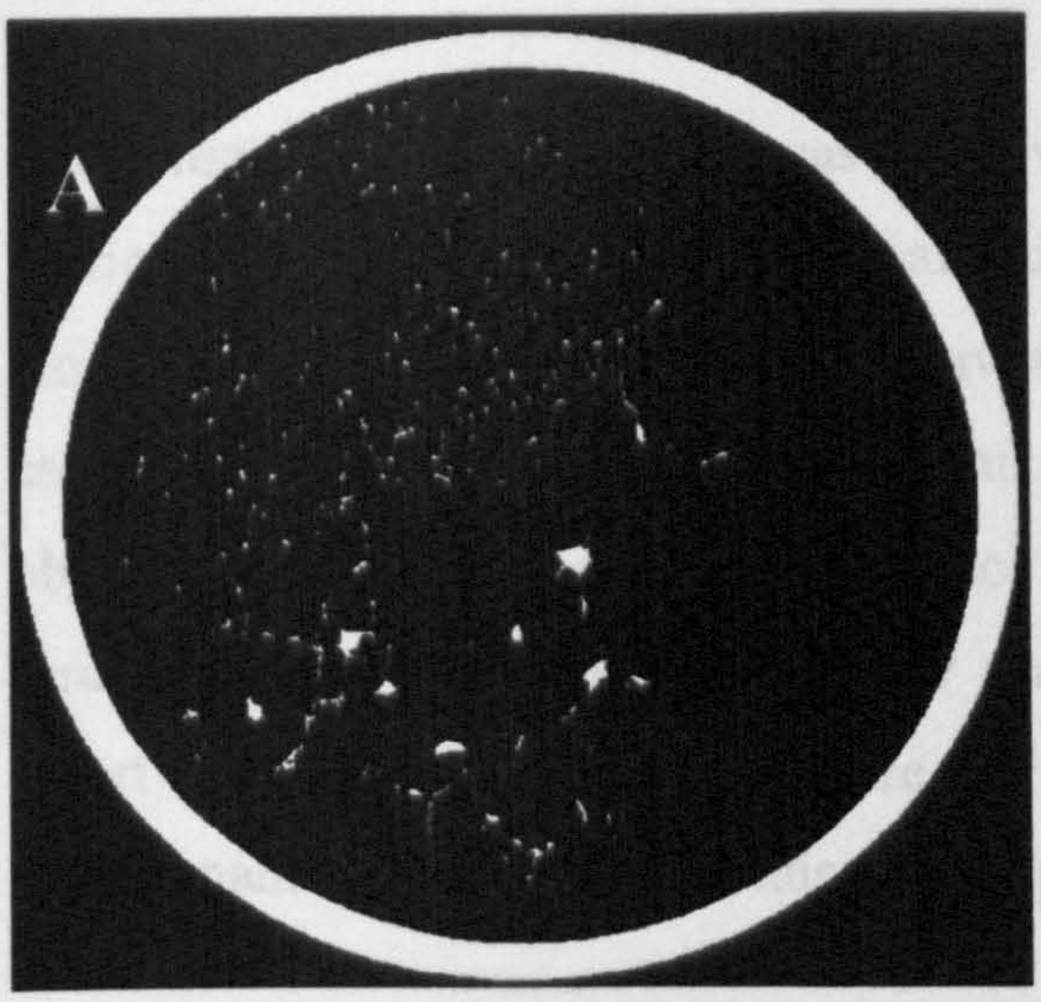

B

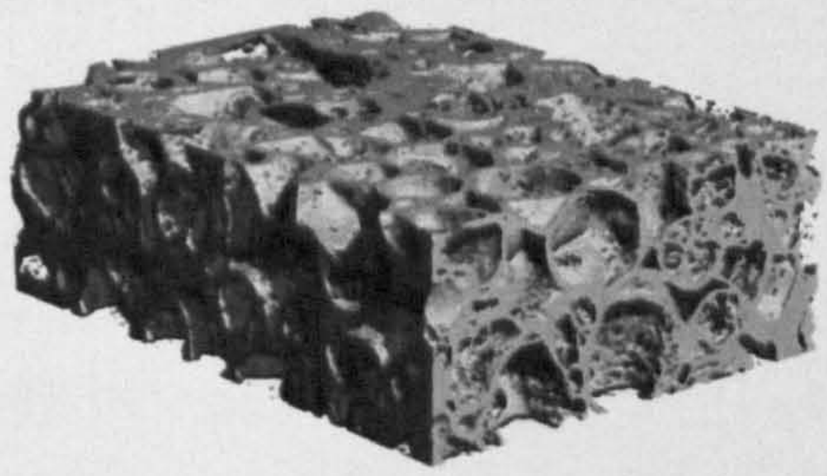

Figure 4-2 Micro-computed tomography images of $P_{DL}LA$ scaffolds fabricated by $scCO_2$ processing at the University of Nottingham. X-rays passed through the sample produce 2D contours or slices (A) that can be compiled into 3D images (B) by the computer software.

4.1.2 Aims

The initial aim of this chapter was to show that porous $P_{DL}LA$ scaffolds could be fabricated in the short time periods already dictated by mammalian cell survival. However, the main aim was then to investigate the effects of mixing mammalian cells with $P_{DL}LA$ and exposing the mixture to $scCO_2$. There were three main objectives within the main aim: (i) to show that cells are evenly distributed throughout the scaffolds, (ii) to show that mammalian cells survive the process (short term and long term) and adhere to the porous structures and (iii) to show that cells remain functional despite this mixing process.

4.2. Methods

4.2.1 Fabrication of $P_{DL}LA$ Scaffolds

The full method for scaffold fabrication can be found in the materials and methods chapter (section 7.2.2). In brief, $P_{DL}LA$ (100 mg) was weighed out into PTFE moulds in triplicate and processed in a 60 ml clamp sealed pressure vessel using $scCO_2$ (74 bar, 35°C) for 10, 30 and 60 seconds, with an additional 40 seconds required for both compression and decompression. This process was repeated three times for each sample and a sample from each replicate was used for light microscopy, SEM or μ–CT analysis.

4.2.2 Characterisation of $P_{DL}LA$ Scaffolds

After fabrication, macroporous $P_{DL}LA$ scaffolds were characterised by a variety of overlapping imaging techniques.

4.2.2.1 Light and Fluorescence Microscopy

Scaffolds were prepared and visualised using the protocol found in the materials and methods chapter (section 7.7.1). In brief, scaffolds were cut transversely using a scalpel, placed on a white background for contrast and the cross sections imaged using a light microscope (Nikon, SMZ1500).

4.2.2.2 Scanning Electron Microscopy

Samples were prepared for non-biological SEM and scanned as described in the materials and methods chapter (section 7.7.2). Briefly, scaffolds were gold coated (Baltzers union, SCD030 sputter coater) before being scanned at 15-20 kV using a Philips 505 scanning electron microscope. The average pore window size (diameter) was calculated from three scaffolds at each processing time by taking 50 random pore measurements and calculating the mean for each scaffold. Histograms of the frequency of pores within each range were constructed to determine the pore size distribution.

4.2.2.3 Micro-Computed Tomography

The process of scanning the polymer scaffolds using μ-CT is described in the materials and methods chapter (section 7.7.3). Briefly, scaffolds were scanned at 55kV and a current of 145mA using a high resolution micro-computed tomography system (μ-CT 40, Scanco Medical, Bassersdorf, Switzerland). Calculations were performed by the Scanco software provided to attain the pore size distribution and total porosity for each scaffold.

4.2.3 Investigation of the Cell/Polymer Mixing Technique

As there is no mixing of the polymer and cell components under pressure, the presentation of the cells to the polymer powder is vital to ensure that the cells are incorporated into final product. Therefore the value of pre-mixing the two components was assessed in terms of the distribution of the suspension in the foamed scaffold.

4.2.3.1 Investigating the Effects of Pre-Mixing a Liquid Dye and $P_{DL}LA$ Powder on the Final Distribution of the Dye in the Scaffold

The distribution of both mixed and unmixed cell suspensions in the final scaffold were compared using a dead cell suspension and food dye. Dead C2C12 cells were collected and a cell count was carried out using trypan blue exclusion as described in the materials and methods chapter (section 7.1.3) to make a stock solution of 1 million cells per ml, which was then re-suspended in complete DMEM (2 ml). A black food dye was then added to the cell suspension to provide contrast against the white polymer. 100 mg of $P_{DL}LA$ powder was then weighed out into 8 PTFE moulds and 200 μl of the cell suspension was either dropped into each well, or mixed into the polymer powder with a small spatula to make a polymer/cell slurry (250,000 cells per well). The cell/polymer mixtures were then processed in $scCO_2$ and observed using light microscopy.

4.2.3.2 Investigating the Effects of Pre-Mixing Cells Fixed with Osmium Tetroxide and $P_{DL}LA$ Powder on the Final Distribution of the Cells in the Scaffold

To show the actual distribution of the cells, live C2C12 cells were fixed in osmium tetroxide to show a contrast against the polymer. Fixing the cells in osmium tetroxide increases their electron density, allowing them to be contrasted against the less electron dense polymer when scanned with the μ-CT system. C2C12 cells were trypsinised and a small sample removed for fixing with 10% formyl saline (Sigma) and then with 1% osmium tetroxide (Fisher, UK) overnight. This cell suspension (200 μl) was then taken and mixed with the polymer as described in section 4.2.3.1. This mixture was then processed in $scCO_2$ and kept for μ-CT analysis.

4.2.3.3 Co-processing Dead and Fixed Cells with $P_{DL}LA$ in Supercritical CO_2

The cells were co processed with the polymer at 74 bar and 35°C as previously described in 4.2.1, for 30 seconds with an additional 40 seconds required for both compression and decompression. After processing the foamed constructs were subject to analysis by either light microscopy or μ-CT.

4.2.3.4 Light Microscopy Analysis

Scaffolds loaded with food dye were viewed under the light microscope to enable comparison between the distribution of the dye in mixed and non-mixed samples. Scaffolds were captured by a digital camera to show their gross morphology and then cut transversely to show the distribution of the food dye within. The full protocol for light microscopy can be found in the materials and methods chapter (section 7.7.1).

4.2.3.5 Micro-Computed Tomographic Analysis of Cell Loaded Scaffolds

The construct was imaged using a high-resolution micro computed tomography system (μ-CT 40, Scanco Medical, Bassersdorf, Switzerland) set to a voltage of 55 kV and a current of 145 mA.

Samples were scanned at 8 μm voxel (3D pixel) resolution with an integration time of 120 ms to produce 3D reconstructed images. The cell-loaded scaffolds were thresholded at 60 (an arbitrary number) to view the porous scaffold and then at 190 to view the osmium stained cells contained within.

4.2.4 Co-Processing Live Cells with $P_{DL}LA$

4.2.4.1 Cell Isolation and Culture

Murine C2C12 cells, 3T3 fibroblasts, rat hepatocytes and ovine fibrochondrocytes, were isolated and/or cultured as described in the materials and methods chapter (sections 7.1.1 and 7.1.2). A viable cell count was carried out with trypan blue to achieve a suitable concentration of cells in suspension, as described in the materials and methods chapter (section 7.1.3).

4.2.4.2 Fabrication of Cell-Loaded $P_{DL}LA$ Scaffolds using Supercritical CO_2

All four mammalian cell types were used for the investigation as detailed in chapter 2. The cell suspensions (250,000 cells in 200 μl) were mixed with the polymer (100 mg) using the technique described in section 4.2.3.3. The cell/polymer slurries were then processed in $scCO_2$ (74 bar and 35°C) for 30 seconds, with an additional 40 seconds required for compression and decompression (80 seconds in total). After processing the foamed constructs were cut into 4 equal pieces, cultured in complete medium for 24 hours and analysed using a variety of techniques.

4.2.4.3 Assessment of Cell Survival in $P_{DL}LA$ Scaffolds

All cell types loaded onto $P_{DL}LA$ scaffolds were assayed for continued metabolic activity using the Alamar Blue™ assay (see materials and methods chapter, section 7.3.1) and compared to untreated controls to provide some quantitative data. Briefly, media was aspirated from the processed cells after 24 hours in culture and replaced by 1ml solution of 10% Alamar Blue™ solution (v/v; Serotech Ltd UK) in, phenol red-free HBSS, Sigma UK). The cells were incubated for 90 minutes before 200 μl of solution from each well was transferred to a 96-well plate (Falcon).

Fluorescence readings were then obtained at an emission wavelength of λ590 nm using λ560 nm excitation. After processing Scaffolds containing C2C12 cells cultured for 34 hours in complete DMEM were stained for continued cell survival using the LIVE/DEAD™ stain (Molecular Probes, UK) at days 1 and 28 as described in the materials and methods chapter (section 7.6.1). Briefly, The cells and polymers were incubated in 10 ml of complete DMEM containing 20 µl of Ethidium Homodimer-1 (to highlight the dead cells red) and 5 µl of Calcein AM (to highlight the live cells green) for 1 hour. The cells were then rinsed (×4) in phosphate buffered saline (PBS) for 1 hour, before being observed using fluorescence microscopy (Leica DM IRB).

4.2.4.4 Histological Assessment of Cell Survival and Distribution

In order to observe the presence and viability of cells in the centre of the constructs, the cell loaded scaffolds were prepared for histology as described in the materials and methods chapter (section 7.6.2) Briefly, the cell loaded scaffolds were fixed in 70% methanol for 30 minutes, before drying overnight and subsequent infiltration with 65°C paraplast wax (Sigma UK). Sections (10 µm) were then cut using a microtome and observed using a fluorescence microscope for either propidium iodide stained nuclei (for identification of the cells location within the scaffolds) or for LIVE/DEAD™ stained cells (to show location and metabolic activity).

4.2.4.5 Scanning Electron Microscopy of Cell Loaded $P_{DL}LA$ Scaffolds

Scanning electron microscopy was used to observe the cells attaching to and spreading on, the surfaces of the scaffolds after supercritical processing. The scaffolds loaded with C2C12 and 3T3 fibroblasts were prepared for biological SEM as described in the materials and methods chapter (section 7.7.2). The samples were then gold coated, using a Balzers Union SCD030 sputter coater, before being scanned at 20 kV with a Philips 505 scanning electron microscope.

4.2.5 Assessment of Cell Function using BMP-2 Induced Alkaline Phosphatase Activity

For functional assessment, an alkaline phosphatase stain and assay was carried out on $scCO_2$ processed scaffolds loaded with C2C12 cells after BMP-2 induced osteogenic differentiation. Two methods were used to deliver the BMP-2 to the cells. In the first method, BMP-2 was delivered to pre-fabricated cell loaded scaffolds by culturing the cell loaded scaffolds in DMEM containing 500 ng/ml of BMP-2 for seven days. In addition, a second method was used whereby the growth factor was included in the fabrication process along with the cells. The use of a one-step $scCO_2$ processing technique for the production of $P_{DL}LA$ scaffolds loaded with BMP-2 has already been reported (Yang *et al*, 2003b, Yang *et al*, 2004). Here, C2C12 cells were mixed with $P_{DL}LA$ pre-loaded with BMP-2 to demonstrate the possibility of a complete tissue engineering construct in a single step.

4.2.5.1 Addition of BMP-2 after Scaffold Fabrication

Cell loaded scaffolds were fabricated by using the method described in 4.2.4.2 and cut into four pieces. After 24 hours culture in complete DMEM, the scaffolds were cultured for a further seven days in osteogenic DMEM containing 500 ng/ml BMP-2.

4.2.5.2 Addition of BMP-2 before Scaffold Fabrication

Before the cells could be processed with the polymer, the BMP-2 was adsorbed onto the surface of the polymer particles by using a freeze drying process. The BMP-2 (3 μg) was suspended in 600 μl added to 600 mg of $P_{DL}LA$ powder and placed into 6 wells of a PTFE plate to give 100 mg $P_{DL}LA$/500 ng BMP-2 per well. The polymer/protein mixtures were then frozen in liquid nitrogen and freeze dried overnight to adsorb the protein to the polymer particles. The cell loaded scaffolds were fabricated by using the method described in 4.2.4.2 and cut into four pieces before seven days culture in complete DMEM.

4.2.5.3 Assay and Stain for Alkaline Phosphatase Activity

After removal from the scaffolds, C2C12 cells were also assayed for alkaline phosphatase activity using the method described in the materials and methods chapter (section 7.4.2). Briefly, cell cultures were fixed in 75% ethanol for 10 minutes and homogenized in 600 µl of distilled water containing 0.001% Tween detergent after 3 cycles of freeze-thawing. The substrate (p-nitrophenyl phosphate) (p-NPP) was added to equal volumes of the cell samples, incubated at 37°C for 1 hour and the rate of conversion into p-nitrophenol (p-NP) measured by a change in fluorescence at 405 nm. Values were compared against known p-NP standards with DNA correction.

As a further measure of the osteogenic status of C2C12 cells, a red color substrate was precipitated on the cells by the action of cellular alkaline phosphatase activity. The substrate system comprised of Napthol AS-MX buffer solution containing 1 mg/ml Fast Violet B salt, as described previously by Oreffo and co-workers (Oreffo *et al*, 1998). This technique is described in full in the materials and methods chapter (section 7.4.3).

4.3 Results & Discussion

4.3.1 Characterisation of $P_{DL}LA$ Scaffolds Fabricated in Supercritical CO_2

Polymer processing time limitations imposed by cell survival only permitted the fabrication of $P_{DL}LA$ scaffolds over 10, 30 and 60 seconds with an additional 80 seconds for compression and decompression. Cross sectional images of these $P_{DL}LA$ foams can be seen in figure 4-3. These images confirm that even over short $scCO_2$ exposure times, highly porous structures can be produced. These macroporous structures are highly heterogeneous with a non-uniform morphology. The SEM images in figure 4-4 also show that there are many closed pores indicating limited interconnectivity and little similarity in pore structure between the samples. This heterogeneity and limited interconnectivity is likely to be due to the limited processing pressure and perhaps more crucially, processing time (Goel & Beckman, 1994a, Parks *et al*, 1996). Despite this, the data in table 4-1 shows that the scaffolds have a high level of porosity (82-88%) with no significant difference between the scaffolds exposed to $scCO_2$ for 10, 30 and 60 seconds. The pore size measurements are in excess of 500 μm for each scaffold, providing large areas in which cells could attach and interact, although a lack of interconnectivity may restrict any interaction between pores. The mean pore size for each scaffold is highly variable, as previously suggested by the microscopic images and is partially dependent upon the method used to calculate it. The mean pore sizes calculated from μ-CT are lower than those observed on the SEM images. Because the μ-CT does not use a subjective method of calculating pore size, many of the smaller pores that are not visible on the SEM, have been included in the calculation. As a result, these pore size measurements are more likely to be an accurate representation of the actual values. The pore size distribution data in figures 4-5 & 4-6 indicates that there is a broad range of pore sizes with a lot of similarity in the patterns for both μ-CT and SEM data. Such a large pore size range is likely to be a result of the fast decompression rate, which has previously been shown to provide control over pore size and distribution (Howdle *et al*, 2001, Watson *et al*, 2002).

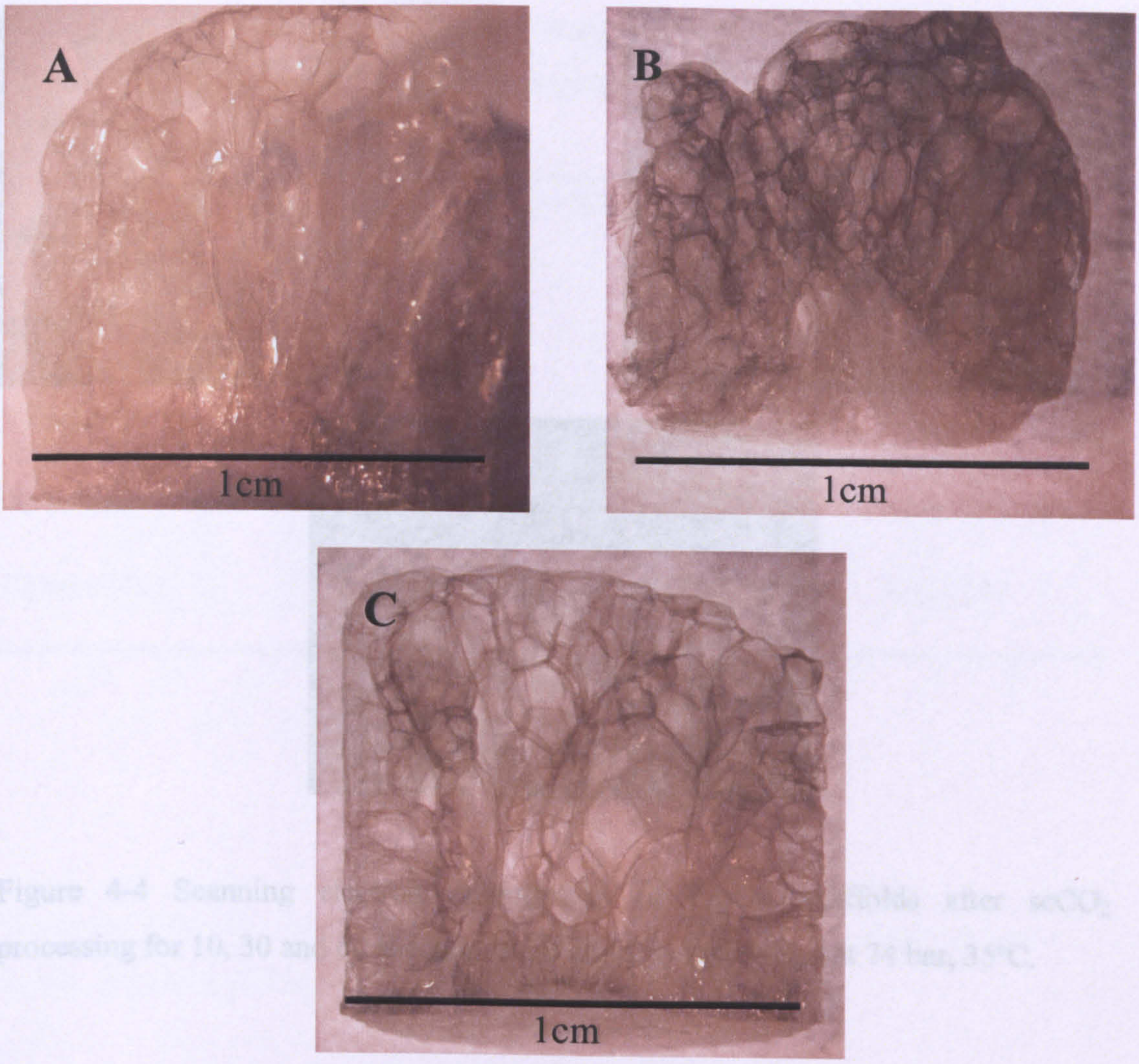

Figure 4-3 Images of $P_{DL}LA$ scaffolds taken using a light microscope after $scCO_2$ processing for 10, 30 and 60 seconds (A, B and C respectively) at 74 bar, 35°C.

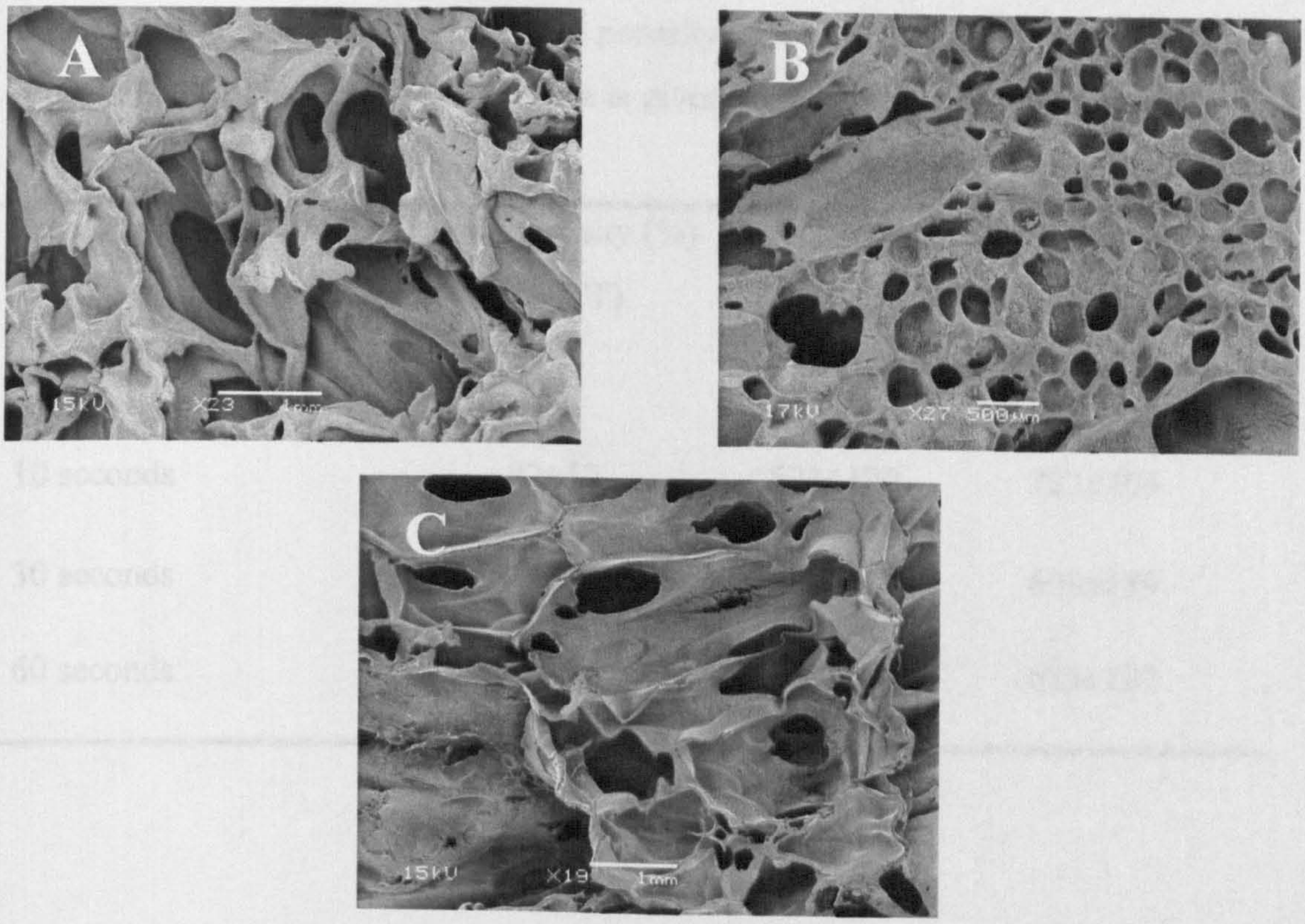

Figure 4-4 Scanning electron micrographs of $P_{DL}LA$ scaffolds after $scCO_2$ processing for 10, 30 and 60 seconds (A, B and C respectively) at 74 bar, 35°C.

Table 4-1 A summary of pore size and porosity data for $P_{DL}LA$ scaffolds after $scCO_2$ processing at 74 bar and 35°C. All data is given with standard deviation.

Processing time at 74 bar	Porosity (%) (μ-CT)	Average pore size μ-CT (μm)	Average pore size SEM (μm)
10 seconds	82±12	623±120	723±205
30 seconds	88±14	589±103	603±189
60 seconds	88±12	604±109	685±187

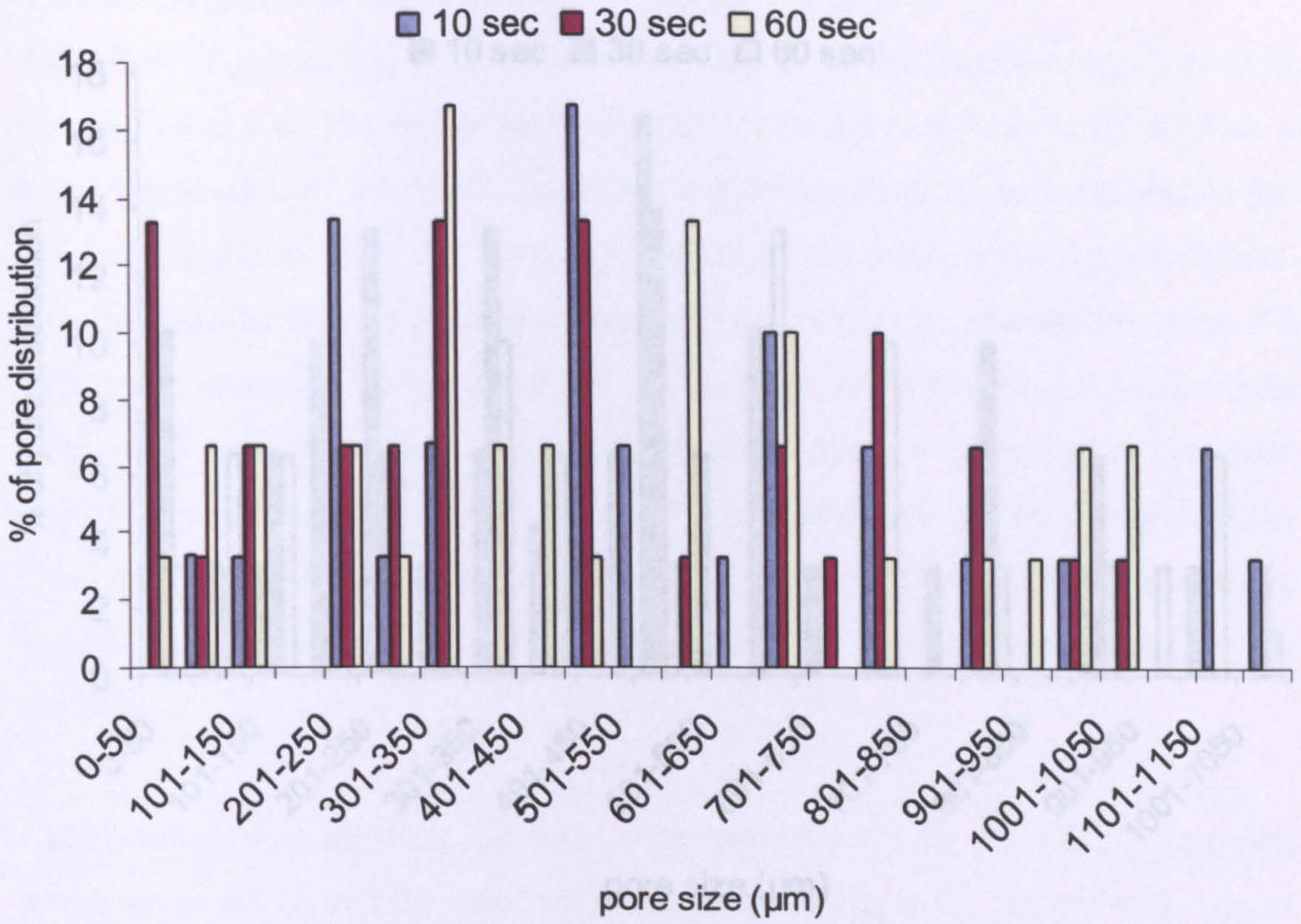

Figure 4-5 Pore size distributions calculated from SEM for $P_{DL}LA$ scaffolds after $scCO_2$ processing for up to 60 seconds at 74 bar, 35°C.

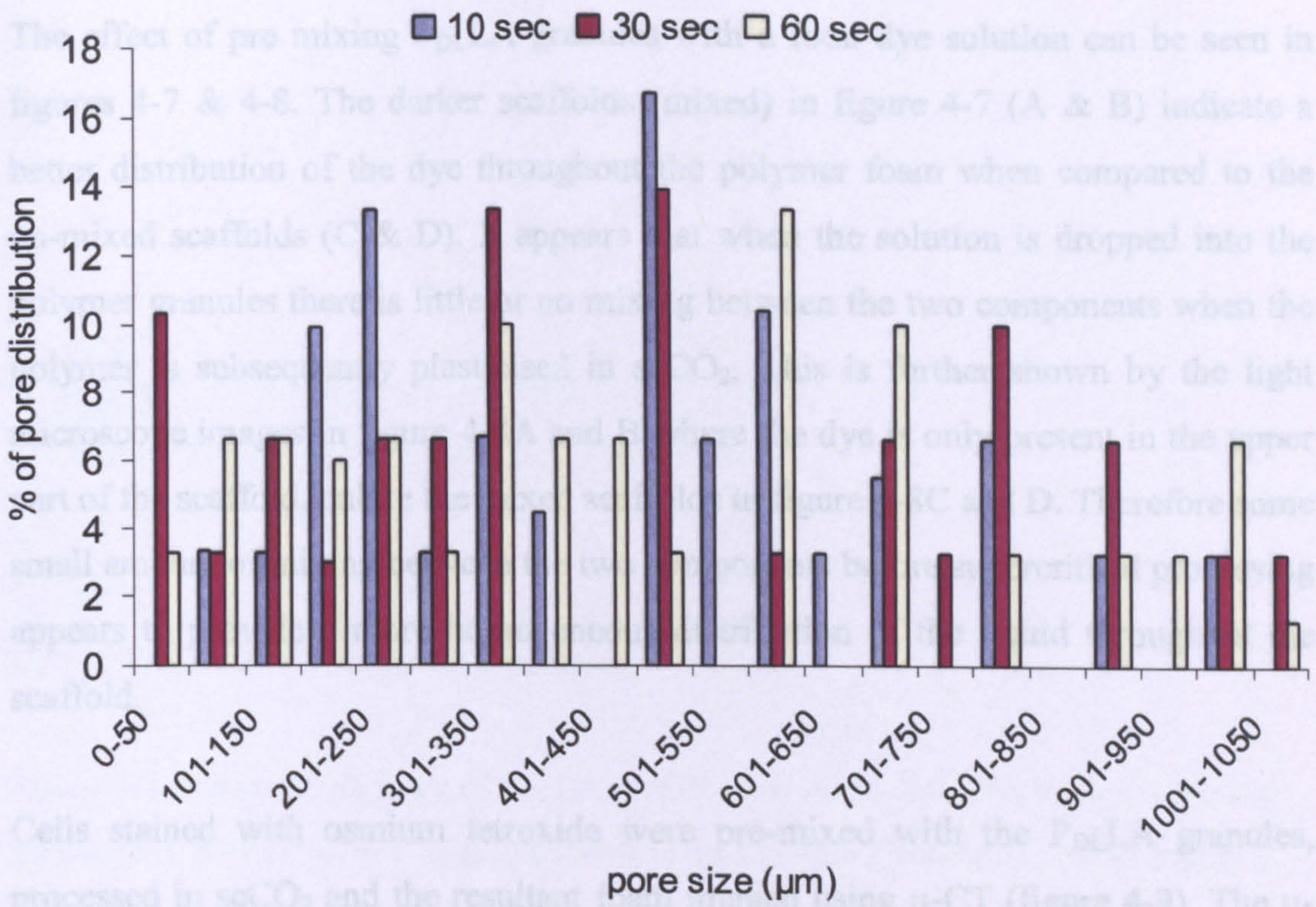

Figure 4-6 Pore size distributions calculated from µ-CT for $P_{DL}LA$ scaffolds after $scCO_2$ processing for up to 60 seconds at 74 bar, 35°C.

4.3.2 Investigation of the Polymer/Cell Mixing Technique

The effect of pre mixing $P_{DL}LA$ granules with a food dye solution can be seen in figures 4-7 & 4-8. The darker scaffolds (mixed) in figure 4-7 (A & B) indicate a better distribution of the dye throughout the polymer foam when compared to the un-mixed scaffolds (C & D). It appears that when the solution is dropped into the polymer granules there is little or no mixing between the two components when the polymer is subsequently plasticised in $scCO_2$. This is further shown by the light microscope images in figure 4-8A and B where the dye is only present in the upper part of the scaffold, unlike the mixed scaffolds in figure 4-8C and D. Therefore some small amount of mixing between the two components before supercritical processing appears to provide a more homogeneous distribution of the liquid throughout the scaffold.

Cells stained with osmium tetroxide were pre-mixed with the $P_{DL}LA$ granules, processed in $scCO_2$ and the resultant foam imaged using μ-CT (figure 4-9). The μ-CT image of a cross section through the porous scaffold (on the left) shows that the cells (on the right) are well distributed throughout the structure. A greater proportion of the cells appear to be present at the base of the scaffold which is most likely a result of gravity and the foaming of the scaffold over the top of the suspension.

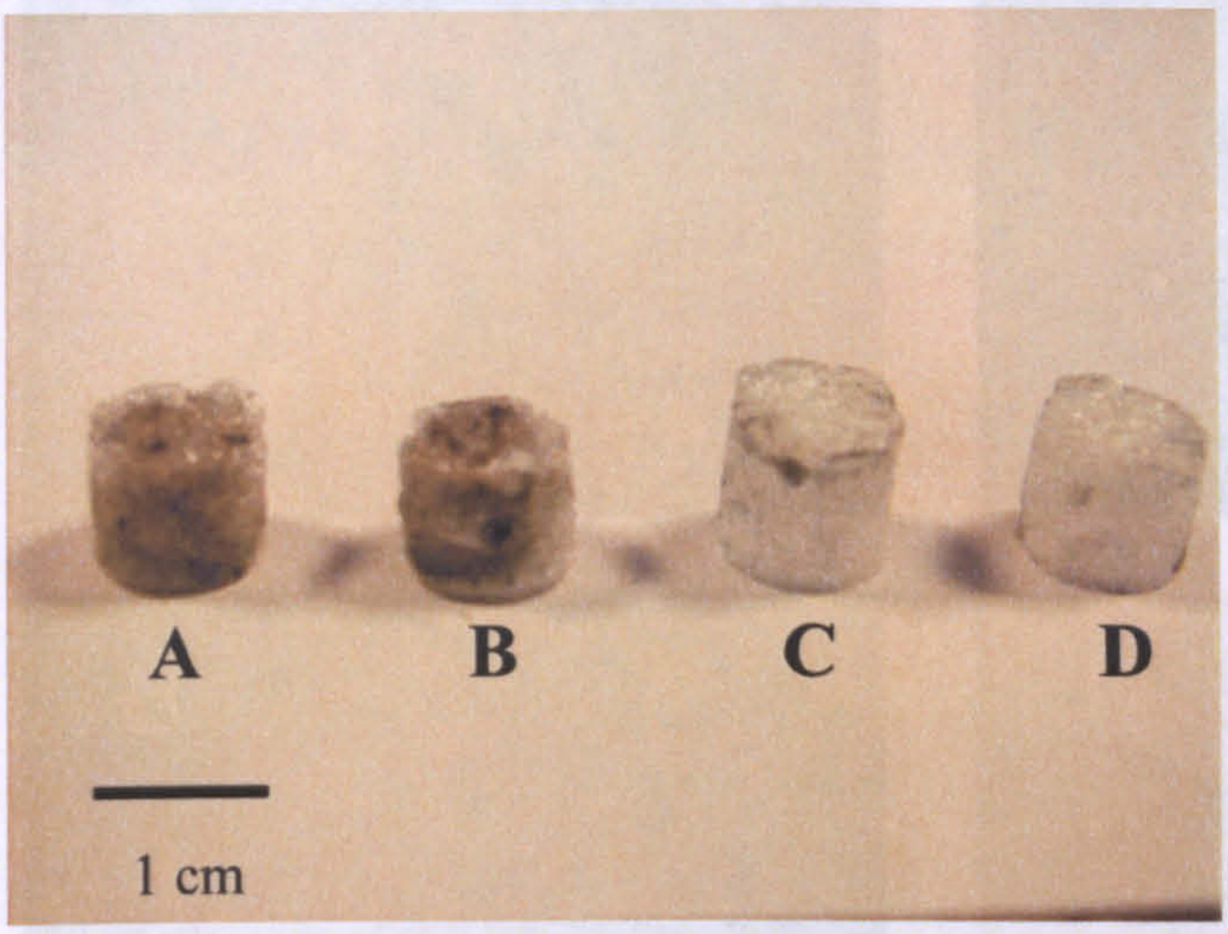

Figure 4-7 Gross morphology of $P_{DL}LA$ scaffolds showing the effects of pre-mixing the polymer powder with a food dye solution on the final distribution of the liquid in the foamed scaffold. Scaffolds A & B show the result of pre-mixing the two components whereas scaffolds C & D show the final scaffolds after no pre-mixing took place.

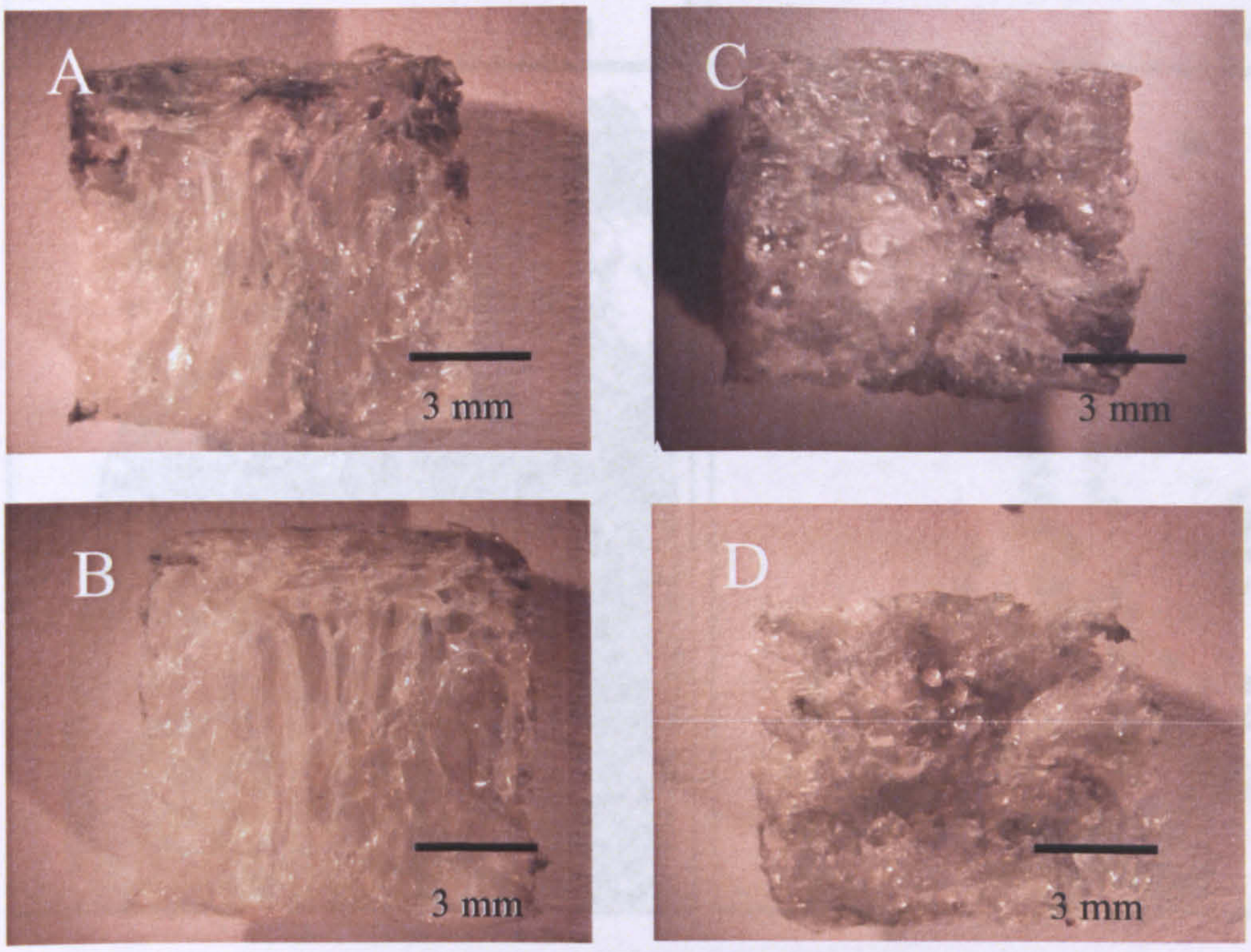

Figure 4-8 Cross-sections of pre-mixed and unmixed $P_{DL}LA$/food dye scaffolds as viewed on the light microscope. The dark areas at the top of scaffolds A & B (unmixed) indicate the need for pre-mixing the solution with the polymer as shown in scaffolds C & D where there are clear patches of black dye present in the central areas of the structures.

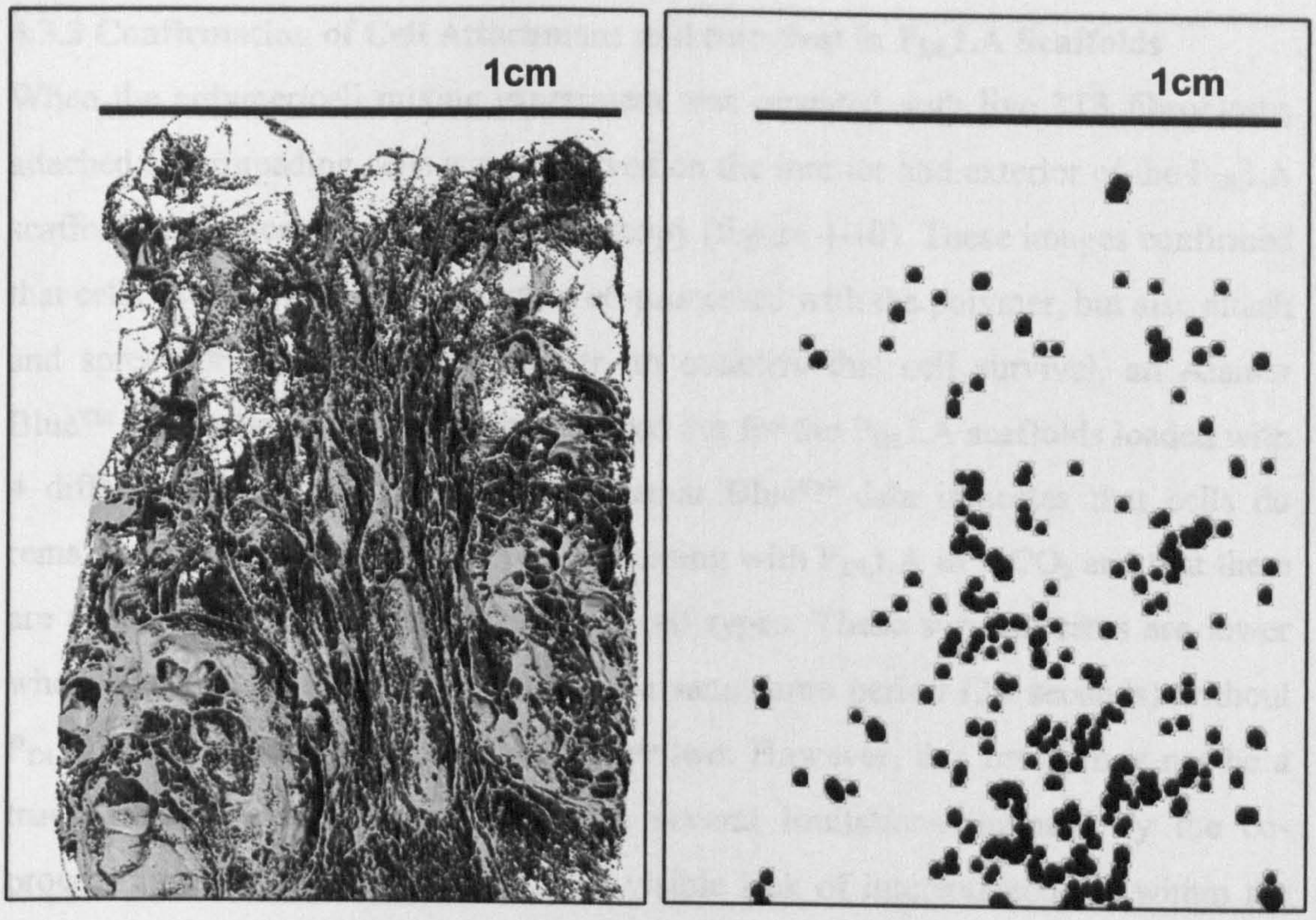

Figure 4-9 Distribution of pre-mixed, osmium stained cells (right) in a $P_{DL}LA$ scaffold (left). Note: the cells have been visually enhanced to show the distribution more clearly.

4.3.3 Confirmation of Cell Attachment and Survival in $P_{DL}LA$ Scaffolds

When the polymer/cell mixing experiment was repeated with live 3T3 fibroblasts, attached and spreading cells were observed on the interior and exterior of the $P_{DL}LA$ scaffolds using scanning electron microscopy (figure 4-10). These images confirmed that cells could not only survive when co-processed with the polymer, but also attach and spread on the surfaces. However, to quantify this cell survival, an Alamar Blue™ metabolic activity assay was carried out for the $P_{DL}LA$ scaffolds loaded with 4 different cell types (figure 4-11). Alamar Blue™ data indicates that cells do remain metabolically active after co-processing with $P_{DL}LA$ in $scCO_2$ and that there are no obvious differences between the cell types. These survival rates are lower when than that of cells processed for the same time period (30 seconds) without $P_{DL}LA$ as previously discussed in chapter two. However, this result may not be a true indication of cell survival due to several limitations imposed by the co-processing of the polymer and cells. A visible lack of interconnectivity within the scaffolds caused by the formation of closed pores may have limited the cells contact with the Alamar Blue™ solution. In addition, the physical process of cutting the scaffolds before cell attachment may have reduced the cell numbers. The control cell samples were not co-processed with the polymer and did therefore not suffer from any of these limitations, possibly skewing the cell survival rates further.

As an additional method of confirming metabolic activity in the short term and in the long term, $P_{DL}LA$ scaffolds loaded with C2C12 cells were cultured in the LIVE/DEAD™ stain after supercritical processing (figure 4-12). The images taken at 24 hours and 6 weeks clearly show a large population of live cells (green) after processing into $P_{DL}LA$ scaffolds. Histological sections of cell loaded scaffolds show that this survival and distribution is not restricted to the outer surfaces of the scaffolds (see figure 4-13). Sections stained for (A) propidium iodide and (B) LIVE/DEAD™ indicate the presence of both cell nuclei and live cells respectively, on the internal surfaces of the scaffolds.

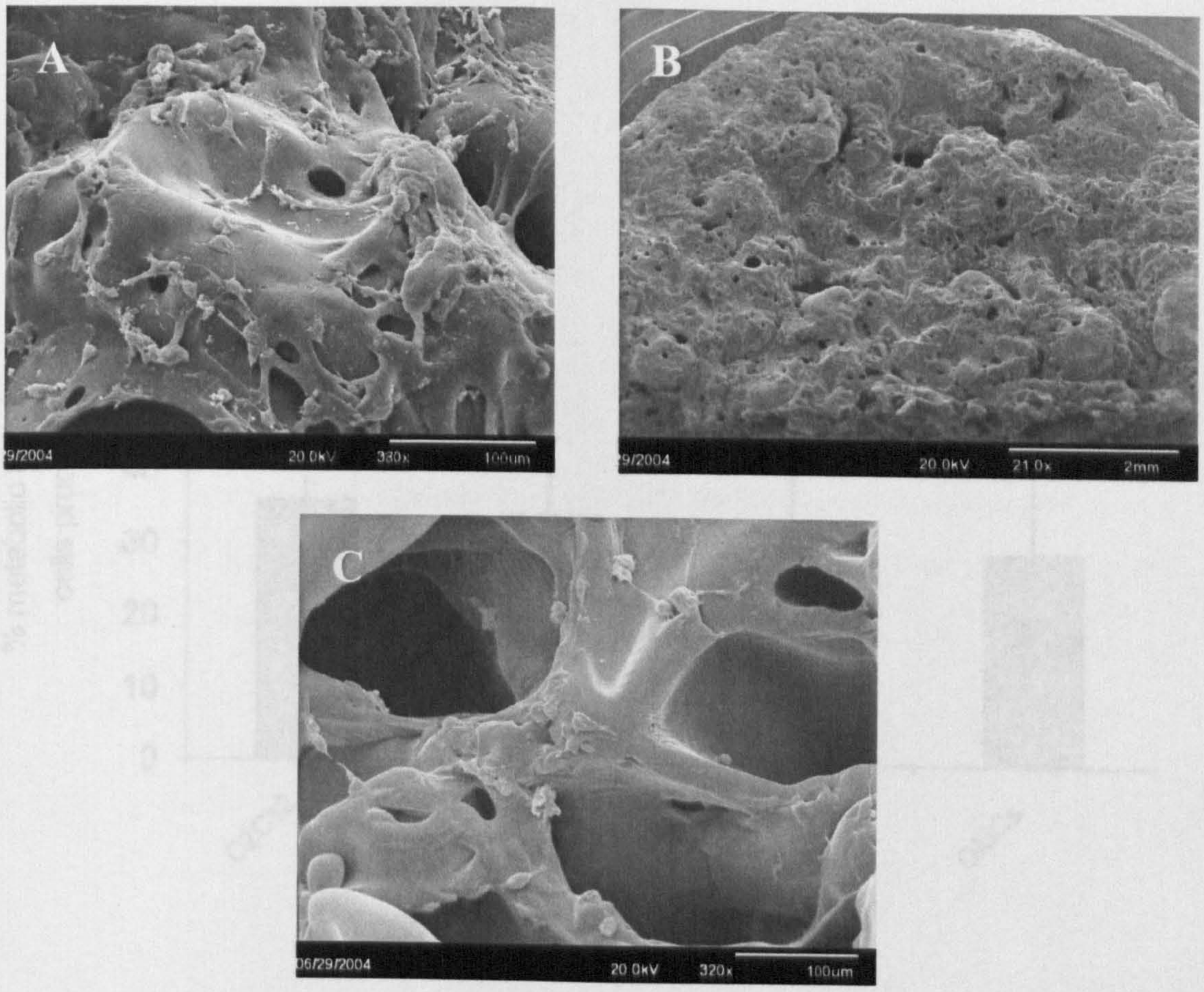

Figure 4-10 SEM images of 3T3 fibroblasts spreading on $P_{DL}LA$ scaffolds. These images clearly show that the cells are attached to both the external (A & B) and internal (C) surfaces.

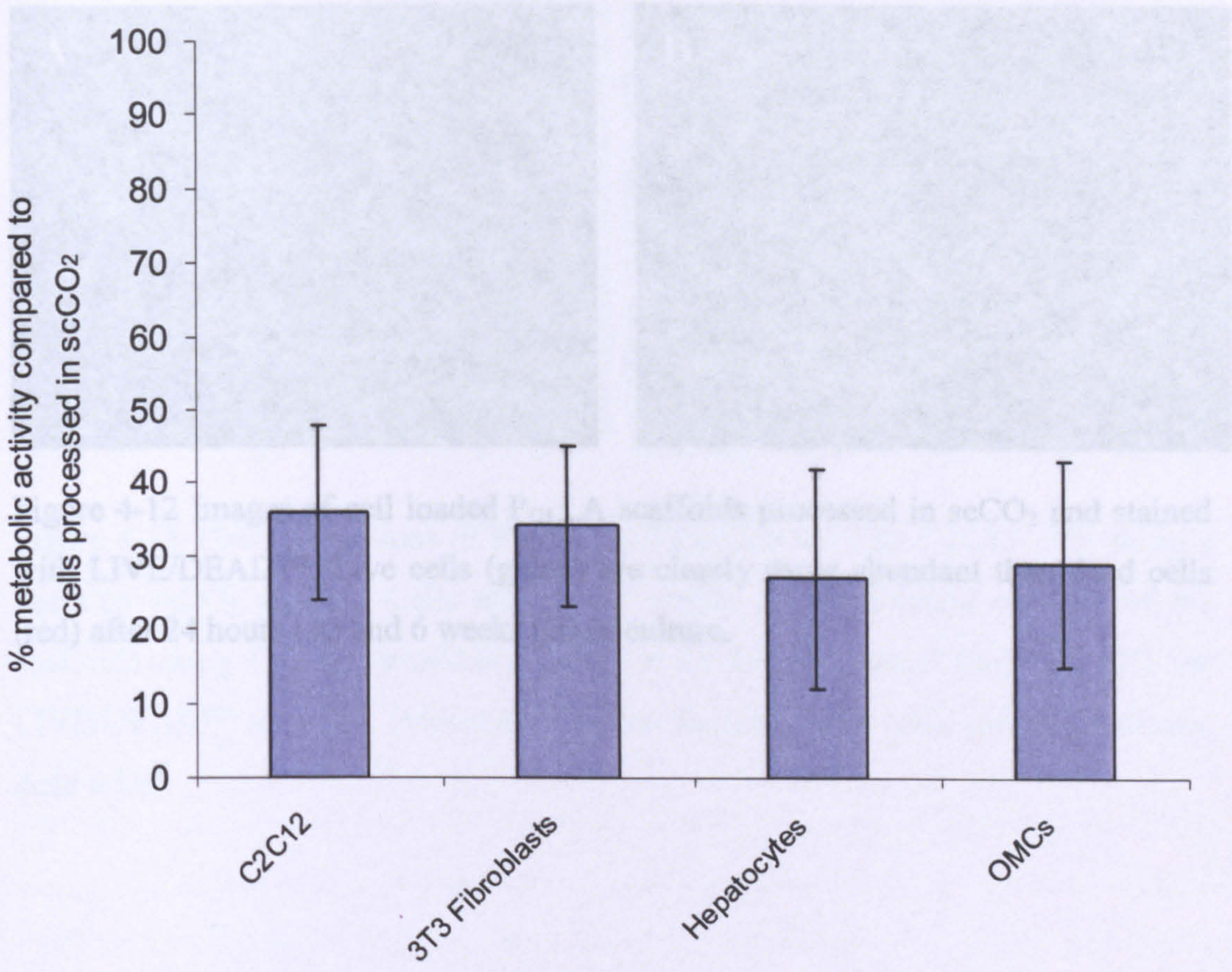

Figure 4-11 Survival data for four cell types after processing into $P_{DL}LA$ scaffolds using $scCO_2$ for 30 seconds as measured by an Alamar Blue assay. Mean (n=4) ± SD.

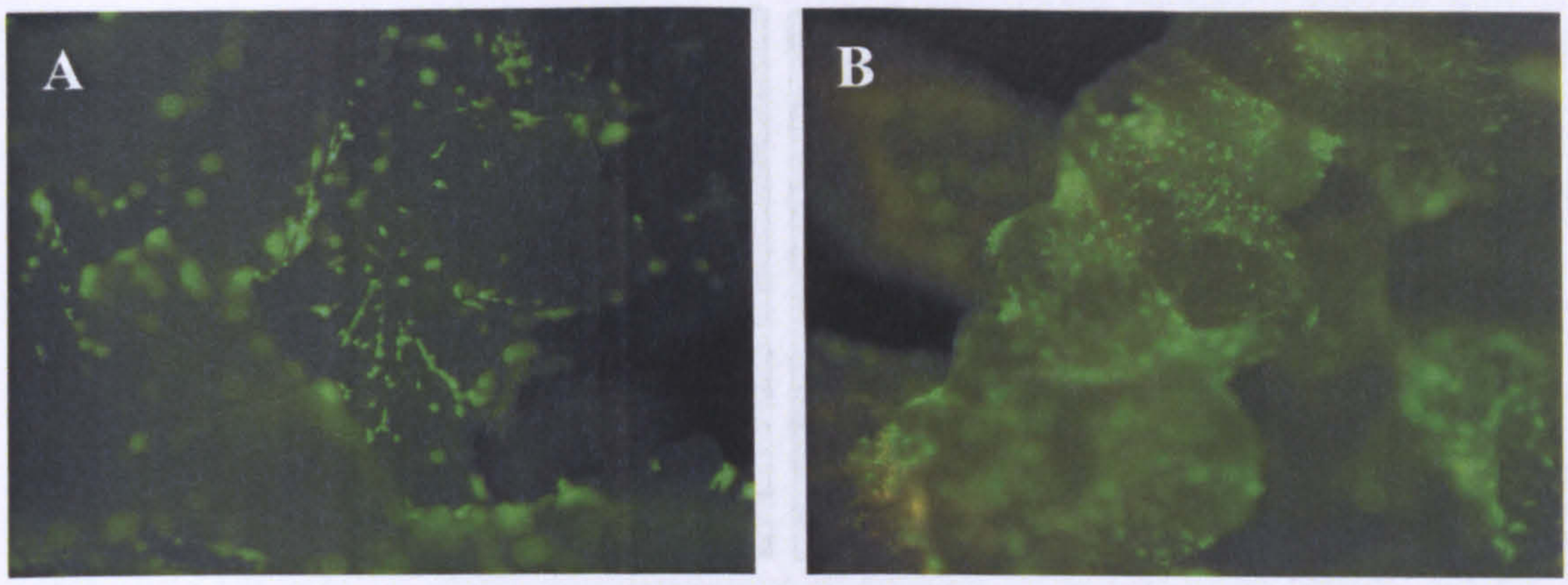

Figure 4-12 Images of cell loaded $P_{DL}LA$ scaffolds processed in $scCO_2$ and stained with LIVE/DEAD™. Live cells (green) are clearly more abundant than dead cells (red) after 24 hours (A) and 6 weeks (B) in culture.

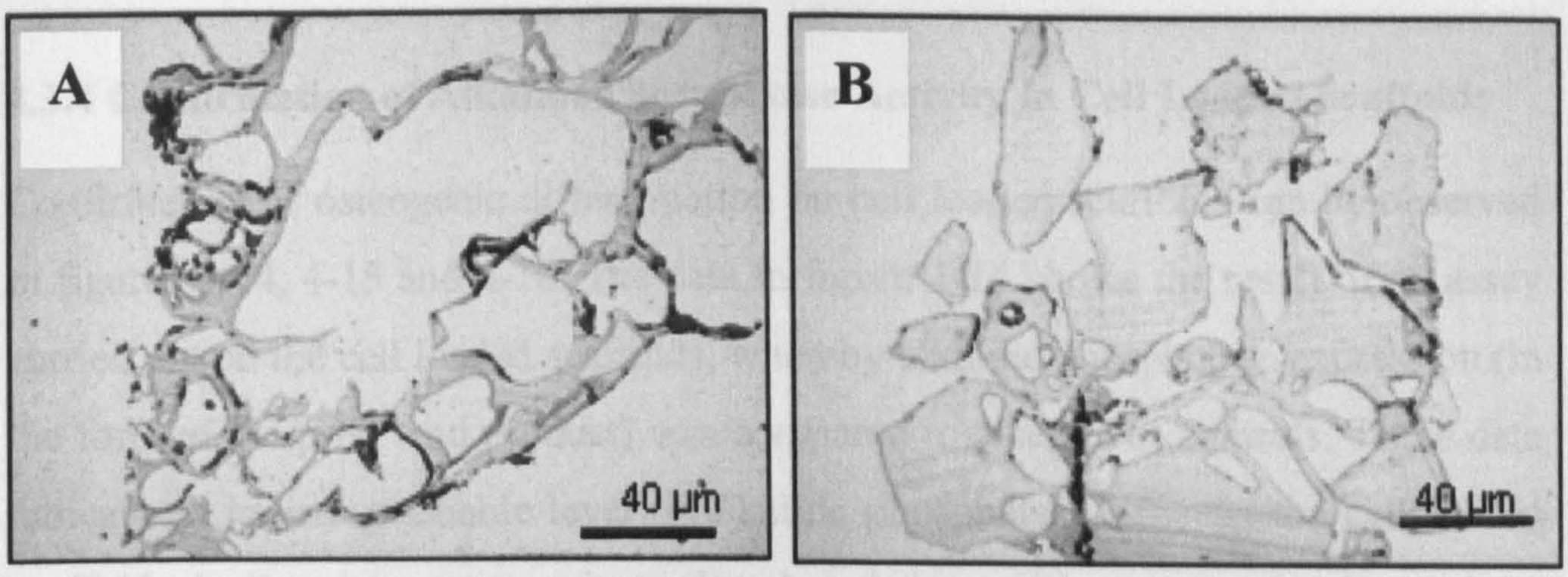

Figure 4-13 Thin cut sections of $P_{DL}LA$ scaffolds loaded with C2C12 cells using a one-step $scCO_2$ process. Cells are clearly visible on the internal surfaces of the scaffolds using (A) the propidium iodide stain for cell nuclei (red) and (B) the LIVE/DEAD™ stain for cytotoxicity (green indicates live cells and red indicates dead cells).

4.3.4 Confirmation of Alkaline Phosphatase Activity in Cell Loaded Scaffolds

Confirmation of osteogenic differentiation on cell loaded scaffolds can be observed in figures 4-14, 4-15 and 4-16. The data in figure 4-14 shows the result of an assay carried out on the cell loaded scaffolds, whereby alkaline phosphatase expression (in the form of the p-NP end product) was compared to a series of controls. These data indicate an indistinguishable level of alkaline phosphatase between the cell-loaded scaffolds (cultured in osteogenic medium) and the $scCO_2$ processed cells without $P_{DL}LA$. This suggests that presence of the polymer did not impair cellular alkaline phosphatase activity any more than the effects of $scCO_2$ alone (when corrected to the levels of DNA retrieved). An alternative method that has already been used to successfully control the release of proteins including BMP-2 (Howdle *et al*, 2001, Yang *et al*, 2003) was also used to induce osteogenic differentiation on $P_{DL}LA$ scaffolds. Here the BMP-2 was adsorbed onto the $P_{DL}LA$ powder and pre-mixed with C2C12 cells before processing into porous foams using $scCO_2$. The levels of alkaline phosphatase activity in these scaffolds are significantly lower than in the scaffolds that were cultured in an osteogenic medium (figure 4-14). The images in figures 4-15 and 4-16 further demonstrate this reduced osteogenic effect, with visibly less red-stained areas in the BMP-2 loaded scaffolds. This would further indicate that the technique of adsorbing the protein onto the $P_{DL}LA$ and thus, allowing release to be controlled by the porous structure, induces a reduced osteogenic response. However, this has previously been shown to be a very effective method of inducing an osteogenic response from $P_{DL}LA$ scaffolds as the BMP-2 activity is not significantly reduced by the $scCO_2$ process (Yang *et al*, 2003b, Yang *et al*, 2004). It is possible that the limitations of the $P_{DL}LA$ scaffolds made using the truncated processing times (as previously discussed) have prevented BMP-2 gaining sufficient access to the cell population to induce the same osteogenic response.

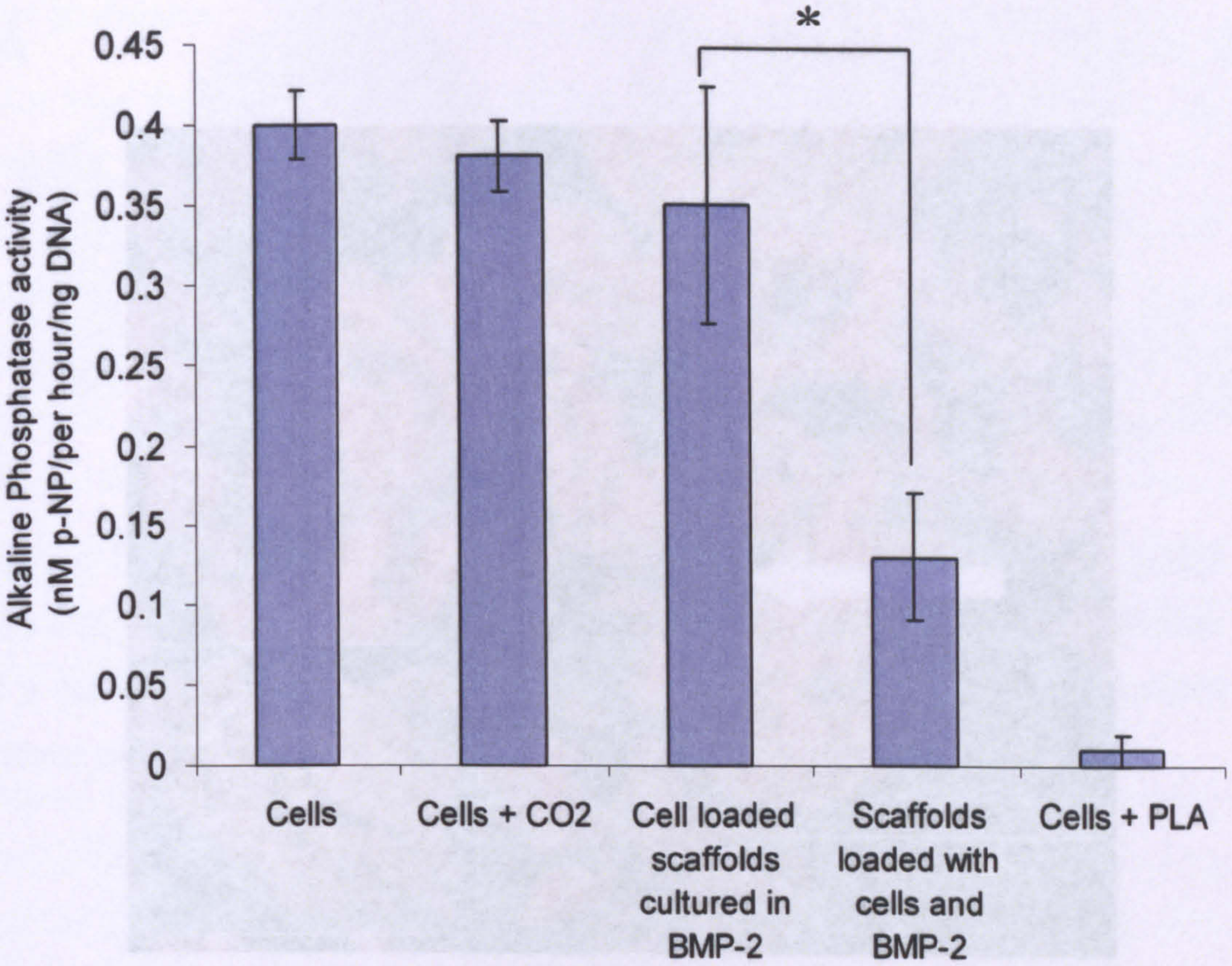

Figure 4-14 Confirmation of alkaline phosphatase activity in $P_{DL}LA$ scaffolds loaded with C2C12 cells using a one-step scCO2 process after induction into the osteogenic lineage with 500 ng/ml rhBMP-2. Mean (n=3) ± SD. * indicates $p<0.05$ using T-test.

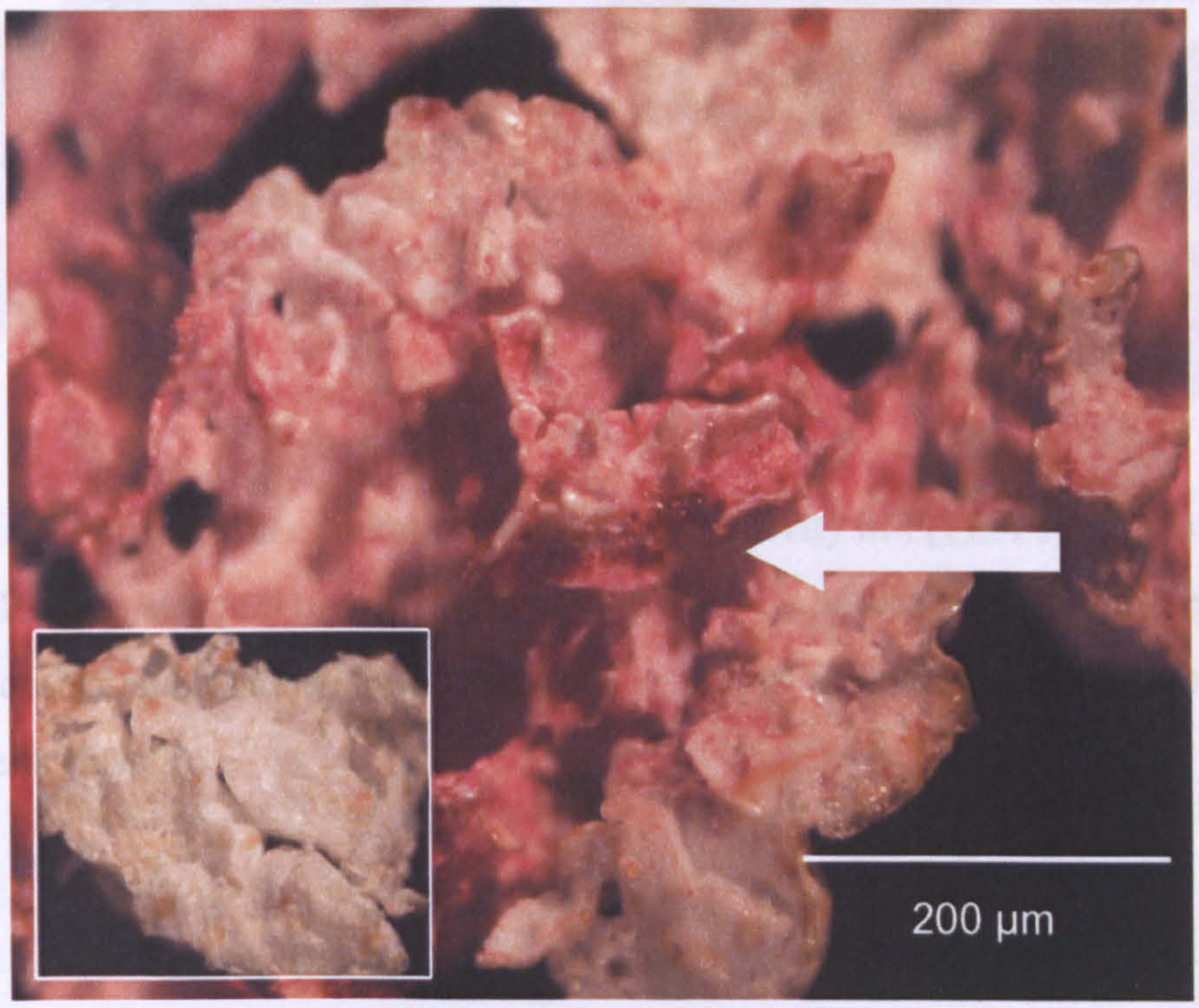

Figure 4-15 Visual confirmation of alkaline phosphatase activity in $P_{DL}LA$ scaffolds loaded with C2C12 cells using $scCO_2$ after subsequent osteogenic culture in 500 ng/ml rhBMP-2. Alkaline phosphatase activity is shown by the precipitation of a red colour substrate indicated by the arrow, compared to a scaffold without cells (inset).

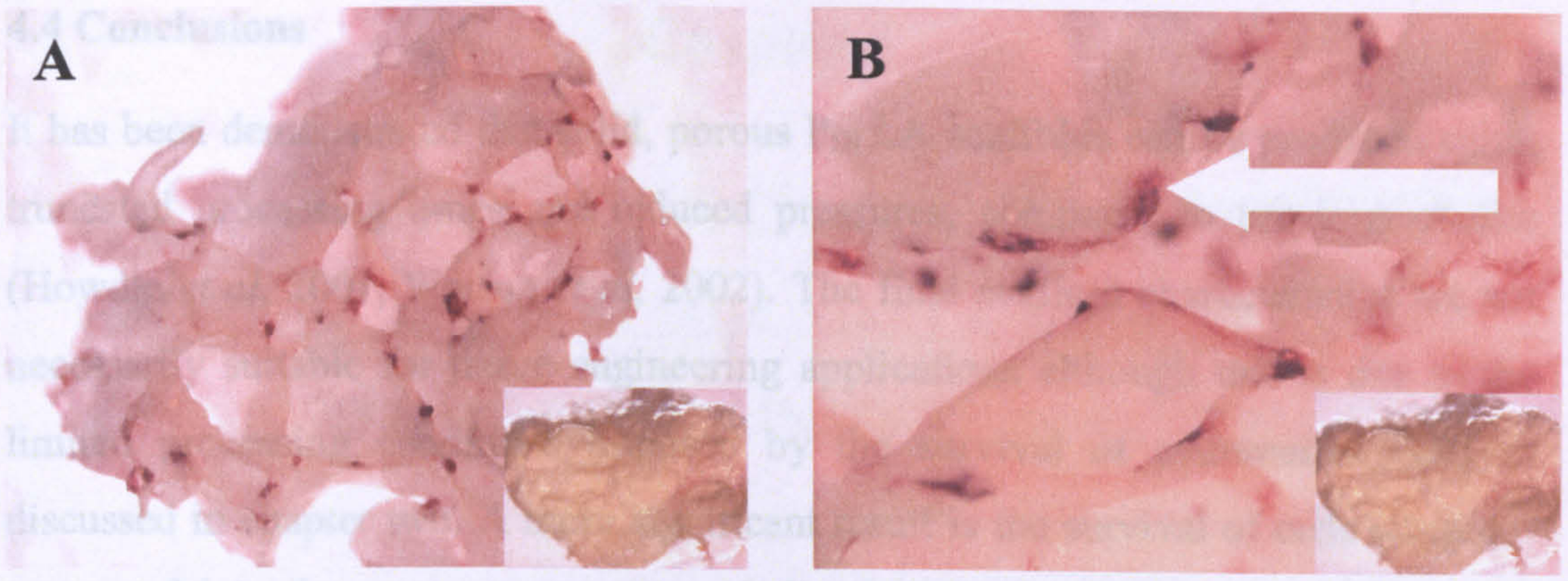

Figure 4-16 Confirmation of alkaline phosphatase activity in $P_{DL}LA$ scaffolds loaded with C2C12 cells and 500 ng of rhBMP-2 using $scCO_2$ processing. The precipitation of a red colour substrate is indicated by the arrow and compared to a scaffold without cells (inset).

4.4 Conclusions

It has been demonstrated that solid, porous $P_{DL}LA$ scaffolds can be produced using truncated processing times and reduced pressures, compared to previous studies (Howdle *et al*, 2001, Watson *et al*, 2002). The final scaffold characteristics are not necessarily suitable for tissue engineering applications although this is due to the limited processing conditions imposed by the survival of mammalian cells as discussed in chapter two. A more significant result is the survival of cells when co-processed into these porous structures, indicating the feasibility of a $scCO_2$-based one-step scaffold seeding process. In addition to surviving the process, the cells were also shown to be evenly distributed throughout the porous scaffolds despite minimal levels of mixing.

Perhaps most remarkably, the attached C2C12 cells have been able to undergo osteogenic differentiation when prompted with BMP-2 before and after processing into the $P_{DL}LA$ scaffold. Thus, it has been shown that growth factors, mammalian cells and polymer powder can be processed into 3D, cell loaded constructs by using a single $scCO_2$ processing step. By addressing the limitations of the polymer processing time, this method could be used to produce cell loaded scaffolds for tissue engineering purposes. In this way, the exposure of the cells to the $scCO_2$ must be minimised, whereas the exposure of the polymer needs to be maximised. This way, the scaffold properties can be tuned to fit the application and cell survival is optimised. This could not be achieved with the equipment used thus far. Therefore some modification to the high pressure apparatus was required to facilitate this.

Chapter 5

PASSING MAMMALIAN CELLS INTO PLASTICISED POLY(DL-LACTIC ACID) USING A HIGH PRESSURE CARBON DIOXIDE INJECTION SYSTEM

5.1 Introduction

When fabricating scaffolds using $scCO_2$, both the pressure and the exposure time are directly linked to the level of porosity and interconnectivity in porous polymer materials as previously discussed (Goel & Beckman, 1994a, Goel & Beckman, 1994b, Park *et al*, 1995, Baldwin *et al*, 1995). By increasing the pressure/processing time, the level of soluble gas molecules in the polymer can also be increased, preventing the depletion of dissolved gas in the regions around the nucleating pores and allowing the pores to become interconnected during decompression. These are desirable properties in tissue engineering scaffolds as they permit cellular interaction and the passage of nutrients to surrounding cells and tissues (Mooney *et al*, 1996). It was therefore important to devise a new method of delivering the cells to the polymer at a later stage of the fabrication process. This would allow the polymer processing time to be extended indefinitely and the exposure of cells to high pressure CO_2 to be minimised. Thus, a new piece of equipment had to be designed in order to achieve this.

5.1.1 Designing the Cell Injection System

The equipment used for the cell injection system was based on the high pressure CO_2 apparatus already used in this study. The cells and the polymer were still processed together inside a 60 ml pressure vessel before controlled decompression with a back pressure regulator. However, a mechanism for delivering the cells into the pressure vessel was required along with the apparatus to facilitate this. As a result, there were three main challenges associated with delivering the cells into a high pressure environment, as described overleaf.

1. The cells had to be delivered into the polymer under pressure (in a plasticised state). This involved using a mechanism of delivery that would allow the cells to be passed from atmospheric pressure into the pressurised vessel. This had to be carried out without compromising both safety and cell survival.
2. Once inside the vessel, the cells had to be delivered to, and penetrate, the surface of the plasticised polymer which was likely to be considerably more viscous than the cell suspension.
3. The cell/polymer mixture had to be contained within a suitable mould that would allow the quick and easy removal of the cell loaded scaffolds upon decompression.

Points one and two provided the biggest challenge due to the delicate nature of the cells. Therefore, to avoid any further complications it was decided that high pressure gas should be used to inject the cells into the vessel. The theory was that by storing a reservoir of CO_2 or N_2 set at a higher pressure than that in the vessel containing the plasticised polymer, the pressure differential would force the cell suspension into the vessel through a piece of tubing. Because frequent re-designing and building of the apparatus was required in this chapter, many small changes were made to the experimental methods along the way. Therefore, the whole process was split into the three distinct stages with each step broken down for optimisation. The original set up for the high pressure injection equipment can be seen in figure 5-1.

5.1.2 Aims

The central aim of this final experimental chapter was to provide evidence for a new technique that would allow mammalian cells to be incorporated into the scaffold fabrication step with cell survival and functionality retained in the final foamed structure. Within this main aim, there were three smaller objectives; (i) to show that this mechanism can be used to deliver cells efficiently into the desired mould, (ii) to show that cells can survive and retain important aspects of functionality despite this high pressure injection process and (iii) to provide evidence for continued cell survival/functionality within the foamed scaffold.

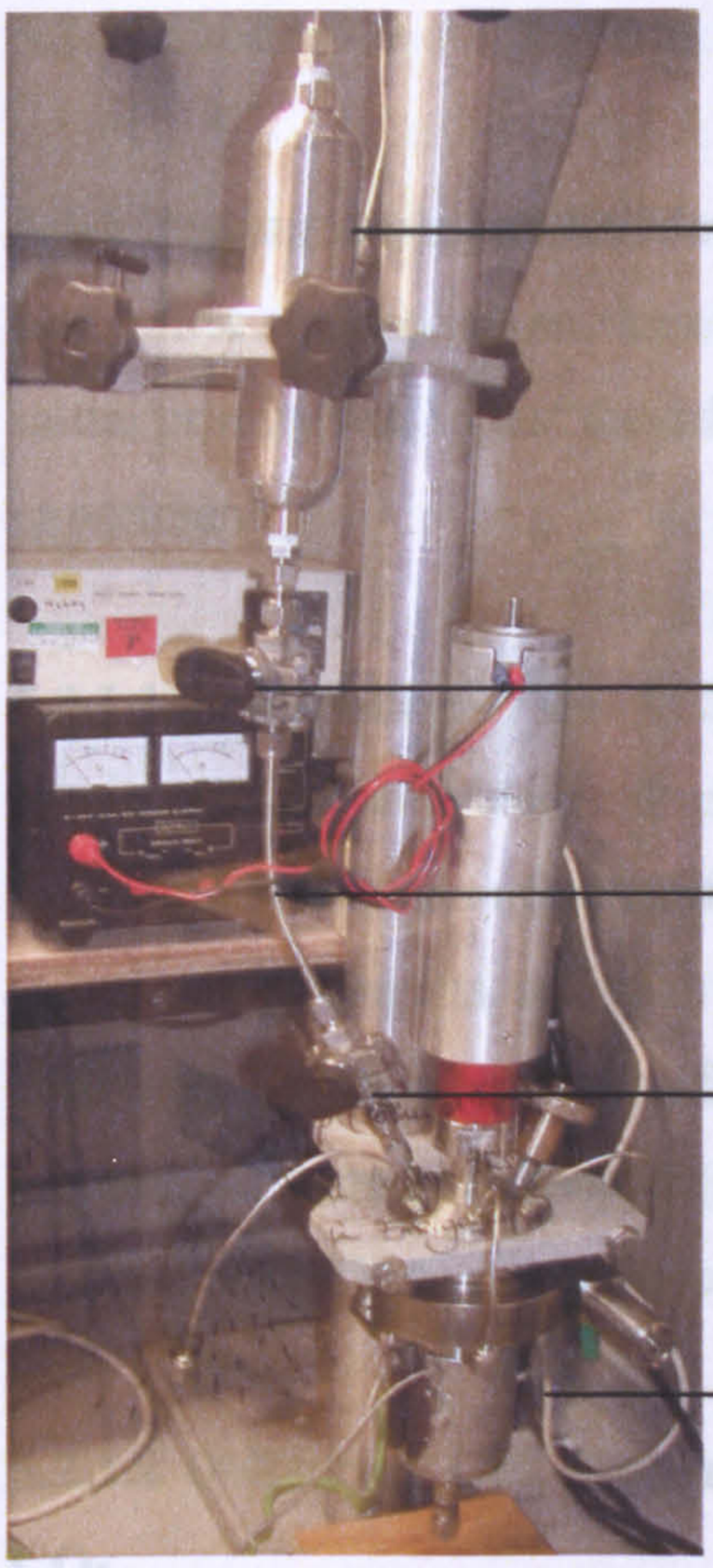

Figure 5-1 Original set-up for the high pressure CO_2 injection system. The gas reservoir was pressurised along with the 60 ml collection vessel. The cell suspension was stored in the ¼ inch stainless steel sample tubing before being injected into the high pressure vessel by opening valves A and B and passing through the ¼ inch tubing. Once inside the vessel, the pressure was quenched and the cell suspension collected.

5.2 Methods

5.2.1 Testing the Injection Mechanism with Dead Cells

In the first of three sub sections describing the progression of this technique, the initial priority was to test the delivery mechanism with a series of simple experiments.

5.2.1.1 Preparation of Dead C2C12 Cells for Injection Experiments

Murine C2C12 cells were cultured as described in the materials and methods chapter (section 7.1.1) over a number of weeks with all dead cells collected and kept for trial injection experiments. A trypan blue cell count was carried out to confirm that the cells were both dead and in sufficient number for the experiment as described in the materials and methods chapter (section 7.1.3). These cells were re-suspended in complete DMEM to retain the correct viscosity of a live cell suspension.

5.2.1.2 Delivering Cell Suspensions into the 60 ml Vessel using High Pressure CO_2

In order to show that liquids can be passed through the tubing and reach the collection vessel with the use of high pressure, it was important to carry out a simple experiment using a liquid suspension. Dead C2C12 cells (250,000) were added to 200 µl of DMEM in order to make a realistic suspension that could be passed through the injection system. The cells were added to the sample tubing and the valves either side closed. The vessel was heated to 35°C and kept at atmospheric pressure. The gas reservoir was then pressurised with 5, 37 and 74 bars of CO_2 and the valves opened sequentially (A then B) to allow the CO_2 to pass through the sample tubing and pass into the vessel, carrying the dead cell suspension. The system was decompressed immediately and the volume of liquid retrieved from the vessel was then recorded as a mean percentage of the initial volume.

5.2.1.3 Delivering Cell Suspensions into a High Pressure CO_2 Environment

To find the minimum pressure differential required to allow the cells to reach the vessel the cells were injected at three different pressures with the pressure in the collection vessel altered accordingly. Dead C2C12 cells (250,000) were suspended in 200 µl DMEM and added to the sample tubing and the gas reservoir was pressurised to 5, 37 and 74 bars of CO_2 as in 5.2.1.2 The pressure inside the vessel was increased to equal that of inside the injection reservoir and then reduced to pressures that were 1 and 5 bars lower (see processing matrix - table 5-1). The vessel was heated to 35°C and the cell suspension was then injected at each pressure by opening the 2 valves sequentially (A then B). The valves were then closed and the decompression stage (40 seconds) was started after 10 seconds at maximum pressure. The volume of liquid retrieved from the vessel was then recorded as a percentage of the initial volume injected.

Table 5-1 Processing matrix for the injection of cells into reduced pressures with CO_2.

Injection pressure (bar)	Vessel pressure -1 (bar)	Vessel pressure -5 (bar)
5	4	0
37	36	32
74	73	69

5.2.1.4 Delivering Cell Suspensions into a Collection Mould using High Pressure CO_2

Although a 60 ml vessel was used in the previous experiment, it was considered that such a relatively large volume may be an inefficient way to collect the sample, with to large a surface area. Therefore, it was decided that a smaller collection mould would be beneficial in terms of retaining the maximum amount of cell suspension after injection. It also facilitates the formation of a $P_{DL}LA$ scaffold with the desired morphology by restricting the foaming to a pre-defined shape. For these reasons, the equipment was modified in order to facilitate a collection mould (see figure 5-2). A thick walled mould was designed from PTFE (see figure 5-3) to provide a collection volume of 15 ml. It was considered that the hydrophobic surface combined with the smaller volume would facilitate improved sample recovery. A piece of ⅛" piping was passed down through a drilled hole (3 mm wide at the top) in the thick surrounding wall of the mould to allow the cell suspension to reach the bottom of the mould. Furthermore, the bottom of the mould was removable to allow easy sample collection after decompression. The mould was then placed into the vessel and the dead C2C12 cells (250,000 suspended in 200 µl DMEM) were loaded into the sample tubing. A pressure difference of one bar was used between sample injection (5, 37 and 74 bar) and the collection vessel (4, 36, 73 bar). The collection vessel was heated to 35°C and the cell suspension was then injected at each pressure by opening the two valves (A & B). The valves were then closed and after 10 seconds at maximum pressure, the system was decompressed over 40 seconds. The volume of liquid retrieved from the vessel was then recorded as a percentage of the initial volume injected.

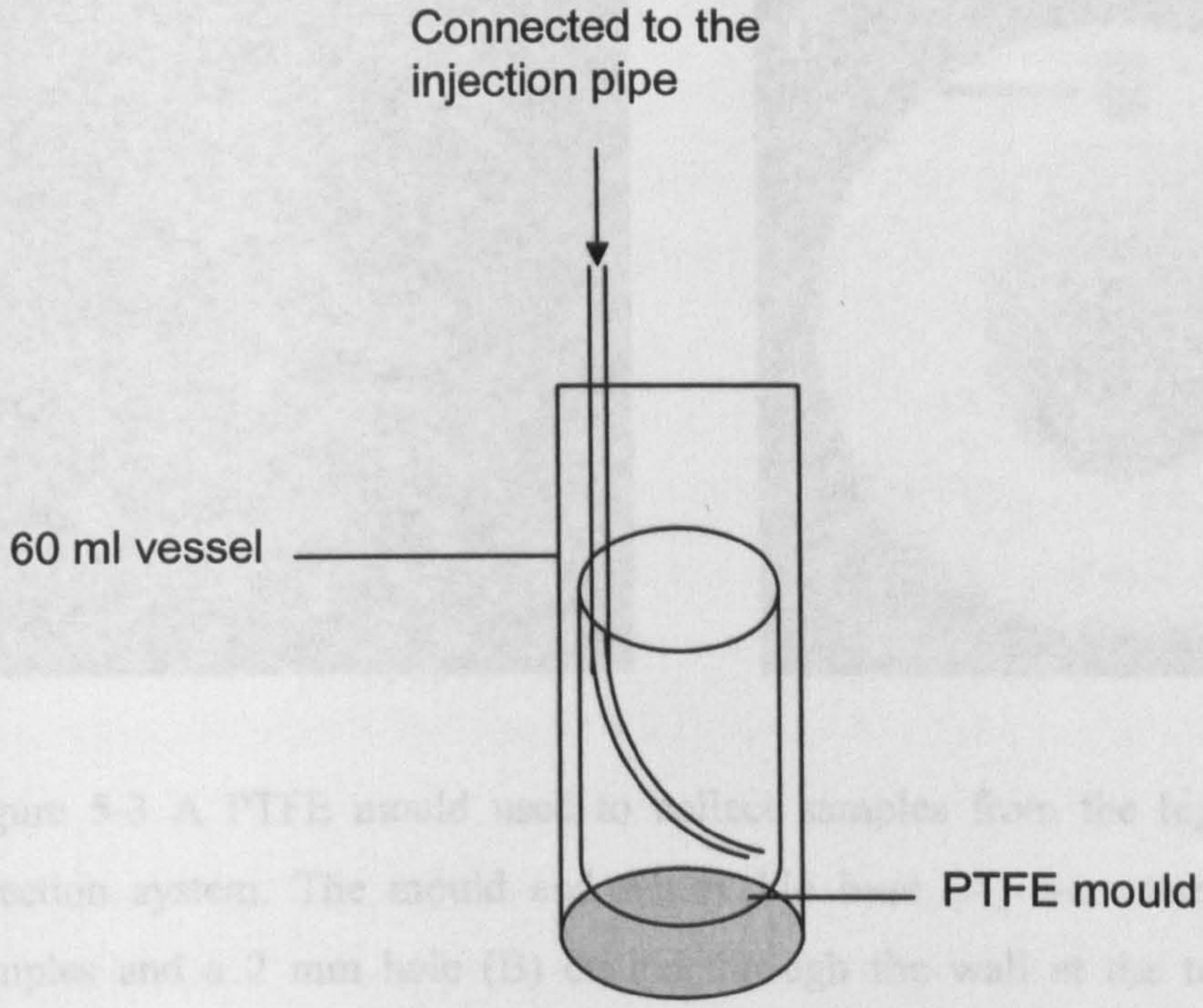

Figure 5-2 Modifications made to the high pressure CO_2 injection system in order to incorporate a collection mould. The bottom of the mould had a diameter of 15 mm with a think wall surrounding it through which the cell delivery tubing was passed.

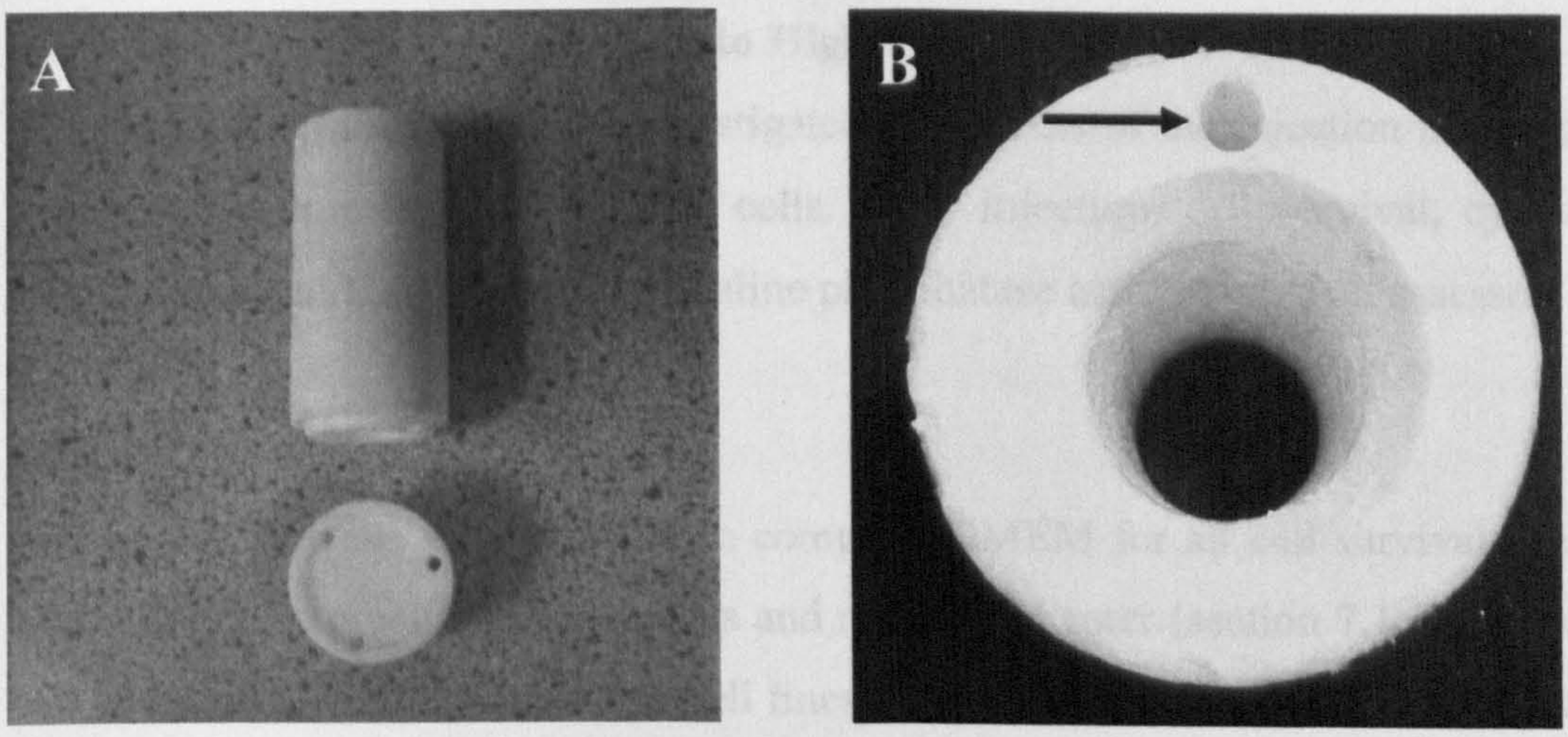

Figure 5-3 A PTFE mould used to collect samples from the high pressure CO_2 injection system. The mould and removable base (A) were used to collect the samples and a 2 mm hole (B) drilled through the wall at the top of the mould allowed the passage of the cell suspension into the base of the mould.

5.2.2. The Injection of Live Cells into High Pressure CO_2

The second step in this process investigated the effects of the injection mechanism and high pressure injection on live cells. After injection, cell survival, cytosolic LDH release and BMP-2 induced alkaline phosphatase activity were all assessed.

5.2.2.1 Cell Culture

Murine C2C12 cells were cultured in complete DMEM for all cell survival studies with full details given in the materials and methods chapter (section 7.1.1). A viable cell count was carried out for both cell lines using trypan blue exclusion, full details of which can be seen in the materials and methods chapter (section 7.1.3).

5.2.2.2 Investigating the Effect of Injection Pressure on Cell Survival

To test the resilience of the murine C2C12 cell line, live cells (250,000) were suspended in 200 µl of DMEM and placed into the cell storage tubing. The high-pressure reservoir above the cell storage tubing was pressurised to 5, 37 and 74 bar and the pressure inside the vessel was increased to 4, 36 and 73 respectively. The higher of the two valves (A) was the opened to expose the cell suspension to the pressurised gas. The second valve (B) was then opened to push the cells through the tubing and into a PTFE mould in the base of the vessel. The system was then decompressed over 40 seconds and the cell suspension removed and placed into DMEM overnight.

5.2.2.3 Investigating the Effects of the Injection Mechanism and Medium on Cell Survival and Function

In order to show any differences between the valve opening sequence two alternative methods were employed. The method is the same as in 5.2.2.2, with the exception of the opening of the valves. In the first alternative, the two valves were opened in the same order (A - B), but at a slower rate (approximately 10 seconds per valve). This would show any difference between an instant increase in pressure and a more gradual increase. In the second alternative, the order of the valve opening was reversed from A-B, to B-A.

This would allow the cells to pass through an already open valve (B) when valve A was opened to allow the cells to be pushed into the vessel. This was done to provide some indication of the effects of the valve mechanism on cell survival at high pressure. In order to further examine the cause of cell death after high pressure injection, high pressure N_2 was also used as a cell storage/injection medium and compared with CO_2. The B-A valve opening sequence was also used before assessment of cellular alkaline phosphatase activity (injection at 35°C/74 bars of CO_2) and LDH release (injection at 35°C/5-74 bars of CO_2).

5.2.2.4 Assessment of Cell Survival after injection with High Pressure CO_2 and N_2

Cells were assayed for metabolic activity using the Alamar Blue™ (Serotech, UK) cell metabolic activity assay as described in the materials and methods chapter (section 7.3.1). Briefly, cells were removed from culture and the complete medium covering the cells replaced with an Alamar Blue™ solution (10% v/v in HBSS, Sigma UK). After a 90 minute incubation at 37°C (5% CO_2) 200 µl of solution from each well was transferred to a 96-well plate (Falcon). Fluorescence readings were then obtained at an emission wavelength of λ590 nm using λ560 nm excitation.

5.2.2.5 Assessment of Cell Membrane Rupture after Injection with High Pressure CO_2

As cells release cytosolic LDH when the membrane is ruptured, an assay for levels of LDH after exposure to $scCO_2$ was carried out as described in the materials and methods chapter (section 7.3.3). Briefly, C2C12 cells (250,000 per well) were removed by centrifugation and the remaining DMEM assayed for release of LDH using an LDH colour substrate system as per manufacturer's instructions (Roche, Penzberg, Germany). The results were then compared to cells processed for 10 seconds at equivalent pressures (5 to 74 bar) using the method previously described in section 2.2.3 as a positive control and dead (lysed) cells used as a negative control.

5.2.2.6 Assessment of Cell Functionality after Injection with High Pressure CO_2

All of the following methods for alkaline phosphatase activity assessment are included in more detail in the materials and methods chapter (section 7.4). For osteogenic culture, C2C12 cells that had been injected using $scCO_2$ for 10 exposure seconds at 74 bar (35°C) were cultured in complete DMEM overnight before addition of 500 ng/ml recombinant human bone morphogenetic protein-2 (rhBMP-2) in 2% FCS supplemented DMEM media. After seven days in culture, C2C12 cells were assayed for the p-NP soluble end product of alkaline phosphatase activity using the assay described in the materials and methods chapter (section 7.4.2). Briefly, cell cultures were fixed in 75% ethanol for 10 minutes and homogenised in 600 µl of distilled water containing 0.001% Tween detergent after 3 cycles of freeze-thawing. The substrate (p-NPP) was added to equal volumes of the cell samples, incubated at 37°C for 1 hour and the rate of conversion into p-NP measured by a change in fluorescence at 405 nm. Values were compared against known p-NP standards, corrected to DNA content and presented as nM of p-NP per hour per ng DNA. The DNA content of the cells was calculated using the method found in the materials and methods chapter (section 7.3.2).

5.2.3 The Injection of Live Cells into Plasticised $P_{DL}LA$

The final step in this part of the study was to investigate the suitability of this high pressure CO_2 injection system for use in tissue engineering and other biotechnological applications. To achieve this, the cells had to be injected into the pre-plasticised polymer (under pressure) before subsequent assessment of cell survival and functionality was carried out on the foamed structures.

5.2.3.1 Cell Culture

Murine C2C12 cells were cultured in complete DMEM for all cell survival studies with full details given in the materials and methods chapter (section 7.1.1). A viable cell count was carried out for both cell lines using trypan blue exclusion, full details of which can be seen in the materials and methods chapter (section 7.1.3).

5.2.3.2 The Injection of Fixed and Live Mammalian Cells into Plasticised $P_{DL}LA$

A method was devised in order to show the distribution of the cells in the scaffold based upon that previously used in section 4.2.3.2. C2C12 cells (1,000,000) were suspended in 800 µl of osmium tetroxide overnight and separated into four × 200 µl aliquots (250,000 cells per aliquot). The aliquots were injected using the method in 5.2.2.3. In brief, each aliquot of the osmium cell suspension was placed in the sample tubing and the $P_{DL}LA$ plasticised in the 60 ml collection vessel at 73 bar (35°C). An injection pressure of 74 bar was used before equilibrating for 10 seconds and decompression over 40 seconds. This experiment was repeated with live C2C12 cells to show the presence of the live and spreading cells on the inner and outer surfaces of the scaffolds.

5.2.3.3 Microscopic Analysis of Foamed $P_{DL}LA$ Scaffolds

In order to show the gross morphology of the injected scaffolds, images of the $P_{DL}LA$ foams were viewed and captured using the light microscope. This technique is described in more detail in the materials and methods chapter (section 7.7.1). Scanning electron microscopy was also used to show the presence of attached and spreading cells. Samples were prepared for biological SEM and scanned as described in the materials and methods chapter (section 7.7.2). In brief, scaffolds were cut, mounted and gold coated (Baltzers union, SCD030 sputter coater) before being scanned at 20 kV using a Philips 505 scanning electron microscope.

5.2.3.4 Micro-Computed Tomographic Analysis of Cell Loaded Scaffolds

Constructs of $P_{DL}LA$ and osmium stained C2C12 cells were kept in tact to observe the distribution of the cells within. These constructs were imaged using a high-resolution micro-computed tomography system (µ-CT 40, Scanco Medical, Bassersdorf, Switzerland). The scanner was set to a voltage of 55 kVp and a current of 145 mA. Samples were scanned at 8 µm voxel (3D pixel) resolution with an integration time of 120 ms to produce 3D reconstructed images.

The cell-loaded scaffolds were thresholded at 60 (arbitrary number) to view the porous scaffold and then at 190 to view the osmium stained cells contained within.

5.2.3.5 Assessment of Cell Survival after Injection into Plasticised $P_{DL}LA$

Both cell viability and location were assessed with the use of the LIVE/DEAD™ stain as described in the materials and methods chapter (section 7.5.1). In brief, the cell loaded $P_{DL}LA$ foams were incubated in 10 ml of complete DMEM containing 20 µl of Ethidium Homodimer-1 (to highlight the dead cells red) and 5 µl of Calcein AM (to highlight the live cells green) for 1 hour. The cells were then rinsed (×4) in phosphate buffered saline (PBS) for 1 hour, before being observed using fluorescence microscopy (Leica DM IRB).

5.2.3.6 Assessment of Cell Functionality after Injection into Plasticised $P_{DL}LA$

For functional assessment, an alkaline phosphatase stain was carried out on the cell loaded scaffolds. In brief, the cell loaded scaffolds were cut into four pieces and cultured for seven days in DMEM containing 500 ng/ml of rhBMP-2. A red colour substrate was then precipitated on the cells by the action of cellular alkaline phosphatase activity. The substrate system comprised of Napthol AS-MX buffer solution containing 1 mg/ml Fast Violet B salt, as described previously by Oreffo and co-workers (Oreffo *et al*, 1998). This technique is described in the materials and methods chapter (section 7.4.3).

5.3 Results and Discussion

5.3.1 Testing the Injection Mechanism

The data presented in figures 5-4 and 5-5 shows that at least 50% of the cell suspension was lost after injection into the vessel, irrespective of the injection pressure. The largest volume of cell suspension recovered after injection into atmospheric pressure was 45±15% (figure 5-4). The effects of injecting into a high pressure environment provided little increase in recovered cell suspension with a maximum value of 53±16% (figure 5-5). However, the addition of a collection mould increased the percentage of recovered cell suspension with minimum of 84±14% at 74 bar and a maximum of 95±4% at 5 bar (figure 5-6). This development, coupled with an additional piece of tubing to allow the cells to pass directly into the mould, increased the levels of recovered cell suspension. This is likely to be due to the restrictions placed upon the final destination of the cells, as without a mould and the associated tubing there is a larger surface area over which the cell suspension can be spread (the 60 ml vessel). In addition, it is possible that the hydrophobic surface provided by the PTFE material facilitates the rapid and efficient collection of the water-based suspension from within the mould.

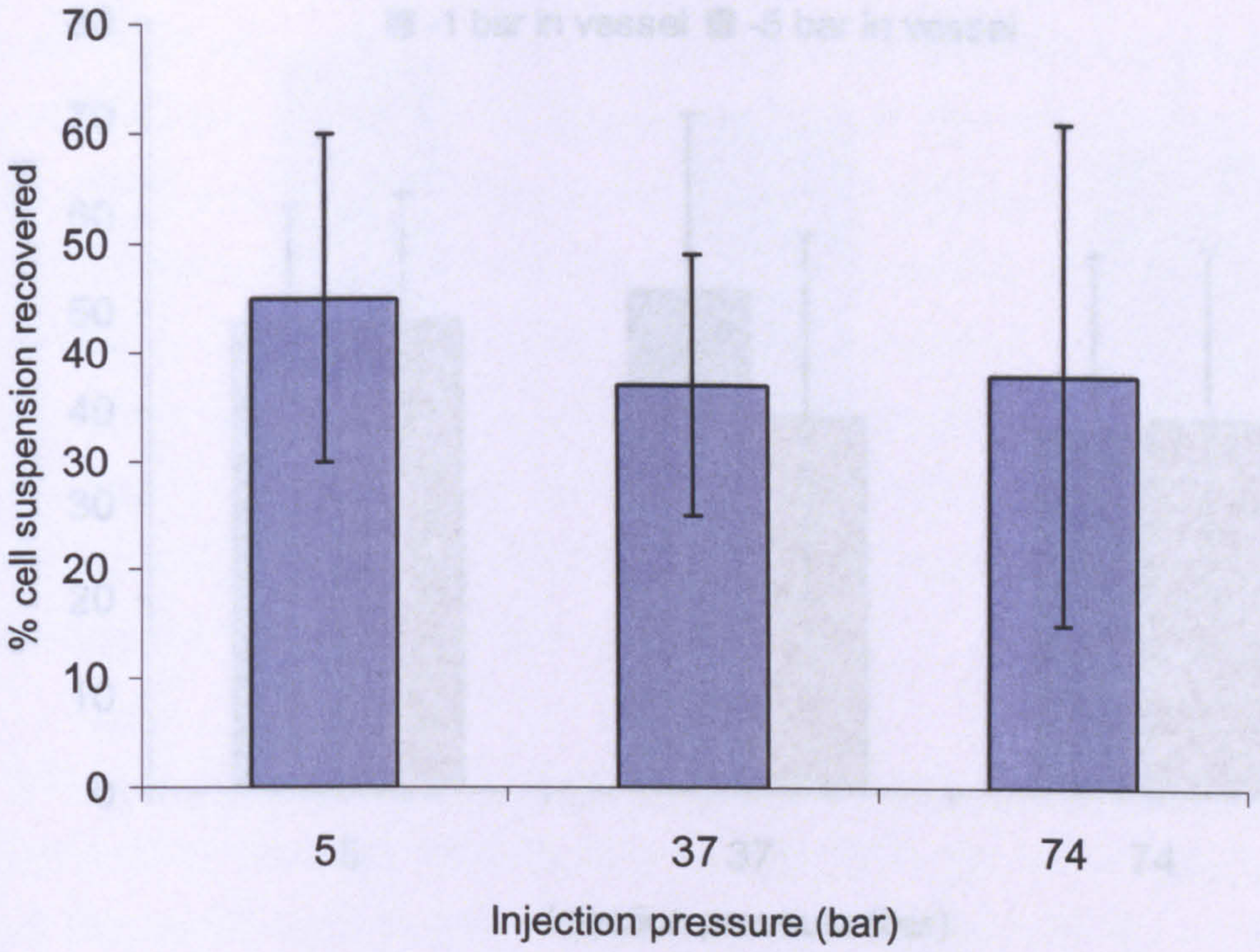

Figure 5-4 Percentage recovery of a dead cell suspension after high pressure CO_2 injection into a 60 ml vessel retained at atmospheric pressure. Mean (n=5) ± SD.

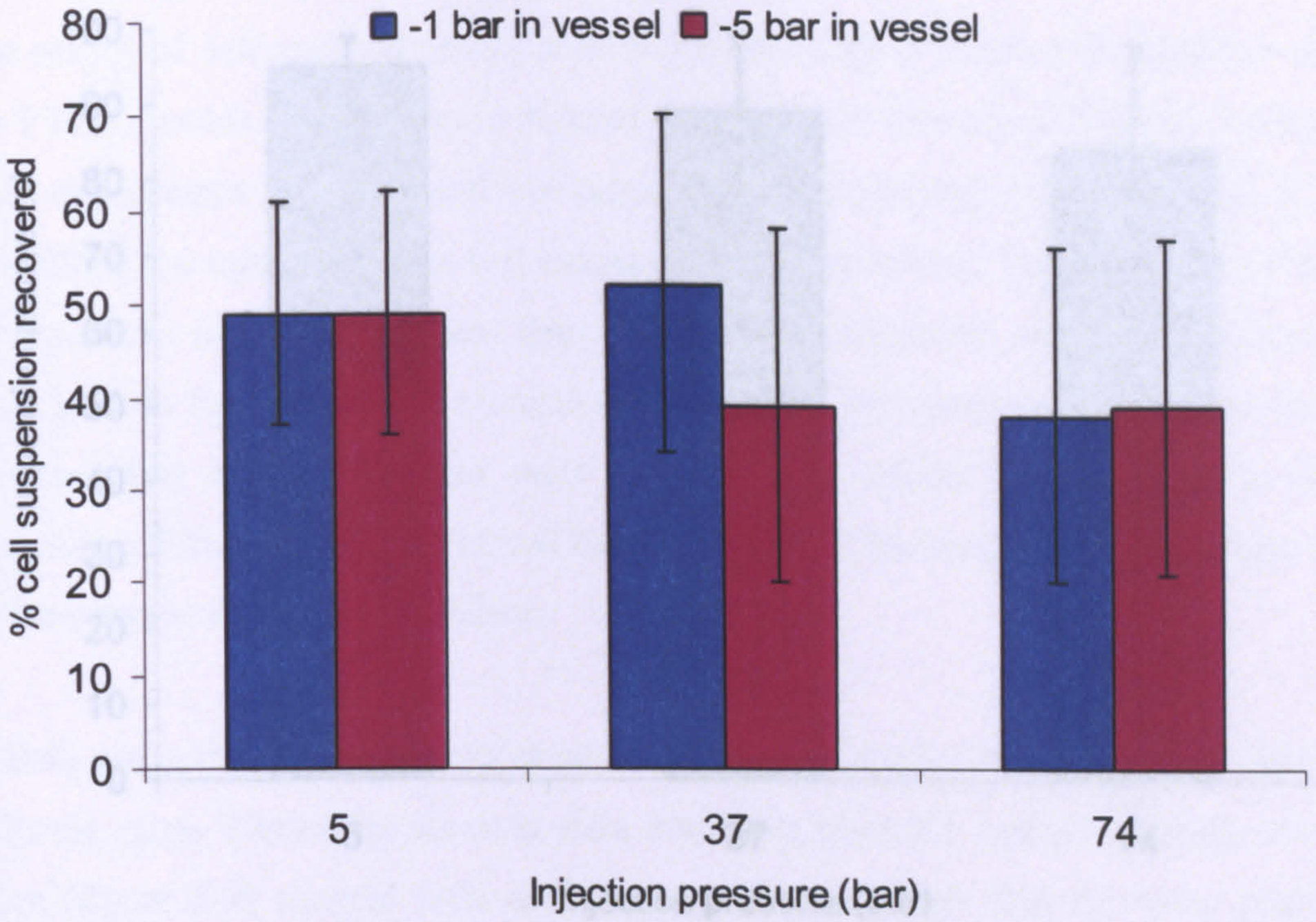

Figure 5-5 Percentage recovery of a dead cell suspension after high pressure CO_2 injection into a vessel already pressurised with CO_2. Mean (n=5) ± SD.

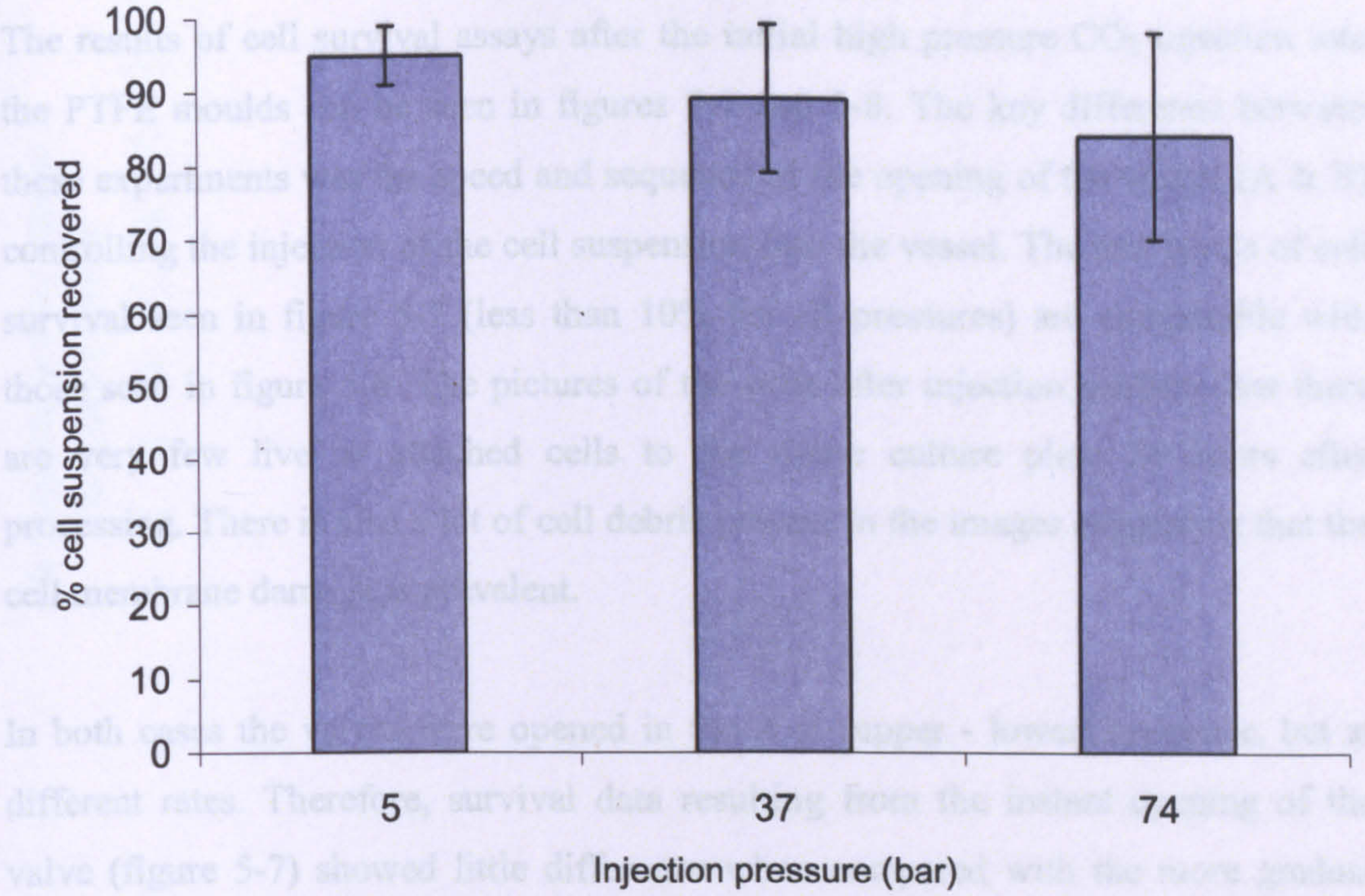

Figure 5-6 Percentage recovery of a dead cell suspension after high pressure CO_2 injection into a PTFE mould within a vessel pressurised with CO_2. Mean (n=5) ± SD.

5.3.2 The Injection of Live Cells into High Pressure CO_2

The results of cell survival assays after the initial high pressure CO_2 injection into the PTFE moulds can be seen in figures 5-7 and 5-8. The key difference between these experiments was the speed and sequence of the opening of the valves (A & B) controlling the injection of the cell suspension into the vessel. The low levels of cell survival seen in figure 5-7 (less than 10% for all pressures) are comparable with those seen in figure 5-8. The pictures of the cells after injection confirm that there are very few live or attached cells to the tissue culture plate 24 hours after processing. There is also a lot of cell debris present in the images suggesting that the cell membrane damage is prevalent.

In both cases the valves were opened in the A-B (upper - lower) sequence, but at different rates. Therefore, survival data resulting from the instant opening of the valve (figure 5-7) showed little difference when compared with the more gradual opening of the valve (figure 5-8). From this it was concluded that it may not be the speed of the release that was affecting the survival.

In a final variation, the lower valve (B) was opened first to allow the CO_2 from the vessel to pressurise the cell suspension and permit the passage of the cells through an already open valve when the second valve (A) was opened to inject the cells. This change in the valve opening sequence from A-B to B-A resulted in a minimum of 45±17% cell survival at 74 bar with a maximum of 54±24% at 37 bar (figure 5-9). This represents a significant improvement in cell survival data when compared with that from the A-B opening sequence. It would appear that the opening of the valve may have caused the cells to be crushed as the valve is only fully open at the very end of the injection process, by which stage many of the cells would have passed through a smaller orifice. When injected with N_2, the data was comparable to that using injected with CO_2, as there was a minimum of 48±23% cell survival at 74 bar and a maximum of 55±13% at 37 bar (figure 5-10). This indicates that the damage caused to the cells is not specific to the effects of CO_2.

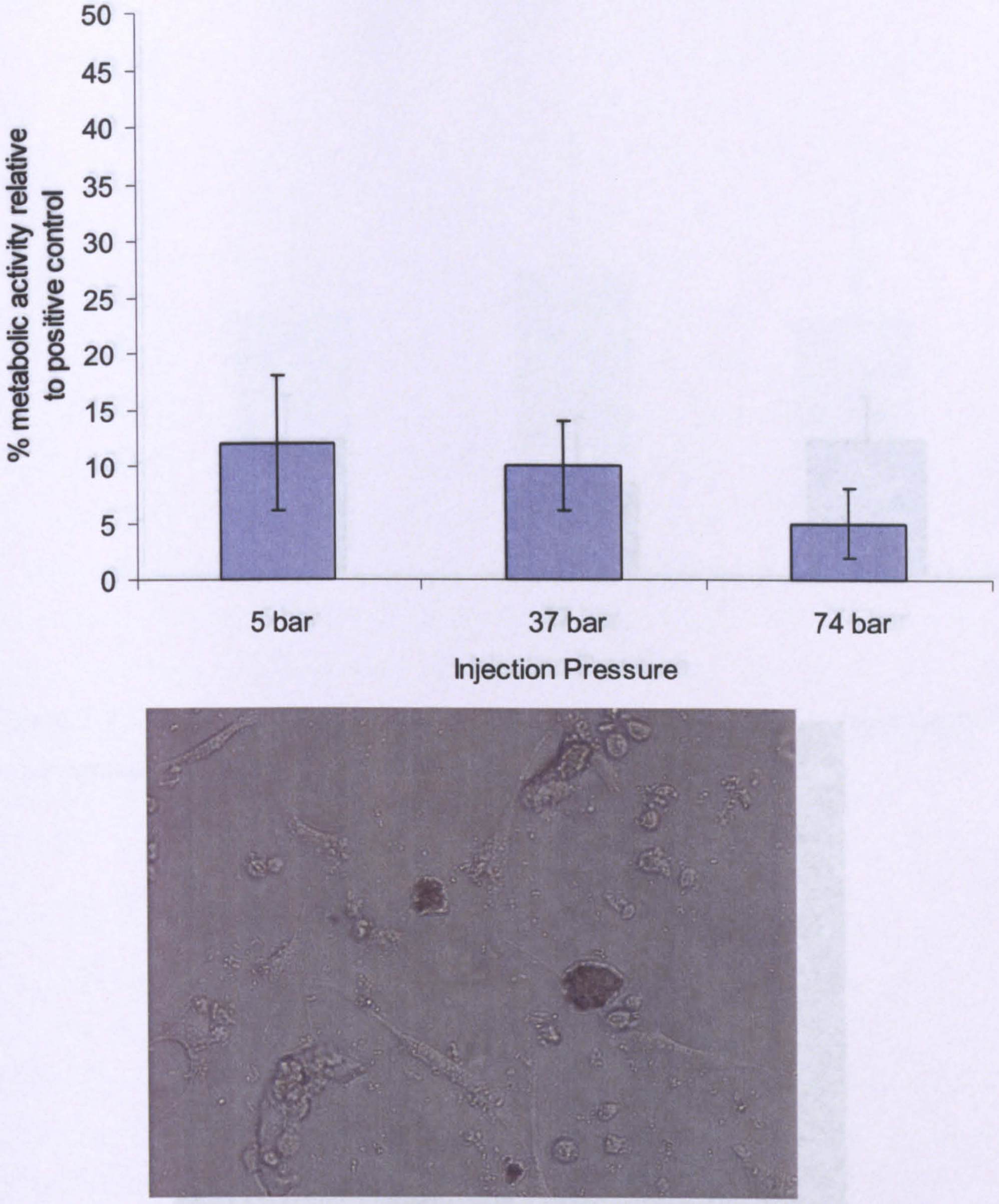

Figure 5-7 Cell survival data and visual confirmation after injection into high pressure CO_2 using the A-B valve opening sequence. Mean (n=3) ± SD. The physical appearance of the cells after injection at the highest pressure (74 bar) can be seen inset. This shows the cell debris that is indicative of damage to the cell membrane.

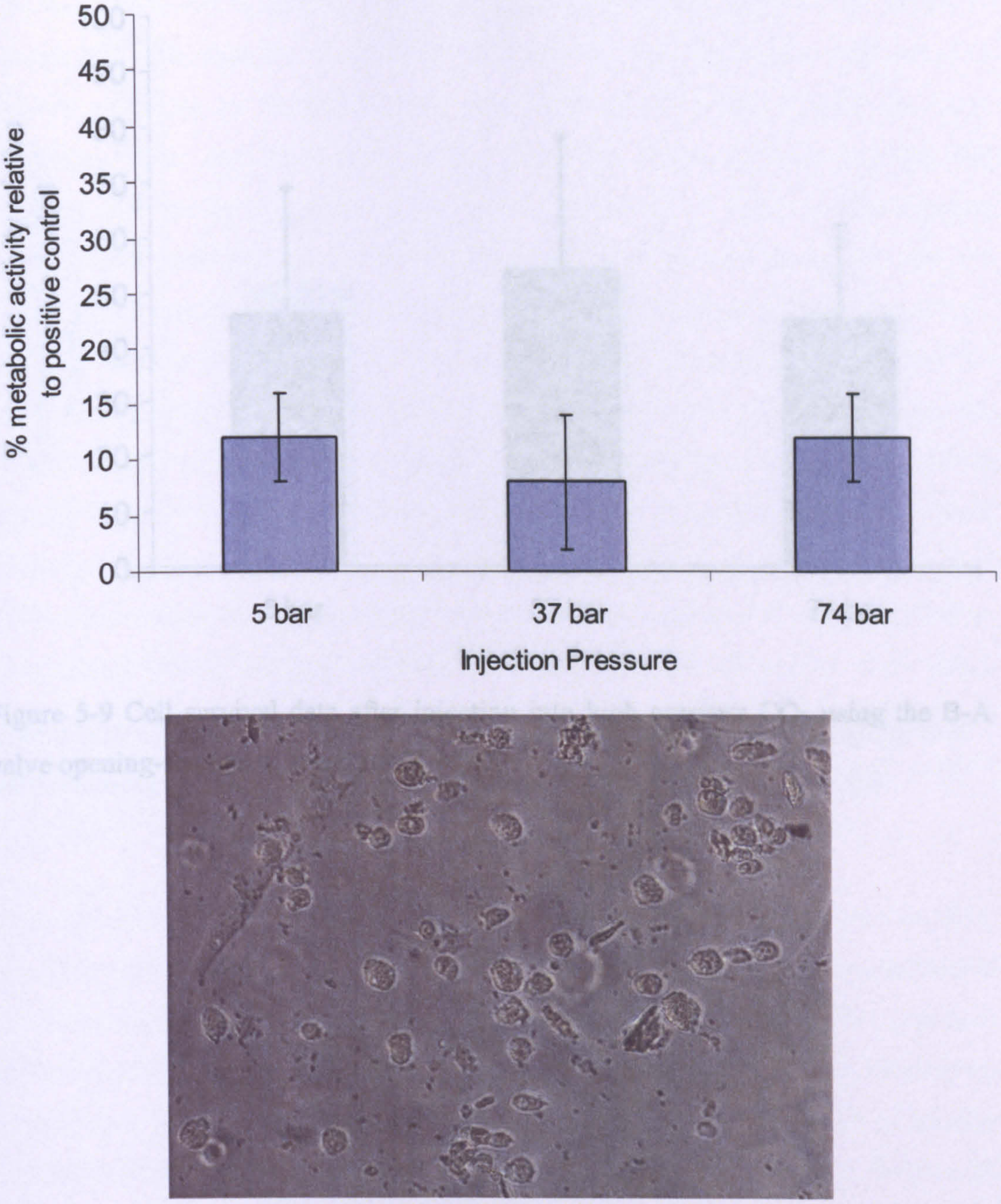

Figure 5-8 Cell survival and visual confirmation after a slow injection into high pressure CO_2 using the A-B valve opening sequence. All data is given with standard deviation. The physical appearance of the cells after injection at the highest pressure (74 bar) can be seen inset. This shows the cell debris that is indicative of damage to the cell membrane.

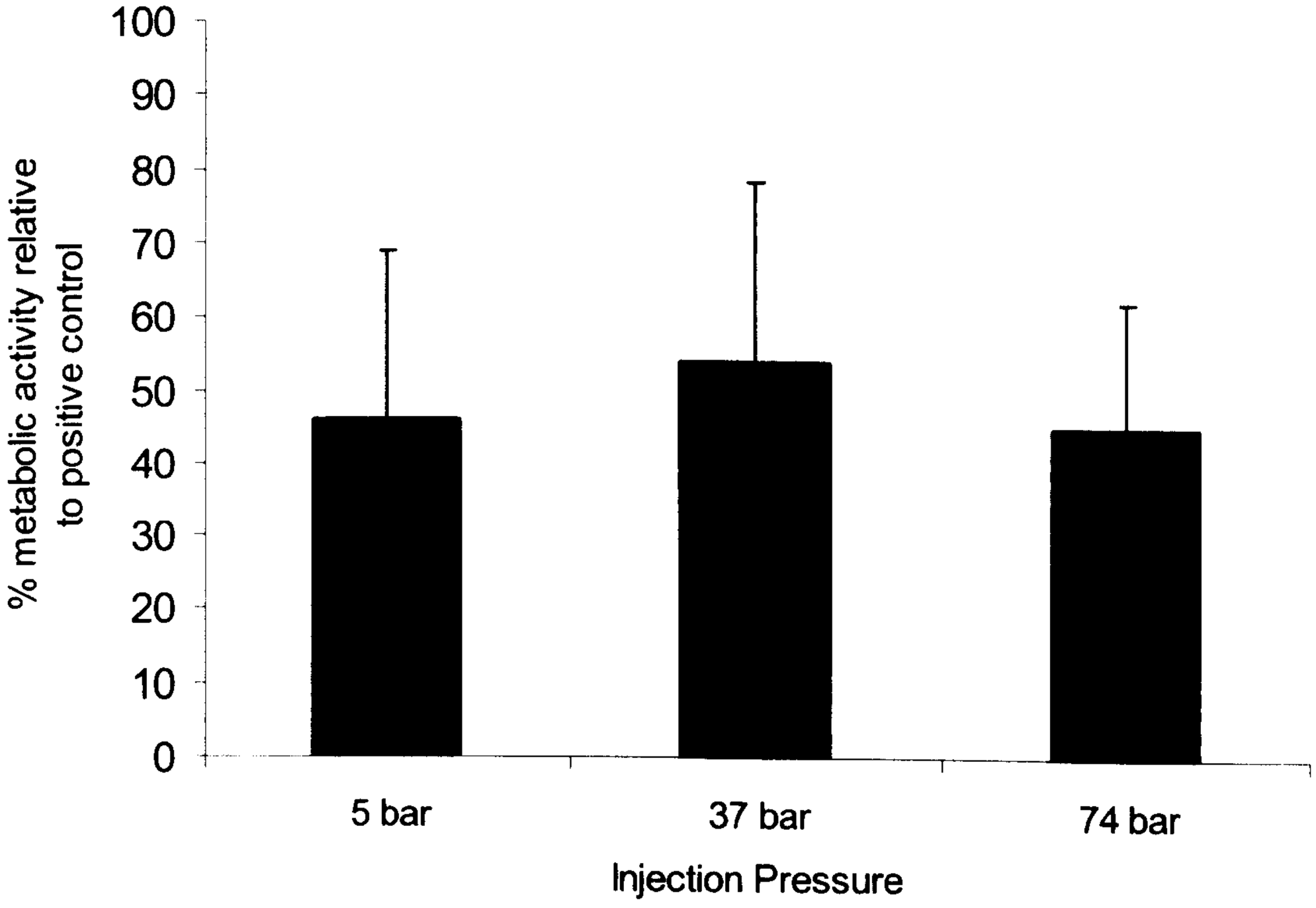

Figure 5-9 Cell survival data after injection into high pressure CO_2 using the B-A valve opening-sequence. Mean (n=3) ± SD.

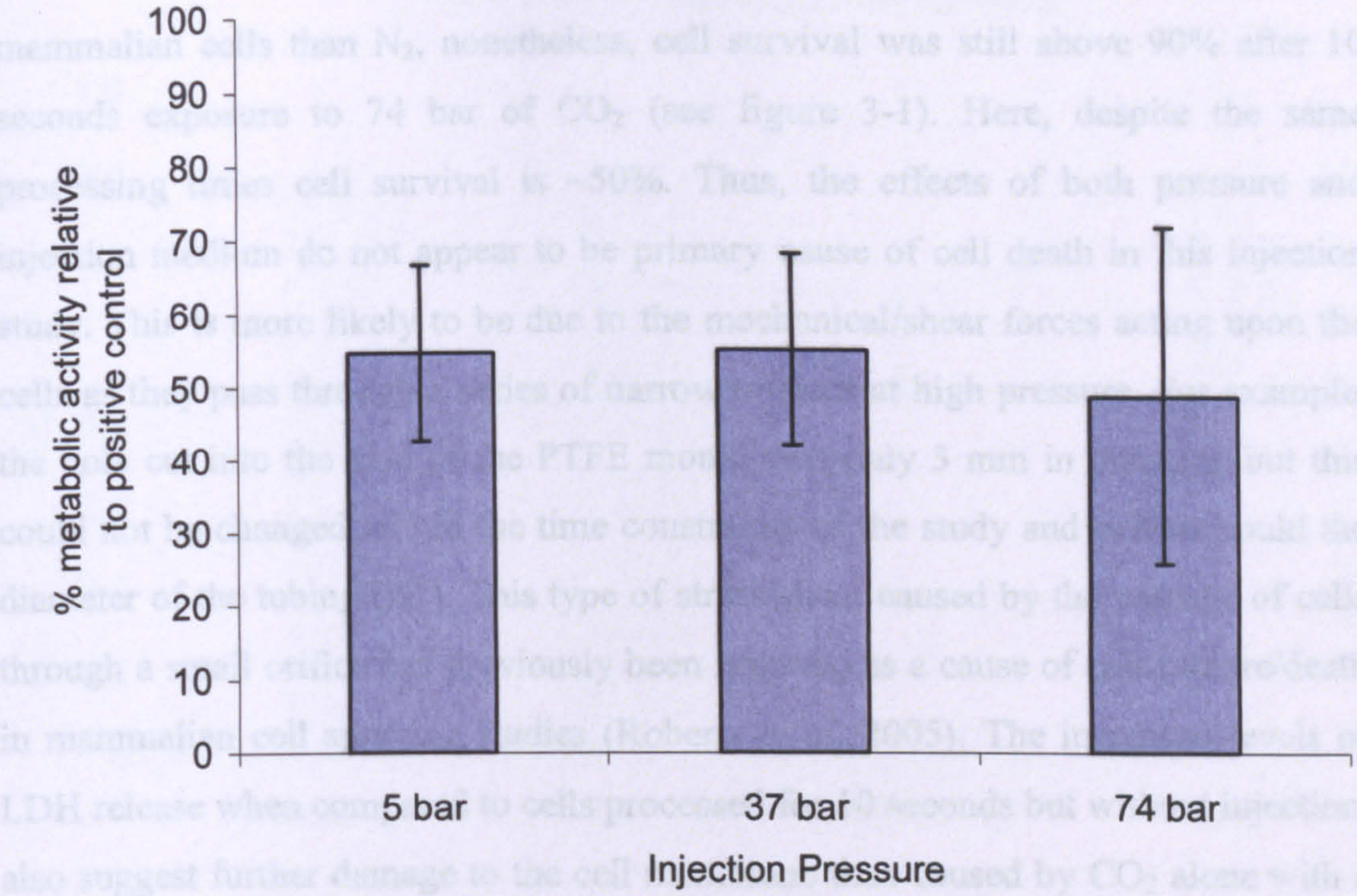

Figure 5-10 Cell survival data after injection into high pressure CO_2 using the B-A valve-opening sequence and N_2 as the injection medium. Mean (n=3) ± SD.

The work described in chapter four indicated that $scCO_2$ had a more toxic effect on mammalian cells than N_2, nonetheless, cell survival was still above 90% after 10 seconds exposure to 74 bar of CO_2 (see figure 3-1). Here, despite the same processing times cell survival is ~50%. Thus, the effects of both pressure and injection medium do not appear to be primary cause of cell death in this injection study. This is more likely to be due to the mechanical/shear forces acting upon the cells as they pass through a series of narrow orifices at high pressure. For example, the hole cut into the side of the PTFE mould was only 3 mm in diameter but this could not be changed within the time constraints of the study and neither could the diameter of the tubing (⅛"). This type of stress/shear caused by the passage of cells through a small orifice has previously been reported as a cause of cell rupture/death in mammalian cell spraying studies (Roberts *et al*, 2005). The increased levels of LDH release when compared to cells processed for 10 seconds but without injection, also suggest further damage to the cell membrane than caused by CO_2 alone with a significant difference at 74 bar (figure 5-11). However, with only minimal cell damage specifically from the effects of CO_2, optimisation of the delivery method may eliminate the additional damage caused by the injection process itself.

With cell (C2C12) survival confirmed after injection using 74 bar pressure of CO_2, the cells were then assessed for functionality after the same process. As described in previous chapters, this was carried out by measuring the capacity of C2C12 cells to differentiate into the osteogenic lineage via BMP-2 induced alkaline phosphatase activity (see figure 5-12). When corrected to the retrievable DNA, levels of alkaline phosphatase are indistinguishable between the control sample and those cells injected at 74 bar. This indicates that providing the cells survive the injection process, they retain their ability to undergo osteogenic differentiation. Therefore once cell survival has been confirmed the cell injection process would appear to have no a detrimental effect upon this aspect of cellular function than the previous method used to process cells in $scCO_2$ (see chapter three).

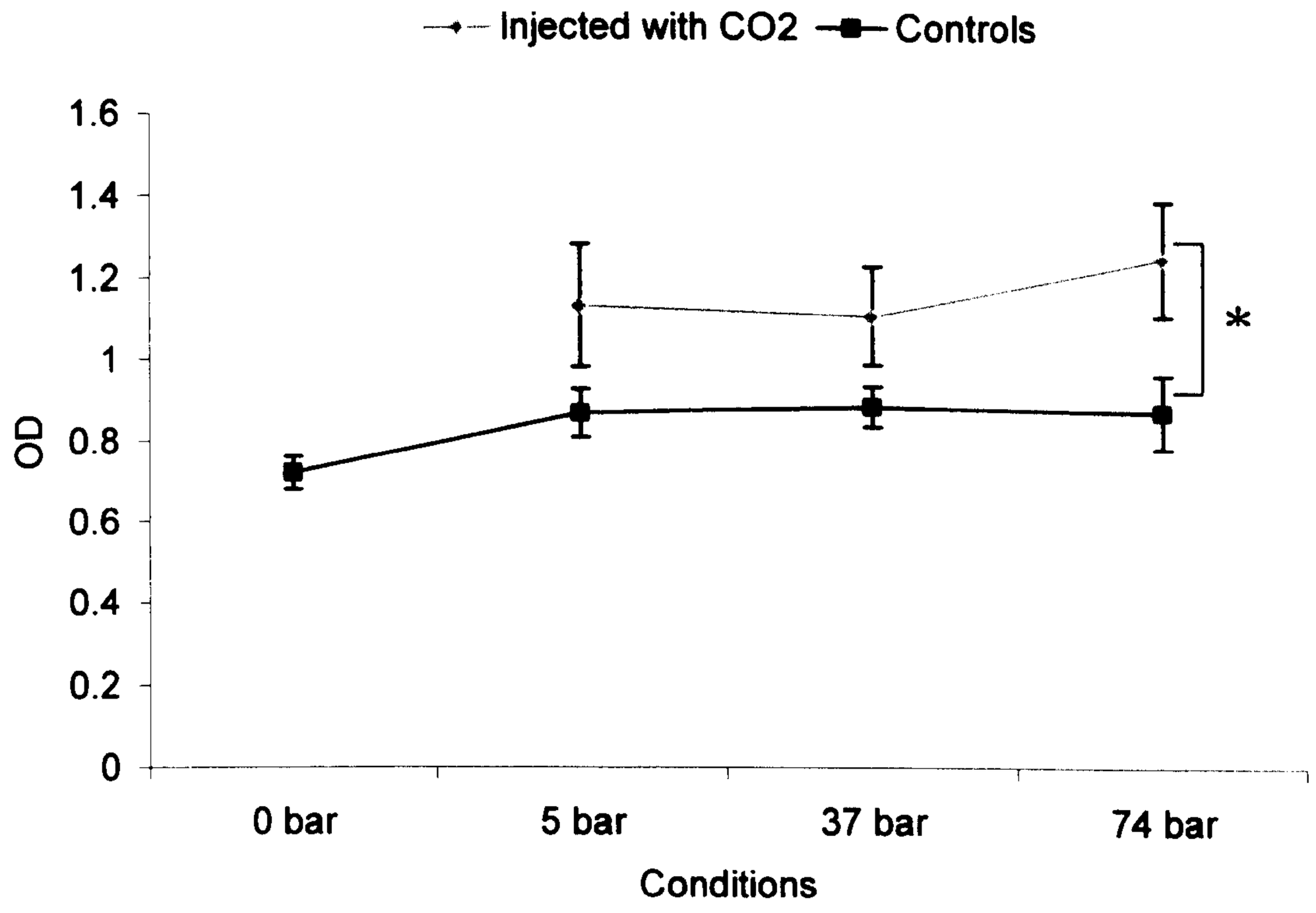

Figure 5-11 Measurement of cell rupture using an LDH assay after exposure of C2C12 cells to increasing pressures of CO_2. Cells were injected using high pressure CO_2 and the resultant LDH levels compared with cells processed in high pressure CO_2 without injection. Mean (n=3) ± SD. * indicates $p<0.05$ using T-test.

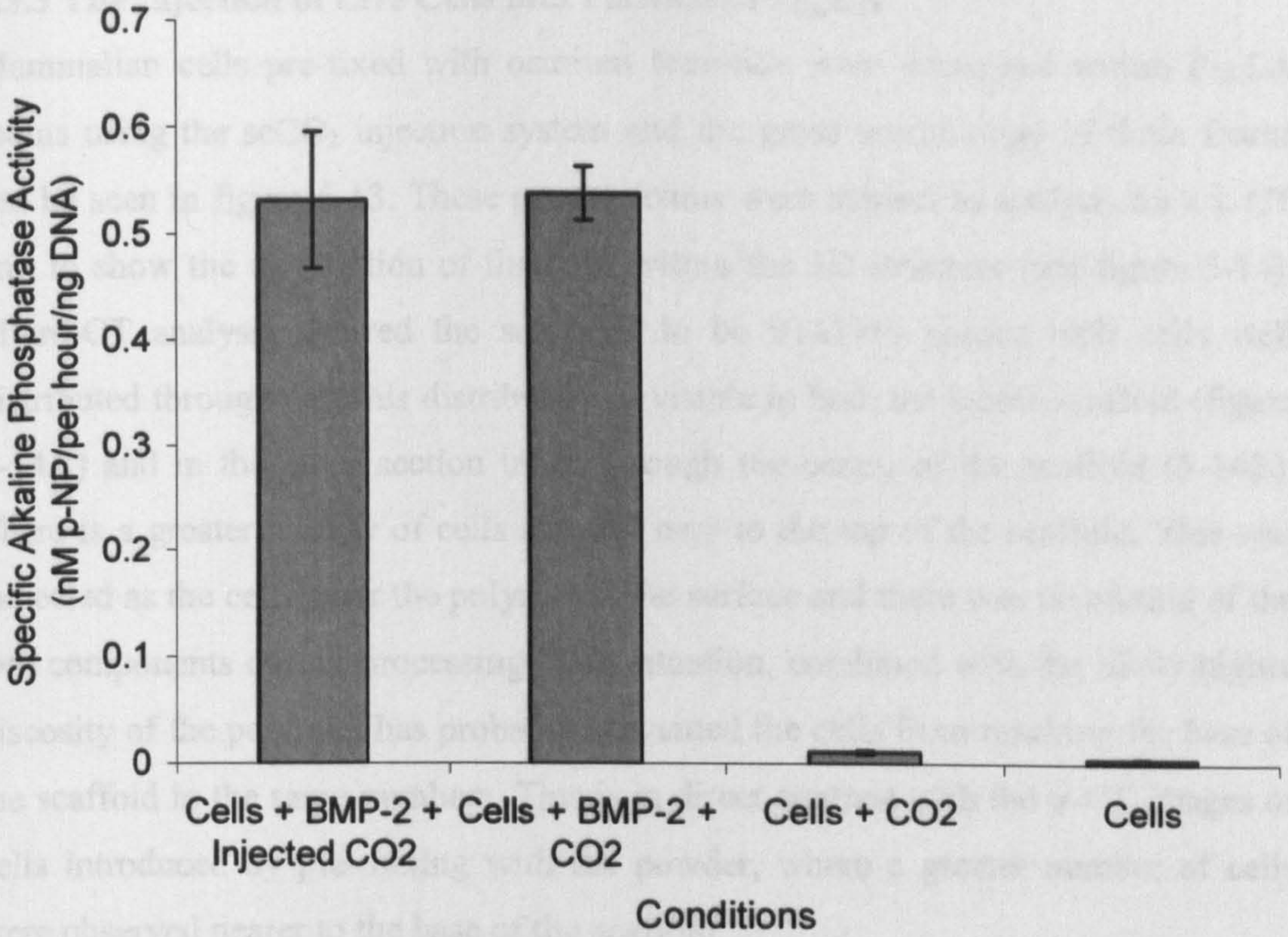

Figure 5-12 Specific alkaline phosphatase activity of C2C12 cells after injection into a high pressure environment with $scCO_2$. Mean (n=3) ± SD.

5.3.3 The Injection of Live Cells into Plasticised $P_{DL}LA$

Mammalian cells pre-fixed with osmium tetroxide were entrapped within $P_{DL}LA$ foams using the $scCO_2$ injection system and the gross morphology of these foams can be seen in figure 5-13. These porous foams were subject to analysis on a μ-CT unit to show the distribution of the cells within the 3D structure (see figure 5-14). Micro-CT analysis showed the scaffolds to be 91±17% porous with cells well distributed throughout. This distribution is visible in both the whole scaffold (figure 5-14A) and in the cross section taken through the centre of the scaffold (5-14B). There is a greater density of cells situated near to the top of the scaffold. This was expected as the cells enter the polymer at the surface and there was no mixing of the two components during processing. This situation, combined with the likely higher viscosity of the polymer, has probably prevented the cells from reaching the base of the scaffold in the same numbers. This is in direct contrast with the μ-CT images of cells introduced by pre-mixing with the powder, where a greater number of cells were observed nearer to the base of the scaffold.

After the injection of live mammalian cells into the $P_{DL}LA$, both SEM and LIVE/DEAD™ analysis were carried out to verify the presence of live and spreading cells. Figure 5-15 shows SEM images of $P_{DL}LA$ scaffolds injected with live 3T3 fibroblasts. It can clearly be observed that the cells are attaching and spreading on the inner and outer surfaces of the porous structure. The LIVE/DEAD™ images in figure 5-16 show that a large proportion of the cells are metabolically active (green). The cells do not appear to be as abundant as in the LIVE/DEAD™ images in chapter four but this is likely to be due to the lower proportion of cells that survived the process (see figures 5-9 and 5-10) when compared with the better survival rates seen in chapter two (figure 2-9). The three images seen in figure 5-16 are representative of the variation in cell survival that exists between the samples.

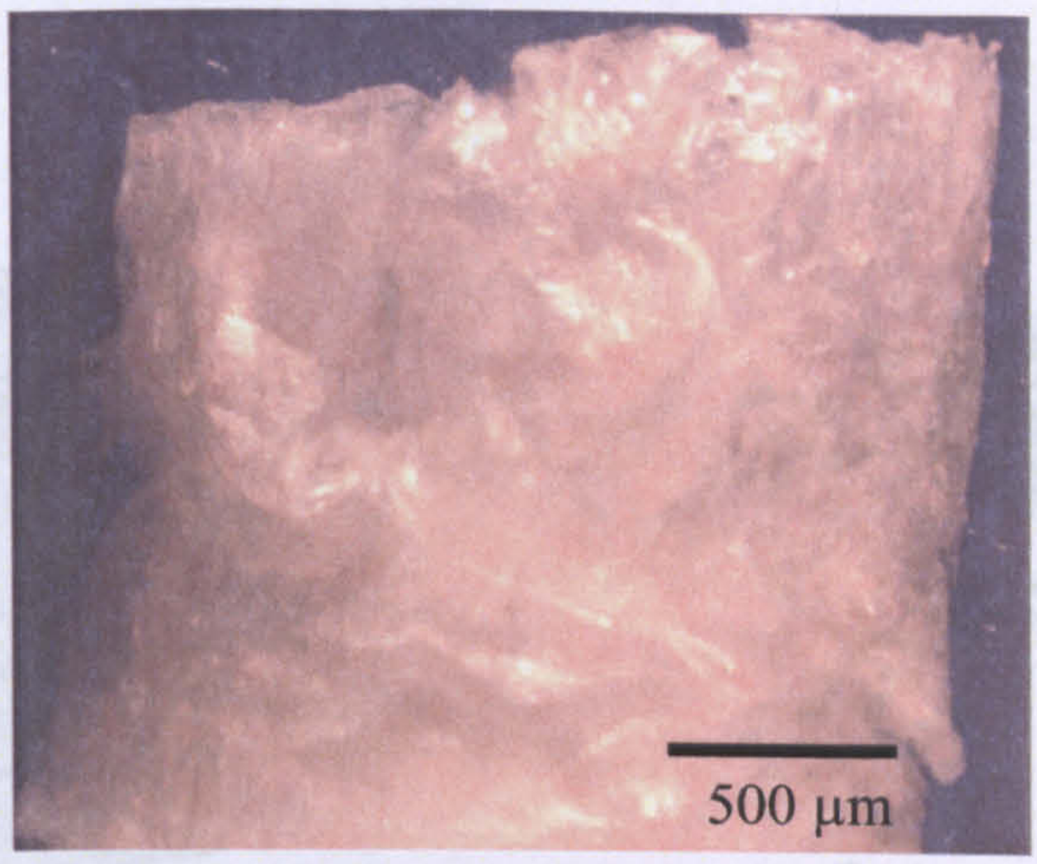

Figure 5-13 Gross morphology of a $P_{DL}LA$ scaffold produced using the $scCO_2$ injection system.

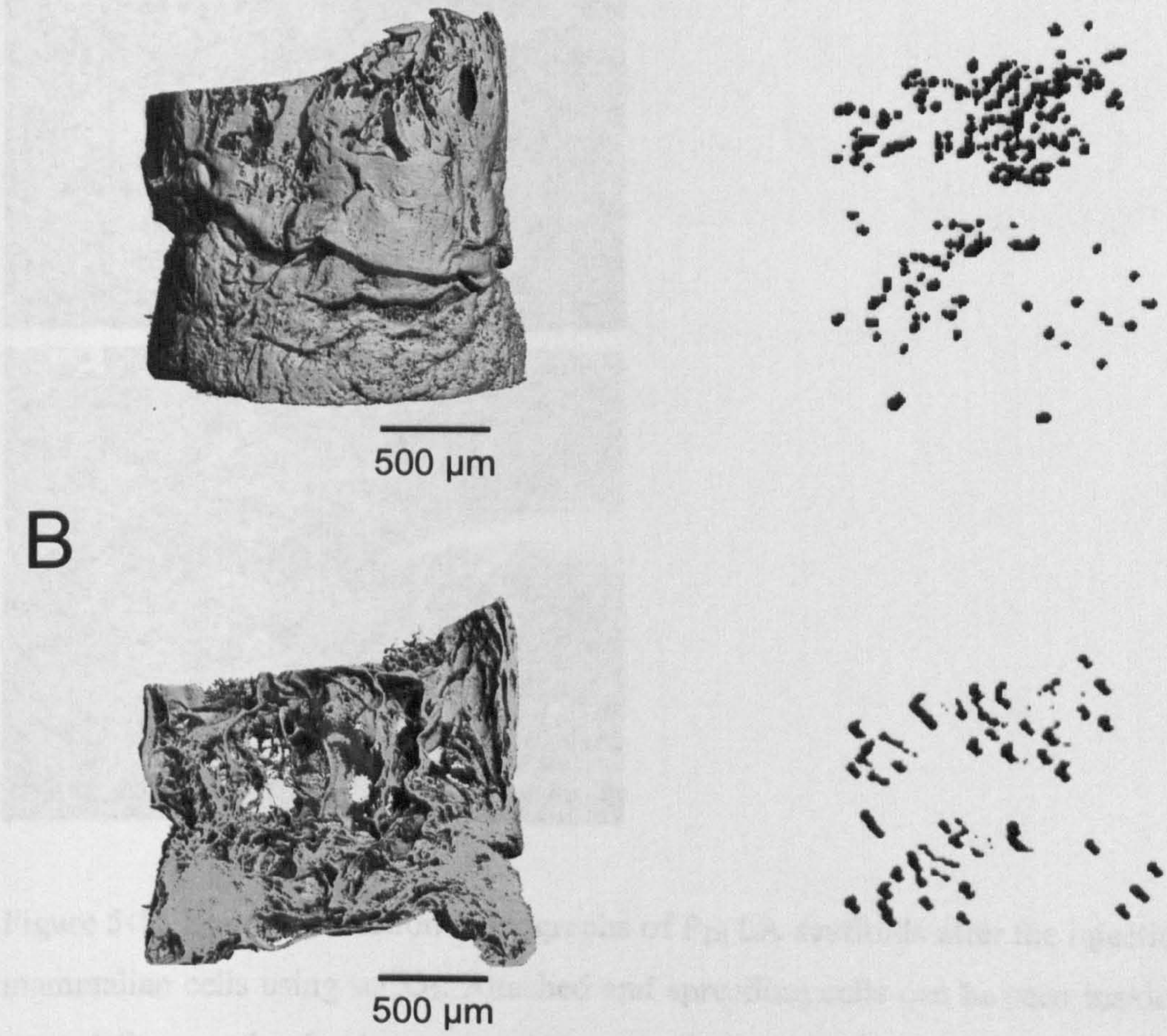

Figure 5-14 Micro-computed tomographic images of (A) whole $P_{DL}LA$ scaffolds and (B) scaffold cross sections, showing the distribution of mammalian cells pre-fixed with electron dense osmium tetroxide and subsequently injected into the polymer using $scCO_2$. The osmium stained cells have been visually enhanced for clarity.

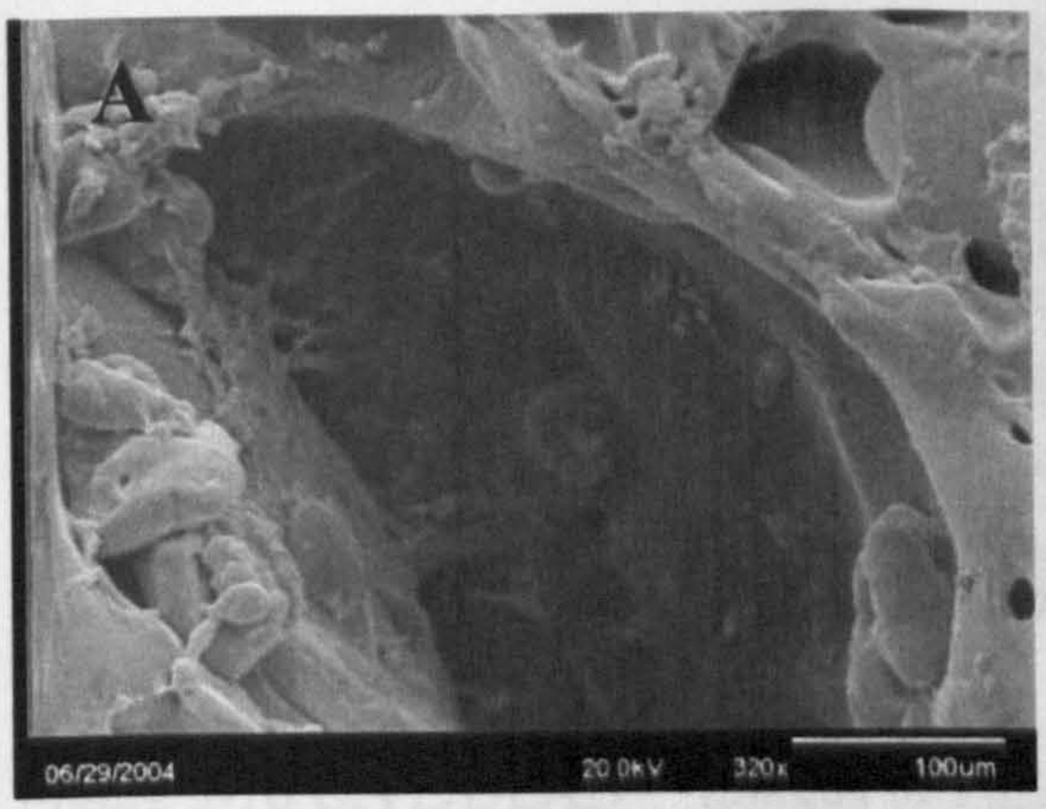

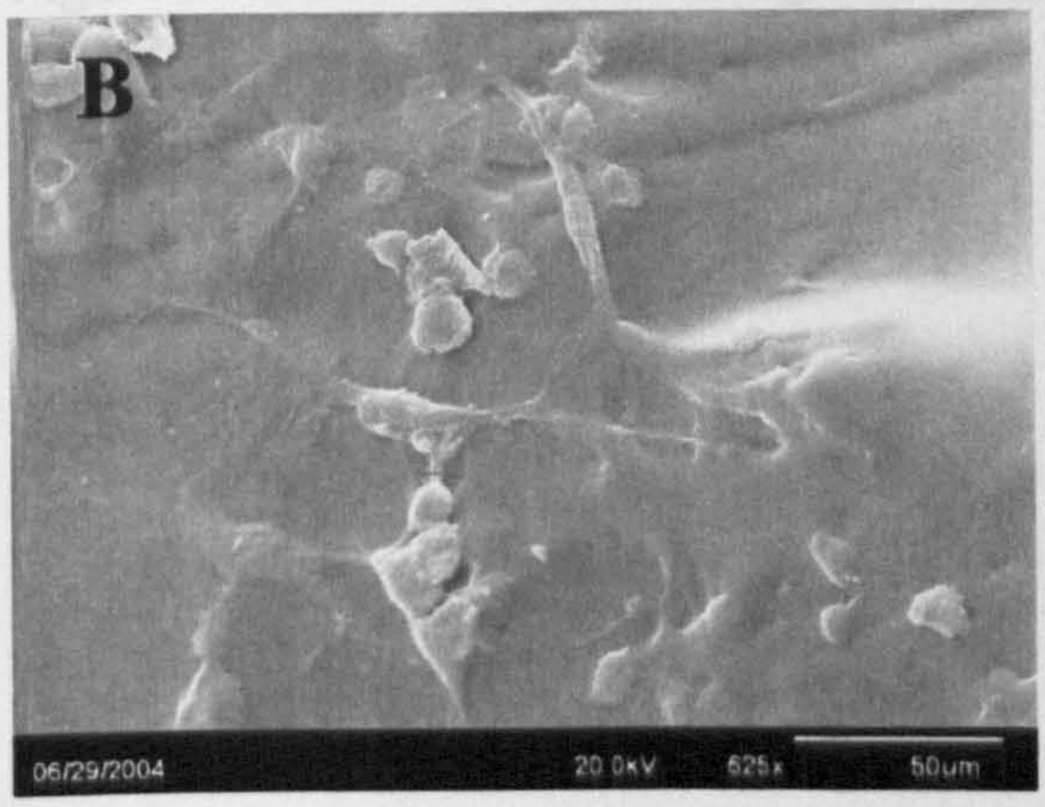

Figure 5-15 Scanning electron micrographs of $P_{DL}LA$ scaffolds after the injection of mammalian cells using $scCO_2$. Attached and spreading cells can be seen inside and around the mouth of a large pore (A) as well as on the flat outer surface of the scaffold (B).

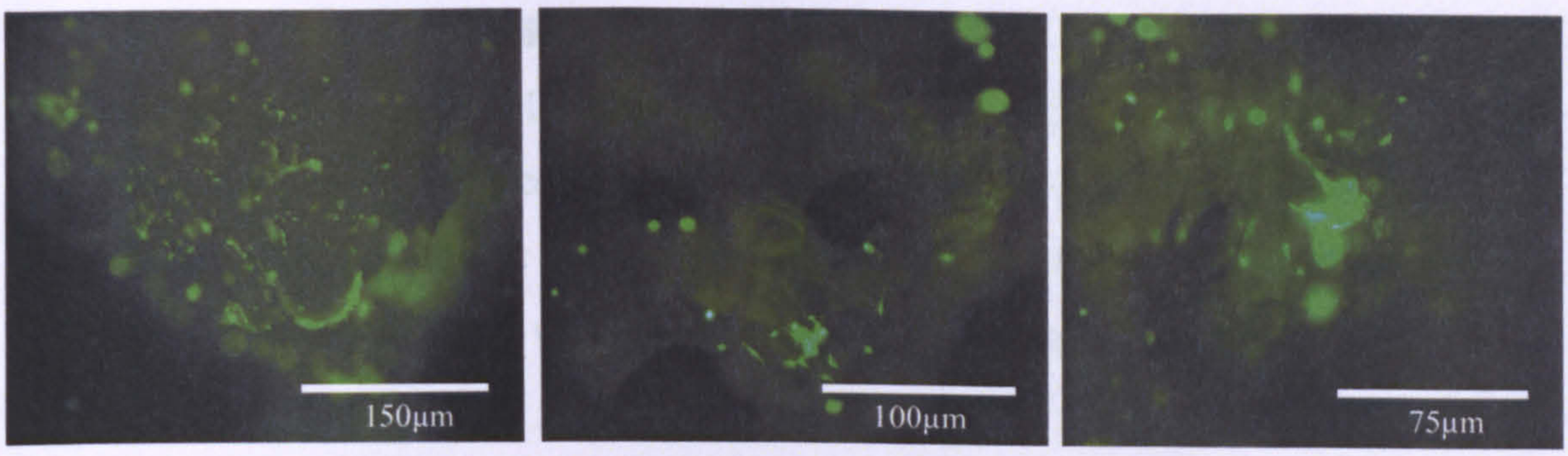

Figure 5-16 LIVE/DEAD™ images of $P_{DL}LA$ scaffolds loaded with mammalian cells using the high pressure CO_2 injection system.

5.3.4 Cell Functionality Studies

Scaffolds injected with C2C12 cells using 74 bar of CO_2 were cultured in an osteogenic medium (DMEM containing 500 ng of BMP-2) and stained for alkaline phosphatase activity. Assays were not carried out on these scaffolds as the subsequent recovery of DNA was inconsistent and there was not sufficient time to repeat the experiment.

The stained scaffolds seen in figure 5-17 do show localised alkaline phosphatase activity, as shown by the red stained areas. This provides evidence of BMP-2 induced osteogenic differentiation of the C2C12 cell line when injected into the $P_{DL}LA$. The stained areas of the scaffold do not appear as abundant as in chapter four, when the cells were pre-mixed with the $P_{DL}LA$ before processing in $scCO_2$. However, the number of live cells present in the injected $P_{DL}LA$ scaffolds was limited to 50% or less as can be seen from the survival data in figure 5-9. This may explain both this apparent reduction in cellular alkaline phosphatase activity and the poor recovery of DNA from the scaffolds. As in the previous chapter, the issue here was merely of proving the concept and this has been achieved.

This injection process may not be as efficient as the pre-mixing technique, but it represents a significant step in the development of a technique for the production of cell loaded tissue engineering scaffolds using a single processing step. Further optimisation of the cell delivery method in the future may result in a more abundant cell population on which to conduct these functionality studies.

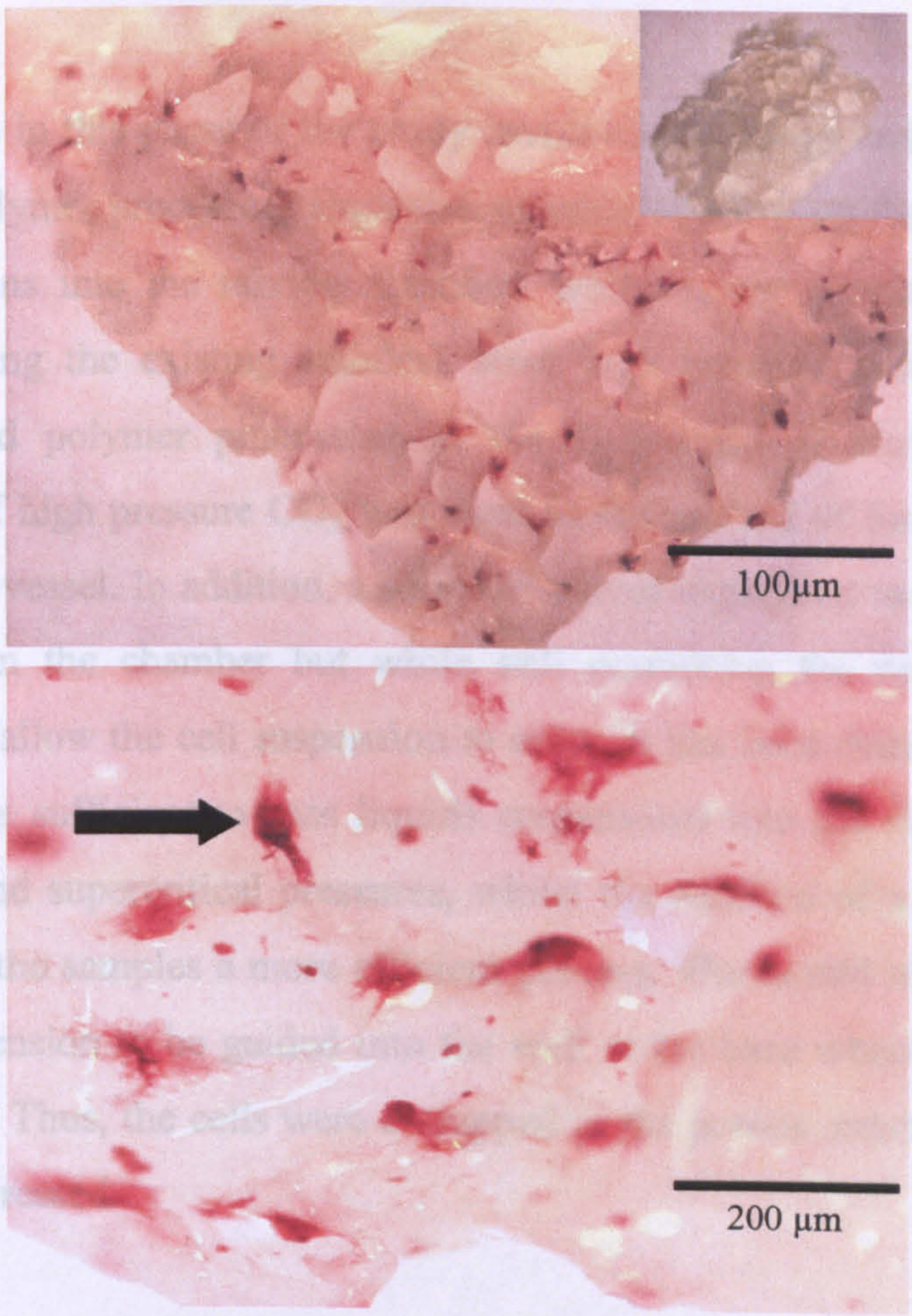

Figure 5-17 $P_{DL}LA$ scaffolds loaded with C2C12 cells using the supercritical CO_2 injection system and stained for BMP-2 induced alkaline phosphatase activity. Red stained cells (arrow) indicate localised alkaline phosphatase activity.

5.4 Conclusions

The main challenge in this phase of the study involved the design and construction of high pressure polymer processing apparatus capable of allowing the introduction of liquid suspensions into the mixing chamber, whilst under pressure. This was achieved by adapting the existing stainless steel high pressure vessels used for polymerisations and polymer processing at the University of Nottingham. An additional source of high pressure CO_2 was used as the method of forcing the cells suspension into the vessel. In addition, a series of valves were used to prevent rapid decompression from the chamber but while still permitting the opening of the mixing chamber to allow the cell suspension to enter. It has been demonstrated that this mechanism was sufficient to pass liquids suspensions into the vessel when at atmospheric, sub and supercritical pressures, whilst the addition of a PTFE mould made collection of the samples a more efficient process. The mould was adapted to allow the cell suspension to be guided into the well at the base where the polymer was pre-plasticised. Thus, the cells were entrapped in the porous structure when the system was decompressed.

Cell survival and function were confirmed despite this injection process, with and without the presence of a polymer scaffold. Despite the convoluted path for the cell suspension to take and the potential level of cellular perturbation, Alamar Blue™ assays indicated that 50% of the cells could survive this process without the addition of the polymer and with no apparent loss of their capacity to differentiate into the osteogenic lineage when prompted with BMP-2. When injected into the polymer, the cells were shown to survive in good numbers as indicated by the LIVE/DEAD™ stained scaffolds. Where viable C2C12 cells were found, their ability to undergo osteogenic differentiation was also demonstrated when prompted with BMP-2.

Chapter 6

GENERAL DISCUSSION AND CONCLUSIONS

6.1 Discussion

The possibility of a rapid, one-step technique for the production of cell-loaded scaffolds for tissue engineering applications is appealing for a number of reasons. Traditional methods of seeding tissue engineering scaffolds are frequently inefficient and time consuming processes that requires a large population of cells to be added to a solid, porous structure followed by weeks or months of careful culture to achieve the desired cell density (Freed *et al*, 1998). If sufficient numbers of cells were introduced into scaffolds during the fabrication process, it could potentially eliminate the requirement for the subsequent scaffold culture stage and also increase the seeding efficiency. In theory, cell loaded scaffolds could be fabricated in surgical theatres with the patients own cell sample, before immediate implantation back into the patient. This would not only make the process more rapid, but it would also be less stressful for the patient as there would be only one surgical procedure necessary with reduced risk of infection.

Therefore, at the start of this study it was hypothesised that if cells could survive and remain functional after exposure to $scCO_2$, it may be possible to co-process mammalian cells and amorphous $P_{DL}LA$ into porous tissue engineering constructs in a single processing step. To achieve this, the study was split into five smaller areas of investigation across four chapters of this PhD thesis.

In chapter two, cells alone were exposed to both high pressure and supercritical CO_2 processing conditions and assessed for metabolic activity. This was carried out not only to confirm the survival of cells and allow the study to proceed further, but also to produce optimal processing conditions for the later stages of this study. A variety of cells demonstrated a time-dependent survival after exposure to $scCO_2$ (74 bar, 35°C) that could be extended by increasing the decompression time to four minutes. The survival of mammalian cells after $scCO_2$ processing has never been recorded in the literature, although it has been reported that similar conditions (75 bar, 38°C) could be used to kill and inactivate bacterial cell populations (Spilimbergo *et al*, 2002).

Exposure time was shown to have the most damaging effects on cell survival with a secondary role taken by pressure along with other conditions such as temperature, gas bubble formation and pH. These factors are already known to have detrimental effects on cell survival (Gregoriades *et al*, 2003, Wu, 1995, Dillow *et al*, 1999). Changes in temperature were recorded and shown to both increase and decrease rapidly during compression and decompression respectively. This was due to the effects of Joule-Thompson heating/cooling, an occurrence which could not be avoided as a result of the short compression and decompression times required to ensure cell viability. The toxic effects of $scCO_2$ did change with cell type, as the secondary cell lines appeared to be more resistant than the primary cells. However, the secondary cell lines are more proliferative when in culture, and therefore this may explain their ability to regain their numbers in the culture period of 24 hours between $scCO_2$ processing and assay.

Despite the reduction in cell survival resulting from the $scCO_2$ process, it must be mentioned that many conventional methods of seeding tissue engineering scaffolds can also affect cell viability. Frequently, the incorporation of cells into scaffolds is carried out by using mechanical agitation (dynamic seeding) due to the reduced seeding efficiencies often associated with static culture methods (Burg *et al*, 2000, Unsworth *et al*, 2002). However, despite increasing cell proliferation in the long-term, dynamic seeding methods have also been shown to reduce the viability of mammalian cells (Kim *et al*, 2004) sometimes by as much as 50% when compared to static or perfusion bioreactor methods alone (Burg *et al*, 2000). Even cells that have been encapsulated within biopolymers such as alginate have shown some reduction in cell viability (5-10%) despite the fact that the encapsulation process used no toxic or harmful treatments (Maguire *et al*, 2005). Therefore, the use of any technique to incorporate cells into porous polymer scaffolds will not be without damage or risk to the cell component and some loss of cell viability is acceptable when producing cell-based tissue engineering devices. Thus, a survival rate of between 70 and 90% after 30 seconds exposure to $scCO_2$ may well not be an issue, particularly if there is a subsequent culture period to increase the cell population.

However, the confirmation of cell survival after using a $scCO_2$ processing step was not the only factor that required investigation. Although it was obvious that prolonged exposure to $scCO_2$ had a toxic effect on mammalian cells, it was necessary to further investigate the some of the potential causes of cell death and to test the functional machinery of the cells after $scCO_2$ processing (chapter three). Mammalian cells were processed under the same conditions (74 bar, 35°C) but using another gas (N_2) to separate the effects of high pressure and processing medium on cell survival. Nitrogen was shown to have a less detrimental effect over the same processing times, indicating a CO_2-specific interaction with the cells with the effects of pressure only a secondary factor. Data from previous studies with bacterial cells has suggested that CO_2 induces cell death by reducing the intracellular pH after first damaging the cell membrane (Dillow *et al*, 1999). Significant damage to the cell membrane was confirmed by an assay for LDH, providing evidence that this combination of events may be the primary cause of cell death. However, CO_2 could not be replaced with N_2 for this application as it neither plasticises nor foams amorphous polymers.

Gene microarray analysis of four RNA samples that were independently exposed to $scCO_2$ confirmed that very few changes in gene expression were induced by the high-pressure CO_2 environment and rapid pressure fluctuations. Of eight genes that were significantly down-regulated, survivin121, clast4 protein, and glutathione *S*-transferase could play a role in a biochemical response from the cell to the extreme changes in environment. Survivin121 is a component of the chromosomal passenger complex that acts as an inhibitor of apoptosis (Wheatley & McNeish, 2005). However, down-regulation of survivin was the only change associated with an apoptotic response here, indicating only a minor role for apoptosis. Further evidence for this was provided by the results of an ELISA, showing low levels of the histone complexes that are indicative of an apoptotic response. Cell enzyme and receptor function were tested by means of induced testosterone metabolism in primary hepatocytes (Seglen, 1987) and the BMP-2 induced osteogenic differentiation of murine C2C12 cells (Katagiri *et al*, 1994).

Despite processing for one minute in $scCO_2$, both cell types were shown to retain their respective functions with no distinguishable difference between $scCO_2$ treated and untreated control cells.

In chapter four, it was confirmed that solid, porous $P_{DL}LA$ scaffolds could be processed within the time limitations imposed by cell survival. Both cells and $P_{DL}LA$ were processed together using the optimal conditions from chapter two (30 seconds at 74 bar/35°C with cells suspended in 200 µl of DMEM). Despite the crude mixing technique, visual assessment of the cell loaded scaffolds by microscopic techniques, indicated that the cells were not only attaching and spreading to the internal surfaces, but also remained viable, as shown by the LIVE/DEAD™ stain. This represents the first time that cells have been incorporated into a synthetic polymer scaffold during the fabrications step with cell viability retained. Furthermore, this was achieved despite the possibility of cell entrapment within closed pores and a potentially more acidic environment due to the combination of water and lactic acid. For this work to be taken further it would require efficient mixing of the cells and polymer during polymer processing. This is vital to achieving a homogeneous distribution of cells throughout the scaffolds and in close proximity to one another, thus, facilitating the important processes that lead to tissue formation such as cell-cell signalling. During the latter stages of the study this problem was addressed by creating a new cell injection system with a static mixer incorporated into the design. The mixer was a simple stainless steel tube containing a series of blades that are specifically designed to mix the two components as they pass through at high pressure. However, this system had yet to be trialled as this PhD thesis was written. Once processed into the $P_{DL}LA$ scaffolds using $scCO_2$, murine C2C12 cells demonstrated their ability to undergo osteogenic differentiation as measured by BMP-2 induced alkaline phosphatase activity. In an interesting development, it was also demonstrated that BMP-2, C2C12 cells and $P_{DL}LA$ could be processed together to form a composite structure, capable of inducing osteogenic differentiation of the attached cells by controlled release of the protein from the scaffold.

After successfully co-processing the cells into the $P_{DL}LA$ scaffolds, the final stage in this study was to design and build a novel high pressure injection system to facilitate the incorporation of the cells into the plasticised polymer. By adding the cells at a later stage in the fabrication process, it would be possible to circumvent the limitations of the polymer processing time imposed by the finite survival time of mammalian cells. Some modification to the high pressure apparatus was required to facilitate this. The main challenge in chapter five of the study involved the design and construction of a high pressure polymer processing apparatus capable of allowing the introduction of liquid cell suspensions into the mixing chamber, already pressurised with CO_2 and containing plasticised polymer. This was achieved by adapting the existing stainless steel high pressure vessels, fabricated in-house at the University of Nottingham, used for polymer synthesis and processing. An additional source of high pressure CO_2 or N_2 at a greater pressure than that in the mixing chamber was used as the method of injecting the cell suspension. Two valves were utilised to allow the cells to be injected into the chamber without loss of pressure. It was demonstrated that this mechanism was sufficient to pass cell suspensions into the vessel when at atmospheric, sub and supercritical pressures and that the addition of a custom-made PTFE mould made collection of the samples a more efficient process.

Despite the longer path for the cell suspension to take and the potential increased level of cellular perturbation through the narrow orifices, Alamar Blue™ assays indicated that more than 50% of the cells could survive this high pressure injection process although cell survival was not pressure dependent over these short times (10 seconds at 5, 37 and 74 bar). This is comparable with the 70%+ cell viability reported by Roberts *et al*, who used either nitrogen or air to propel bovine chondrocytes and epithelial cells through an atomizer onto a microscope slide (Roberts *et al*, 2005). Despite the use of a different orifice size (0.8 mm), carrier medium (phosphate buffered saline) and a gas that is not CO_2, this acts of further evidence for the potential of such a high pressure cell delivery system to be used.

In this study, the difference in cell survival after injection with CO_2 and N_2 was indistinguishable indicating that high pressure CO_2 was not the only cause of cell death in this system. An increase in the release of cytosolic LDH was observed from the injected C2C12 cells when compared to cells processed in CO_2 using the method described in chapter two, indicating further mechanical rupture of the cell membrane. Furthermore, alkaline phosphatase data indicated that those C2C12 cells that did survive the injection process did not lose their capacity to differentiate into the osteogenic lineage when prompted with BMP-2.

Finally the cells were injected into plasticised $P_{DL}LA$ before subsequent decompression caused the polymer to foam with the cells entrapped within the porous structure. A proportion of these cells were shown to survive within indicated by the LIVE/DEAD™ stained scaffolds. Where live C2C12 cells were found, their ability to undergo BMP-2 induced osteogenic differentiation was also demonstrated. This injection step represents an important proof of concept for the addition of cells to a pre-plasticised polymer. If mechanical damage to the cells could be reduced by the use of an optimised delivery method, this technique could be used for the fabrication of cell loaded scaffolds in single step process that is free of some of the processing restrictions imposed by the pre-mixing technique. One approach could be to change the cell entry method or to create a pressure gradient as the cells are passed into the vessel to reduce the levels of trauma they are subjected to. Cell survival could be further optimised with a more sterile environment retained throughout the process. This could be implemented by moving the high pressure processing equipment into a sterile tissue culture facility and the routine sterilisation of the pressure vessel. With cell survival optimised, the final issue is that of the scaffold micro-architecture as in order to produce scaffolds capable of supporting tissue formation, the polymer processing conditions would have to be optimised. The advantage of using $scCO_2$ is that the processing conditions such as the temperature, pressure and decompression rate can easily be tuned to provide scaffolds with the desired characteristics (Goel & Beckman, 1994b, Howdle *et al*, 2001) and permit tissue formation in vivo (Yang *et al*, 2003b, Yang *et al*, 2004).

6.2 Conclusions

This study shows that mammalian cells are able to survive exposure to $scCO_2$ for sufficient time for the $scCO_2$ to plasticise and foam $P_{DL}LA$. This study has provided evidence for a rapid, one-step technique for combining mammalian cells and synthetic polymers into biodegradable scaffolds without the use of toxic solvents or elevated temperatures. After exposure to $scCO_2$ and rapid decompression, both C2C12 cells and primary hepatocytes demonstrated retention of functionality. In addition, the effects of $scCO_2$ exposure upon gene expression were minimal in the C2C12 cell line. $ScCO_2$ was found to have a more detrimental effect on cell survival than N_2 under the same conditions, although N_2 could not replace CO_2 for this application as it neither plasticises nor foams amorphous polymers.

Cells were shown to survive and remain functional after co-processing with the polymer although this did place restrictions on the polymer processing time. However, the implementation of a new high pressure CO_2 injection system succeeded in allowing the cells to be introduced into the pre-plasticised polymer. This could facilitate the extension of polymer processing times/pressures and enable cell loaded scaffolds to be fabricated with pre-determined characteristics that fit the application.

In addition to tissue engineering, this technology could be used in other applications where mammalian cells are combined with synthetic polymers. For example, cells and synthetic polymers are combined in cell therapy strategies (Emerich *et al*, 1992) and recombinant protein production, where cell anchorage is necessary for the production of protein drugs and enzymes (Ryu *et al*, 2003).

Chapter 7

MATERIALS AND METHODS

7.1 Cell Culture

7.1.1 Culture of Primary and Secondary Cells

Complete medium for 3T3 fibroblasts, ovine meniscal fibrochondrocytes and murine C2C12 cells contained Dulbecco's Modified Eagle's Medium (DMEM) supplemented with 10% foetal calf serum (FCS), 2% non-essential amino acids, 2% L-glutamine and 2% antibiotic/antimycotic solution. In addition, the complete medium for the chondrocyte cells contained L-proline (Fisher Scientific) and ascorbic acid-2-phosphate (Sigma, UK). Complete medium for hepatocytes contained Williams Medium E (InVitrogen), supplemented with 10% FCS and 20 mM L-glutamine containing penicillin. Murine C2C12 and 3T3 fibroblasts were cultured in T75 cell culture flasks (Falcon) and chondrocytes in T180 flasks (Falcon) until 80% confluent, before removal by a three minute incubation with an EDTA/trypsin solution (2 ml per flask) (Sigma). Hepatocytes were used on the day of the isolation due to their sensitivity to trypsin and short life span in culture. The C2C12 cells were kindly provided by Dr Richard Oreffo (University of Southampton).

7.1.2 Isolation of Primary Cells

Ovine knee joints were kindly provided by Broomhill's Butchers (Gloucestershire, UK) on the morning of the isolation. The fibrochondrocytes were isolated from the ovine knee joint meniscus using a method adapted from the one previously described by Collier and Ghosh (1995) and is detailed in figure 7-1. The menisci were then each placed in 50 ml universals (Falcon) containing 20 ml of phosphate buffered saline (PBS). The tissue was then diced into 2 mm^3 pieces and incubated for 2 hours in a pronase E solution (5 mg in 50 ml DMEM) (VWR international) at 37°C and 5% CO_2. This solution was aspirated and replaced with a type II collagenase solution (100 mg in 50 ml DMEM) (Lorne laboratories, UK) and left overnight. This enzymatic digestion process was necessary to remove the cells from the extra cellular matrix proteins. The following day, the cloudy cell suspension was passed through a 70 μm nylon filter (Sartorius) to remove any large pieces of tissue.

The cells were centrifuged using 1200 rpm (Sigma 3K15, SciQuip) for five minutes before being re-suspended in complete medium.

Hepatocytes were isolated from healthy rat liver using a method modified from Seglen (1976). Rats were sacrificed on the morning of isolation using cervical dislocation. The body cavity of the animal was then opened and the liver carefully removed, avoiding damage to the lobes. The liver was then placed on a petri-dish (Nunc, Denmark) and lobes removed. An incision was then made along the edge the lobe to expose the large central vessels. The lobes were then perfused for 10 minutes using EGTA (ethylene-glycol tetra-acetic acid) metal ion chelating buffer solution, followed by a 20 minute perfusion using a solution containing collagenase type II and IV (Sigma). After perfusion, each lobe was placed in a petri-dish containing complete tissue culture medium. The cells, tissue and media were then poured through sterile gauze (64 μm) into two 50 ml universals (Falcon). Released parenchymal cells were further purified from other cell types using a percol (Sigma) density gradient.

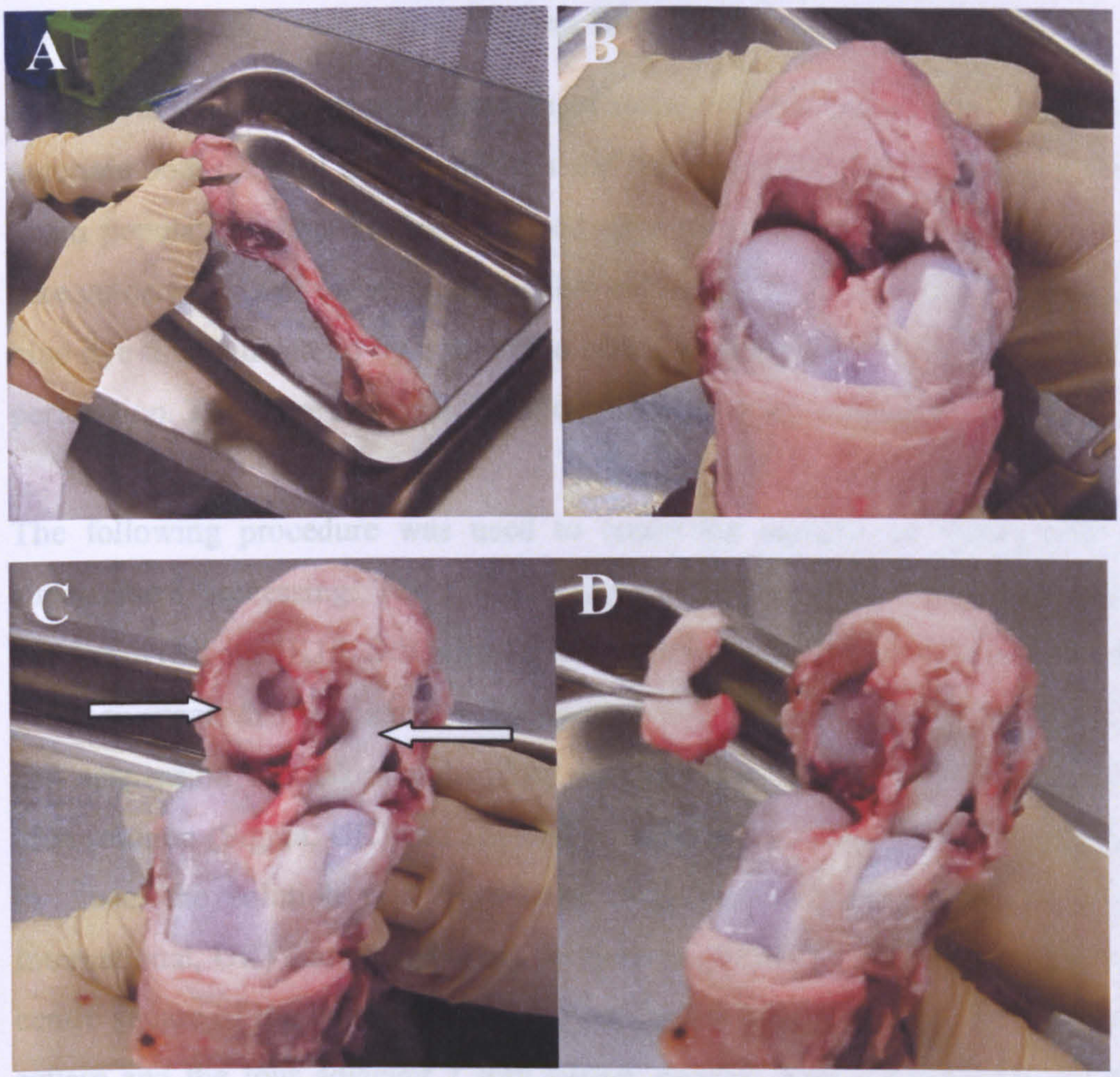

Figure 7-1 Isolation of the cartilage menisci from the ovine knee joint. The leg is first transferred to a class I cabinet (A) before an incision is made across the top of the knee joint with a size 22 scalpel blade and the connective tissue cut away (B). The ligaments are then severed to expose the two menisci (C – with arrows) before they are cut away from the surrounding connective tissue (D).

7.1.3 Viable Cell Counts using Trypan Blue Exclusion

In order to determine correct numbers of cells, a viable cell count is carried out to ascertain both the total number of cells and the number of viable (live) cells within a given population. This method is based upon the principle that viable cells do no take up certain dyes, where as non-viable cells do. Trypan blue is a commonly used blue dye that is taken up by non-viable cells, normally as a result of cell membrane perforation. Therefore any cells that are stained blue are counted as non-viable.

The following procedure was used to count the number of viable cells before supercritical processing: The cell suspension to be counted was centrifuged using 1200 rpm (Sigma 3K15, SciQuip) for 5 minutes, the supernatant removed to and the pellet re-suspended in a small volume of complete medium. A 50 µl aliquot of the cell suspension was taken and mixed with an equal volume of 0.4% (w/v) trypan blue solution (Sigma, UK) and allowed to stand for 5-10 minutes. With a cover-slip in place, the solution was transferred to a haemocytometer (Weber Scientific International, UK) and placed under a microscope (10× objective). Starting with the centre square of the haemocytometer, (see figure 7-2) the cells in the 1 mm middle square and the four adjacent 1 mm corner squares were counted (see figure 7-2). Each square of the haemocytometer represents a total volume 0.1 mm^3. As 1 cm^3 is equivalent to approximately 1 ml, the subsequent cell concentration per ml (and total number of cells) was determined using the following equations.

Average total number of cells in 1×0.1 mm^3:

= total number viable cells + total number of non-viable cells

Cell concentration (cells/ml):

= Total number of cells in 1×0.1 mm^3 square $\times (1 \times 10^4) \times 2$

(1×10^4 is the multiplication factor used to gain cells in volume of 1 ml and 2 is the dilution factor of the trypan blue)

Total number of cells:

= total number cells (viable and non-viable) × original volume of cell suspension

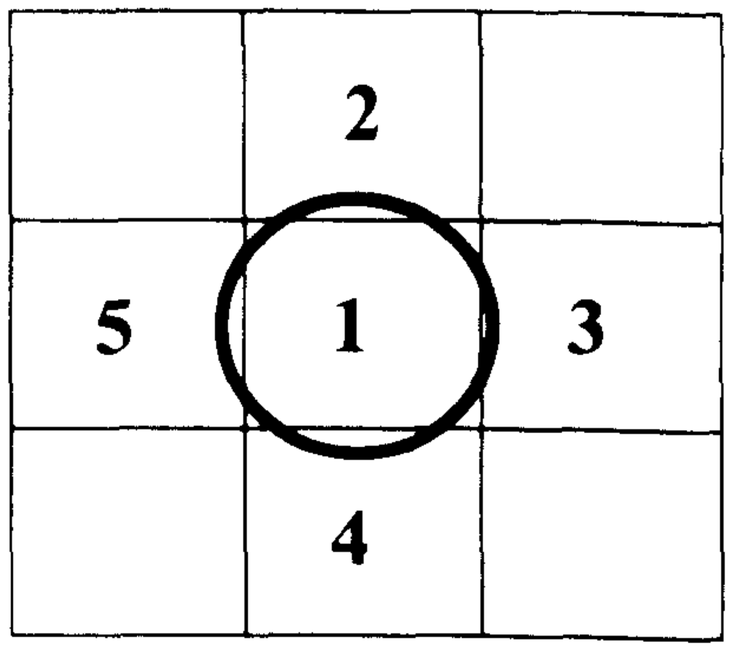

Figure 7-2 Layout of the five chambers on the haemocytometer (1-5) used to calculate cell number.

7.2 High Pressure Carbon Dioxide Processing

7.2.1 Processing of Mammalian Cells in High Pressure CO_2 and N_2

In these experiments, four cell types were exposed to a variety of high pressure CO_2 conditions to show their effect on cell survival. The set up of the equipment used can be seen in figure 7-3. The high pressure equipment was all made in-house (School of Chemistry workshops) with the exception of the back pressure regulator (Bronkhorst, Netherlands), the steel tubing and the fittings (Manchester Fluid Systems, UK).

The cell types used were murine 3T3 fibroblasts and C2C12 cells, along with primary rat hepatocytes and ovine fibrochondrocytes. Cells were cultured using the protocols given in section 7.1. After isolation/culture, cells were removed from cell culture flasks (if necessary) and a cell count was performed. The cells were then re-suspended in complete media to provide the required concentration, before being placed in custom-made poly(tetrafluoroethylene) (PTFE) 8-well tissue culture moulds at 2×10^5 cells per well (see figure 7-4A). The moulds were then placed into a 60 ml clamp-sealed pressure vessel (see figure 7-4B) that was pre heated to a specific temperature (dependent upon experiment). The cells were then pressurised in 40 seconds and exposed to pressures from 5 to 74 bars of CO_2 (food grade CO_2 supplied by Cryoservice UK) or nitrogen (BOC gases, UK) for a set time limit thereafter. The exposure times used were 10, 30, 60, 120 and 180 seconds (dependent upon the experiment). The process was controlled using a Bronkhorst High-Tec BV series flow meter connected to a PC. This acted as a sensitive back pressure regulator (BPR) and allowed the pressure to be ramped up and down within very short time periods. Once the system had depressurised, the clamp was removed from the vessel and the cells removed. The cells were re-suspended in complete media (1 ml per well) and cultured for 24 hours in tissue culture treated plates (Primaria & Falcon).

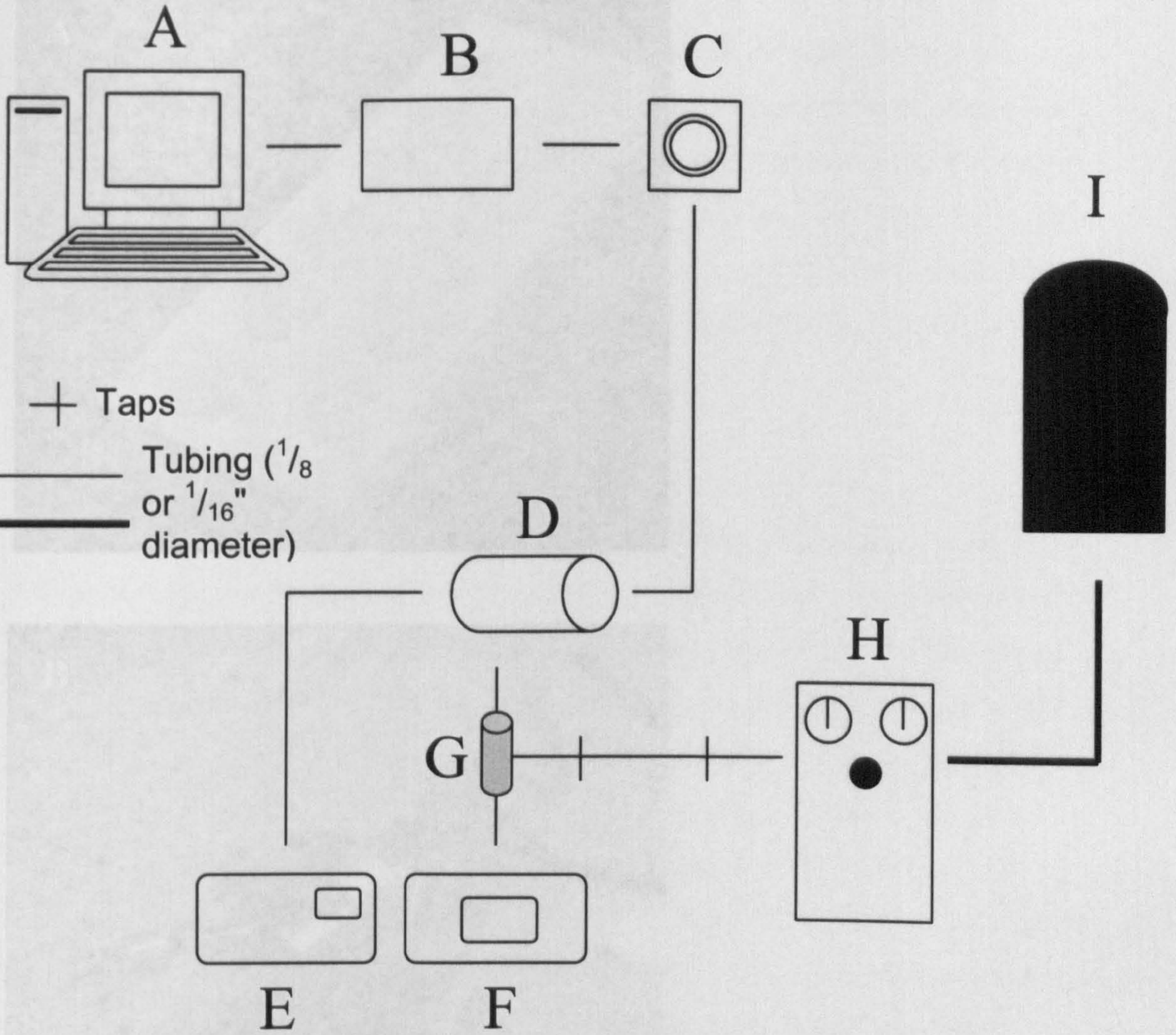

Figure 7-3 Schematic of the equipment used to process mammalian cells and synthetic polymers in high pressure and supercritical CO_2. The PTFE mould is placed in the 60 ml pressure vessel (D) and the temperature is set and controlled via a thermocouple on the inside of the vessel and read on the monitor (E). The CO_2 is then released from the cylinder (I) and pumped into the vessel via a Pickel pump (H) and two taps. The pressure inside the vessel is measured by a pressure transducer (G) and the pressure displayed on the pressure monitor (F). The pressure is controlled by a back pressure regulator (C) attached to a power source (B) and a PC (A).

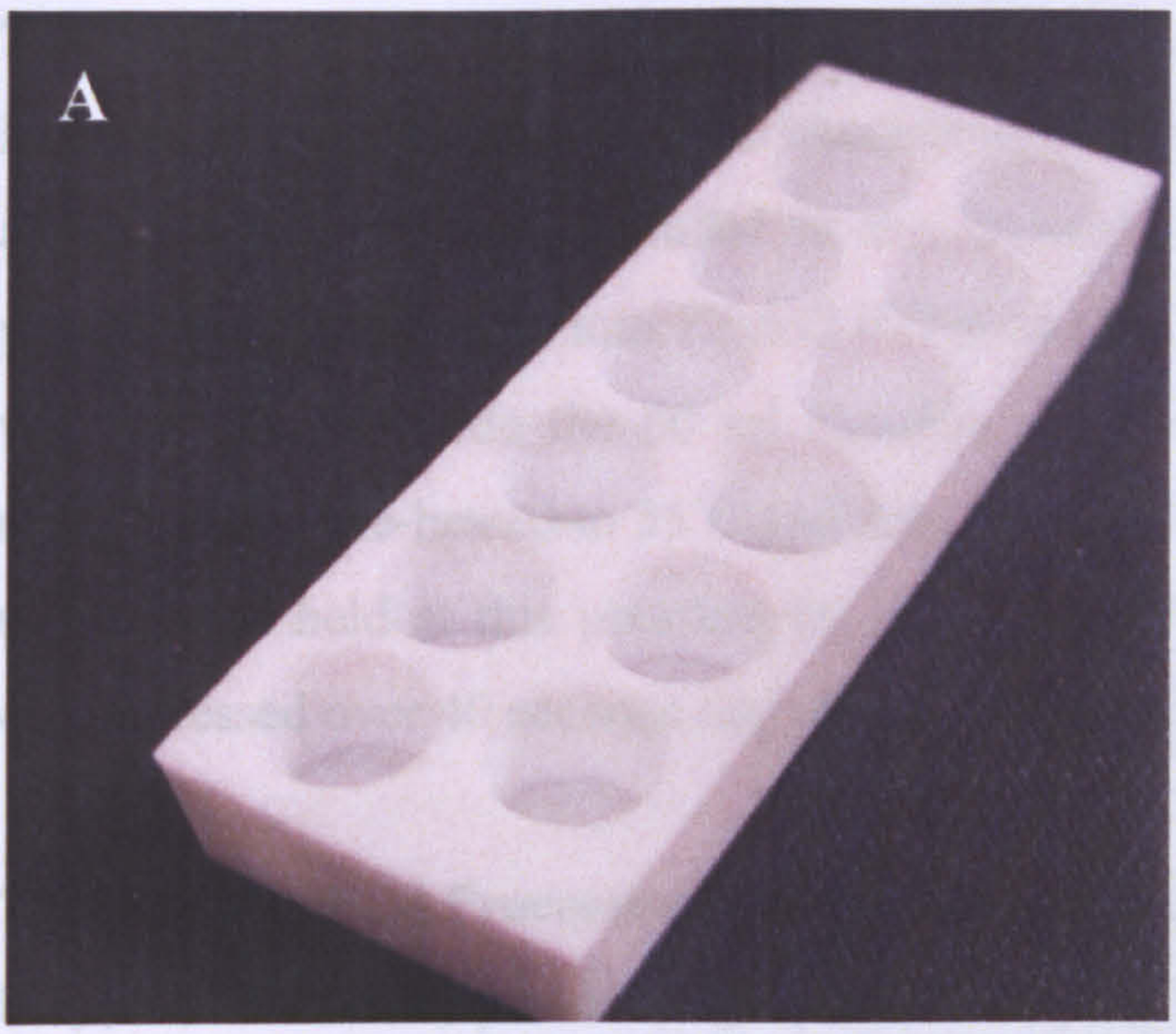

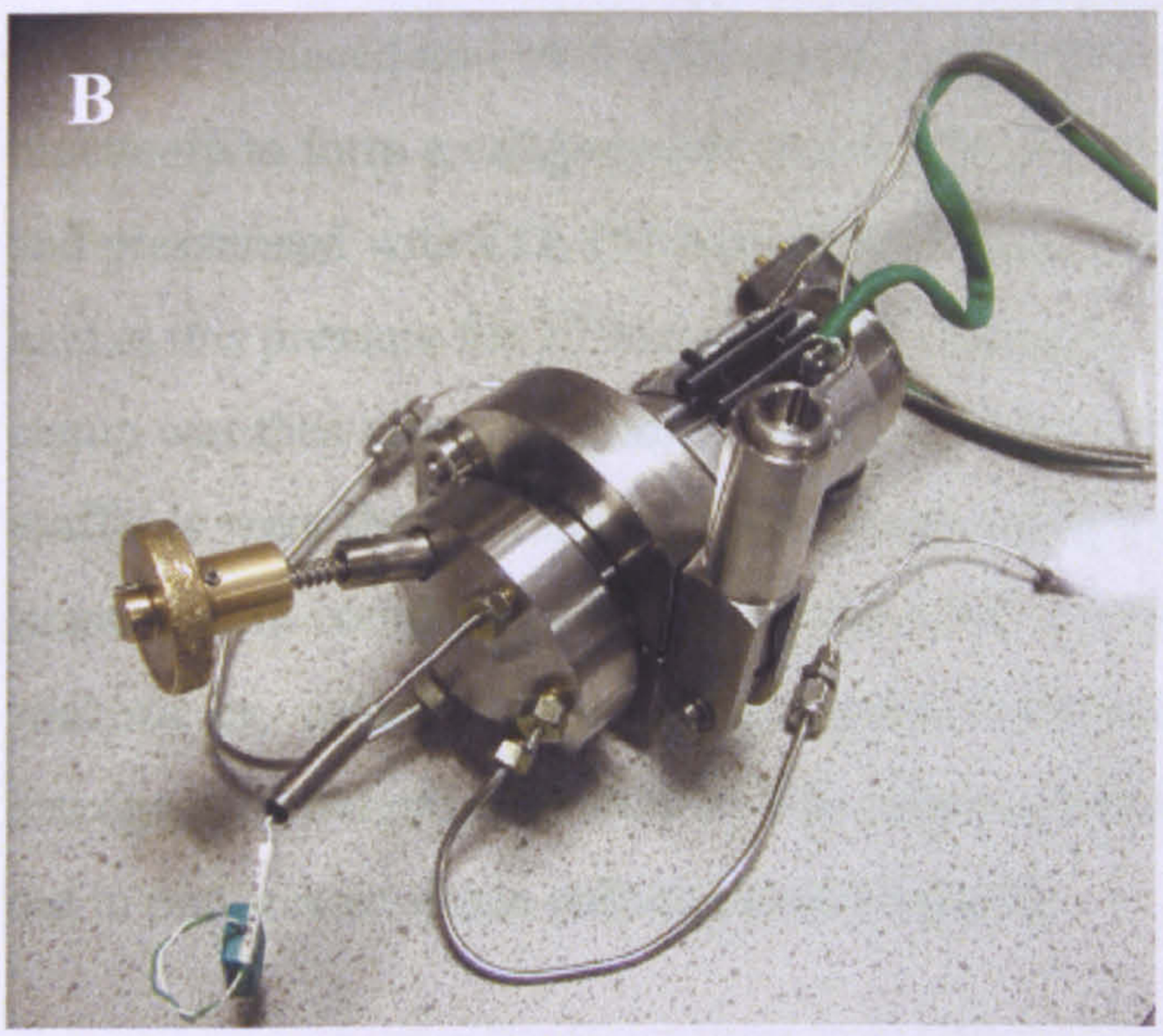

Figure 7-4 Apparatus used to process of both mammalian cells and $P_{DL}LA$ scaffolds in high pressure and supercritical CO_2. The cell suspension and or polymer was added to the poly(tetrafluoroethylene) (PTFE) mould (A) before inserting the mould into the 60 ml clamp sealed pressure vessel (B).

7.2.2 Supercritical Processing of $P_{DL}LA$ Scaffolds

In order to produce scaffolds for characterisation purposes only, neither cells nor additional proteins were included in the fabrication process. Poly(DL-lactic acid) powder was weighed out into 12 well PTFE moulds (see figure 7-4A) at 100 mg per well and placed inside the 60 ml stainless steel vessel seen in figure 7-4B. The autoclave was pre-heated to 35˚C and the system pressurised to 74 bars of CO_2 in 40 seconds and held at this pressure for 10, 30 or 60 seconds. The system was then decompressed over 40 seconds and the scaffolds removed for analysis.

7.2.3 Supercritical Processing of Live Mammalian Cells with $P_{DL}LA$

Poly(DL-lactic acid) powder was weighed out into 8 well PTFE moulds (see figure 7-4) at 100 mg per well. Aliquots of cell suspension (200 µl containing 250,000 cells) were placed into each well containing the polymer and gently stirred in using a pipette tip to form a cell/polymer slurry. The pressure vessel was pre-heated to 35˚C and pressurised with CO_2 (74 bar) inside 40 seconds. The cell/polymer mixture was held at this pressure for 30 seconds before being decompressed over 40 seconds. The clamp was then removed from the vessel and the cell loaded scaffolds removed. The scaffolds were then cut into 4 equal pieces using a size 22 scalpel blade and either, suspended in complete media (1 ml per well) for 24 hours/six weeks before further analysis or, cultured in complete media containing 500 ng/ml of rhBMP-2 for osteogenic differentiation studies. The culture of all cell loaded scaffolds was carried out in non-treated tissue culture plates (Falcon).

7.2.4 Injecting Cells into High Pressure Environments and $P_{DL}LA$

In the polymer injection process $P_{DL}LA$ powder (100 mg) was first weighed out into the cylindrical PTFE mould (see figure 7-5) and the mould placed in the 60 ml clamp sealed autoclave. In all experiments: the sample (250,000 cells in 200 µl or the dye solution) was placed in the tubing separated from the pressure reservoir and the 60 ml vessel by two valves (A & B). The tubing and the valves were then closed and the 60 ml vessel was pre-heated to 35˚C. The vessel was then slowly pressurised with CO_2 (pressure dependent upon experiment).

During this time, the pressure reservoir above the 60 ml vessel was also pressurised with CO_2 or N_2 (pressure dependent upon experiment) and after the polymer had been exposed to $scCO_2$ for a minimum of ten seconds, the valves (A and B) were opened to allow the cells to pass into the 60 ml vessel by a combination of pressure and gravity. The valves were then closed immediately and after 10 seconds the system was decompressed over 40 seconds. The clamp was then removed from the vessel and the cells or cell loaded scaffolds removed. Cells were then either cultured for 24 hours in complete medium before being assessed for metabolic activity or, cultured in osteogenic medium containing 500 ng/ml of rhBMP-2 and assessed for alkaline phosphatase activity. The scaffolds were either retained in whole for μ-CT analysis, or, cut into four equal pieces using a size 22 scalpel blade and suspended in complete media (1 ml per well) for 24 hours before further analysis or cultured in 500 ng/ml complete media containing rhBMP-2 for osteogenic differentiation studies. The culture of all cell loaded scaffolds was carried out in non-treated tissue culture plates (Falcon).

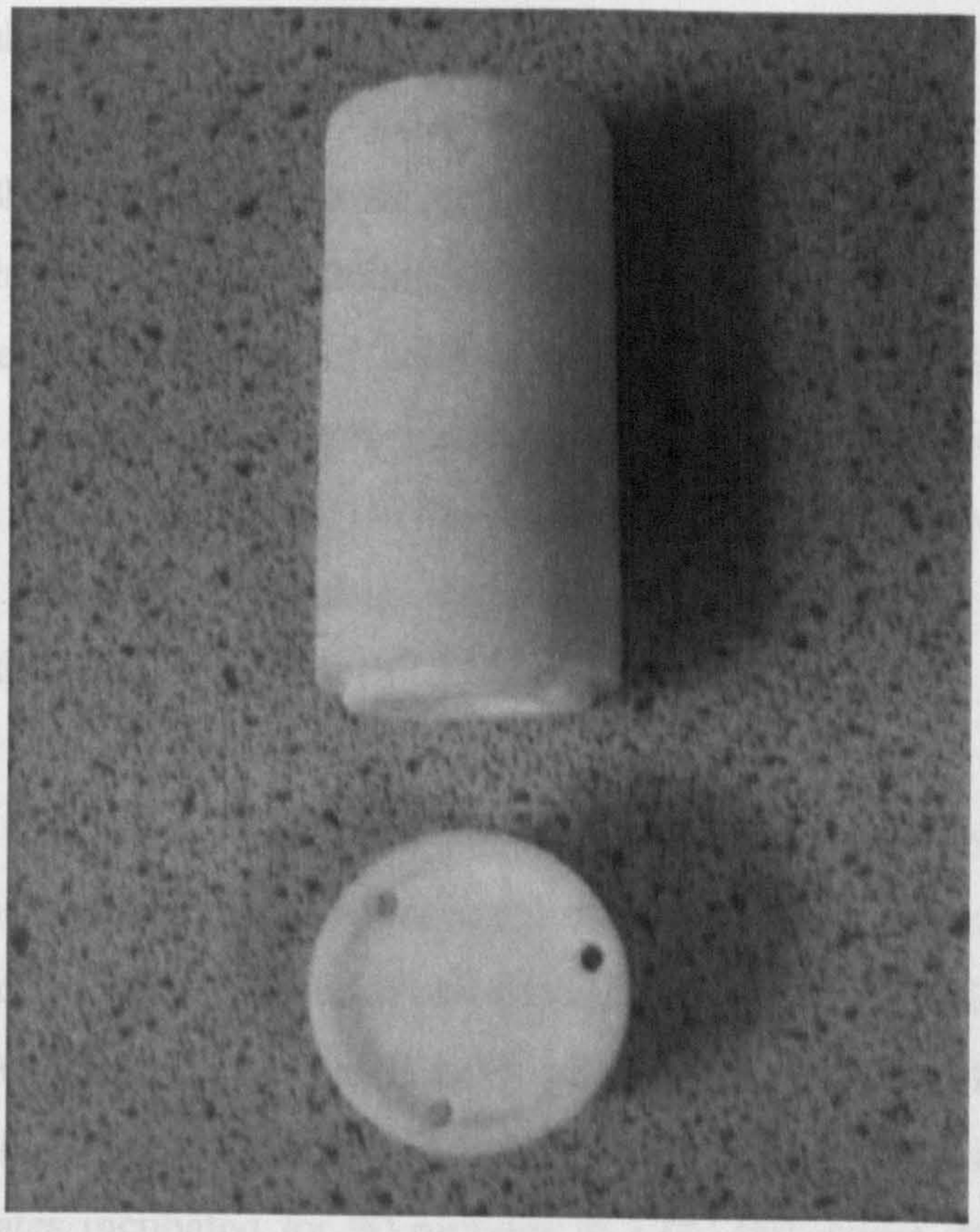

Figure 7-5 A PTFE mould used to collect samples from the high pressure injection system.

7.3 Biochemical Assays

7.3.1 Alamar Blue™ Cell Metabolic Activity Assay

The Alamar Blue™ assay is a relatively simple but extremely sensitive way to measure the metabolic activity of cells in culture. The Alamar Blue™ substrate (Serotech, UK) incorporates a colorimetric indicator that turns from an oxidised form (blue) to a reduced form (red) in the presence of metabolic activity. This colour change can be measured by using absorbance or fluorescence and is directly proportional to the level of cellular mitochondrial activity.

The following procedure was used to measure cell metabolic activity after supercritical processing: After 24 hours in culture, cell culture medium was aspirated from the cells or cell loaded scaffolds and the cells/scaffolds washed with phosphate buffered saline (PBS). The Alamar Blue™ solution (10% v/v in Hank's Balanced Salt Solution, HBSS) was then added in 1 ml aliquots to each of the wells containing cells and the plates incubated for 90 minutes at 37°C (5% CO_2). After 90 minutes had elapsed, 200 µl aliquots were taken from each well in triplicate and transferred to a 96–well plate (Falcon). This solution was then read on the plate reader (Cytofluor, Perceptive Biosystems) at 530 nm excitation and 590 nm emission. After data retrieval, the fluorescence readings were compared to that of untreated controls to give a percentage of normal cellular metabolic activity and thus, the percentage survival for each cell type.

7.3.2 DNA Assay

In order to calculate the specific levels of alkaline phosphatase or testosterone expressed in the cell population after supercritical processing, the values were corrected to the quantity of DNA present to give a more accurate representation. DNA content was estimated using Hoechst 33258 dye binding, as modified from a previously described method (Cesarone *et al*, 1979). Cell cultures were first washed in PBS before being fixed in 75% ethanol and homogenised in 600 µl of distilled water containing 0.01% tween detergent (Triton x-100) to lyse the cells, thus releasing the DNA. The cell homogenate (50 µl) was added to a 96 well plate (Falcon) and 100 µl of 2 µg/ml Hoechst 33258 added. Fluorescence was detected at an emission wavelength of λ460 nm using λ360 nm excitation and compared to a series of DNA standards from 0 to 20 µg/ml. A standard curve of fluorescence against DNA content was plotted using the DNA standards to calculate the amount of DNA in each sample.

7.3.3 Assay for LDH Release from Mammalian Cells as an Indicator of Cell Rupture

This colorimetric assay for the quantification of cell death and cell lysis is based on the measurement of lactate dehydrogenase (LDH) activity released from the cytosol of damaged cells into the supernatant. Therefore a simple assay for levels of LDH was carried out to determine the extent of any damage to the cell membrane after exposure to or injection into high pressure or supercritical CO_2. C2C12 cells were either, exposed to scCO_2 in DMEM (without phenol red and FCS) for increasing exposure times (10 seconds to three minutes) or, injected into a pressurised PTFE mould using high pressure CO_2. The cells were then separated and removed by centrifugation for two minutes (8000 g rpm, SciQuip 3K15) and 100 µl of the DMEM supernatant assayed for release of LDH using an equal volume of the LDH substrate/dye reaction mixture in a 96-well plate (Roche, Penzberg, Germany). Absorbance readings were detected at an emission wavelength of λ490 nm using λ600 nm as a reference. Results were then compared to a set of controls.

7.3.4 Enzyme–Linked Immunosorbent Assay for Histone Complexes as an Indicator of Apoptosis

To further elucidate the cause of cell death, C2C12 cells were assessed for $scCO_2$ induced apoptosis by way of an enzyme-linked immuno sorbent assay (ELISA) used to detect the histone-DNA complexes indicative of apoptotic cells. After processing in $scCO_2$ (74 bar, 35°C) for increasing exposure times (10 seconds to three minutes) cells were cultured for a further three hours in fresh DMEM (so as to observe apoptosis rather than cell mechanical damage). The cells were then assayed using the cell death detection ELISA plus (Roche, Penzberg, Germany) used as per manufacturers instructions. In brief, cells from each processing cycle were lysed using the provided buffer, centrifuged (200 × g for 10 minutes) and 20 µl of the lysate supernatant added to a streptavidin coated ELISA plate. 80 µl of the immunoreagent (containing the enzyme-linked antibody) was added to each well and the plate was incubated at room temperature (with slight agitation for two hours). The solution was then removed from each well and replaced with 100 µl of an ABTS solution before a 20 minute incubation to allow the green color to develop in the sample wells. Absorbance readings were detected at an emission wavelength of λ490 nm using λ600 nm as a reference.

7.3.5 Testosterone Assay for Cytochrome P450 Activity using High Performance Liquid Chromatography

The function of cytochrome P450 (CYP450) enzymes in cultured hepatocytes was assayed via the hydroxylation of testosterone and detection of the resultant metabolites. Presence of these metabolites was detected via the use of high performance liquid chromatography (HPLC). The following procedure was used to measure testosterone activity after $scCO_2$ processing for 10, 30 and 60 seconds. Rat cell cultures were incubated for 1 hour at 37°C in 1.5 ml or 320 µl respectively of Earl's buffered saline solution (EBSS) supplemented with 1 mM Ca^{2+}, 1 mM Mg^{2+} and containing 100 µM testosterone. The supernatant was centrifuged to remove cell debris, and analysed using a Beckman HPLC 1090 fitted with a Zorbax 300 SB-C18 4.6 mm x 15 cm column maintained at 50°C.

Mobile phase A consisted of 450 ml H_2O, 50 ml acetonitrile and 250 µl formic acid, whilst mobile phase B consisted of 50 ml H_2O, 450 ml acetonitrile, 75 µl formic acid. Mobile phase A was run at 1 ml/minute, starting at 15% B, increasing linearly over 10 minutes to 50% B. UV absorbance was detected at 245 nm using an integral diode array detector. The sample injection volume was 40 µl and each run was controlled by intermittent injection of an external standard of 6β-hydroxytestosterone, as well as a mix of all metabolite standards. The peak height of each sample was recorded, corrected to DNA retrieved from the cell samples and compared to untreated controls to calculate the percentage of each metabolite present in each sample.

7.4 Alkaline Phosphatase Studies using the Murine C2C12 Cell Line

In order to measure cell function, the differentiation of myogenic C2C12 cells was investigated as this cell line has been shown to be pluri-potent dependent upon the cell environment (Ichida *et al*, 2004). The osteoblast lineage can be induced in the C2C12 cell line by bone morphogenetic protein-2 (BMP-2), an indicator of which is alkaline phosphatase activity (Okubo *et al*, 1999, Han *et al*, 2003). Alkaline phosphatase acts by converting p-nitrophenyl phosphate (p-NPP) into p-nitrophenol (p-NP) and inorganic orthophosphate. Therefore the rate of this conversion to p-NP is given as a measure of alkaline phosphatase activity and thus, evidence of osteogenesis (Katagiri *et al*, 1994).

7.4.1 BMP-2 Induced Osteogenic Differentiation of the C2C12 Cell Line

After culture in complete DMEM, cells were further cultured for seven days in DMEM supplemented with 2% FCS (v/v) and 500 ng/ml rhBMP-2 (for osteogenic differentiation) using a method modified from that already described (Oreffo *et al*, 1998). Scaffolds loaded with C2C12 cells were cut into four equal pieces and cultured for 24 hours in complete DMEM. Once attached to the $P_{DL}LA$ scaffold, the cells were further cultured for seven days in DMEM supplemented with 2% FCS (v/v) and 500 ng/ml rhBMP-2 (for osteogenic differentiation).

7.4.2 p-NPP Assay for Alkaline Phosphatase Activity

Murine C2C12 cells were processed in high pressure or supercritical CO_2 before subsequent culture in an osteogenic medium containing 500 ng/ml of BMP-2. Cells were fixed in 75% ethanol for 10 minutes and homogenized in 600 µl of distilled water containing 0.01% Tween (Triton-X 100) detergent after three cycles of freeze-thawing. The assay for alkaline phosphatase is based on a method used by Tare *et al* (2002) and was carried out as follows:

The p-NPP substrate (1 mg/ml) was added to equal volumes of the cell samples, incubated at 37°C for 1 hour and the rate of conversion into p-nitrophenol (p-NP) measured by a change in fluorescence at 405 nm. Values were compared against known p-NP standards (0 – 1 mg/ml), multiplied by the dilution factor and matched to DNA content to compensate for changes in cell number. Because the assay was carried out over one hour, the final expression of alkaline phosphatase activity is given as nM of p-NP per ng of DNA per hour. This process was repeated in triplicate over four experiments for osteogenically prompted C2C12 cells.

For assessment of alkaline phosphatase activity in $P_{DL}LA$ scaffolds, C2C12 cells were removed by a process of repeatedly pipetting distilled water containing 0.01% of Triton-X 100 detergent and assayed for alkaline phosphatase activity using the method previously described.

7.4.3 Alkaline Phosphatase Staining of the C1C12 Cell Line

As a measure of the osteogenic status of C2C12 cells, a red color substrate was precipitated on the cells by the action of cellular alkaline phosphatase activity. After osteogenic culture, each cell loaded scaffold was washed in PBS (1 ml) and then incubated at room temperature in 1 ml of the active substrate. The substrate system comprised 9.6 ml of dH_2O, 400 µl of Napthol AS-MX buffer solution and 10 mg of fast violet B salt. After 30 minutes at room temperature the scaffolds were viewed using a light microscope (Nikon, SMZ1500).

7.5 Genomic Analysis

Gene expression profiling or microarray analysis enables the measurement of thousands of genes in a single RNA sample. The principal behind the technique is simple: a glass slide is arrayed with DNA fragments or oligonucleotides that represent specific gene coding regions. Purified RNA is then fluorescently labelled and hybridised to the slide. The raw data is obtained by scanning the array using a laser and a number of statistical tests can then be carried out. Here, hybridisation was carried out on a number of RNA samples retrieved from murine C2C12 cells after supercritical processing. Hybridisation was simultaneously carried out with reference or control RNA to facilitate a comparison of data between processed and non-processed cells.

7.5.1 RNA Isolation, Purification and Hybridisation

Batches of C2C12 cells (N=4) were assessed for changes in gene expression using an OciChip™ 30k set-A microarray (Ocimum Biosolutions). Murine C2C12 cells (1 million per batch) were processed for one minute at 74 bar and 35˚C as described in section 7.2.1) and cultured for a further three hours in DMEM. Cells were then rinsed in 1 ml PBS and homogenised in an RLT buffer containing β-mercaptoethanol (10 µl per ml) before overnight freezing at -20°C. When thawed, total RNA content of the cell homogenate was assessed using the RNeasy kit (Qiagen, Germany). Ethanol (70%) was first added to the cell homogenate and mixed thoroughly by pipetting. The sample (700 µl) was added to an RNeasy mini spin column and centrifuged for 15 seconds at 8000g (10,000 rpm) before removal of the flow through. This process was repeated with all of the samples and untreated controls using a series of buffers supplied with the kit (RW1 and RPE x 2). Finally, 50 µl of nuclease free water was pipetted directly onto the membrane and the sample centrifuged for 1 minute at 8000g (10,000 rpm) to elute the purified RNA. The concentration and quality of the eluted RNA was checked on the nanodrop and agilent bioanalyser and the sample stored at -70°C.

Indirectly labelled probes were generated from 5 μg of total sample RNA with ambion messageamp II amplification (as per manufacturer's protocols). The probes were labelled with alexa 555 or 647 NHS ester dyes (InVitrogen) and 0.5 μg (approximately 40 ρM of dye-label) of each was used for each channel of 2 colour hybridisations. Hybridisations were performed for 16 hours on a TEcan HTS 4800 hybridisation station with moderate agitation, using the Ocimum recommended solutions and temperatures.

7.5.2 Microarray Analysis

Arrays were scanned with a GenePix 4000b laser scanner and primary data obtained using GenePix Pro 6.0 software (Axon). Filtering of array data and normalization using the LOWESS algorithm were performed within the University of Nottingham microarray database (a version of BASE v1.2.16, Lund University, Sweden). Further analysis was performed on this data set using Multi Experiment Viewer (MEV) software and the statistical analysis of microarrays (SAM) algorithm.

7.6 Biological Stains and Histology

7.6.1 Ethidium Homodimer-1: Calcein AM (LIVE/DEAD™) Stain

Both cell viability and location in cell loaded scaffolds were assessed with the use of LIVE/DEAD™ stain (Molecular Probes, UK). The LIVE/DEAD™ stain uses ubiquitous intracellular esterase activity to distinguish live cells from dead. In live cells, the cell permeant calcein AM is converted into the fluorescent calcein which is retained within the cell and produces a uniform green fluorescence. In dead cells, the ethidium homodimer-1 enters cells through the damaged membrane, where it binds to nucleic acids to produce a fluorescent red colour. After $scCO_2$ processing cell loaded polymers scaffolds were incubated in 10 ml of complete DMEM containing 20 µl of ethidium homodimer-1 (to highlight the dead cells red) and 5 µl of calcein AM (to highlight the live cells green) for 1 hour. The cells were then rinsed (×4) in phosphate buffered saline (PBS) for 1 hour, before being observed using fluorescence microscopy (Leica DM IRB).

7.6.2 Histology of Cell Loaded Scaffolds with LIVE/DEAD™ and Propidium Iodide Staining

Poly(DL-lactic acid) ($P_{DL}LA$) scaffolds containing C2C12 cells were prepared for histology by fixing in 70% methanol for 30 minutes, drying overnight and subsequent infiltration with 65°C paraplast wax (Sigma UK). 10 µm sections were cut using a microtome (Leica RM2165) and observed using a fluorescence microscope for either propidium iodide stained nuclei to identify cell location or for LIVE/DEAD™ stained cells to show cell activity within the scaffolds.

7.7 Techniques used in the Characterisation of Polymer Scaffolds

7.7.1 Light and Fluorescence Microscopy

Two light/fluorescence microscopes were used for visualisation of all the samples (Nikon, SMZ1500 & Leica DM IRB). Samples were observed using a variety of methods. Mammalian cells were visualised *in situ* using normal light. Cells on scaffolds were visualised using fluorescent light for the LIVE/DEAD™ stain after the scaffold had been cut into four sections and placed upon the stage piece by piece in the most suitable orientation. Polymer scaffolds were either cut transversely and placed on the microscope stage for scaffold characterisation or, cut into smaller pieces for identification of areas stained for alkaline phosphatase and then placed upon the microscope stage. All scaffolds viewed without fluorescent light were placed on a piece of plain white paper to act as a suitable background. Histological samples were visualised with fluorescent light to indicate the areas stained with either LIVE/DEAD™ or propidium iodide.

7.7.2 Scanning Electron Microscopy

7.7.2.1 Preparation of Samples

The degree of preparation was dependent upon the type of sample used. For non-biological samples (no cells attached) the polymer scaffolds required no preparation before sputter coating. However, if the polymer scaffolds were loaded with cells (biological samples) the scaffolds were fixed to preserve the in vivo state of the cells. This was done by first pre-fixing each scaffold in 1 ml of glutaraldehyde (3%) (Fisher, UK) overnight at 4°C. A solution of 1% osmium tetroxide (Fisher, UK) was then added to the scaffolds (1 ml per scaffold) before a two hour incubation step at room temperature. Osmium tetroxide fixes the cells further and provides a conductive coating of osmium, which improves the final image quality by reducing the charging of the sample under the electron beam and by enhancing the secondary electron emission. The scaffolds were then washed three times in distilled water and dehydrated using increasing concentrations of ethanol from 25% to 100%.

Finally, sufficient hexamethyldisilazane (HMDS) (Fisher, UK) was added to cover the scaffolds and left on for five minutes × 2 (to chemically dry the scaffolds). The scaffolds were then washed in distilled water and left to dry overnight.

7.7.2.2 Gold (Sputter) Coating

Before polymer samples were examined under the electron microscope, they needed to be gold (sputter) coated. This process allows the electron beam to interact with the polymer surface. Scaffolds were cut transversely and correctly orientated to show the area of interest before being mounted on aluminium stubs using adhesive carbon disks to eliminate background charge. The samples were then placed in the vacuum-sealed sputter coater and a coating cycle run for 4 minutes using an argon pressure of 13 Pa and a current of 14 mA.

7.7.2.3 Imaging and Scaffold Characterisation

For pore measurements, the $P_{DL}LA$ scaffolds were prepared for non-biological SEM, placed inside the sample chamber of the microscope (Philips 505 SEM). When under vacuum, the filament was switched on and the scaffolds were scanned at 15-20 kV with the spot size set to 50. The diameter across the pores of the scaffolds was measured using the supplied SEMICAPS software and was taken as the widest part of the open-pore windows. Pore diameters were counted randomly beginning at the centre and travelling set distances from this point. Only 50 pores were counted: this was limited by the number of pores and the large pore size. Histograms of the frequency of each diameter were constructed to determine the pore size distribution and the mean pore size. Cell loaded scaffolds were prepared for biological SEM and scanned at 20kV with a spot size of 50. The magnification control was slowly increased (up to 380×) and the contrast altered to distinguish any clusters of cells that were attached the surface of the scaffold.

7.7.3 Micro-Computed Tomography

Samples were scanned using this technique to both determine the physical characteristics of, and look for the distribution of cells within, $P_{DL}LA$ scaffolds. Scaffolds were placed inside a plastic sample tube in an upright position, packed with polyurethane foam and loaded into the micro-computed tomography (μ-CT) unit. The scanner was set to a voltage of 55 kV and a current of 145 mA using a high resolution μ-CT unit (μ-CT 40, Scanco Medical, Bassersdorf, Switzerland). Scaffolds were scanned at 8 μm voxel 13D pixel resolution with an integration time of 120 ms to produce a set of slices or contours (400 per scaffold) from which 3D reconstructed images could be formed.

The characteristics of the 3D scaffolds were evaluated by defining a region of interest (ROI) for each slice or contour and using the Scanco software provided to calculate both the average pore size and total porosity for each scaffold within that ROI. Histograms of the frequency of each pore diameter were constructed to provide the pore size distribution. A threshold of 60 (arbitrary number) was used to view the porous polymer scaffolds and a threshold of 190 was used to observe the cells entrapped within when appropriate. Note: by altering the threshold value the contrast of the image can be changed. Too high a threshold may result in a loss of sample data whereas too low a threshold value and the level of noise in the image will be increased.

References

Alsberg, E., Hill, E.E. and Mooney, D.J. (2001) Craniofacial tissue engineering. *Critical Reviews in Oral Biology and Medicine*, **12**, 64-75.

Anderson, D.G., Levenberg, S. and Langer, R. (2004) Nanoliter-scale synthesis of arrayed biomaterials and application to human embryonic stem cells. *Nature Biotechnology*, **22**, 863-866.

Anson, D.S., Austen, D.E.G. and Brownlee, G.G. (1995) Expression of active human clotting factor IX from recombinant DNA clones in mammalian cells. *Nature*, **315**, 683-685.

Arora, K.A., Lesser, A.J. and McCarthy, T.J. (1998) Preparation and characterization of microcellular polystyrene foams processed in supercritical carbon dioxide. *Macromolecules*, **31**, 4614-4620.

Atala, A., Cima, L.G., Kim, W., Paige, K.T., Vacanti, J. P., Retik., A.B. and Vacanti., C.A. (1993) Injectable alginate seeded with chondrocytes as a potential treatment for vesicoureteral reflux. *Journal of Urology*, **150**, 745-747 Part 2.

Au, A., Polotsky, A., Krzyminski, K., Gutowska, A., Hungerford, D.S. and Frondoza, C.G. (2004) Evaluation of thermoreversible polymers containing fibroblast factor -9 (FGF-9) for chondrocyte culture. *Journal of Biomedical Materials Research - Part A*, **69A**, 367-372.

Auger, F.A., Lopez Valle, C.A., Guingard, R., Tremblay, N., Noel, B., Goulet, F. and Germain, L. (1995) Skin equivalent produced with human collagen. *In-Vitro Cellular and Developmental Biology – Animal*, **31**, 432-439.

Baldwin, D.F., Shimbo, M. and Suh, N.P. (1995) The role of gas dissolution and induced crystallisation during microcellular polymer processing: a study of poly(ethylene terephthalate) and carbon dioxide systems. *Journal of Engineering and Materials Technology*, **117**, 62-74.

Baldwin, D.F., Park, C. B. and Suh, N.P. (1996a) A Microcellular Processing Study of Poly(Ethylene Terephthalate) in the Amorphous and Semicrystalline States. Part I: Microcellular nucleation. *Polymer Engineering and Science*, **36**, 1437-1445.

Baldwin, D.F., Park, C.B. and Suh, N.P. (1996b) A Microcellular Processing Study of Poly(Ethylene Terephthalate) in the Amorphous and Semi-crystalline States. Part II: Cell Growth and Process Design. *Polymer Engineering and Science*, **36**, 1446-1453.

Barry, J.A., Gidda, H.S., Scotchford, C.A. and Howdle, S.M. (2004) Porous methacrylate scaffolds: supercritical fluid fabrication and in vitro chondrocyte responses, *Biomaterials*, **25**, 3559-3568.

Barry, J.J.A., Silva, M.M.C.G., Shakesheff, K.M., Howdle, S.M. and Alexander, M.R. (2005) Using plasma deposits to promote cell populations of the porous interior of three-dimensional poly(DL-lactic acid) tissue engineering scaffolds. *Advanced Functional Materials*, **15**, 1134-1140.

Berscht, P.C., Nies, B., Liebendorfer, A. and Kreuter, J. (1994) Incorporation of basic fibroblast growth factor into methylpyrrolidinone chitosan fleeces and determination of the in vitro release characteristics. *Biomaterials*, **15**, 593-600.

Bhandari, R.N.B, Riccalton, L.A., Lewis, A.L., Fry, J.R., Hammond, A.H., Tendler, S.J.B., Shakesheff, K.M.S. (2001) Liver tissue engineering: A role for co-culture systems in modifying hepatocyte function and viability, *Tissue Engineering*, **7**, 345-357.

Bleich, J., Muller, B.W., Wassmus, W. (1993) *International Journal of Pharmaceutics*, **97,** 111-117.

Bonassar, L.J. and Vacanti, C.A. (1998) Tissue Engineering: the first decade and beyond, *Journal of Cellular Biochemistry Supplements*, **30/31**, 297.

Brewer, W.E., Galipo, R.C., Sellers, K.W. and Morgan, S.L. (2001) Analysis of cocaine, benzoylecgonine, codeine, and morphine in hair by supercritical fluid extraction with carbon dioxide modified with methanol. *Analytical Chemistry*, **73**, 2371-2376.

Briscoe, B.J. and Kelly, C.T. (1995) The plasticization of a polyurethane by carbon dioxide at high pneumatic stresses. *Polymer*, **36**, 3099-3102.

Brittberg, M., Tallheden, T., Sjoren-Jansson, B. and Peterson, L. (2001) Autologous chondrocytes used for articular cartilage repair – an update, *Clinical Orthopaedics and Related Research*, **391**, S337.

Burg, K. J. L., Holder, W. D., Culberson, C. R., Beiler, R. J., Greene, K. G, Loebsack, A. B, Roland, W. D, Eiselt, P., Mooney, D. J. and Halberstadt, C.R.(2000) Comparative study of seeding methods for three-dimensional polymeric scaffolds. *Journal of Biomedical Materials Research*, **51**, 642-649.

Busby, A.J., Zhang, J.X., Naylor, A., Roberts, C.J., Davies, M.C., Tendler, S.J.B. and Howdle, S.M. (2003) The preparation of novel nano-structured polymer blends of ultra high molecular weight polyethylene with polymethacrylates using supercritical carbon dioxide. *Journal of Materials Chemistry*, **13**, 2838-2844.

Cadoni, E., De Giorgi, M.R., Medda, E. and Poma, G. (1999) Supercritical carbon dioxide extraction of lycopene and beta-carotene from ripe tomatoes. *Dyes & Pigments*, **44**, 27-32.

Cannizzaro, S. M., Padera, R. F., Langer, R., Rogers, R. A., Black, F. E., Davies, M. C., Tendler, S. J. B. and Shakesheff, K. M. (1998) A novel biotinylated degradable polymer for cell-interactive applications. *Biotechnology & Bioengineering*, **58**, 529-535.

Cao, Y.L., Rodriguez, A., Vacanti, M., Ibarra, C., Arevalo, C. and Vacanti, C.A. (1998) Comparative study of the use of poly(glycolic acid), calcium alginate and pluronics in the engineering of porcine cartilage. *Journal of Biomaterials Science - Polymer Edition*, **9**, 475-487.

Cao, X. and Shoichet, M.S. (1999) Delivering neuroactive molecules from biodegradable microspheres for application in central nervous system disorders, *Biomaterials.*, **20**, 329-339.

Cartmell, S., Huynh, K., Lin, A., Nagaraja, S. and Guldberg, R. (2004) Quantitative micro computed tomography analysis of mineralization within three-dimensional scaffolds in vitro. *Journal of Biomedical Materials Research - A*, **69**, 97–104.

Cesarone, C. F, Bolognesi, C. and Santi, L. (1979) Improved micro-fluorometric DNA determination in biological material using 33258 HOECHST. *Analytical Biochemistry*, **100**, 188-197.

Charoenchaitrakool, M., Dehghani, F., Foster, N.R. and Chan, H.K. (2000) Micronisation by rapid expansion of supercritical solutions to enhance the dissolution rate of poorly water-soluble molecules. *Industrial and Engineering Chemistry Research*, **39**, 4794-4802.

Chen, G.P., Ito, Y. and Imanishi, Y. (1997) Photo-immobilization of epidermal growth factor enhances its mitogenic effect by artificial juxtacrine signalling, *Biochemica et Biophysica ACTA -Molecular Cell Research*, **1358**, 200-208.

Collier, S. and Ghosh, P. (1995) Effects of transforming growth factor beta on proteoglycan synthesis by cell and explant cultures derived from the knee-joint meniscus. *Osteoarthritis & Cartilage*, **3**, 127-138.

Cooper, A. I. (2000) Polymer synthesis and processing in supercritical carbon dioxide. *Journal of Materials Chemistry,* **10**, 207-234.

Côté, M.F., Laroche, G., Gagnon, E., Chevallier, P. and Doillon, C.J. (2004) Denatured collagen as support for a FGF-2 delivery system: physiological characterizations and *in vitro* release kinetics and bioactivity. *Biomaterials*, **25**, 3761-3772.

Darling, E.M. and Athanasiou, K.A. (2003) Articular cartilage bioreactors and bioprocesses, *Tissue Engineering*, **9**, 9-26.

Darr, J. A. and Poliakoff, M. (1999) New directions in inorganic and metal-organic coordination chemistry in supercritical fluids. *Chemical Reviews*, **99**, 495-541.

Debenedetti, P.G., Tom, J.W., Kwauk, X. and Yeo, S.D. (1993) Rapid expansion of supercritical solutions (RESS) – fundamentals and applications. *Fluid Phase Equilibria*, **82**, 311-321.

Deng, W., Obrocka, M., Fischer, I. and Prockop, D.J. (2001) In vitro differentiation of human marrow stromal cells into early progenitors of neural cells by conditions that increase intracellular cyclic AMP. *Biochemical and Biophysical Research Communications*, **282**, 148–152.

Denry, I.L. (1996) Recent advances in ceramics for dentistry. *Critical Reviews in Oral Biology & Medicine*, **7**, 134-143.

Dillow, A.K., Dehghani, F., Hrkach, J.S., Foster, N.R. & Langer, R. (1999) Bacterial inactivation by using near and supercritical carbon dioxide. *Proceedings of the National Academy of Sciences of the United States of America,* **96**, 10344-10348.

Dixit, V. (1994) Development of a bioartificial liver using isolated hepatocytes, *Artificial Organs*, **18**, 371-384.

Draget, K.I., Skjak-Braek, G. and Smidsrod, O. (1997) Alginate-based new materials. *International Journal of Biological Macromolecules*, **21**, 47-55.

Dsouza, S.E, Ginsberg, M.H. and Plow, E.F. (1991) Arginyl-Glycyl-Aspartic Acid (RGD) – a cell adhesion mofif. *Trends in Biochemical Sciences*, **16**, 246-250.

Ducheyne, P. and Qui, Q. (1999) Bioactive ceramics: the effect of surface reactivity on bone formation and bone cell function. *Biomaterials*, **20**, 2287-2303.

Dunkelman, N.S., Zimber, M.P., Lebaron, R.G., Pavelec, R., Kwan, M. and Purchio, A.F. (1995) Cartilage production by rabbit articular chondrocytes on PGA scaffolds in a closed bioreactor system. *Biotechnology and Bioengineering*, **46**, 299-305.

Dutt, K., Douglas, P., Layne, D., Harris-Hooker, S., Tufon, R. and Hunt, R. (2000) Tissue engineering: Human retinal pre-cursors and retinal pigment epithelial cell co-cultures in NASA bioreactor, *Investigative. Ophthalmology & Visual Science*, **41**, S858-S858.

Emerich, D.F., Winn, D.F., Christenson, L., Palmatier, M.A., Gentile, F.T. and Sanberg, P.R. (1992) A novel approach to neural transplantation in Parkinsons disease – use of polymer-encapsulated cell therapy. *Neuroscience and Biobehavioral Reviews*, **16**, 437-447.

Eming, S.A., Smola, H. and Krieg, T. (2002) Treatment of chronic wounds: State of the art and future concepts. *Cells, Tissues, Organs,* **172**, 105-117.

Enomoto A., Nakamura K., Nagai K., Hashimoto T. and Hakoda, M. (1997) Inactivation of food microorganisms by high-pressure carbon dioxide treatment with or without explosive decompression. *Bioscience, Biotechnology and Biochemistry*, **61**, 1133-1137.

Falk, R., Randolph, T.W., Meyer, J.D., Kelly, R.M. and Manning, M.C. (1997) Controlled release of ionic compounds from poly (L-lactide) microspheres produced by precipitation with a compressed antisolvent. *Journal of Controlled Release*, **44**, 77-85.

Falk, R.F. and Randolph, T.W. (1998) Process variable implications for residual solvent removal and polymer morphology in the formation of gentamycin-loaded poly(L-lactide) microparticles. *Pharmaceutical Res*earch, **15**, 1233-1237.

Foster, J.W., Cowan, R.M., Maag, T.A. (1962) Rupture of bacteria by explosive decompression. *Journal of Bacteriology,* **83**, 330-334.

Foster, N., Mammucari, R., Dehghani, F., Barrett, A., Bezanehtak, K., Coen, E., Combes, G., Meure, L., Ng, A., Regtop, H.L. and Tandya, A. (2003) Processing pharmaceutical compounds using dense gas technology. *Industrial and Engineering Chemistry Research*, **42**, 6476-6493.

Fraser, D. (1951) Bursting bacteria by release of gas pressure. *Nature,* **167**, 33-34.

Freed, L.E., Marquis, J.C., Nohria, A., Emmanual, J., Mikos, A.G. and Langer, R. (1993a) Neocartilage formation in vitro and in vivo using cells cultured on synthetic biodegradable polymers. *Journal of Biomedical Materials Research*, **27**, 11-23.

Freed, L.E., Hollander, A.P., Martin, I., Barry, J.R., Langer, R. and Vunjak-Novakovic G. (1998) Chondrogenesis in a cell-polymer-bioreactor system, *Experimental Cell Research*, **240**, 58-65.

Freed, L.E. and Vunjak-Novakovic, G. (1998) Culture of organised cell communities. *Advanced Drug Delivery Reviews*, **33**, 15-30.

Fuchs, J.R., Hannouche, D., Terada, S., Zand, S., Vacanti, J.P. and Fauza, D.O. (2005) Cartilage engineering from ovine umbilical cord blood mesenchymal progenitor cells. *Stem Cells*, **23**, 958-964.

Goel, S.K. and Beckman, E.J. (1993a) Plasticization of poly(methyl methacrylate) (PMMA) networks by supercritical carbon-dioxide. *Polymer*, **34**, 7, 1410-1417.

Goel, S.K. and Beckman, E.J. (1993b) Generation of micro-cellular polymers using supercritical carbon dioxide. *Cellular Polymers*, **12**, 251-274.

Goel, S.K. and Beckman, E.J. (1994a) Generation of micro-cellular polymeric foams using supercritical carbon dioxide. 1: Effect of pressure and temperature on nucleation. *Polymer Engineering and Science,* **34**, 1137-1147.

Goel, S.K. and Beckman, E.J. (1994b) Generation of micro-cellular polymeric foams using supercritical carbon dioxide. 2: Cell growth and skin formation. *Polymer Engineering and Science,* **34**, 1148-1156.

Goodpaster, J. V., Bishop, J. J. and Benner, B. A. (2003) Forensic analysis of hair surface components using off-line supercritical fluid extraction and large volume injection. *Journal of Separation Science*, **26**, 137-141.

Göpferich, A. Mechanisms of polymer degradation and erosion. (1996) *Biomaterials.*, **17**, 103-111.

Gregoriades, N., Luzardo, M. and Lucquet, B. (2003) Heat inactivation of mammalian cell cultures for biowaste kill system design. *Biotechnology Progress*, **19**, 14-20.

Griffith, L.G., Wu, B., Cima, M.J., Powers, M.J., Chaignaud, B. and Vacanti, J.P. (1997) In vitro organogenesis of liver tissue, *Annals of the New York Academy of Sciences*, **831**, 382-397.

Guney, O. and Akgerman, A. (2000) Solubilities of 5-fluorouracil and ss-estradiol in supercritical carbon dioxide *Journal of Chemical Engineering Data*, **45**, 1049-1052.

Guney, O. and Akgerman, A. (2002) Synthesis of controlled-release in supercritical medium. *AIChE J*ournal, **48**, 856-866.

Guo, J.F, Jourdian G.W. and MacCallum D.K. (1989) Culture and growth characteristics of chondrocytes encapsulated in alginate beads. *Connective Tissue Research*, **19**, 277–297.

Haas, G.J., Prescott, H.E., Dudley, E., Dir, R., Hintlian, C. and Keane, L. (1989) Inactivation of microorganisms by carbon dioxide under pressure. *Journal of Food Safety,* **9**, 253-265.

Han, B., Tang, B. and Nimni, M.E. (2003) Quantitative and sensitive in vitro assay for osteoinductive activity of demineralized bone matrix. *Journal of Orthopedic Research*, **21**, 648-654.

Han, D.K. and Hubbell, J. A. (1997) Synthesis of polymer network scaffolds from L-lactide and poly(ethylene glycol) and their interaction with cells. *Macromolecules*, **30**, 6077-6083.

Hanna, M.H., and York, P. (1995) *Method and apparatus for the formulation of particles*. Patent WO 96/00 610.

Hao, J.Y., Whitaker, M.J., Wong, B., Serhatkulu, G., Shakesheff, K.M. and Howdle, S.M. (2004) Plasticization and spraying of poly (DL-lactic acid) using supercritical carbon dioxide: Control of particle size. *Journal Pharmaceutical Sci*ences, **93**, 1083-1090.

Hao, J.Y., Whitaker, M.J., Serhatkulu, G., Shakesheff, K.M. and Howdle, S.M. (2005) Supercritical fluid assisted melting of poly(ethylene glycol): a new solvent-free route to microparticles. *Journal of Materials Chem*istry, **15**, 1148-1153.

Harris, L.D., Kim, B.S. and Mooney, D.J. (1998) Open pore biodegradable matrices formed with gas foaming. *Journal of Biomedical Materials Research*, **42**, 396-402.

Hayman, M.W., Smith, K.H., Cameron, N.R. and Przyborski, S.A. (2005) Growth of human stem cell-derived neurons on solid three-dimensional polymers. *Journal of Biochemical and Biophysical Methods*, **62**, 231-240.

Hile, D.D., Amirpour, M.L., Akgerman, A. and Pishko, M.V. (2000) Active growth factor delivery from poly(D,L-lactide-co-glycolide) foams prepared in supercritical CO_2. *Journal of Controlled Release*, **66**, 177-185.

Holmes, J.D., Ziegler, K.J., Audriani, M., Ted Lee Jr, C., Bhargava, P.A., Steytler, D.C. and Johnston, K.P. (1999) Buffering the Aqueous Phase pH in Water-in-CO_2 Microemulsions. *Journal of Physical Chemistry –B*, **103**, 5703-5711.

Hou, Q-P., Freeman, R., Buttery, L.D.K. and Shakesheff, K.M. (2005) Novel surface entrapment process for the incorporation of bioactive molecules within pre-formed alginate fibres. *Biomacromolecules*, **6**, 734-740.

Howard, D., Partridge, K., Yang, X.B., Clarke, N.M.P., Okubo, Y., Bessho, K., Howdle, S.M., Shakesheff, K.M. and Oreffo, R.O.C. (2002) Immunoselection and adenoviral genetic modulation of human osteoprogenitors: in vivo bone formation on PLA scaffold. *Biochemical and Biophysical Research Communications*, **299**, 208-215.

Howdle, S.M., Watson, M.S., Whitaker, M.J., Popov, V.K., Davies, M.C., Mandel, F.S., Wang, J.D. and Shakesheff, K.M. (2001) Supercritical fluid mixing: preparation of thermally sensitive polymer composites containing bioactive materials. *Chemical Communications*, **1**, 109-110.

Huang, Y., Onyeri, S., Mbonda, S., Moshfeghain, A. and Madihally, S. V. (2005) In vitro characterization of chitosan-gelatin scaffolds for tissue engineering. *Biomaterials*, **26** 7616–7627.

Humes, H.D., MacKay, S.M., Funke, A.J. and Buffington, D.A. (1999) Tissue engineering of a bioartificial renal tubule assist device: In vitro transport and metabolic characteristics. *Kidney International*, **55**, 2502-2514.

Ishaug-Riley, S.L., Crane-Kruger, G.M., Yaszemski, M.J. and Mikos, A.G. (1998) Three-dimensional culture of rat calvarial osteoblasts in porous biodegradable polymers. *Biomaterials*, **19**, 1405-1412.

Ishihara, M., Obara, K., Ishizuka, T., Fujita, M., Sato, M., Masuoka, K., Saito, Y., Yura, H., Matsui, T., Hattori, H., Kikuchi, M. and Kurita, A, (2003) Controlled release of fibroblast growth factors and heparin from photo-crosslinked chitosan hydrogels and subsequent effect on *in vivo* vascularization. *Journal of Biomedical Materials Research – Part A*, **64A**, 551-559.

Jang, J. and Shea, L. D. (2003) Controllable delivery of non-viral DNA from porous scaffolds. *Journal of Controlled Release*, **86**, 157-168.

Kanematsu, A., Yamamoto, S., Ozeki, M., Tetsuya, N., Kanatani, I., Ogawa, O., and Tabata, Y. (2004) Collagenous matrices as release carriers of exogenous growth factors, *Biomaterials*, **25**, 4513-4520.

Katagiri, T., Yamaguchi, A., Komaki, M., Abe, E., Takahashi, N., Ikeda, T., Rosen, V., Wozney, J.M., Fujisawasehara, A. and Suda, T. (1994) Bone morphogenetic protein two converts the differentiation pathway of C2C12 myoblasts into the osteoblast lineage. *Journal of Cell Biology*, **127**, 1755-1766.

Kayrak, D., Akman, U. and Hortacsu, O. (2003) Micronization of ibuprofen by RESS. *Journal of Supercritical Fluids*, **26**, 17-31.

Kazarian, S.G., Vincent, M.F., Bright, F.V., Liotta, C.L. and Eckert, C.A. (1996) Specific intermolecular interaction of carbon dioxide with polymers. *Journal of the American Chemical Society*, **118**, 1729-1736.

Kellner, K., Lang, K., Papadimitriou, A., Leser, U., Milz, S., Shulz, M.B., Blunk, T. and Göpferich, A. (2002) Effects of hedgehog proteins on tissue engineering of cartilage in vitro. *Tissue Engineering*, **8**, 541-572.

Keswani, J. and Frank, J.F. (1998) Thermal inactivation of mycobacterium paratuberculosis in milk. *Journal of Food Protection*, **61**, 974-978.

Kim, D.I., Park, H.J., Eo, H.S., Suh, S.W., Hong, J.H., Lee, M.J., Kim, J.S., Jang, I.S. and Kim, B.S. (2004) Comparative study of seeding and culture methods to vascular smooth muscle cells on biodegradable scaffolds. *Journal of Microbiology and Biotechnology*, **14**, 707-714.

Klawitte, J.J. and Hulbert, S.F. (1973) Kinetics and mechanisms of tissue in-growth into porous ceramic implants. *American Ceramic Society Bulletin*, **52**, 430-430.

Klawitte, J.J., Bagwell, J.G., Weinstein, A.M., Sauer, B.W. and Pruitt, J.R. (1976) Evaluation of bone growth into porous high density polyethylene. *Journal of Biomedical Materials Research*, **10**, 311-323.

Kotobuki, N., Hirose, M., Takakura, Y. and Ohgushi, H. (2004) Cultured autologous human cells for hard tissue regeneration: preparation and characterization of mesenchymal stem cells from bone marrow. *Artificial Organs*, **28**, 33-39.

Krewson, C.E. and Saltzman, W.M. (1996) Transport and elimination of recombinant human NGF during long-term delivery to the brain, *Brain Res*earch, **727**, 169-181.

Kulig, K.M and Vacanti, J.R. (2004) Hepatic tissue engineering, *Transplant Immunology*, **12**, 303-310.

Kunas, K.T. and Papoutsakis, E.T. (1990) Damage mechanisms of suspended animal cells in agitated bioreactors with and without bubble entrainment. *Biotechnology and Bioengineering*, **36**, 476-483.

Laurencin C.T., Attawia M.A., Elgendy, H.E. and Hebert, K.M. (1996) Tissue engineered bone regeneration using degradable polymers: the formation of mineralized matrices, *Bone*, **19**, S93-S99.

LeBaron, R.G. and Athanasiou, K.A. (2000) Ex-vivo synthesis of articular cartilage, *Biomaterials*, **21**, 2575-2587.

Ledley, F.D. (1996) Pharmaceutical approach to somatic gene therapy. *Pharmaceutical Research*, **13**, 1595-1614.

Langer, R. and Vacanti, J. P. (1993) Tissue Engineering. *Science*, **260**, 920-926.

Langer, R. and Vacanti, J.P. (1999) Tissue engineering: the challenges ahead, *Scientific American*, **280**, 86.

Levenberg, S. and Langer, R. (2004) Advances in Tissue Engineering. *Current Topics in Developmental Biology*, **61**, 113-134.

Levenberg, S., Rouwkema, J., Macdonald, M., Garfein, E.S., Kohane, D. S., Darland, D. C., Marini, R., van Blitterswijk, C. A., Mulligan, R. C., D'Amore, P. A. and Langer, R. (2005) Engineering vascularized skeletal muscle tissue. *Nature Biotechnology*, **23**, 879-884.

L'Heureux, N., Paquet, S., Labbe, R., Germain, L. and Auger, F. A. (1998) A completely biological tissue-engineered human blood vessel, *Faseb Journal*, **12**, 47-56.

Li, W.J., Laurencin, C.T., Caterson, E.J., Tuan, R.S. and Ko, F.K. (2002) Electrospun nanofibrous structure: A novel scaffold for tissue engineering. *Journal of Biomedical Materials Research*, **60**, 613-621.

Lin, A.S., Barrows, T.H., Cartmell, S.H. and Guldberg, R.E. (2003) Microarchitectural and mechanical characterization of oriented porous polymer scaffolds. *Biomaterials*, **24**, 481–489.

Lind, M., Overgaard, S., Glerup, H., Soballe, K. and Bunger, C. (2001) Transforming growth factor-beta 1 adsorbed to tricalciumphosphate coated implants increases peri-implant bone remodelling. *Biomaterials.*, **22**, 189-193.

Lu, L. and Mikos, A.G. (1996) The importance of new processing techniques in tissue engineering, *Materials Research Society Bulletin.*, **21**, 28-32.

Lu, L., Peter, S.J., Lyman, M.D., Lai, H-L., Leite, S.M., Tamada, J.A., Vacanti, J.P., Langer, R. and Mikos, A.G. (2000a) In vitro degradation of porous poly(L-lactic acid) foams, *Biomaterials*, **21**, 1595-1605.

Lu, L., Peter, S.J., Lyman, M.B., Lai, H-L., Leite, S.M., Tamada, J.A., Uyama, S., Vacanti, J.P., Langer, R. and Mikos, A.G. (2000b) In vitro and in vivo degradation of porous poly(D,L-lactic-co-glycolic acid). *Biomaterials*, **21**, 1837-1845.

Lohmann, C.H., Schwartz, Z., Niederauer, G.G., Carnes, D.L., Dean, D.D. and Boyan, B.B. (2000) Pre-treatment with platelet derived growth factor-BB modulates the ability of costochondral resting zone chondrocytes incorporated into PLA/PGA scaffolds to form new cartilage in vivo, *Biomaterials,* **21**, 49-61.

Maddocks, R.R. and Gibson, J. (1977) Supercritical extraction of coal. *Chemical Engineering Progress*, **73**, 59-63.

Maguire, T., Novik, E., Schloss, R. and Yarmush, M. (2005) Alginate-PLL encapsulation: effect on the differentiation of embryonic stem cells into hepatocytes. *Biotechnology and Bioengineering*, **93**, 581-591.

Makino, S., Fukuda, K., Miyoshi, S., Konishi, F., Kodama, H., Pan, J., Sano, M., Takahashi, T., Hori, S., Abe, H., Hata, J., Umezawa, A. and Ogawa, S. (1999) Cardiomyocytes can be generated from marrow stromal cells in vitro. *Journal of Clinical Investigation,* **103**, 697–705.

Mann, B.K., Schmedlen, R.H. and West, J.L. (2001) Tethered-TGF-beta increases extracellular matrix production of vascular smooth muscle cells. *Biomaterials*, **22**, 439-444.

Maquet, V. and Jerome, R. (1997) Design of macroporous biodegradable polymer scaffolds for cell transplantation. *Materials Science Forum*, **250**, 15-42.

Martinsen, A., Skjak-Braek, G. and Smidsrod, O. (1989) Alginate as immobilization material: I. correlation between chemical and physical properties of alginate gel beads. *Biotechnology and Bioengineering*, **33**, 79–89.

Matson, D.W., Petersen, R.C. and Smith, R.D. (1986) *Materials Letters*, **4**, 429-432.

Matson, D.W., Petersen, R.C. and Smith, R.D. (1987) *Journal of Materials Science*, **22**, 1919-1928.

Mckay, I.A. and Leigh, I. (1993) *Growth Factors; a practical approach*, IRL press, Oxford.

Mironov, V., Boland, T., Trusk, T., Forgacs, G. and Markwald, R. R. (2003) Organ printing: computer-aided jet-based 3D tissue engineering. *Trends in Biotechnology*, **21**, 157-161.

Moon, J.S., Jeon, H.M, Meng, W., Awaike, T. and Kang, I.K. (2005) Morphology and metabolism of hepatocytes microencapsulated with acrylic terpolymer-alginate using gelatin and poly(vinyl alcohol) as extracellular matrices. *Journal of Biomaterials Science-Polymer Edition,* **16**, 1245-1259.

Mooney, D. J., Baldwin, D. F., Suh, N.P., Vacanti, L. P., and Langer. R. (1996a) Novel approach to fabricate porous sponges of poly(D,L-lactic-co-glycolic acid) without the use of organic solvents, *Biomaterials*, **17**, 1417.

Mooney, D.J., Kaufmann, P.M., Sano, K., Schwendeman, S.P., Majahod, K., Schloo, B., Vacanti, J.P. and Langer, R. (1996b) Localized delivery of epidermal growth factor improves the survival of transplanted hepatocytes. *Biotechnology and Bioengineering*, **50**, 422-429.

Nakamura, K., Enomoto, A., Fukushima, H., Nagai, K. and Hakoda, M. (1994) Disruption of microbial cells by the flash discharge of high-pressure carbon dioxide. *Bioscience, Biotechnology and Biochemistry,* **58**, 1297-1301.

Nicoll, S.B., Denker, A.E. and Tuan, R.S. (1995) *In vitro* characterization of transforming growth factor-beta 1-loaded composites of biodegradable polymer and mesenchymal cells. *Cells and Materials*, **5**, 231-244.

Oghushi, H. and Caplan, A.I. (1999) Stem cell technology and bioceramics: From cell to gene engineering. *Journal of Biomedical Materials Research*, **48**, 913-927.

Okubo, Y., Bessho, K., Fujimura, K., Iizuka, T. and Miyatake, S. (1999) Expression of bone morphogenetic protein-2 via adenoviral vector in C2C12 myoblasts induces differentiation into the osteoblast lineage. *Biochemical and Biophysical Research Communications*, **262**, 739-743.

Oreffo, R.O., Bennett, A., Carr, A.J. and Triffitt, J.T. (1998) Patients with primary osteoarthritis show no change with ageing in the number of osteogenic precursors. *Scandinavian Journal of Rheumatology*, **27**, 415-424.

Orgill, D.P. and Skrabut, E.M. (1985) Engineering artificial skin, *Technology Review*, **88**, 56-56.

Otterlei, M., Ostgaard., K, Skjak-Braek., G, Smidsrod., O, Soon-Shiong., T. and Espevik, T. (1991) Induction of cytokine production from human monocytes stimulated with alginate. *Journal of Immunotherapy*, **10**, 286-291.

Paige, K.T., Cima, L.G., Yaremchuk, M.J., Vacanti. J.P. and Vacanti CA. (1995) Injectable cartilage. *Plastic Reconstructive Surgery*, **96**, 1390–1400.

Park, C.B., Baldwin, D.F. and Suh, N.P. (1995) Cell nucleation by rapid pressure drop in continuous processing of microcellular plastics. *Polymer Engineering & Science*, **35**, 432-440.

Park, Y.J., Lee, Y.M., Lee, J.Y., Seol, Y.J., Chung, C.P. and Lee, S.J. (2000a) Controlled release of platelet-derived growth factor-BB from chondroitin sulfate-chitosan sponge for guided bone regeneration. *Journal of Controlled Release*, **67**, 385-394.

Park, Y.J., Lee, Y.M., Park, S.N., Sheen, S.Y., Chung, C.P. and Lee, S.J. (2000b) Platelet derived growth factor releasing chitosan sponge for periodontal bone regeneration. *Biomaterials*, **21**,153-159.

Park, S.S., Jin, H.R., Chi, D.H. and Taylor, R.S. (2004) Characteristics of tissue engineered cartilage from human articular chondrocytes. *Biomaterials*, **25**, 2363-2369.

Parks, K., Sparacio, D. and Beckman, E.J. (1996) Formation of microcellular polymeric materials via polymerization in carbon dioxide. *Abstracts of Papers of the American Chemical Society*, **211**, 142-PMSE Part 2.

Parenteau, N.L., Bilbo, P., Nolte, C.J.M., Mason, V. S. and Rosenberg. (1992) The organotypic culture of human skin keratinocytes and fibroblasts to achieve form and function. *Cytotechnology*, **9**, 163-171.

Partridge, K., Yang, X.B., Clarke, N.M.P., Okubo, Y., Bessho, K., Sebald, W., Howdle, S.M., Shakesheff, K.M. and Oreffo, R.O.C. (2002) Adenoviral BMP-2 gene transfer in mesenchymal stem cells: In vitro and in vivo bone formation on biodegradable polymer scaffolds. *Biochemical and Biophysical Research Communications*, **292**, 144-152.

Patz, T.M., Doraiswamy, A., Narayan, R.J., Modi, R. and Chrisey, D.B. (2005) Two-dimensional differential adherence and alignment of C2C12 myoblasts. *Materials Science and Engineering B – Solid State Materials for Advanced Technology*, **123**, 242-247.

Peker, H, Srinivasan, M.P., Smith, J.M. and McCoy, B.J. (1992) Caffeine extraction rates from coffee beans with supercritical carbon dioxide. *AIChE Journal,* **38**, 761-770.

Peters, M.C., Polverini, P.J. and Mooney, D.J. (2002) Engineering vascular networks in porous polymer matrices, *Journal of Biomedical Materials Research*, **60**, 668-678.

Popov, V. K., Evseev, A. V., Ivanov, A. L., Roginski, V. V., Volozhin, A. I. and Howdle, S. M. (2004) Laser stereolithography and supercritical fluid processing for custom-designed implant fabrication. *Journal of Materials Science – Materials in Medicine*, **15**, 123-128.

Quarto, R., Mastrogiacomo, M., Cancedda, R., Kutepov, S.M., Mukhachev, V., Lavroukov, A., Kon, E. and Marcacci, M. (2001) Repair of large bone defects with the use of autologous bone marrow stromal cells. *New England Journal of Medicine*, **344**, 385–386.

Rauen, U. and de Groot, H. (1998) Cold-induced release of reactive oxygen species as a decisive mediator of hypothermia injury to cultured liver cells. *Free Radical Biology and Medicine*, **24**, 1316–1323.

Reyes, M., Dudek, A., Jahagirdar, B., Koodie, L., Marker, P.H. and Verfaillie, C.M. (2002) Origin of endothelial progenitors in human postnatal bone marrow. *Journal of Clinical Investigation*, **109**, 337–346.

Riccalton-Banks, L., Liew, C., Bhandari, R., Fry, J. and Shakesheff, K.M. (2003) Long term culture of functional liver tissue: three dimensional co-culture of primary hepatocytes and stellate cells. *Tissue Engineering*, **9**, 401-410.

Richardson, T.P., Peters, M.C., Ennet, A.B. and Mooney, D.J. (2001) Polymeric system for dual growth factor delivery. *Nature Biotechnology*, **19**, 1029-1034.

Reichelt, H.W. and Joyner, C.A. (1965) Use of gelatin as a food-bonding agent. *Progressive Fish Culturist*, **27**, 66-∞.

Reverchon, E. (2002) Supercritical-assisted atomization to produce micro- and/or nanoparticles of controlled size and distribution. *Industrial and Engineering Chemistry Research*, **41**, 2405-2411.

Roberts, C.J. and Debenedetti, P.G. (2002) Engineering pharmaceutical stability with amorphous solids. *AIChE Journal*, **48**, 1140-1144.

Roberts, A., Wyslouzil, B.E. and Bonassar, L. (2005) Aerosol delivery of mammalian cells for tissue engineering. *Biotechnology & Bioengineering*, **9**, 801-807.

Roether, J.A., Gough, J.E., Boccaccini, A.R., Hench, L.L., Maquet, V. and Jerome, R. (2002) Novel bioresorbable and bioactive composites based on bioactive glass and polylactide foams for bone tissue engineering. *Journal of Materials Science – Materials in Medicine*, **13**, 1207-1214.

Rose, F.R.A.J, Cyster, L.A., Grant, D.M., Scotchford, C.A., Howdle, S.M. and Shakesheff, K.M. (2004) In vitro assessment of cell penetration into porous hydroxyapatite scaffolds with a central aligned channel. *Biomaterials*, **25**, 5507-5514.

Ryu, J., Oh, D. J., Choi, C. Y. and Kim, B.S. (2003) Suspension culture of anchorage-dependent animal cells using nanospheres of the biodegradable polymer, poly(lactic-co-glycolic acid). *Biotechnology Lett*ers, **25**, 1363-1367.

Sakiyama-Elbert, S.E. and Hubbell, J.A. (2000b) Controlled release of nerve growth factor from a heparin-containing fibrin-based cell in-growth matrix. *Journal of Controlled Release*, **69**,149-158.

Sarasam, A. and Madihally, S.V. (2005) Characterization of chitosan–polycaprolactone blends for tissue engineering applications. *Biomaterials*, **26**, 5500–5508.

Schwartz, R.E., Reyes, M., Koodie, L., Jiang, Y.H., Blackstad, M., Lund, T., Lenvik, T., Johnson, S., Hu, W. S. and Verfaillie, C. M. (2002) Multi-potential adult progenitor cells from bone marrow differentiation into functional hepatocyte-like cells. *Journal of Clinical Investigation,* **109**, 1291–1302.

Sencar-Bozic, P., Srcic, S., Knez, Z. and Kerc, J. (1997) Improvement of nifedipine dissolution characteristics using supercritical CO_2. *International Journal of Pharmaceutics*, **148**, 123-130.

Service, R.F. (2005) Tissue engineering - technique uses body as 'bioreactor' to grow new bone. *Science*, **309**, 683-683.

Shea, L.D., Smiley, B., Bonadio, J. and Mooney, D.J. (1999) DNA delivery from polymer matrices for tissue engineering. *Nature Biotechnology*, **17**, 551-554.

Sheridan, M.H., Shea, L.D., Peters, M.C. and Mooney, D.J. (2000) Bioabsorbable polymer scaffolds for tissue engineering capable of sustained growth factor delivery. *Journal of Controlled Release*, **64**, 91-102.

Singh, L., Kumar, V. and Ratner, B.D. (2004) Generation of porous microcellular 85/15 poly (DL-lactide-co-glycolide) foams for biomedical applications. *Biomaterials*, **25**, 2611-2617.

Smidsrod, O. and Skjak-Braek, G. (1990) Alginate as an immobilization matrix for cells. *Trends in Biotechnology*, **8**, 71-78.

Sohier, J., Haan, R.E., de Groot, K. and Bezemer, J.M. (2003) A novel method to obtain protein release from porous polymer scaffolds: emulsion coating, *Journal of Controlled Release*, **87**, 57-68.

Sonderfan, A.J., Arlotto, M.P., Dutton, D.R, McMillen, A.K. and Parkinson, A. (1987) Regulation of testosterone hydroxylation by rat-liver microsomal cytochrome-P-450. *Archives of Biochemistry and Biophysics*, **255**, 27-41.

Sonderfan, A.J., Arlotto, M.P. and Parkinson, A. (1989) Identification of the cytochrome-P-450 isozymes responsible for testosterone oxidation in rat lung, kidney, and testis – evidence that cytochrome-P-450A (P450IIA1) is the physiologically important testosterone-7-alpha-hydroxylase in rat testi. *Endocrinology*, **125**, 857-866.

Spilimbergo, S., Elvassore, N. and Bertucco, A. (2002) Microbial inactivation by high-pressure. *Journal of Supercritical Fluids*, **22**, 55-63.

Sproule, T. L., Lee, J. A., Li, H. B., Lannutti, J. J. and Tomasko, D. L. (2004) Bioactive polymer surfaces via supercritical fluids. *Journal of Supercritical Fluids*, **28**, 241-248.

Stevens, M.M., Marini, R.P., Schaefer, D., Aronson, J., Langer, R. and Shastri, V.P. (2005) In vivo engineering of organs: The bone bioreactor. *Proceedings of the National Academy of Sciences of the Unites States of America*, **102**, 11450-11455.

Sun, Q.H., Chen, R., Mooney, D.J., Rajagopalan, S. and Grossman, P.M. (2004) Biodegradable scaffolds incorporating vascular endothelial factor as a novel sustained delivery platform to induce angiogenesis. *Journal of the American College of Cardiology*, **43**, 473A-473A.

Suh, J.K. and Howard, W.T. (2000) Application of chitosan-based polysaccharide biomaterials in cartilage tissue engineering: a review. *Biomaterials*, **21**, 2589–2598.

Tabata, Y., Miyao, M., Ozeki, M. and Ikada, Y. (2000) Controlled release of vascular endothelial growth factor by use of collagen hydrogels. *Journal of Biomaterials Science – Polymer Edition*, **11**, 915-930.

Talwar, R., Di Silvio, L., Hughes, F.J. and King, G.N. (2001) Effects of carrier release kinetics on bone morphogenetic protein-2-induced periodontal regeneration in vivo. *Journal of Clinical Periodontology*, **28**, 340–347.

Tare, R.S., Oreffo, R.O., Clarke, N.M. and Roach, H.I. (2002) Pleiotrophin/ Osteoblast-stimulating factor 1: Dissecting its diverse functions in bone formation. *Journal of Bone and Mineral Research*, **17**, 2009-2020.

Thurner, P., Muller, B., Beckmann, F., Weitkamp, T., Rau, C., Muller, R., Hubbell, J.A. and Sennhauser, U. (2003) Tomography studies of human foreskin fibroblasts on polymer yarns. *Nuclear Instruments & Methods in Physics Research Section B – Beam Interactions with Materials & Atoms*, **200**, 397-405 (2003).

Thurner, P., Muller, B., Sennhauser, U., Hubbell, J.A. and Muller, R. (2004) Tomography studies of biological cells on polymer scaffolds. *Journal of Physics – Condensed Matter*, **16**, S3499-S3510.

Tom, J.W. and Debenedetti, P.G. (1991) Formation of bioerodible polymeric microspheres and microparticles by rapid expansion of supercritical solutions. *Biotechnology Prog*ress, **7**, 403-411.

Tomford W.W. (1995) Transmission of disease through transplantation of musculoskeletal allografts. *Journal of Bone and Joint Surgery American Volume*, **77**, 1742–1754.

Uematsu, K., Hattori, K., Ishimoto, Y., Yamauchi, J., Habata, T.,Takakura, Y., Ohgushi, H., Fukuchi, T. and Sato, M. (2005) Cartilage regeneration using mesenchymal stem cells and a three-dimensional poly-lactic-glycolic acid (PLGA) scaffold. *Biomaterials*, **26**, 4273–4279.

Unsworth, J.M., Rose, F.R.A.J., Wright, E., Scotchford, C.A. and Shakesheff, K.M. (2003) Seeding cells into needled felt scaffolds for tissue engineering applications. *Journal of Biomedical Materials Research Part A*, **66A**, 425-431.

Van de Vord, P.J., Nasser, S. and Wooley, P.H. (2005) Immunological responses to bone soluble proteins in recipients of bone allografts. *Journal of Orthopedic Research,* **23**, 1059-1064.

Van de Weert, M., Hoechstetter, J, Hennink, W.E. and Crommelin, D.J.A. (2000) The effect of a water/organic solvent interface on the structural stability of lysozyme. *Journal of Controlled Release*, **68**, 351-359.

Venugopal, J., Ma, L. L., Yong, T. and Ramakrishna, S. (2005) In vitro study of smooth muscle cells on polycaprolactone and collagen nanofibrous matrices. *Cell Biology International*, **29**, 861-867.

von Recum, H., Kikuchi, A., Yamato, M., Sakurai, Y., Okano, T. and Kim, S.W. (1999) Growth factor and matrix molecules preserve cell function on thermally responsive culture surfaces. *Tissue Engineering*, **5**, 251-265.

Wallace, D.G. and Rosenblatt, J. (2003) Collagen gel systems for sustained delivery and tissue engineering. *Advanced Drug Delivery Reviews*, **55**, 1631-1649.

Wangerin, K. and Wottge, H.U. (1994) Immunological reactions against collagen. *European journal of Plastic Surgery*, **17**, 287-291.

Watson, M.S., Whitaker, M.J., Howdle, S.M. and Shakesheff, K.M. (2002) Incorporation of proteins into polymer materials by a novel supercritical fluid processing method. *Advanced Materials*, **14**, 1802-1804.

Weatherford, D.A., Sackman, J.E., Reddick, T.T. and Freeman, M.B. (1996) Vascular endothelial growth factor and heparin in a biologic glue promotes human aortic endothelial cell proliferation with aortic smooth muscle cell inhibition, Stevens, S.L, Goldman, M.H. *Surgery*, **120**, 433-439.

Wheatley S.P. and McNeish A. (2005) *International Reviews in Cytology*, **247**, 35-88.

Whitaker, M.J., Hao, J.Y., Davies, O.R., Serhatkulu, G., Stolnik-Trenkic, S., Howdle, S.M. and Shakesheff, K.M. (2005) The production of protein-loaded microparticles by supercritical fluid enhanced mixing and spraying. *Journal of Controlled Release*, **101**, 85-92.

Widmer, M.S., Gupta, P.K., Lu, L.C., Meszlenyi, R.K., Evans, G.R.D., Brandt, K., Savel, T., Gurlek, A., Patrick, C.W. and Mikos, A.G. (1998) Manufacture of porous biodegradable polymer conduits by an extrusion process for guided tissue regeneration. *Biomaterials*, **19**, 1945-1955.

Wood, J.H. (1965) In vivo drug release rate from hard gelatin capsules. *Journal of Pharmaceutical Sciences*, **54**, 1207-∞.

Woods, H.M., Silva, M.M.C.G., Nouvel, C., Shakesheff, K.M. and Howdle, S.M. (2004) Materials processing in supercritical carbon dioxide: surfactants, polymers and biomaterials. *Journal of Materials Chemistry,* **14**, 1663-1678.

Wu, J. (1995) Mechanisms of animal cell damage associated with gas bubbles and cell protection by medium additives. *Journal of Biotechnology, **43**, 81-94.*

Xynos, I.D., Hukkanen, M.V.J., Batten, J.J., Buttery, L.D., Hench, L.L. and Polak, J. M. (2000) Bioglass® 45S5 stimulates osteoblast turnover and enhances bone formation in vitro: Implications and applications for bone tissue engineering. *Calcified Tissue Engineering*, **67**, 321-329.

Yang, X.B., Roach, H.I., Clarke, N.M.P., Howdle, S.M., Quirk, R., Shakesheff, K.M. and Oreffo, R.O.C. (2001) Synthetic biodegradable structures after surface modification. *Bone*, **29**, 523-531.

Yang, X.B., Roach, H.I., Clarke, N.M., Howdle, S.M., Shakesheff, K.M. and Oreffo, R.O.C. (2002) Induction of bone formation in vivo using human osteoprogenitor and osteoblast stimulating factor-1 adsorbed scaffold constructs, *Journal of Bone and Mineral Research*, **17**, 47-57.

Yang, X.B., Tare, R.S., Partridge, K.A., Roach, H.I., Clarke, N.M., Howdle, S.M., Shakesheff, K.M. and Oreffo, R.O.C. (2003a) Induction of human osteoprogenitor chemotaxis, proliferation, differentiation, and bone formation by osteoblast stimulating factor-1/pleiotrophin: osteoconductive biomimetic scaffolds for tissue engineering, *Journal of Bone and Mineral Research*, **18**, 47-57.

Yang, X.B., Whitaker, M.J., Clarke, N.M., Sebald, W., Howdle, S.M., Shakesheff, K.M. and Oreffo, R.O.C (2003b) In vivo human bone and cartilage formation using porous polymer scaffolds encapsulated with bone morphogenetic protein-2 (BMP-2), *Journal of Bone and Mineral Research*, **18**, 1366-1366.

Yang, X.B.B., Whitaker, M.J., Sebald, W., Clarke, N., Howdle, S.M., Shakesheff, K.M.S. and Oreffo, R. O. C. (2004) Human osteoprogenitor bone formation using encapsulated morphogenetic protein-2 in porous polymer scaffolds. *Tissue Engineering*, **10**, 1037-1045.

Yeo, S-D., Lim, G.B., Debenedetti, P.G. and Bernstein, H. (1993) Formation of microparticulate protein powders using a supercritical antisolvent. *Biotechnology and Bioengineering*, **41**, 341-346.

Young, T.J., Johnston, K.P., Mishima, K. and Tanaka, H. (1999) Encapsulation of lysozyme in a biodegradable polymer by precipitation with a vapor-over-liquid antisolvent. *Journal of Pharmaceutical Science*, **88**, 640-650.

Zhang, S.G., Holmes, T.C., Dipersio, C.M., Hynes, R.O., Su, X. and Rich, A. (1995) Self complimentary matrices support mammalian cell attachment. *Biomaterials*, **16**, 1385-1393.

Zhang, Y.Z., Venugopal, J., Huang, Z.M., Lim, C.T., Ramakrishna, S. (2005) Characterization of the surface biocompatibility of the electrospun PCL-collagen nanofibers using fibroblasts. *Biomacromolecules*, **6**, 2583-2589.

Zisch, A.H., Lutolf, M.P., Hubbell, J.A. (2003) Biopolymeric delivery matrices for angiogenic growth factors. *Cardiovascular Pathology*, **12**, 295-310.

General Reference Material

Principles of tissue engineering – 2nd edition 2000. Lanza, R. P., Langer, R. and Vacanti, J. P. Academic Press Inc. London.